Electric Machinery

Sixth Edition

A. E. Fitzgerald
Late Vice President for Academic Affairs
and Dean of the Faculty
Northeastern University

Charles Kingsley, Jr.
Late Associate Professor of Electrical
Engineering, Emeritus
Massachusetts Institute of Technology

Stephen D. Umans
Principal Research Engineer
Department of Electrical Engineering and
Computer Science
Laboratory for Electromagnetic and
Electronic Systems
Massachusetts Institute of Technology

Boston Burr Ridge, IL Dubuque, IA Madison, WI New York San Francisco St. Louis
Bangkok Bogotá Caracas Kuala Lumpur Lisbon London Madrid Mexico City
Milan Montreal New Delhi Santiago Seoul Singapore Sydney Taipei Toronto

McGraw-Hill Higher Education

*A Division of The **McGraw-Hill** Companies*

ELECTRIC MACHINERY, SIXTH EDITION

Published by McGraw-Hill, a business unit of The McGraw-Hill Companies, Inc., 1221 Avenue of the Americas, New York, NY 10020. Copyright © 2003, 1990, 1983, 1971, 1961, 1952 by The McGraw-Hill Companies, Inc. All rights reserved. Copyright renewed 1980 by Rosemary Fitzgerald and Charles Kingsley, Jr. All rights reserved. No part of this publication may be reproduced or distributed in any form or by any means, or stored in a database or retrieval system, without the prior written consent of The McGraw-Hill Companies, Inc., including, but not limited to, in any network or other electronic storage or transmission, or broadcast for distance learning.

Some ancillaries, including electronic and print components, may not be available to customers outside the United States.

This book is printed on acid-free paper.

International 1 2 3 4 5 6 7 8 9 0 DOC/DOC 0 9 8 7 6 5 4 3 2
Domestic 1 2 3 4 5 6 7 8 9 0 DOC/DOC 0 9 8 7 6 5 4 3 2

ISBN 0-07-366009-4
ISBN 0-07-112193-5 (ISE)

Publisher: *Elizabeth A. Jones*
Developmental editor: *Michelle L. Flomenhoft*
Executive marketing manager: *John Wannemacher*
Project manager: *Rose Koos*
Production supervisor: *Sherry L. Kane*
Media project manager: *Jodi K. Banowetz*
Senior media technology producer: *Phillip Meek*
Coordinator of freelance design: *Rick D. Noel*
Cover designer: *Rick D. Noel*
Cover image courtesy of: *Rockwell Automation/Reliance Electric*
Lead photo research coordinator: *Carrie K. Burger*
Compositor: *Interactive Composition Corporation*
Typeface: *10/12 Times Roman*
Printer: *R. R. Donnelley & Sons Company/Crawfordsville, IN*

Library of Congress Cataloging-in-Publication Data

Fitzgerald, A. E. (Arthur Eugene), 1909–
Electric machinery / A. E. Fitzgerald, Charles Kingsley, Jr., Stephen D. Umans. —6th ed.
p. cm. —(McGraw-Hill series in electrical engineering. Power and energy)
Includes index.
ISBN 0-07-366009-4—ISBN 0-07-112193-5
1. Electric machinery. I. Kingsley, Charles, 1904–. II. Umans, Stephen D. III. Title.
IV. Series.

TK2181 .F5 2003
621.31′042—dc21 2002070988
CIP

INTERNATIONAL EDITION ISBN 0-07-112193-5
Copyright © 2003. Exclusive rights by The McGraw-Hill Companies, Inc., for manufacture and export. This book cannot be re-exported from the country to which it is sold by McGraw-Hill. The International Edition is not available in North America.

www.mhhe.com

McGraw-Hill Series in Electrical and Computer Engineering

Stephen W. Director, University of Michigan, Ann Arbor, *Senior Consulting Editor*

Circuits and Systems
Communications and Signal Processing
Computer Engineering
Control Theory and Robotics
Electromagnetics
Electronics and VLSI Circuits
Introductory
Power
Antennas, Microwaves, and Radar

Ronald N. Bracewell, Colin Cherry, James F. Gibbons, Willis W. Harman, Hubert Heffner, Edward W. Herold, John G. Linvill, Simon Ramo, Ronald A. Rohrer, Anthony E. Siegman, Charles Susskind, Frederick E. Terman, John G. Truxal, Ernst Weber, and John R. Whinnery, *Previous Consulting Editors*

This book is dedicated to my mom, Nettie Umans, and my aunt, Mae Hoffman, and in memory of my dad, Samuel Umans.

ABOUT THE AUTHORS

The late **Arthur E. Fitzgerald** was Vice President for Academic Affairs at Northeastern University, a post to which he was appointed after serving first as Professor and Chairman of the Electrical Engineering Department, followed by being named Dean of Faculty. Prior to his time at Northeastern University, Professor Fitzgerald spent more than 20 years at the Massachusetts Institute of Technology, from which he received the S.M. and Sc.D., and where he rose to the rank of Professor of Electrical Engineering. Besides *Electric Machinery,* Professor Fitzgerald was one of the authors of *Basic Electrical Engineering,* also published by McGraw-Hill. Throughout his career, Professor Fitzgerald was at the forefront in the field of long-range power system planning, working as a consulting engineer in industry both before and after his academic career. Professor Fitzgerald was a member of several professional societies, including Sigma Xi, Tau Beta Pi, and Eta Kappa Nu, and he was a Fellow of the IEEE.

The late **Charles Kingsley, Jr.** was Professor in the Department of Electrical Engineering and Computer Science at the Massachusetts Institute of Technology, from which he received the S.B. and S.M. degrees. During his career, he spent time at General Electric, Boeing, and Dartmouth College. In addition to *Electric Machinery,* Professor Kingsley was co-author of the textbook *Magnetic Circuits and Transformers*. After his retirement, he continued to participate in research activities at M.I.T. He was an active member and Fellow of the IEEE, as well as its predecessor society, the American Institute of Electrical Engineers.

Stephen D. Umans is Principal Research Engineer in the Electromechanical Systems Laboratory and the Department of Electrical Engineering and Computer Science at the Massachusetts Institute of Technology, from which he received the S.B., S.M., E.E., and Sc.D. degrees, all in electrical engineering. His professional interests include electromechanics, electric machinery, and electric power systems. At MIT, he has taught a wide range of courses including electromechanics, electromagnetics, electric power systems, circuit theory, and analog electronics. He is a Fellow of the IEEE and an active member of the Power Engineering Society.

PREFACE

The chief objective of *Electric Machinery* continues to be to build a strong foundation in the basic principles of electromechanics and electric machinery. Through all of its editions, the emphasis of *Electric Machinery* has been on both physical insight and analytical techniques. Mastery of the material covered will provide both the basis for understanding many real-world electric-machinery applications as well as the foundation for proceeding on to more advanced courses in electric machinery design and control.

Although much of the material from the previous editions has been retained in this edition, there have been some significant changes. These include:

- A chapter has been added which introduces the basic concepts of power electronics as applicable to motor drives.
- Topics related to machine control, which were scattered in various chapters in the previous edition, have been consolidated in a single chapter on speed and torque control. In addition, the coverage of this topic has been expanded significantly and now includes field-oriented control of both synchronous and induction machines.
- MATLAB®[1] examples, practice problems, and end-of-chapter problems have been included in the new edition.
- The analysis of single-phase induction motors has been expanded to cover the general case in which the motor is running off both its main winding and its auxiliary winding (supplied with a series capacitor).

Power electronics are a significant component of many contemporary electric-machine applications. This topic is included in Chapter 10 of this edition of *Electric Machinery* in recognition of the fact that many electric-machinery courses now include a discussion of power electronics and drive systems. However, it must be emphasized that the single chapter found here is introductory at best. One chapter cannot begin to do justice to this complex topic any more than a single chapter in a power-electronics text could adequately introduce the topic of electric machinery.

The approach taken here is to discuss the basic properties of common power electronic components such as diodes, SCRs, MOSFETs, and IGBTs and to introduce simple models for these components. The chapter then illustrates how these components can be used to achieve two primary functions of power-electronic circuits in drive applications: rectification (conversion of ac to dc) and inversion (conversion of dc to ac). Phase-controlled rectification is discussed as a technique for controlling the dc voltage produced from a fixed ac source. Phase-controlled rectification can be used

[1] MATLAB is a registered trademark of The MathWorks, Inc.

to drive dc machines as well as to provide a controllable dc input to inverters in ac drives. Similarly, techniques for producing stepped and pulse-width-modulated waveforms of variable amplitudes and frequency are discussed. These techniques are at the heart of variable-speed drive systems which are commonly found in variable-speed ac drives.

Drive-systems based upon power electronics permit a great deal of flexibility in the control of electric machines. This is especially true in the case of ac machines which used to be found almost exclusively in applications where they were supplied from the fixed-frequency, fixed-voltage power system. Thus, the introduction to power electronics in Chapter 10 is followed by a chapter on the control of electric machines.

Chapter 11 brings together material that was distributed in various chapters in the previous edition. It is now divided into three main sections: control of dc motors, control of synchronous motors, and control of induction motors. A brief fourth section discusses the control of variable-reluctance motors. Each of these main sections begins with a discussion of speed control followed by a discussion of torque control.

Many motor-drive systems are based upon the technique of field-oriented control (also known as vector control). A significant addition to this new edition is the discussion of field-oriented control which now appears in Chapter 11. This is somewhat advanced material which is not typically found in introductory presentations of electric machinery. As a result, the chapter is structured so that this material can be omitted or included at the discretion of the instructor. It first appears in the section on torque control of synchronous motors, in which the basic equations are derived and the analogy with the control of dc machines is discussed. It appears again in its most commonly used form in the section on the torque control of induction motors.

The instructor should note that a complete presentation of field-oriented control requires the use of the dq0 transformation. This transformation, which appeared for synchronous machines in Chapter 6 of the previous edition, is now found in Appendix C of this edition. In addition, the discussion in this appendix has been expanded to include a derivation of the dq0 transformation for induction machines in which both stator and rotor quantities must be transformed.

Although very little in the way of sophisticated mathematics is required of the reader of this book, the mathematics can get somewhat messy and tedious. This is especially true in the analyis of ac machines in which there is a significant amount of algebra involving complex numbers. One of the significant positive developments in the last decade or so is the widespread availability of programs such as MATLAB which greatly facilitate the solution of such problems. MATLAB is widely used in many universities and is available in a student version.[2]

In recognition of this development, this edition incorporates MATLAB in examples and practice problems as well as in end-of-chapter problems. It should be emphasized, though, that the use of MATLAB is not in any way a requirement for the adoption or use of *Electric Machinery*. Rather, it is an enhancement. The book

[2] The MATLAB Student Version is published and distributed by The MathWorks, Inc. (http://www.mathworks.com).

now includes interesting examples which would have otherwise been too mathematically tedious. Similarly, there are now end-of-chapter problems which are relatively straightforward when done with MATLAB but which would be quite impractical if done by hand. Note that each MATLAB example and practice problem has been notated with the symbol , found in the margin of the book. End-of-chapter problems which suggest or require MATLAB are similarly notatated.

It should be emphasized that, in addition to MATLAB, a number of other numerical-analysis packages, including various spread-sheet packages, are available which can be used to perform calculations and to plot in a fashion similar to that done with MATLAB. If MATLAB is not available or is not the package of preference at your institution, instructors and students are encouraged to select any package with which they are comfortable. Any package that simplifies complex calculations and which enables the student to focus on the concepts as opposed to the mathematics will do just fine.

In addition, it should be noted that even in cases where it is not specifically suggested, most of the end-of-chapter problems in the book can be worked using MATLAB or an equivalent program. Thus, students who are comfortable using such tools should be encouraged to do so to save themselves the need to grind through messy calculations by hand. This approach is a logical extension to the use of calculators to facilitate computation. When solving homework problems, the students should still, of course, be required to show on paper how they formulated their solution, since it is the formulation of the solution that is key to understanding the material. However, once a problem is properly formulated, there is typically little additional to be learned from the number crunching itself. The learning process then continues with an examination of the results, both in terms of understanding what they mean with regard to the topic being studied as well as seeing if they make physical sense.

One additional benefit is derived from the introduction of MATLAB into this edition of *Electric Machinery*. As readers of previous editions will be aware, the treatment of single-phase induction motors was never complete in that an analytical treatment of the general case of a single-phase motor running with both its main and auxiliary windings excited (with a capacitor in series with the auxiliary winding) was never considered. In fact, such a treatment of single-phase induction motors is not found in any other introductory electric-machinery textbook of which the author is aware.

The problem is quite simple: this general treatment is mathematically complex, requiring the solution of a number of simultaneous, complex algebraic equations. This, however, is just the sort of problem at which programs such as MATLAB excel. Thus, this new edition of *Electric Machinery* includes this general treatment of single-phase induction machines, complete with a worked out quantitative example and end-of-chapter problems.

It is highly likely that there is simply too much material in this edition of *Electric Machinery* for a single introductory course. However, the material in this edition has been organized so that instructors can pick and choose material appropriate to the topics which they wish to cover. As in the fifth edition, the first two chapters introduce basic concepts of magnetic circuits, magnetic materials, and transformers. The third

chapter introduces the basic concept of electromechanical energy conversion. The fourth chapter then provides an overview of and on introduction to the various machine types. Some instructors choose to omit all or most of the material in Chapter 3 from an introductory course. This can be done without a significant impact to the understanding of much of the material in the remainder of the book.

The next five chapters provide a more in-depth discussion of the various machine types: synchronous machines in Chapter 5, induction machines in Chapter 6, dc machines in Chapter 7, variable-reluctance machines in Chapter 8, and single/two-phase machines in Chapter 9. Since the chapters are pretty much independent (with the exception of the material in Chapter 9 which builds upon the polyphase-induction-motor discussion of Chapter 6), the order of these chapters can be changed and/or an instructor can choose to focus on one or two machine types and not to cover the material in all five of these chapters.

The introductory power-electronics discussion of Chapter 10 is pretty much stand-alone. Instructors who wish to introduce this material should be able to do so at their discretion; there is no need to present it in a course in the order that it is found in the book. In addition, it is not required for an understanding of the electric-machinery material presented in the book, and instructors who elect to cover this material in a separate course will not find themselves handicapped in any way by doing so.

Finally, instructors may wish to select topics from the control material of Chapter 11 rather than include it all. The material on speed control is essentially a relatively straightforward extension of the material found in earlier chapters on the individual machine types. The material on field-oriented control requires a somewhat more sophisticated understanding and builds upon the dq0 transformation found in Appendix C. It would certainly be reasonable to omit this material in an introductory course and to delay it for a more advanced course where sufficient time is available to devote to it.

McGraw-Hill has set up a website, **www.mhhe.com/umans**, to support this new edition of *Electric Machinery*. The website will include a downloadable version of the solutions manual (for instructors only) as well as PowerPoint slides of figures from the book. This being a new feature of *Electric Machinery,* we are, to a great extent, starting with a blank slate and will be exploring different options for supplementing and enhancing the text. For example, in recognition of the fact that instructors are always looking for new examples and problems, we will set up a mechanism so that instructors can submit examples and problems for publication on the website (with credit given to their authors) which then can be shared with other instructors.

We are also considering setting up a section of the website devoted to MATLAB and other numerical analysis packages. For users of MATLAB, the site might contain hints and suggestions for applying MATLAB to *Electric Machinery* as well as perhaps some Simulink®[3] examples for instructors who wish to introduce simulations into their courses. Similarly, instructors who use packages other than MATLAB might

[3] Simulink is a registered trademark of The MathWorks, Inc.

want to submit their suggestions and experiences to share with other users. In this context, the website would appear again to be an ideal resource for enhancing interaction between instructors.

Clearly, the website will be a living document which will evolve in response to input from users. I strongly urge each of you to visit it frequently and to send in suggestions, problems, and examples, and comments. I fully expect it to become a valuable resource for users of *Electric Machinery* around the world.

Professor Kingsley first asked this author to participate in the fourth edition of *Electric Machinery;* the professor was actively involved in that edition. He participated in an advisory capacity for the fifth edition. Unfortunately, Professor Kingsley passed away since the publication of the fifth edition and did not live to see the start of the work on this edition. He was a fine gentleman, a valued teacher and friend, and he is missed.

I wish to thank a number of my colleagues for their insight and helpful discussions during the production of this edition. My friend, Professor Jeffrey Lang, who also provided invaluable insight and advice in the discussion of variable-reluctance machines which first appeared in the fifth edition, was extremely helpful in formulating the presentations of power electronics and field-oriented control which appear in this edition. Similarly, Professor Gerald Wilson, who served as my graduate thesis advisor, has been a friend and colleague throughout my career and has been a constant source of valuable advice and insight.

On a more personal note, I would like to express my love for my wife Denise and our children Dalya and Ari and to thank them for putting up with the many hours of my otherwise spare time that this edition required. I promised the kids that I would read the Harry Potter books when work on this edition of *Electric Machinery* was completed and I had better get to it! In addition, I would like to recognize my life-long friend David Gardner who watched the work on this edition with interest but who did not live to see it completed. A remarkable man, he passed away due to complications from muscular dystrophy just a short while before the final draft was completed.

Finally, I wish to thank the reviewers who participated in this project and whose comments and suggestions played a valuable role in the final form of this edition. These include Professors:

Ravel F. Ammerman, *Colorado School of Mines*
Juan Carlos Balda, *University of Arkansas, Fayetteville*
Miroslav Begovic, *Georgia Institute of Technology*
Prasad Enjeti, *Texas A&M University*
Vernold K. Feiste, *Southern Illinois University*
Thomas G. Habetler, *Georgia Institute of Technology*
Steven Hietpas, *South Dakota State University*
Heath Hofmann, *Pennsylvania State University*
Daniel Hutchins, *U.S. Naval Academy*
Roger King, *University of Toledo*

Alexander E. Koutras, *California Polytechnic State University, Pomona*
Bruno Osorno, *California State University, Northridge*
Henk Polinder, *Delft University of Technology*
Gill Richards, *Arkansas Tech University*
Duane F. Rost, *Youngstown State University*
Melvin Sandler, *The Cooper Union*
Ali O. Shaban, *California Polytechnic State University, San Luis Obispo*
Alan Wallace, *Oregon State University*

I would like to specifically acknowledge Professor Ibrahim Abdel-Moneim Abdel-Halim of Zagazig University, whose considerable effort found numerous typos and numerical errors in the draft document.

Stephen D. Umans
Cambridge, MA
March 5, 2002

BRIEF CONTENTS

Preface x

1 Magnetic Circuits and Magnetic Materials 1

2 Transformers 57

3 Electromechanical-Energy-Conversion Principles 112

4 Introduction to Rotating Machines 173

5 Synchronous Machines 245

6 Polyphase Induction Machines 306

7 DC Machines 357

8 Variable-Reluctance Machines and Stepping Motors 407

9 Single- and Two-Phase Motors 452

10 Introduction to Power Electronics 493

11 Speed and Torque Control 559

Appendix A Three-Phase Circuits 628

Appendix B Voltages, Magnetic Fields, and Inductances of Distributed AC Windings 644

Appendix C The dq0 Transformation 657

Appendix D Engineering Aspects of Practical Electric Machine Performance and Operation 668

Appendix E Table of Constants and Conversion Factors for SI Units 680

Index 681

CONTENTS

Preface x

Chapter 1

Magnetic Circuits and Magnetic Materials 1

1.1 Introduction to Magnetic Circuits 2
1.2 Flux Linkage, Inductance, and Energy 11
1.3 Properties of Magnetic Materials 19
1.4 AC Excitation 23
1.5 Permanent Magnets 30
1.6 Application of Permanent Magnet Materials 35
1.7 Summary 42
1.8 Problems 43

Chapter 2

Transformers 57

2.1 Introduction to Transformers 57
2.2 No-Load Conditions 60
2.3 Effect of Secondary Current; Ideal Transformer 64
2.4 Transformer Reactances and Equivalent Circuits 68
2.5 Engineering Aspects of Transformer Analysis 73
2.6 Autotransformers; Multiwinding Transformers 81
2.7 Transformers in Three-Phase Circuits 85
2.8 Voltage and Current Transformers 90
2.9 The Per-Unit System 95
2.10 Summary 103
2.11 Problems 104

Chapter 3

Electromechanical-Energy-Conversion Principles 112

3.1 Forces and Torques in Magnetic Field Systems 113
3.2 Energy Balance 117
3.3 Energy in Singly-Excited Magnetic Field Systems 119
3.4 Determination of Magnetic Force and Torque from Energy 123
3.5 Determination of Magnetic Force and Torque from Coenergy 129
3.6 Multiply-Excited Magnetic Field Systems 136
3.7 Forces and Torques in Systems with Permanent Magnets 142
3.8 Dynamic Equations 151
3.9 Analytical Techniques 155
3.10 Summary 158
3.11 Problems 159

Chapter 4

Introduction to Rotating Machines 173

4.1 Elementary Concepts 173
4.2 Introduction to AC and DC Machines 176
4.3 MMF of Distributed Windings 187
4.4 Magnetic Fields in Rotating Machinery 197
4.5 Rotating MMF Waves in AC Machines 201
4.6 Generated Voltage 208
4.7 Torque in Nonsalient-Pole Machines 214
4.8 Linear Machines 227
4.9 Magnetic Saturation 230

4.10 Leakage Fluxes 233
4.11 Summary 235
4.12 Problems 237

Chapter **5**
Synchronous Machines 245

5.1 Introduction to Polyphase Synchronous Machines 245
5.2 Synchronous-Machine Inductances; Equivalent Circuits 248
5.3 Open- and Short-Circuit Characteristics 256
5.4 Steady-State Power-Angle Characteristics 266
5.5 Steady-State Operating Characteristics 275
5.6 Effects of Salient Poles; Introduction to Direct- and Quadrature-Axis Theory 281
5.7 Power-Angle Characteristics of Salient-Pole Machines 289
5.8 Permanent-Magnet AC Motors 293
5.9 Summary 295
5.10 Problems 297

Chapter **6**
Polyphase Induction Machines 306

6.1 Introduction to Polyphase Induction Machines 306
6.2 Currents and Fluxes in Polyphase Induction Machines 311
6.3 Induction-Motor Equivalent Circuit 313
6.4 Analysis of the Equivalent Circuit 317
6.5 Torque and Power by Use of Thevenin's Theorem 322
6.6 Parameter Determination from No-Load and Blocked-Rotor Tests 330
6.7 Effects of Rotor Resistance; Wound and Double-Squirrel-Cage Rotors 340
6.8 Summary 347
6.9 Problems 348

Chapter **7**
DC Machines 357

7.1 Introduction 357
7.2 Commutator Action 364
7.3 Effect of Armature MMF 367
7.4 Analytical Fundamentals: Electric-Circuit Aspects 370
7.5 Analytical Fundamentals: Magnetic-Circuit Aspects 374
7.6 Analysis of Steady-State Performance 379
7.7 Permanent-Magnet DC Machines 384
7.8 Commutation and Interpoles 390
7.9 Compensating Windings 393
7.10 Series Universal Motors 395
7.11 Summary 396
7.12 Problems 397

Chapter **8**
Variable-Reluctance Machines and Stepping Motors 407

8.1 Basics of VRM Analysis 408
8.2 Practical VRM Configurations 415
8.3 Current Waveforms for Torque Production 421
8.4 Nonlinear Analysis 430
8.5 Stepping Motors 437
8.6 Summary 446
8.7 Problems 448

Chapter **9**
Single- and Two-Phase Motors 452

9.1 Single-Phase Induction Motors: Qualitative Examination 452
9.2 Starting and Running Performance of Single-Phase Induction and Synchronous Motors 455
9.3 Revolving-Field Theory of Single-Phase Induction Motors 463
9.4 Two-Phase Induction Motors 470

9.5 Summary 488
9.6 Problems 489

Chapter **10**
Introduction to Power Electronics 493

10.1 Power Switches 494
10.2 Rectification: Conversion of AC to DC 507
10.3 Inversion: Conversion of DC to AC 538
10.4 Summary 550
10.5 Bibliography 552
10.6 Problems 552

Chapter **11**
Speed and Torque Control 559

11.1 Control of DC Motors 559
11.2 Control of Synchronous Motors 578
11.3 Control of Induction Motors 595
11.4 Control of Variable-Reluctance Motors 613
11.5 Summary 616
11.6 Bibliography 618
11.7 Problems 618

Appendix **A**
Three-Phase Circuits 628

A.1 Generation of Three-Phase Voltages 628
A.2 Three-Phase Voltages, Currents, and Power 631
A.3 Y- and Δ-Connected Circuits 635
A.4 Analysis of Balanced Three-Phase Circuits; Single-Line Diagrams 641
A.5 Other Polyphase Systems 643

Appendix **B**
Voltages, Magnetic Fields, and Inductances of Distributed AC Windings 644

B.1 Generated Voltages 644
B.2 Armature MMF Waves 650
B.3 Air-Gap Inductances of Distributed Windings 653

Appendix **C**
The dq0 Transformation 657

C.1 Transformation to Direct- and Quadrature-Axis Variables 657
C.2 Basic Synchronous-Machine Relations in dq0 Variables 660
C.3 Basic Induction-Machine Relations in dq0 Variables 664

Appendix **D**
Engineering Aspects of Practical Electric Machine Performance and Operation 668

D.1 Losses 668
D.2 Rating and Heating 670
D.3 Cooling Means for Electric Machines 674
D.4 Excitation 676
D.5 Energy Efficiency of Electric Machinery 678

Appendix **E**
Table of Constants and Conversion Factors for SI Units 680

Index 681

CHAPTER 1

Magnetic Circuits and Magnetic Materials

The objective of this book is to study the devices used in the interconversion of electric and mechanical energy. Emphasis is placed on electromagnetic rotating machinery, by means of which the bulk of this energy conversion takes place. However, the techniques developed are generally applicable to a wide range of additional devices including linear machines, actuators, and sensors.

Although not an electromechanical-energy-conversion device, the transformer is an important component of the overall energy-conversion process and is discussed in Chapter 2. The techniques developed for transformer analysis form the basis for the ensuing discussion of electric machinery.

Practically all transformers and electric machinery use ferro-magnetic material for shaping and directing the magnetic fields which act as the medium for transferring and converting energy. Permanent-magnet materials are also widely used. Without these materials, practical implementations of most familiar electromechanical-energy-conversion devices would not be possible. The ability to analyze and describe systems containing these materials is essential for designing and understanding these devices.

This chapter will develop some basic tools for the analysis of magnetic field systems and will provide a brief introduction to the properties of practical magnetic materials. In Chapter 2, these results will then be applied to the analysis of transformers. In later chapters they will be used in the analysis of rotating machinery.

In this book it is assumed that the reader has basic knowledge of magnetic and electric field theory such as given in a basic physics course for engineering students. Some readers may have had a course on electromagnetic field theory based on Maxwell's equations, but an in-depth understanding of Maxwell's equations is not a prerequisite for study of this book. The techniques of magnetic-circuit analysis, which represent algebraic approximations to exact field-theory solutions, are widely used in the study of electromechanical-energy-conversion devices and form the basis for most of the analyses presented here.

1.1 INTRODUCTION TO MAGNETIC CIRCUITS

The complete, detailed solution for magnetic fields in most situations of practical engineering interest involves the solution of Maxwell's equations along with various constitutive relationships which describe material properties. Although in practice exact solutions are often unattainable, various simplifying assumptions permit the attainment of useful engineering solutions.[1]

We begin with the assumption that, for the systems treated in this book, the frequencies and sizes involved are such that the displacement-current term in Maxwell's equations can be neglected. This term accounts for magnetic fields being produced in space by time-varying electric fields and is associated with electromagnetic radiation. Neglecting this term results in the magneto-quasistatic form of the relevant Maxwell's equations which relate magnetic fields to the currents which produce them.

$$\oint_C \mathbf{H}d\mathbf{l} = \int_S \mathbf{J} \cdot d\mathbf{a} \tag{1.1}$$

$$\oint_S \mathbf{B} \cdot d\mathbf{a} = 0 \tag{1.2}$$

Equation 1.1 states that the line integral of the tangential component of the *magnetic field intensity* **H** around a closed contour C is equal to the total current passing through any surface S linking that contour. From Eq. 1.1 we see that the source of **H** is the *current density* **J**. Equation 1.2 states that the *magnetic flux density* **B** is conserved, i.e., that no net flux enters or leaves a closed surface (this is equivalent to saying that there exist no monopole charge sources of magnetic fields). From these equations we see that the magnetic field quantities can be determined solely from the instantaneous values of the source currents and that time variations of the magnetic fields follow directly from time variations of the sources.

A second simplifying assumption involves the concept of the *magnetic circuit*. The general solution for the magnetic field intensity **H** and the magnetic flux density **B** in a structure of complex geometry is extremely difficult. However, a three-dimensional field problem can often be reduced to what is essentially a one-dimensional circuit equivalent, yielding solutions of acceptable engineering accuracy.

A magnetic circuit consists of a structure composed for the most part of high-permeability magnetic material. The presence of high-permeability material tends to cause magnetic flux to be confined to the paths defined by the structure, much as currents are confined to the conductors of an electric circuit. Use of this concept of

[1] Although exact analytical solutions cannot be obtained, computer-based numerical solutions (the finite-element and boundary-element methods form the basis for a number of commercial programs) are quite common and have become indespensible tools for analysis and design. However, such techniques are best used to refine analyses based upon analytical techniques such as are found in this book. Their use contributes little to a fundamental understanding of the principles and basic performance of electric machines and as a result they will not be discussed in this book.

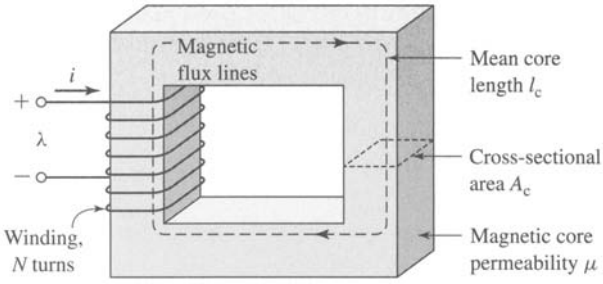

Figure 1.1 Simple magnetic circuit.

the magnetic circuit is illustrated in this section and will be seen to apply quite well to many situations in this book.[2]

A simple example of a magnetic circuit is shown in Fig. 1.1. The core is assumed to be composed of magnetic material whose permeability is much greater than that of the surrounding air ($\mu \gg \mu_0$). The core is of uniform cross section and is excited by a winding of N turns carrying a current of i amperes. This winding produces a magnetic field in the core, as shown in the figure.

Because of the high permeability of the magnetic core, an exact solution would show that the magnetic flux is confined almost entirely to the core, the field lines follow the path defined by the core, and the flux density is essentially uniform over a cross section because the cross-sectional area is uniform. The magnetic field can be visualized in terms of flux lines which form closed loops interlinked with the winding.

As applied to the magnetic circuit of Fig. 1.1, the source of the magnetic field in the core is the ampere-turn product Ni. In magnetic circuit terminology Ni is the *magnetomotive force* (mmf) $\mathcal{F}$ acting on the magnetic circuit. Although Fig. 1.1 shows only a single coil, transformers and most rotating machines have at least two windings, and Ni must be replaced by the algebraic sum of the ampere-turns of all the windings.

The *magnetic flux* ϕ crossing a surface S is the surface integral of the normal component of $\mathbf{B}$; thus

$$\phi = \int_S \mathbf{B} \cdot \mathbf{da} \tag{1.3}$$

In SI units, the unit of ϕ is the *weber* (Wb).

Equation 1.2 states that the net magnetic flux entering or leaving a closed surface (equal to the surface integral of $\mathbf{B}$ over that closed surface) is zero. This is equivalent to saying that all the flux which enters the surface enclosing a volume must leave that volume over some other portion of that surface because magnetic flux lines form closed loops.

---

[2] For a more extensive treatment of magnetic circuits see A. E. Fitzgerald, D. E. Higgenbotham, and A. Grabel, *Basic Electrical Engineering,* 5th ed., McGraw-Hill, 1981, chap. 13; also E. E. Staff, M.I.T., *Magnetic Circuits and Transformers,* M.I.T. Press, 1965, chaps. 1 to 3.

These facts can be used to justify the assumption that the magnetic flux density is uniform across the cross section of a magnetic circuit such as the core of Fig. 1.1. In this case Eq. 1.3 reduces to the simple scalar equation

$$\phi_c = B_c A_c \tag{1.4}$$

where ϕ_c = flux in core
B_c = flux density in core
A_c = cross-sectional area of core

From Eq. 1.1, the relationship between the mmf acting on a magnetic circuit and the magnetic field intensity in that circuit is.[3]

$$\mathcal{F} = Ni = \oint \mathbf{H}d\mathbf{l} \tag{1.5}$$

The core dimensions are such that the path length of any flux line is close to the mean core length l_c. As a result, the line integral of Eq. 1.5 becomes simply the scalar product $H_c l_c$ of the magnitude of **H** and the mean flux path length l_c. Thus, the relationship between the mmf and the magnetic field intensity can be written in magnetic circuit terminology as

$$\mathcal{F} = Ni = H_c l_c \tag{1.6}$$

where H_c is average magnitude of **H** in the core.

The direction of H_c in the core can be found from the *right-hand rule,* which can be stated in two equivalent ways. (1) Imagine a current-carrying conductor held in the right hand with the thumb pointing in the direction of current flow; the fingers then point in the direction of the magnetic field created by that current. (2) Equivalently, if the coil in Fig. 1.1 is grasped in the right hand (figuratively speaking) with the fingers pointing in the direction of the current, the thumb will point in the direction of the magnetic fields.

The relationship between the magnetic field intensity **H** and the magnetic flux density **B** is a property of the material in which the field exists. It is common to assume a linear relationship; thus

$$\mathbf{B} = \mu \mathbf{H} \tag{1.7}$$

where μ is known as the *magnetic permeability*. In SI units, **H** is measured in units of *amperes per meter,* **B** is in *webers per square meter,* also known as *teslas* (T), and μ is in *webers per ampere-turn-meter,* or equivalently *henrys per meter.* In SI units the permeability of free space is $\mu_0 = 4\pi \times 10^{-7}$ henrys per meter. The permeability of linear magnetic material can be expressed in terms of μ_r, its value relative to that of free space, or $\mu = \mu_r \mu_0$. Typical values of μ_r range from 2000 to 80,000 for materials used

[3] In general, the mmf drop across any segment of a magnetic circuit can be calculated as $\int \mathbf{H}d\mathbf{l}$ over that portion of the magnetic circuit.

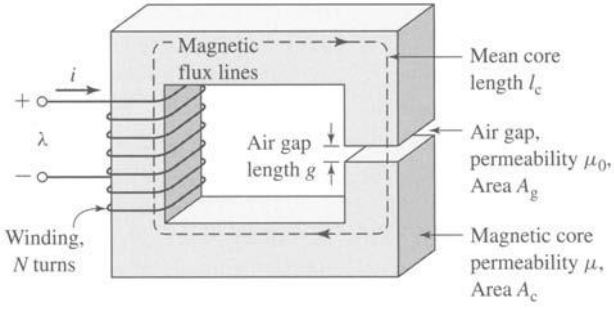

Figure 1.2 Magnetic circuit with air gap.

in transformers and rotating machines. The characteristics of ferromagnetic materials are described in Sections 1.3 and 1.4. For the present we assume that μ_r is a known constant, although it actually varies appreciably with the magnitude of the magnetic flux density.

Transformers are wound on closed cores like that of Fig. 1.1. However, energy conversion devices which incorporate a moving element must have air gaps in their magnetic circuits. A magnetic circuit with an air gap is shown in Fig. 1.2. When the air-gap length g is much smaller than the dimensions of the adjacent core faces, the magnetic flux ϕ will follow the path defined by the core and the air gap and the techniques of magnetic-circuit analysis can be used. If the air-gap length becomes excessively large, the flux will be observed to "leak out" of the sides of the air gap and the techniques of magnetic-circuit analysis will no longer be strictly applicable.

Thus, provided the air-gap length g is sufficiently small, the configuration of Fig. 1.2 can be analyzed as a magnetic circuit with two series components: a magnetic core of permeability μ, cross-sectional area A_c, and mean length l_c, and an air gap of permeability μ_0, cross-sectional area A_g, and length g. In the core the flux density can be assumed uniform; thus

$$B_c = \frac{\phi}{A_c} \tag{1.8}$$

and in the air gap

$$B_g = \frac{\phi}{A_g} \tag{1.9}$$

where ϕ = the flux in the magnetic circuit.

Application of Eq. 1.5 to this magnetic circuit yields

$$\mathcal{F} = H_c l_c + H_g g \tag{1.10}$$

and using the linear B-H relationship of Eq. 1.7 gives

$$\mathcal{F} = \frac{B_c}{\mu} l_c + \frac{B_g}{\mu_0} g \tag{1.11}$$

Here the $\mathcal{F} = Ni$ is the mmf applied to the magnetic circuit. From Eq. 1.10 we see that a portion of the mmf, $\mathcal{F}_c = H_c l_c$, is required to produce magnetic field in the core while the remainder, $\mathcal{F}_g = H_g g$, produces magnetic field in the air gap.

For practical magnetic materials (as is discussed in Sections 1.3 and 1.4), B_c and H_c are not simply related by a known constant permeability μ as described by Eq. 1.7. In fact, B_c is often a nonlinear, multivalued function of H_c. Thus, although Eq. 1.10 continues to hold, it does not lead directly to a simple expression relating the mmf and the flux densities, such as that of Eq. 1.11. Instead the specifics of the nonlinear B_c-H_c relation must be used, either graphically or analytically. However, in many cases, the concept of constant material permeability gives results of acceptable engineering accuracy and is frequently used.

From Eqs. 1.8 and 1.9, Eq. 1.11 can be rewritten in terms of the total flux ϕ as

$$\mathcal{F} = \phi\left(\frac{l_c}{\mu A_c} + \frac{g}{\mu_0 A_g}\right) \tag{1.12}$$

The terms that multiply the flux in this equation are known as the *reluctance* $\mathcal{R}$ of the core and air gap, respectively,

$$\mathcal{R}_c = \frac{l_c}{\mu A_c} \tag{1.13}$$

$$\mathcal{R}_g = \frac{g}{\mu_0 A_g} \tag{1.14}$$

and thus

$$\mathcal{F} = \phi(\mathcal{R}_c + \mathcal{R}_g) \tag{1.15}$$

Finally, Eq. 1.15 can be inverted to solve for the flux

$$\phi = \frac{\mathcal{F}}{\mathcal{R}_c + \mathcal{R}_g} \tag{1.16}$$

or

$$\phi = \frac{\mathcal{F}}{\frac{l_c}{\mu A_c} + \frac{g}{\mu_0 A_g}} \tag{1.17}$$

In general, for any magnetic circuit of total reluctance $\mathcal{R}_{tot}$, the flux can be found as

$$\phi = \frac{\mathcal{F}}{\mathcal{R}_{tot}} \tag{1.18}$$

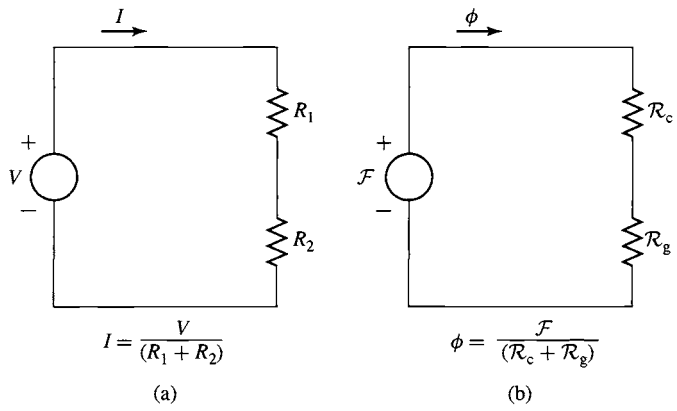

Figure 1.3 Analogy between electric and magnetic circuits. (a) Electric circuit, (b) magnetic circuit.

The term which multiplies the mmf is known as the *permeance* $\mathcal{P}$ and is the inverse of the reluctance; thus, for example, the total permeance of a magnetic circuit is

$$\mathcal{P}_{\text{tot}} = \frac{1}{\mathcal{R}_{\text{tot}}} \tag{1.19}$$

Note that Eqs. 1.15 and 1.16 are analogous to the relationships between the current and voltage in an electric circuit. This analogy is illustrated in Fig. 1.3. Figure 1.3a shows an electric circuit in which a voltage V drives a current I through resistors R_1 and R_2. Figure 1.3b shows the schematic equivalent representation of the magnetic circuit of Fig. 1.2. Here we see that the mmf $\mathcal{F}$ (analogous to voltage in the electric circuit) drives a flux ϕ (analogous to the current in the electric circuit) through the combination of the reluctances of the core $\mathcal{R}_c$ and the air gap $\mathcal{R}_g$. This analogy between the solution of electric and magnetic circuits can often be exploited to produce simple solutions for the fluxes in magnetic circuits of considerable complexity.

The fraction of the mmf required to drive flux through each portion of the magnetic circuit, commonly referred to as the *mmf drop* across that portion of the magnetic circuit, varies in proportion to its reluctance (directly analogous to the voltage drop across a resistive element in an electric circuit). From Eq. 1.13 we see that high material permeability can result in low core reluctance, which can often be made much smaller than that of the air gap; i.e., for $(\mu A_c/l_c) \gg (\mu_0 A_g/g)$, $\mathcal{R}_c \ll \mathcal{R}_g$ and thus $\mathcal{R}_{\text{tot}} \approx \mathcal{R}_g$. In this case, the reluctance of the core can be neglected and the flux and hence B can be found from Eq. 1.16 in terms of $\mathcal{F}$ and the air-gap properties alone:

$$\phi \approx \frac{\mathcal{F}}{\mathcal{R}_g} = \frac{\mathcal{F}\mu_0 A_g}{g} = Ni\,\frac{\mu_0 A_g}{g} \tag{1.20}$$

As will be seen in Section 1.3, practical magnetic materials have permeabilities which are not constant but vary with the flux level. From Eqs. 1.13 to 1.16 we see that as

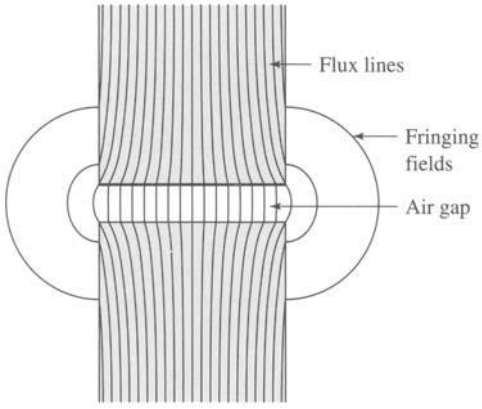

Figure 1.4 Air-gap fringing fields.

long as this permeability remains sufficiently large, its variation will not significantly affect the performance of the magnetic circuit.

In practical systems, the magnetic field lines "fringe" outward somewhat as they cross the air gap, as illustrated in Fig. 1.4. Provided this fringing effect is not excessive, the magnetic-circuit concept remains applicable. The effect of these *fringing fields* is to increase the effective cross-sectional area A_g of the air gap. Various empirical methods have been developed to account for this effect. A correction for such fringing fields in short air gaps can be made by adding the gap length to each of the two dimensions making up its cross-sectional area. In this book the effect of fringing fields is usually ignored. If fringing is neglected, $A_g = A_c$.

In general, magnetic circuits can consist of multiple elements in series and parallel. To complete the analogy between electric and magnetic circuits, we can generalize Eq. 1.5 as

$$\mathcal{F} = \oint \mathbf{H}d\mathbf{l} = \sum_k \mathcal{F}_k = \sum_k H_k l_k \tag{1.21}$$

where $\mathcal{F}$ is the mmf (total ampere-turns) acting to drive flux through a closed loop of a magnetic circuit,

$$\mathcal{F} = \int_S \mathbf{J} \cdot d\mathbf{a} \tag{1.22}$$

and $\mathcal{F}_k = H_k l_k$ is the *mmf drop* across the k'th element of that loop. This is directly analogous to Kirchoff's voltage law for electric circuits consisting of voltage sources and resistors

$$V = \sum_k R_k i_k \tag{1.23}$$

where V is the source voltage driving current around a loop and $R_k i_k$ is the voltage drop across the k'th resistive element of that loop.

Similarly, the analogy to Kirchoff's current law

$$\sum_n i_n = 0 \tag{1.24}$$

which says that the sum of currents into a node in an electric circuit equals zero is

$$\sum_n \phi_n = 0 \tag{1.25}$$

which states that the sum of the flux into a node in a magnetic circuit is zero.

We have now described the basic principles for reducing a magneto-quasistatic field problem with simple geometry to a *magnetic circuit model.* Our limited purpose in this section is to introduce some of the concepts and terminology used by engineers in solving practical design problems. We must emphasize that this type of thinking depends quite heavily on engineering judgment and intuition. For example, we have tacitly assumed that the permeability of the "iron" parts of the magnetic circuit is a constant known quantity, although this is not true in general (see Section 1.3), and that the magnetic field is confined soley to the core and its air gaps. Although this is a good assumption in many situations, it is also true that the winding currents produce magnetic fields outside the core. As we shall see, when two or more windings are placed on a magnetic circuit, as happens in the case of both transformers and rotating machines, these fields outside the core, which are referred to as *leakage fields,* cannot be ignored and significantly affect the performance of the device.

EXAMPLE 1.1

The magnetic circuit shown in Fig. 1.2 has dimensions $A_c = A_g = 9\ \text{cm}^2$, $g = 0.050$ cm, $l_c = 30$ cm, and $N = 500$ turns. Assume the value $\mu_r = 70{,}000$ for core material. (*a*) Find the reluctances $\mathcal{R}_c$ and $\mathcal{R}_g$. For the condition that the magnetic circuit is operating with $B_c = 1.0$ T, find (*b*) the flux ϕ and (*c*) the current i.

■ Solution

a. The reluctances can be found from Eqs. 1.13 and 1.14:

$$\mathcal{R}_c = \frac{l_c}{\mu_r \mu_0 A_c} = \frac{0.3}{70{,}000\,(4\pi \times 10^{-7})(9 \times 10^{-4})} = 3.79 \times 10^3 \ \frac{\text{A} \cdot \text{turns}}{\text{Wb}}$$

$$\mathcal{R}_g = \frac{g}{\mu_0 A_g} = \frac{5 \times 10^{-4}}{(4\pi \times 10^{-7})(9 \times 10^{-4})} = 4.42 \times 10^5 \ \frac{\text{A} \cdot \text{turns}}{\text{Wb}}$$

b. From Eq. 1.4,

$$\phi = B_c A_c = 1.0(9 \times 10^{-4}) = 9 \times 10^{-4}\ \text{Wb}$$

c. From Eqs. 1.6 and 1.15,

$$i = \frac{\mathcal{F}}{N} = \frac{\phi(\mathcal{R}_c + \mathcal{R}_g)}{N} = \frac{9 \times 10^{-4}(4.46 \times 10^5)}{500} = 0.80\ \text{A}$$

Practice Problem 1.1

Find the flux ϕ and current for Example 1.1 if (*a*) the number of turns is doubled to $N = 1000$ turns while the circuit dimensions remain the same and (*b*) if the number of turns is equal to $N = 500$ and the gap is reduced to 0.040 cm.

Solution

a. $\phi = 9 \times 10^{-4}$ Wb and $i = 0.40$ A
b. $\phi = 9 \times 10^{-4}$ Wb and $i = 0.64$ A

EXAMPLE 1.2

The magnetic structure of a synchronous machine is shown schematically in Fig. 1.5. Assuming that rotor and stator iron have infinite permeability ($\mu \to \infty$), find the air-gap flux ϕ and flux density B_g. For this example $I = 10$ A, $N = 1000$ turns, $g = 1$ cm, and $A_g = 2000$ cm^2.

■ Solution

Notice that there are two air gaps in series, of total length $2g$, and that by symmetry the flux density in each is equal. Since the iron permeability here is assumed to be infinite, its reluctance is negligible and Eq. 1.20 (with g replaced by the total gap length $2g$) can be used to find the flux

$$\phi = \frac{NI\mu_0 A_g}{2g} = \frac{1000(10)(4\pi \times 10^{-7})(0.2)}{0.02} = 0.13 \text{ Wb}$$

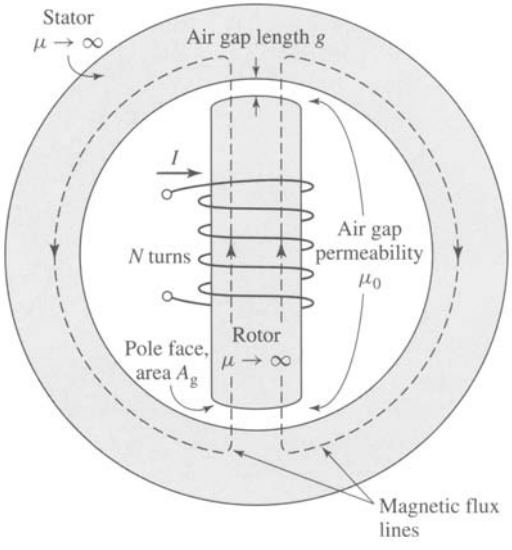

Figure 1.5 Simple synchronous machine.

and

$$B_g = \frac{\phi}{A_g} = \frac{0.13}{0.2} = 0.65\ \text{T}$$

Practice Problem 1.2

For the magnetic structure of Fig. 1.5 with the dimensions as given in Example 1.2, the air-gap flux density is observed to be $B_g = 0.9$ T. Find the air-gap flux ϕ and, for a coil of $N = 500$ turns, the current required to produce this level of air-gap flux.

Solution

$\phi = 0.18$ Wb and $i = 28.6$ A.

1.2 FLUX LINKAGE, INDUCTANCE, AND ENERGY

When a magnetic field varies with time, an electric field is produced in space as determined by *Faraday's law:*

$$\oint_C \mathbf{E} \cdot \mathbf{ds} = -\frac{d}{dt} \int_S \mathbf{B} \cdot \mathbf{da} \tag{1.26}$$

Equation 1.26 states that the line integral of the *electric field intensity* **E** around a closed contour C is equal to the time rate of change of the magnetic flux linking (i.e. passing through) that contour. In magnetic structures with windings of high electrical conductivity, such as in Fig. 1.2, it can be shown that the **E** field in the wire is extremely small and can be neglected, so that the left-hand side of Eq. 1.26 reduces to the negative of the *induced voltage*[4] e at the winding terminals. In addition, the flux on the right-hand side of Eq. 1.26 is dominated by the core flux ϕ. Since the winding (and hence the contour C) links the core flux N times, Eq. 1.26 reduces to

$$e = N\frac{d\varphi}{dt} = \frac{d\lambda}{dt} \tag{1.27}$$

where λ is the *flux linkage* of the winding and is defined as

$$\lambda = N\varphi \tag{1.28}$$

Flux linkage is measured in units of webers (or equivalently weber-turns). The symbol φ is used to indicate the instantaneous value of a time-varying flux.

In general the flux linkage of a coil is equal to the surface integral of the normal component of the magnetic flux density integrated over any surface spanned by that coil. Note that the direction of the induced voltage e is defined by Eq. 1.26 so that if

[4] The term *electromotive force* (emf) is often used instead of *induced voltage* to represent that component of voltage due to a time-varying flux linkage.

the winding terminals were short-circuited, a current would flow in such a direction as to oppose the change of flux linkage.

For a magnetic circuit composed of magnetic material of constant magnetic permeability or which includes a dominating air gap, the relationship between ϕ and i will be linear and we can define the *inductance* L as

$$L = \frac{\lambda}{i} \tag{1.29}$$

Substitution of Eqs. 1.5, 1.18 and 1.28 into Eq. 1.29 gives

$$L = \frac{N^2}{\mathcal{R}_{\text{tot}}} \tag{1.30}$$

From which we see that the inductance of a winding in a magnetic circuit is proportional to the square of the turns and inversely proportional to the reluctance of the magnetic circuit associated with that winding.

For example, from Eq. 1.20, under the assumption that the reluctance of the core is negligible as compared to that of the air gap, the inductance of the winding in Fig. 1.2 is equal to

$$L = \frac{N^2}{(g/\mu_0 A_g)} = \frac{N^2 \mu_0 A_g}{g} \tag{1.31}$$

Inductance is measured in *henrys* (H) or *weber-turns per ampere*. Equation 1.31 shows the dimensional form of expressions for inductance; inductance is proportional to the square of the number of turns, to a magnetic permeability, and to a cross-sectional area and is inversely proportional to a length. It must be emphasized that, strictly speaking, the concept of inductance requires a linear relationship between flux and mmf. Thus, it cannot be rigorously applied in situations where the nonlinear characteristics of magnetic materials, as is discussed in Sections 1.3 and 1.4, dominate the performance of the magnetic system. However, in many situations of practical interest, the reluctance of the system is dominated by that of an air gap (which is of course linear) and the nonlinear effects of the magnetic material can be ignored. In other cases it may be perfectly acceptable to assume an average value of magnetic permeability for the core material and to calculate a corresponding average inductance which can be used for calculations of reasonable engineering accuracy. Example 1.3 illustrates the former situation and Example 1.4 the latter.

EXAMPLE 1.3

The magnetic circuit of Fig. 1.6a consists of an N-turn winding on a magnetic core of infinite permeability with two parallel air gaps of lengths g_1 and g_2 and areas A_1 and A_2, respectively.

Find (*a*) the inductance of the winding and (*b*) the flux density B_1 in gap 1 when the winding is carrying a current i. Neglect fringing effects at the air gap.

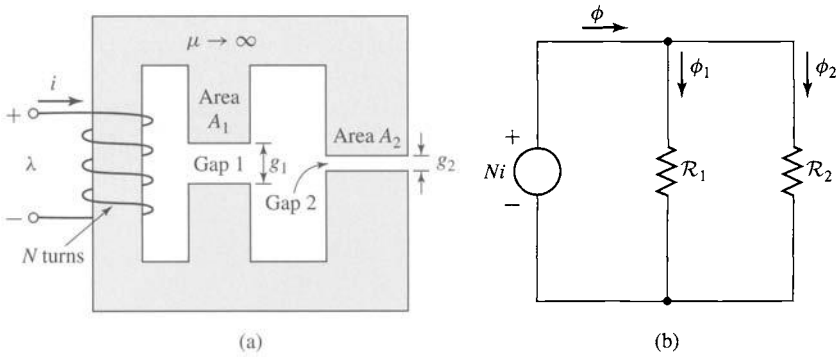

Figure 1.6 (a) Magnetic circuit and (b) equivalent circuit for Example 1.3.

■ Solution

a. The equivalent circuit of Fig. 1.6b shows that the total reluctance is equal to the parallel combination of the two gap reluctances. Thus

$$\phi = \frac{Ni}{\frac{\mathcal{R}_1\mathcal{R}_2}{\mathcal{R}_1+\mathcal{R}_2}}$$

where

$$\mathcal{R}_1 = \frac{g_1}{\mu_0 A_1} \qquad \mathcal{R}_2 = \frac{g_2}{\mu_0 A_2}$$

From Eq. 1.29,

$$L = \frac{\lambda}{i} = \frac{N\phi}{i} = \frac{N^2(\mathcal{R}_1 + \mathcal{R}_2)}{\mathcal{R}_1\mathcal{R}_2}$$

$$= \mu_0 N^2 \left(\frac{A_1}{g_1} + \frac{A_2}{g_2} \right)$$

b. From the equivalent circuit, one can see that

$$\phi_1 = \frac{Ni}{\mathcal{R}_1} = \frac{\mu_0 A_1 N i}{g_1}$$

and thus

$$B_1 = \frac{\phi_1}{A_1} = \frac{\mu_0 N i}{g_1}$$

EXAMPLE 1.4

In Example 1.1, the relative permeability of the core material for the magnetic circuit of Fig. 1.2 is assumed to be $\mu_r = 70{,}000$ at a flux density of 1.0 T.

a. For this value of μ_r calculate the inductance of the winding.
b. In a practical device, the core would be constructed from electrical steel such as M-5

electrical steel which is discussed in Section 1.3. This material is highly nonlinear and its relative permeability (defined for the purposes of this example as the ratio B/H) varies from a value of approximately $\mu_r = 72{,}300$ at a flux density of $B = 1.0$ T to a value of on the order of $\mu_r = 2900$ as the flux density is raised to 1.8 T. (a) Calculate the inductance under the assumption that the relative permeability of the core steel is 72,300. (b) Calculate the inductance under the assumption that the relative permeability is equal to 2900.

■ Solution

a. From Eqs. 1.13 and 1.14 and based upon the dimensions given in Example 1.1,

$$\mathcal{R}_c = \frac{l_c}{\mu_r \mu_0 A_c} = \frac{0.3}{72{,}300\,(4\pi \times 10^{-7})(9 \times 10^{-4})} = 3.67 \times 10^3\ \frac{\text{A} \cdot \text{turns}}{\text{Wb}}$$

while $\mathcal{R}_g$ remains unchanged from the value calculated in Example 1.1 as $\mathcal{R}_g = 4.42 \times 10^5$ A · turns / Wb.

Thus the total reluctance of the core and gap is

$$\mathcal{R}_{tot} = \mathcal{R}_c + \mathcal{R}_g = 4.46 \times 10^5\ \frac{\text{A} \cdot \text{turns}}{\text{Wb}}$$

and hence from Eq. 1.30

$$L = \frac{N^2}{\mathcal{R}_{tot}} = \frac{500^2}{4.46 \times 10^5} = 0.561\ \text{H}$$

b. For $\mu_r = 2900$, the reluctance of the core increases from a value of 3.79×10^3 A · turns / Wb to a value of

$$\mathcal{R}_c = \frac{l_c}{\mu_r \mu_0 A_c} = \frac{0.3}{2900\,(4\pi \times 10^{-7})(9 \times 10^{-4})} = 9.15 \times 10^4\ \frac{\text{A} \cdot \text{turns}}{\text{Wb}}$$

and hence the total reluctance increases from 4.46×10^5 A · turns / Wb to 5.34×10^5 A · turns / Wb. Thus from Eq. 1.30 the inductance decreases from 0.561 H to

$$L = \frac{N^2}{\mathcal{R}_{tot}} = \frac{500^2}{5.34 \times 10^5} = 0.468\ \text{H}$$

This example illustrates the linearizing effect of a dominating air gap in a magnetic circuit. In spite of a reduction in the permeablity of the iron by a factor of $72{,}300/2900 = 25$, the inductance decreases only by a factor of $0.468/0.561 = 0.83$ simply because the reluctance of the air gap is significantly larger than that of the core. In many situations, it is common to assume the inductance to be constant at a value corresponding to a finite, constant value of core permeability (or in many cases it is assumed simply that $\mu_r \to \infty$). Analyses based upon such a representation for the inductor will often lead to results which are well within the range of acceptable engineering accuracy and which avoid the immense complication associated with modeling the nonlinearity of the core material.

Practice Problem 1.3

Repeat the inductance calculation of Example 1.4 for a relative permeability $\mu_r = 30{,}000$.

Solution

$L = 0.554$ H

EXAMPLE 1.5

Using MATLAB,† plot the inductance of the magnetic circuit of Example 1.1 and Fig. 1.2 as a function of core permeability over the range $100 \leq \mu_r \leq 100{,}000$.

■ Solution

Here is the MATLAB script:

```
clc
clear
% Permeability of free space
mu0 = pi*4.e-7;
%All dimensions expressed in meters
Ac = 9e-4; Ag = 9e-4; g = 5e-4; lc = 0.3;
N = 500;
%Reluctance of air gap
Rg = g/(mu0*Ag);
for n = 1:101
mur(n) = 100 + (100000 - 100)*(n-1)/100;
%Reluctance of core
Rc(n) = lc/(mur(n)*mu0*Ac);
Rtot = Rg+Rc(n);
%Inductance
L(n) = N^2/Rtot;
end
plot(mur,L)
xlabel('Core relative permeability')
ylabel('Inductance [H]')
```

The resultant plot is shown in Fig. 1.7. Note that the figure clearly confirms that, for the magnetic circuit of this example, the inductance is quite insensitive to relative permeability until the relative permeability drops to on the order of 1000. Thus, as long as the effective relative permeability of the core is "large" (in this case greater than 1000), any nonlinearities in the properties of the core material will have little effect on the terminal properties of the inductor.

† MATLAB is a registered trademark of The MathWorks, Inc.

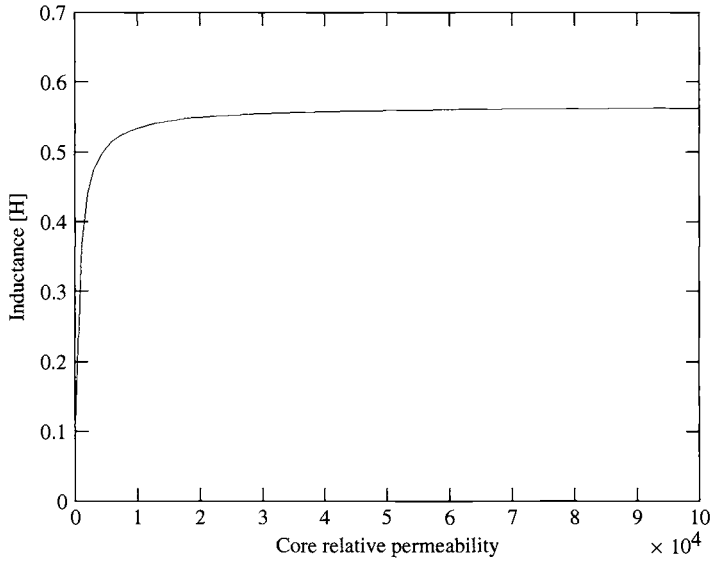

Figure 1.7 MATLAB plot of inductance vs. relative permeability for Example 1.5.

Practice Problem 1.4

Write a MATLAB script to plot the inductance of the magnetic circuit of Example 1.1 with $\mu_r = 70{,}000$ as a function of air-gap length as the the air-gap is varied from 0.01 cm to 0.10 cm.

Figure 1.8 shows a magnetic circuit with an air gap and two windings. In this case note that the mmf acting on the magnetic circuit is given by the *total ampere-turns* acting on the magnetic circuit (i.e., the net ampere turns of both windings) and that the reference directions for the currents have been chosen to produce flux in the same direction. The total mmf is therefore

$$\mathcal{F} = N_1 i_1 + N_2 i_2 \tag{1.32}$$

and from Eq. 1.20, with the reluctance of the core neglected and assuming that $A_c = A_g$, the core flux ϕ is

$$\phi = (N_1 i_1 + N_2 i_2)\frac{\mu_0 A_c}{g} \tag{1.33}$$

In Eq. 1.33, ϕ is the *resultant core flux* produced by the total mmf of the two windings. It is this resultant ϕ which determines the operating point of the core material.

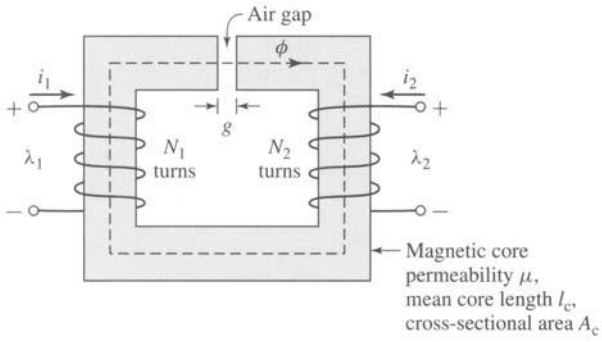

Figure 1.8 Magnetic circuit with two windings.

If Eq. 1.33 is broken up into terms attributable to the individual currents, the resultant flux linkages of coil 1 can be expressed as

$$\lambda_1 = N_1\phi = N_1^2\left(\frac{\mu_0 A_c}{g}\right)i_1 + N_1N_2\left(\frac{\mu_0 A_c}{g}\right)i_2 \tag{1.34}$$

which can be written

$$\lambda_1 = L_{11}i_1 + L_{12}i_2 \tag{1.35}$$

where

$$L_{11} = N_1^2\frac{\mu_0 A_c}{g} \tag{1.36}$$

is the *self-inductance* of coil 1 and $L_{11}i_1$ is the flux linkage of coil 1 due to its own current i_l. The *mutual inductance* between coils 1 and 2 is

$$L_{12} = N_1N_2\frac{\mu_0 A_c}{g} \tag{1.37}$$

and $L_{12}i_2$ is the flux linkage of coil 1 due to current i_2 in the other coil. Similarly, the flux linkage of coil 2 is

$$\lambda_2 = N_2\phi = N_1N_2\left(\frac{\mu_0 A_c}{g}\right)i_1 + N_2^2\left(\frac{\mu_0 A_c}{g}\right)i_2 \tag{1.38}$$

or

$$\lambda_2 = L_{21}i_1 + L_{22}i_2 \tag{1.39}$$

where $L_{21} = L_{12}$ is the mutual inductance and

$$L_{22} = N_2^2\frac{\mu_0 A_c}{g} \tag{1.40}$$

is the self-inductance of coil 2.

It is important to note that the resolution of the resultant flux linkages into the components produced by i_l and i_2 is based on superposition of the individual effects and therefore implies a linear flux-mmf relationship (characteristic of materials of constant permeability).

Substitution of Eq. 1.29 in Eq. 1.27 yields

$$e = \frac{d}{dt}(Li) \tag{1.41}$$

for a magnetic circuit with a single winding. For a static magnetic circuit, the inductance is fixed (assuming that material nonlinearities do not cause the inductance to vary), and this equation reduces to the familiar circuit-theory form

$$e = L\frac{di}{dt} \tag{1.42}$$

However, in electromechanical energy conversion devices, inductances are often time-varying, and Eq. 1.41 must be written as

$$e = L\frac{di}{dt} + i\frac{dL}{dt} \tag{1.43}$$

Note that in situations with multiple windings, the total flux linkage of each winding must be used in Eq. 1.27 to find the winding-terminal voltage.

The power at the terminals of a winding on a magnetic circuit is a measure of the rate of energy flow into the circuit through that particular winding. The *power, p,* is determined from the product of the voltage and the current

$$p = ie = i\frac{d\lambda}{dt} \tag{1.44}$$

and its unit is *watts* (W), or *joules per second.* Thus the change in *magnetic stored energy* ΔW in the magnetic circuit in the time interval t_1 to t_2 is

$$\Delta W = \int_{t_1}^{t_2} p\,dt = \int_{\lambda_1}^{\lambda_2} i\,d\lambda \tag{1.45}$$

In SI units, the magnetic stored energy W is measured in *joules* (J).

For a single-winding system of constant inductance, the change in magnetic stored energy as the flux level is changed from λ_1 to λ_2 can be written as

$$\Delta W = \int_{\lambda_1}^{\lambda_2} i\,d\lambda = \int_{\lambda_1}^{\lambda_2} \frac{\lambda}{L}\,d\lambda = \frac{1}{2L}(\lambda_2^2 - \lambda_1^2) \tag{1.46}$$

The total magnetic stored energy at any given value of λ can be found from setting λ_1 equal to zero:

$$W = \frac{1}{2L}\lambda^2 = \frac{L}{2}i^2 \tag{1.47}$$

EXAMPLE 1.6

For the magnetic circuit of Example 1.1 (Fig. 1.2), find (*a*) the inductance L, (*b*) the magnetic stored energy W for $B_c = 1.0$ T, and (*c*) the induced voltage e for a 60-Hz time-varying core flux of the form $B_c = 1.0 \sin \omega t$ T where $\omega = (2\pi)(60) = 377$.

■ Solution

a. From Eqs. 1.16 and 1.29 and Example 1.1,

$$L = \frac{\lambda}{i} = \frac{N\phi}{i} = \frac{N^2}{\mathcal{R}_c + \mathcal{R}_g}$$

$$= \frac{500^2}{4.46 \times 10^5} = 0.56 \text{ H}$$

Note that the core reluctance is much smaller than that of the gap ($\mathcal{R}_c \ll \mathcal{R}_g$). Thus to a good approximation the inductance is dominated by the gap reluctance, i.e.,

$$L \approx \frac{N^2}{\mathcal{R}_g} = 0.57 \text{ H}$$

b. In Example 1.1 we found that when $B_c = 1.0$ T, $i = 0.80$A. Thus from Eq. 1.47,

$$W = \frac{1}{2}Li^2 = \frac{1}{2}(0.56)(0.80)^2 = 0.18 \text{ J}$$

c. From Eq. 1.27 and Example 1.1,

$$e = \frac{d\lambda}{dt} = N\frac{d\varphi}{dt} = NA_c\frac{dB_c}{dt}$$

$$= 500 \times (9 \times 10^{-4}) \times (377 \times 1.0 \cos(377t))$$

$$= 170 \cos(377t) \quad V$$

Practice Problem 1.5

Repeat Example 1.6 for $B_c = 0.8$ T, assuming the core flux varies at 50 Hz instead of 60 Hz.

Solution

a. The inductance L is unchanged.
b. W = 0.115 J
c. $e = 113 \cos(314t)$ V

1.3 PROPERTIES OF MAGNETIC MATERIALS

In the context of electromechanical energy conversion devices, the importance of magnetic materials is twofold. Through their use it is possible to obtain large magnetic flux densities with relatively low levels of magnetizing force. Since magnetic forces and energy density increase with increasing flux density, this effect plays a large role in the performance of energy-conversion devices.

In addition, magnetic materials can be used to constrain and direct magnetic fields in well-defined paths. In a transformer they are used to maximize the coupling between the windings as well as to lower the excitation current required for transformer operation. In electric machinery, magnetic materials are used to shape the fields to obtain desired torque-production and electrical terminal characteristics. Thus a knowledgeable designer can use magnetic materials to achieve specific desirable device characteristics.

Ferromagnetic materials, typically composed of iron and alloys of iron with cobalt, tungsten, nickel, aluminum, and other metals, are by far the most common magnetic materials. Although these materials are characterized by a wide range of properties, the basic phenomena responsible for their properties are common to them all.

Ferromagnetic materials are found to be composed of a large number of domains, i.e., regions in which the magnetic moments of all the atoms are parallel, giving rise to a net magnetic moment for that domain. In an unmagnetized sample of material, the domain magnetic moments are randomly oriented, and the net resulting magnetic flux in the material is zero.

When an external magnetizing force is applied to this material, the domain magnetic moments tend to align with the applied magnetic field. As a result, the domain magnetic moments add to the applied field, producing a much larger value of flux density than would exist due to the magnetizing force alone. Thus the *effective permeability* μ, equal to the ratio of the total magnetic flux density to the applied magnetic-field intensity, is large compared with the permeability of free space μ_0. As the magnetizing force is increased, this behavior continues until all the magnetic moments are aligned with the applied field; at this point they can no longer contribute to increasing the magnetic flux density, and the material is said to be fully *saturated.*

In the absence of an externally applied magnetizing force, the domain magnetic moments naturally align along certain directions associated with the crystal structure of the domain, known as *axes of easy magnetization.* Thus if the applied magnetizing force is reduced, the domain magnetic moments relax to the direction of easy magnetism nearest to that of the applied field. As a result, when the applied field is reduced to zero, although they will tend to relax towards their initial orientation, the magnetic dipole moments will no longer be totally random in their orientation; they will retain a net magnetization component along the applied field direction. It is this effect which is responsible for the phenomenon known as *magnetic hysteresis.*

Due to this hystersis effect, the relationship between B and H for a ferromagnetic material is both nonlinear and multivalued. In general, the characteristics of the material cannot be described analytically. They are commonly presented in graphical form as a set of empirically determined curves based on test samples of the material using methods prescribed by the American Society for Testing and Materials (ASTM).[5]

---

[5] Numerical data on a wide variety of magnetic materials are available from material manufacturers. One problem in using such data arises from the various systems of units employed. For example, magnetization may be given in oersteds or in ampere-turns per meter and the magnetic flux density in gauss, kilogauss, or teslas. A few useful conversion factors are given in Appendix E. The reader is reminded that the equations in this book are based upon SI units.

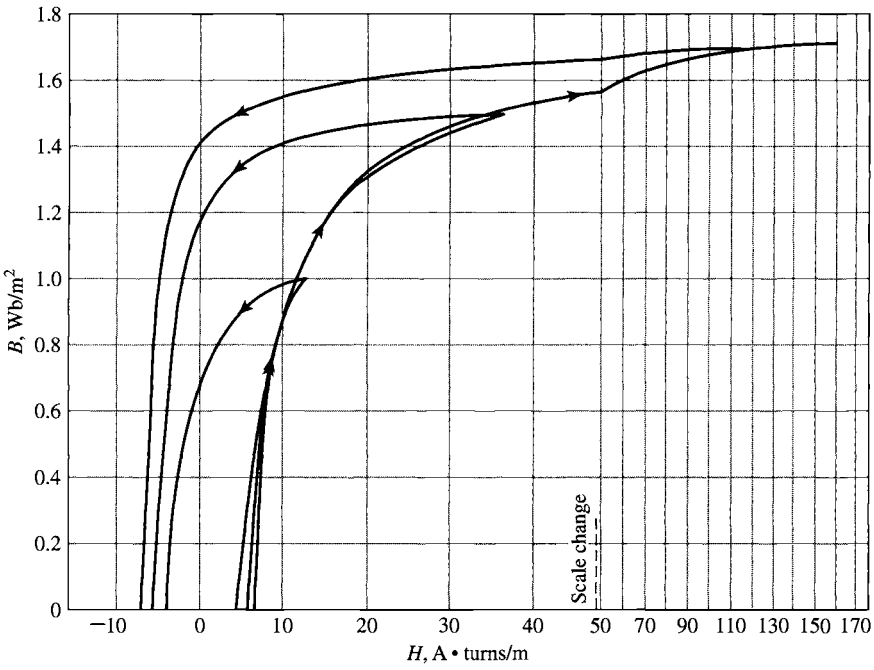

Figure 1.9 *B-H* loops for M-5 grain-oriented electrical steel 0.012 in thick. Only the top halves of the loops are shown here. (*Armco Inc.*)

The most common curve used to describe a magnetic material is the *B-H curve* or *hysteresis loop*. The first and second quadrants (corresponding to $B \geq 0$) of a set of hysteresis loops are shown in Fig. 1.9 for M-5 steel, a typical grain-oriented electrical steel used in electric equipment. These loops show the relationship between the magnetic flux density B and the magnetizing force H. Each curve is obtained while cyclically varying the applied magnetizing force between equal positive and negative values of fixed magnitude. Hysteresis causes these curves to be multivalued. After several cycles the *B-H* curves form closed loops as shown. The arrows show the paths followed by B with increasing and decreasing H. Notice that with increasing magnitude of H the curves begin to flatten out as the material tends toward saturation. At a flux density of about 1.7 T, this material can be seen to be heavily saturated.

Notice that as H is decreased from its maximum value to zero, the flux density decreases but not to zero. This is the result of the relaxation of the orientation of the magnetic moments of the domains as described above. The result is that there remains a *remanant magnetization* when H is zero.

Fortunately, for many engineering applications, it is sufficient to describe the material by a single-valued curve obtained by plotting the locus of the maximum values of B and H at the tips of the hysteresis loops; this is known as a *dc* or *normal magnetization curve*. A dc magnetization curve for M-5 grain-oriented electrical steel

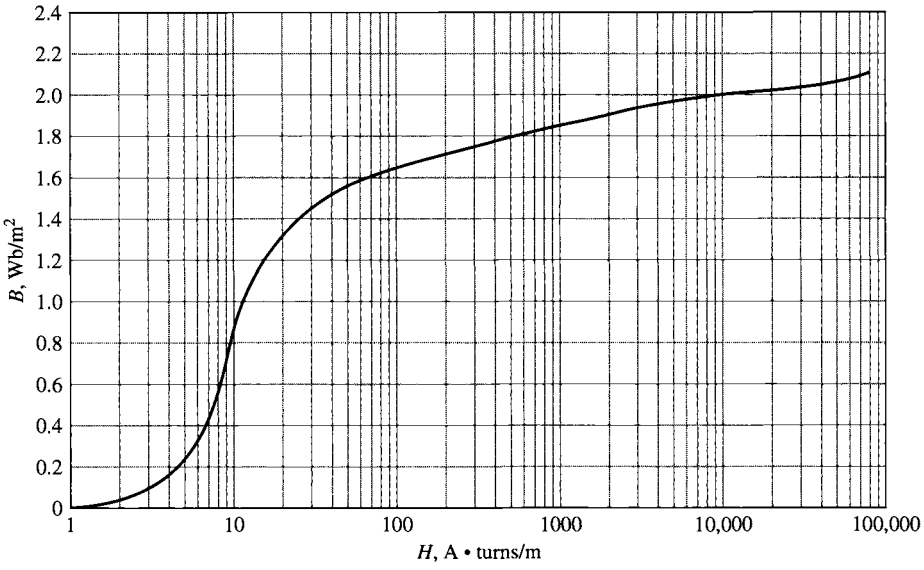

Figure 1.10 Dc magnetization curve for M-5 grain-oriented electrical steel 0.012 in thick. (*Armco Inc.*)

is shown in Fig. 1.10. The dc magnetization curve neglects the hysteretic nature of the material but clearly displays its nonlinear characteristics.

EXAMPLE 1.7

Assume that the core material in Example 1.1 is M-5 electrical steel, which has the dc magnetization curve of Fig. 1.10. Find the current i required to produce $B_c = 1$ T.

■ Solution

The value of H_c for $B_c = 1$ T is read from Fig. 1.10 as

$$H_c = 11 \text{ A} \cdot \text{turns/m}$$

The mmf drop for the core path is

$$\mathcal{F}_c = H_c l_c = 11(0.3) = 3.3 \text{ A} \cdot \text{turns}$$

The mmf drop across the air gap is

$$\mathcal{F}_g = H_g g = \frac{B_g g}{\mu_0} = \frac{5 \times 10^{-4}}{4\pi \times 10^{-7}} = 396 \text{ A} \cdot \text{turns}$$

The required current is

$$i = \frac{\mathcal{F}_c + \mathcal{F}_g}{N} = \frac{399}{500} = 0.80 \text{ A}$$

Practice Problem 1.6

Repeat Example 1.7 but find the current i for $B_c = 1.6$ T. By what factor does the current have to be increased to result in this factor of 1.6 increase in flux density?

Solution

The current i can be shown to be 1.302 A. Thus, the current must be increased by a factor of $1.302/0.8 = 1.63$. Because of the dominance of the air-gap reluctance, this is just slightly in excess of the fractional increase in flux density in spite of the fact that the core is beginning to significantly saturate at a flux density of 1.6 T.

1.4 AC EXCITATION

In ac power systems, the waveforms of voltage and flux closely approximate sinusoidal functions of time. This section describes the excitation characteristics and losses associated with steady-state ac operation of magnetic materials under such operating conditions. We use as our model a closed-core magnetic circuit, i.e., with no air gap, such as that shown in Fig. 1.1 or the transformer of Fig. 2.4. The magnetic path length is l_c, and the cross-sectional area is A_c throughout the length of the core. We further assume a sinusoidal variation of the core flux $\varphi(t)$; thus

$$\varphi(t) = \phi_{max} \sin \omega t = A_c B_{max} \sin \omega t \tag{1.48}$$

where ϕ_{max} = amplitude of core flux φ in webers
B_{max} = amplitude of flux density B_c in teslas
ω = angular frequency = $2\pi f$
f = frequency in Hz

From Eq. 1.27, the voltage induced in the N-turn winding is

$$e(t) = \omega N \phi_{max} \cos(\omega t) = E_{max} \cos \omega t \tag{1.49}$$

where

$$E_{max} = \omega N \phi_{max} = 2\pi f N A_c B_{max} \tag{1.50}$$

In steady-state ac operation, we are usually more interested in the *root-mean-square* or *rms* values of voltages and currents than in instantaneous or maximum values. In general, the rms value of a periodic function of time, $f(t)$, of period T is defined as

$$F_{rms} = \sqrt{\left(\frac{1}{T}\int_0^T f^2(t)\,dt\right)} \tag{1.51}$$

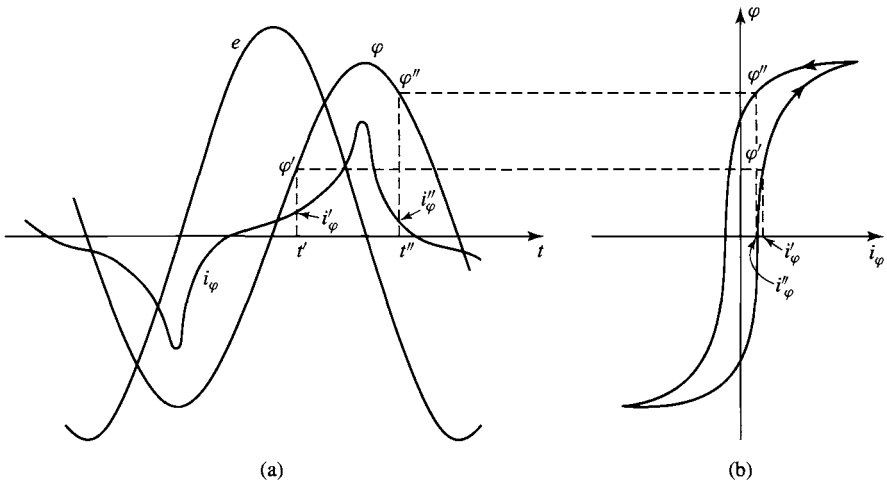

Figure 1.11 Excitation phenomena. (a) Voltage, flux, and exciting current; (b) corresponding hysteresis loop.

From Eq. 1.51, the rms value of a sine wave can be shown to be $1/\sqrt{2}$ times its peak value. Thus the rms value of the induced voltage is

$$E_{\text{rms}} = \frac{2\pi}{\sqrt{2}} f N A_c B_{\max} = \sqrt{2}\pi f N A_c B_{\max} \tag{1.52}$$

To produce magnetic flux in the core requires current in the exciting winding known as the *exciting current,* i_φ.[6] The nonlinear magnetic properties of the core require that the waveform of the exciting current differs from the sinusoidal waveform of the flux. A curve of the exciting current as a function of time can be found graphically from the magnetic characteristics of the core material, as illustrated in Fig. 1.11a. Since B_c and H_c are related to φ and i_φ by known geometric constants, the ac hysteresis loop of Fig. 1.11b has been drawn in terms of $\varphi = B_c A_c$ and is $i_\varphi = H_c l_c / N$. Sine waves of induced voltage, e, and flux, φ, in accordance with Eqs. 1.48 and 1.49, are shown in Fig. 1.11a.

At any given time, the value of i_φ corresponding to the given value of flux can be found directly from the hysteresis loop. For example, at time t' the flux is φ' and the current is i'_φ; at time t'' the corresponding values are φ'' and i''_φ. Notice that since the hysteresis loop is multivalued, it is necessary to be careful to pick the rising-flux values (φ' in the figure) from the rising-flux portion of the hysteresis loop; similarly the falling-flux portion of the hysteresis loop must be selected for the falling-flux values (φ'' in the figure).

[6] More generally, for a system with multiple windings, the exciting mmf is the net ampere-turns acting to produce flux in the magnetic circuit.

Notice that, because the hysteresis loop "flattens out" due to saturation effects, the waveform of the exciting current is sharply peaked. Its rms value $I_{\varphi,\text{rms}}$ is defined by Eq. 1.51, where T is the period of a cycle. It is related to the corresponding rms value $H_{\text{c,rms}}$ of H_{c} by the relationship

$$I_{\varphi,\text{rms}} = \frac{l_{\text{c}} H_{\text{c,rms}}}{N} \tag{1.53}$$

The ac excitation characteristics of core materials are often described in terms of rms voltamperes rather than a magnetization curve relating B and H. The theory behind this representation can be explained by combining Eqs. 1.52 and 1.53. Thus, from Eqs. 1.52 and 1.53, the rms voltamperes required to excite the core of Fig. 1.1 to a specified flux density is equal to

$$\begin{aligned} E_{\text{rms}} I_{\varphi,\text{rms}} &= \sqrt{2}\pi f N A_{\text{c}} B_{\text{max}} \frac{l_{\text{c}} H_{\text{rms}}}{N} \\ &= \sqrt{2}\pi f B_{\text{max}} H_{\text{rms}} (A_{\text{c}} l_{\text{c}}) \end{aligned} \tag{1.54}$$

In Eq. 1.54, the product $A_{\text{c}} l_{\text{c}}$ can be seen to be equal to the volume of the core and hence the rms exciting voltamperes required to excite the core with sinusoidal can be seen to be proportional to the frequency of excitation, the core volume and the product of the peak flux density and the rms magnetic field intensity. For a magnetic material of mass density ρ_{c}, the mass of the core is $A_{\text{c}} l_{\text{c}} \rho_{\text{c}}$ and the *exciting rms voltamperes per unit mass,* P_a, can be expressed as

$$P_a = \frac{E_{\text{rms}} I_{\varphi,\text{rms}}}{\text{mass}} = \frac{\sqrt{2}\pi f}{\rho_{\text{c}}} B_{\text{max}} H_{\text{rms}} \tag{1.55}$$

Note that, normalized in this fashion, the rms exciting voltamperes can be seen to be a property of the material alone. In addition, note that they depend only on B_{max} because H_{rms} is a unique function of B_{max} as determined by the shape of the material hysteresis loop at any given frequency f. As a result, the ac excitation requirements for a magnetic material are often supplied by manufacturers in terms of rms voltamperes per unit weight as determined by laboratory tests on closed-core samples of the material. These results are illustrated in Fig. 1.12 for M-5 grain-oriented electrical steel.

The exciting current supplies the mmf required to produce the core flux and the power input associated with the energy in the magnetic field in the core. Part of this energy is dissipated as losses and results in heating of the core. The rest appears as reactive power associated with energy storage in the magnetic field. This reactive power is not dissipated in the core; it is cyclically supplied and absorbed by the excitation source.

Two loss mechanisms are associated with time-varying fluxes in magnetic materials. The first is ohmic I^2R heating, associated with induced currents in the core material. From Faraday's law (Eq. 1.26) we see that time-varying magnetic fields give rise to electric fields. In magnetic materials these electric fields result in induced

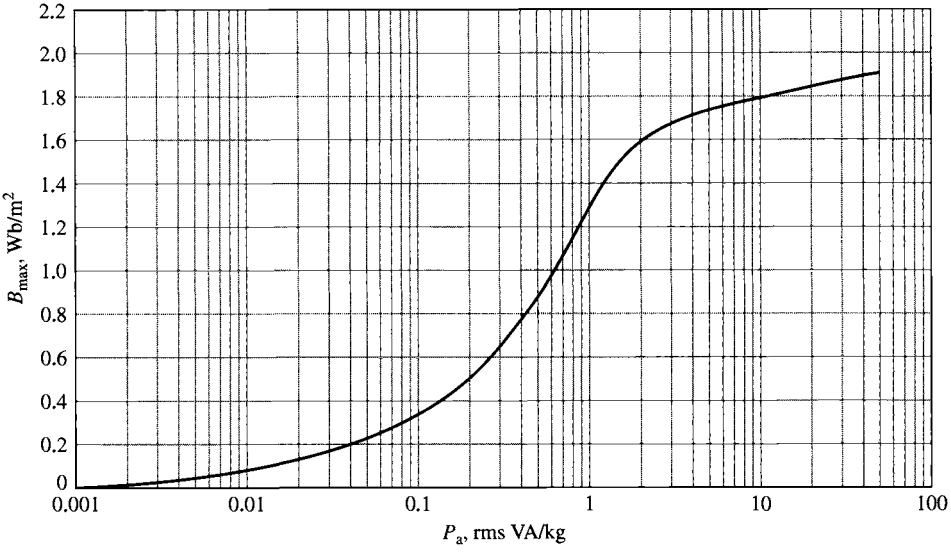

Figure 1.12 Exciting rms voltamperes per kilogram at 60 Hz for M-5 grain-oriented electrical steel 0.012 in thick. (*Armco Inc.*)

currents, commonly referred to as *eddy currents,* which circulate in the core material and oppose changes in flux density in the material. To counteract the corresponding demagnetizing effect, the current in the exciting winding must increase. Thus the resultant "dynamic" B-H loop under ac operation is somewhat "fatter" than the hysteresis loop for slowly varying conditions, and this effect increases as the excitation frequency is increased. It is for this reason that the characteristics of electrical steels vary with frequency and hence manufacturers typically supply characteristics over the expected operating frequency range of a particular electrical steel. Note for example that the exciting rms voltamperes of Fig. 1.12 are specified at a frequency of 60 Hz.

To reduce the effects of eddy currents, magnetic structures are usually built of thin sheets of laminations of the magnetic material. These laminations, which are aligned in the direction of the field lines, are insulated from each other by an oxide layer on their surfaces or by a thin coat of insulating enamel or varnish. This greatly reduces the magnitude of the eddy currents since the layers of insulation interrupt the current paths; the thinner the laminations, the lower the losses. In general, eddy-current loss tends to increase as the square of the excitation frequency and also as the square of the peak flux density.

The second loss mechanism is due to the hysteretic nature of magnetic material. In a magnetic circuit like that of Fig. 1.1 or the transformer of Fig. 2.4, a time-varying excitation will cause the magnetic material to undergo a cyclic variation described by a hysteresis loop such as that shown in Fig. 1.13.

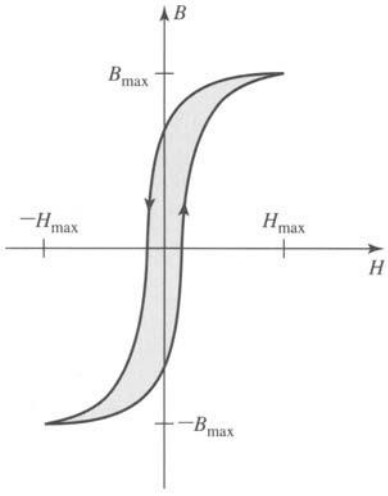

Figure 1.13 Hysteresis loop; hysteresis loss is proportional to the loop area (shaded).

Equation 1.45 can be used to calculate the energy input W to the magnetic core of Fig. 1.1 as the material undergoes a single cycle

$$W = \oint i_\varphi \, d\lambda = \oint \left(\frac{H_c l_c}{N}\right)(A_c N \, dB_c) = A_c l_c \oint H_c \, dB_c \tag{1.56}$$

Recognizing that $A_c l_c$ is the volume of the core and that the integral is the area of the ac hysteresis loop, we see that each time the magnetic material undergoes a cycle, there is a net energy input into the material. This energy is required to move around the magnetic dipoles in the material and is dissipated as heat in the material. Thus for a given flux level, the corresponding *hysteresis losses* are proportional to the area of the hysteresis loop and to the total volume of material. Since there is an energy loss per cycle, hysteresis power loss is proportional to the frequency of the applied excitation.

In general, these losses depend on the metallurgy of the material as well as the flux density and frequency. Information on core loss is typically presented in graphical form. It is plotted in terms of watts per unit weight as a function of flux density; often a family of curves for different frequencies are given. Figure 1.14 shows the core loss P_c for M-5 grain-oriented electrical steel at 60 Hz.

Nearly all transformers and certain sections of electric machines use sheet-steel material that has highly favorable directions of magnetization along which the core loss is low and the permeability is high. This material is termed *grain-oriented steel.* The reason for this property lies in the atomic structure of a crystal of the silicon-iron

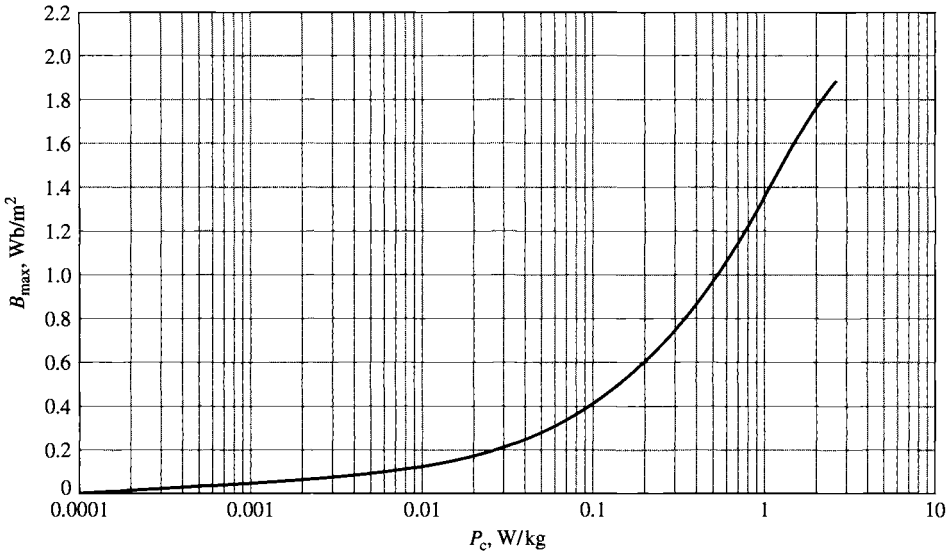

Figure 1.14 Core loss at 60 Hz in watts per kilogram for M-5 grain-oriented electrical steel 0.012 in thick. (*Armco Inc.*)

alloy, which is a body-centered cube; each cube has an atom at each corner as well as one in the center of the cube. In the cube, the easiest axis of magnetization is the cube edge; the diagonal across the cube face is more difficult, and the diagonal through the cube is the most difficult. By suitable manufacturing techniques most of the crystalline cube edges are aligned in the rolling direction to make it the favorable direction of magnetization. The behavior in this direction is superior in core loss and permeability to *nonoriented steels* in which the crystals are randomly oriented to produce a material with characteristics which are uniform in all directions. As a result, oriented steels can be operated at higher flux densities than the nonoriented grades.

Nonoriented electrical steels are used in applications where the flux does not follow a path which can be oriented with the rolling direction or where low cost is of importance. In these steels the losses are somewhat higher and the permeability is very much lower than in grain-oriented steels.

EXAMPLE 1.8

The magnetic core in Fig. 1.15 is made from laminations of M-5 grain-oriented electrical steel. The winding is excited with a 60-Hz voltage to produce a flux density in the steel of $B = 1.5 \sin \omega t$ T, where $\omega = 2\pi 60 \approx 377$ rad/sec. The steel occupies 0.94 of the core cross-sectional area. The mass-density of the steel is 7.65 g/cm^3. Find (*a*) the applied voltage, (*b*) the peak current, (*c*) the rms exciting current, and (*d*) the core loss.

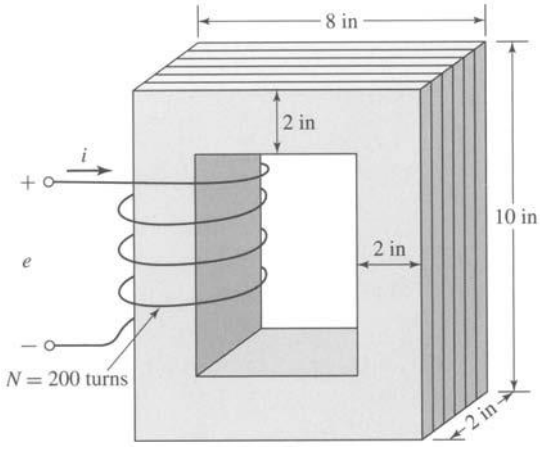

Figure 1.15 Laminated steel core with winding for Example 1.8.

■ Solution

a. From Eq. 1.27 the voltage is

$$e = N\frac{d\varphi}{dt} = NA_c\frac{dB}{dt}$$

$$= 200 \times 4\text{ in}^2 \times 0.94 \times \left(\frac{1.0\text{ m}^2}{39.4^2\text{ in}^2}\right) \times 1.5 \times (377\cos(377t))$$

$$= 274\cos(377t)\text{ V}$$

b. The magnetic field intensity corresponding to $B_{max} = 1.5$ T is given in Fig. 1.10 as $H_{max} = 36$ A turns/m. Notice that, as expected, the relative permeability $\mu_r = B_{max}/(\mu_0 H_{max}) = 33{,}000$ at the flux level of 1.5 T is lower than the value of $\mu_r = 72{,}300$ found in Example 1.4 corresponding to a flux level of 1.0 T, yet significantly larger than the value of 2900 corresponding to a flux level of 1.8 T.

$$l_c = (6+6+8+8)\text{ in}\left(\frac{1.0\text{ m}}{39.4\text{ in}}\right) = 0.71\text{ m}$$

The peak current is

$$I = \frac{H_{max}l_c}{N} = \frac{36(0.71)}{200} = 0.13\text{ A}$$

c. The rms current is obtained from the value of P_a of Fig. 1.12 for $B_{max} = 1.5$ T.

$$P_a = 1.5\text{ VA/kg}$$

The core volume and weight are

$$V_c = (4\text{ in}^2)(0.94)(28\text{ in}) = 105.5\text{ in}^3$$

$$W_c = (105.5\text{ in}^3)\left(\frac{2.54\text{ cm}}{1.0\text{ in}}\right)^3\left(\frac{7.65\text{ g}}{1.0\text{ cm}^3}\right) = 13.2\text{ kg}$$

The total rms voltamperes and current are

$$P_a = (1.5\ \text{VA/kg})(13.2\ \text{kg}) = 20\ \text{VA}$$

$$I_{\varphi,\text{rms}} = \frac{P_a}{E_{\text{rms}}} = \frac{20}{275(0.707)} = 0.10\ \text{A}$$

d. The core-loss density is obtained from Fig. 1.14 as $P_c = 1.2$ W/kg. The total core loss is

$$P_c = (1.2\ \text{W/kg})(13.2\ \text{kg}) = 16\ \text{W}$$

Practice Problem 1.7

Repeat Example 1.8 for a 60-Hz voltage of $B = 1.0 \sin \omega t$ T.

Solution

a. $V = 185 \cos 377t$ V
b. $I = 0.04$ A
c. $I_\varphi = 0.061$ A
d. $P_c = 6.7$ W

1.5 PERMANENT MAGNETS

Figure 1.16a shows the second quadrant of a hysteresis loop for Alnico 5, a typical permanent-magnet material, while Fig. 1.16b shows the second quadrant of a hysteresis loop for M-5 steel.[7] Notice that the curves are similar in nature. However, the hysteresis loop of Alnico 5 is characterized by a large value of *residual flux density* or *remanent magnetization,* B_r, (approximately 1.22 T) as well as a large value of *coercivity,* H_c, (approximately −49 kA/m).

The remanent magnetization, B_r, corresponds to the flux density which would remain in a closed magnetic structure, such as that of Fig. 1.1, made of this material, if the applied mmf (and hence the magnetic field intensity H) were reduced to zero. However, although the M-5 electrical steel also has a large value of remanent magnetization (approximately 1.4 T), it has a much smaller value of coercivity (approximately −6 A/m, smaller by a factor of over 7500). The coercivity H_c corresponds to the value of magnetic field intensity (which is proportional to the mmf) required to reduce the material flux density to zero.

The significance of remanent magnetization is that it can produce magnetic flux in a magnetic circuit in the absence of external excitation (such as winding currents). This is a familiar phenomenon to anyone who has afixed notes to a refrigerator with small magnets and is widely used in devices such as loudspeakers and permanent-magnet motors.

[7] To obtain the largest value of remanent magnetization, the hysteresis loops of Fig. 1.16 are those which would be obtained if the materials were excited by sufficient mmf to ensure that they were driven heavily into saturation. This is discussed further in Section 1.6.

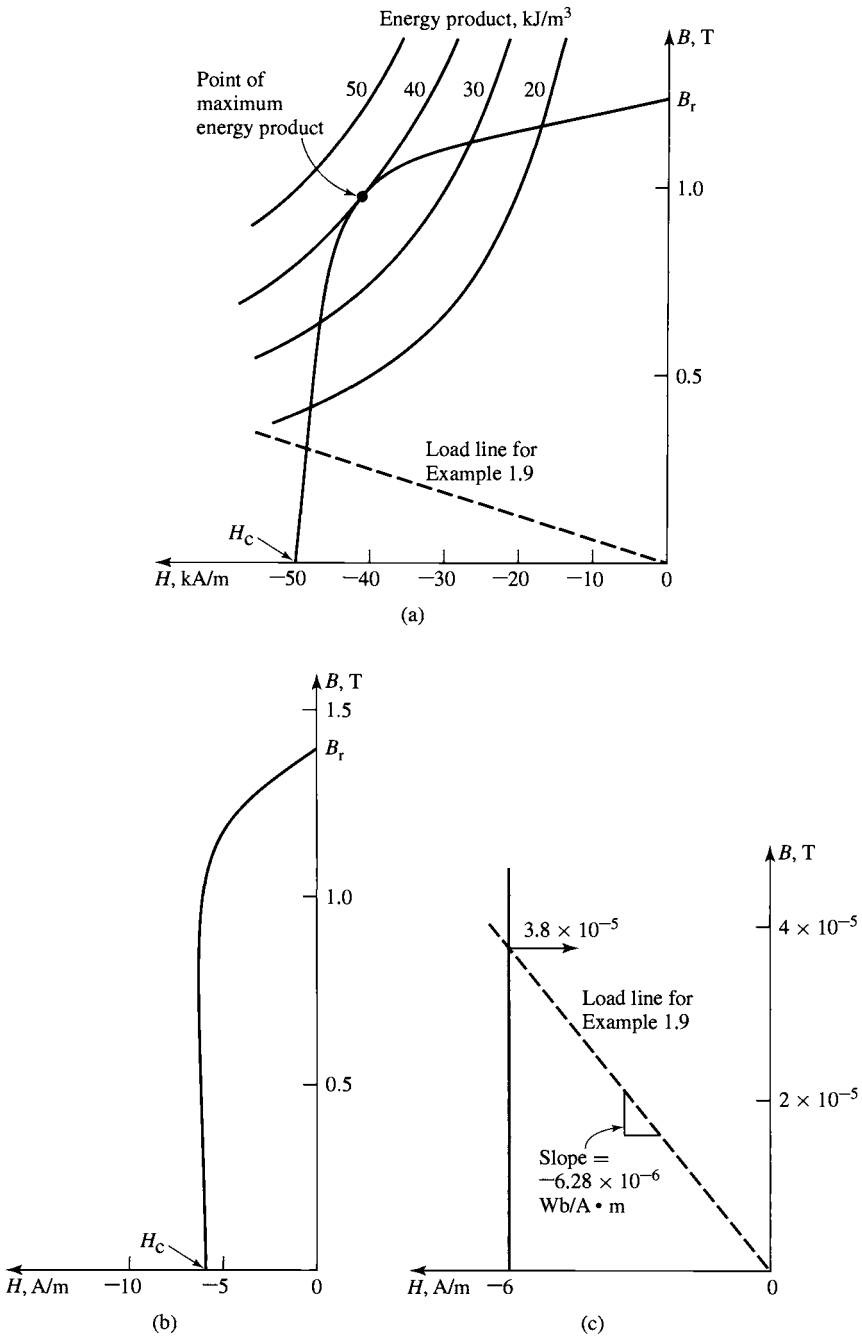

Figure 1.16 (a) Second quadrant of hysteresis loop for Alnico 5; (b) second quadrant of hysteresis loop for M-5 electrical steel; (c) hysteresis loop for M-5 electrical steel expanded for small B. (*Armco Inc.*)

From Fig. 1.16, it would appear that both Alnico 5 and M-5 electrical steel would be useful in producing flux in unexcited magnetic circuits since they both have large values of remanent magnetization. That this is not the case can be best illustrated by an example.

EXAMPLE 1.9

As shown in Fig. 1.17, a magnetic circuit consists of a core of high permeability ($\mu \to \infty$), an air gap of length $g = 0.2$ cm, and a section of magnetic material of length $l_m = 1.0$ cm. The cross-sectional area of the core and gap is equal to $A_m = A_g = 4$ cm^2. Calculate the flux density B_g in the air gap if the magnetic material is (*a*) Alnico 5 and (*b*) M-5 electrical steel.

■ Solution

a. Since the core permeability is assumed infinite, H in the core is negligible. Recognizing that the mmf acting on the magnetic circuit of Fig. 1.17 is zero, we can write

$$\mathcal{F} = 0 = H_g g + H_m l_m$$

or

$$H_g = -\left(\frac{l_m}{g}\right) H_m$$

where H_g and H_m are the magnetic field intensities in the air gap and the magnetic material, respectively.

Since the flux must be continuous through the magnetic circuit,

$$\phi = A_g B_g = A_m B_m$$

or

$$B_g = \left(\frac{A_m}{A_g}\right) B_m$$

where B_g and B_m are the magnetic flux densities in the air gap and the magnetic material, respectively.

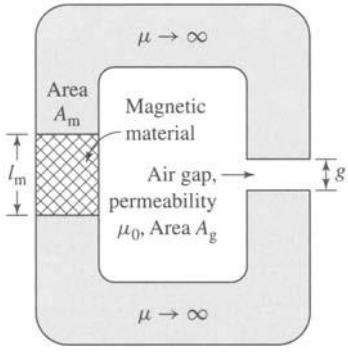

Figure 1.17 Magnetic circuit for Example 1.9.

These equations can be solved to yield a linear relationship for B_m in terms of H_m

$$B_m = -\mu_0 \left(\frac{A_g}{A_m}\right)\left(\frac{l_m}{g}\right) H_m = -5\,\mu_0\,H_m = -6.28 \times 10^{-6} H_m$$

To solve for B_m we recognize that for Alnico 5, B_m and H_m are also related by the curve of Fig. 1.16a. Thus this linear relationship, also known as a *load line,* can be plotted on Fig. 1.16a and the solution obtained graphically, resulting in

$$B_g = B_m = 0.30\ \text{T}$$

b. The solution for M-5 electrical steel proceeds exactly as in part (*a*). The load line is the same as that of part (*a*) because it is determined only by the permeability of the air gap and the geometries of the magnet and the air gap. Hence from Fig. 1.16c

$$B_g = 3.8 \times 10^{-5}\ \text{T} = 0.38\ \text{gauss}$$

which is much less than the value obtained with Alnico 5.

Example 1.9 shows that there is an immense difference between permanent-magnet materials (often referred to as *hard magnetic materials*) such as Alnico 5 and *soft magnetic materials* such as M-5 electrical steel. This difference is characterized in large part by the immense difference in their coercivities H_c. The coercivity can be thought of as a measure of the magnitude of the mmf required to demagnetize the material. As seen from Example 1.9, it is also a measure of the capability of the material to produce flux in a magnetic circuit which includes an air gap. Thus we see that materials which make good permanent magnets are characterized by large values of coercivity H_c (considerably in excess of 1 kA/m).

A useful measure of the capability of permanent-magnet material is known as its *maximum energy product.* This corresponds to the largest B-H product $(B - H)_{max}$, which corresponds to a point on the second quadrant of the hysteresis loop. As can be seen from Eq. 1.56, the product of B and H has the dimensions of energy density (joules per cubic meter). We now show that operation of a given permanent-magnet material at this point will result in the smallest volume of that material required to produce a given flux density in an air gap. As a result, choosing a material with the largest available maximum energy product can result in the smallest required magnet volume.

In Example 1.9, we found an expression for the flux density in the air gap of the magnetic circuit of Fig. 1.17:

$$B_g = \frac{A_m}{A_g} B_m \tag{1.57}$$

We also found that the ratio of the mmf drops across the magnet and the air gap is equal to -1:

$$\frac{H_m l_m}{H_g g} = -1 \tag{1.58}$$

Equation 1.58 can be solved for H_g, and the result can be multiplied by μ_0 to obtain $B_g = \mu_0 H_g$. Multiplying by Eq. 1.57 yields

$$B_g^2 = \mu_0 \left(\frac{l_m A_m}{g A_g} \right) (-H_m B_m)$$

$$= \mu_0 \left(\frac{\text{Vol}_{\text{mag}}}{\text{Vol}_{\text{air gap}}} \right) (-H_m B_m) \tag{1.59}$$

or

$$\text{Vol}_{\text{mag}} = \frac{\text{Vol}_{\text{air gap}} B_g^2}{\mu_0(-H_m B_m)} \tag{1.60}$$

where Vol_{mag} is the volume of the magnet, $\text{Vol}_{\text{air gap}}$ is the air-gap volume, and the minus sign arises because, at the operating point of the magnetic circuit, H in the magnet (H_m) is negative.

Equation 1.60 is the desired result. It indicates that to achieve a desired flux density in the air gap, the required volume of the magnet can be minimized by operating the magnet at the point of the largest possible value of the B-H product $H_m B_m$, i.e., the point of maximum energy product. Furthermore, the larger the value of this product, the smaller the size of the magnet required to produce the desired flux density. Hence the maximum energy product is a useful performance measure for a magnetic material, and it is often found as a tabulated "figure of merit" on data sheets for permanent-magnet materials.

Note that Eq. 1.59 appears to indicate that one can achieve an arbitrarily large air-gap flux density simply by reducing the air-gap volume. This is not true in practice because as the flux density in the magnetic circuit increases, a point will be reached at which the magnetic core material will begin to saturate and the assumption of infinite permeability will no longer be valid, thus invalidating the derivation leading to Eq. 1.59.

Note also that a curve of constant B-H product is a hyperbola. A set of such hyperbolas for different values of the B-H product is plotted in Fig. 1.16a. From these curves, we see that the maximum energy product for Alnico 5 is 40 kJ/m^3 and that this occurs at the point $B = 1.0$ T and $H = -40$ kA/m.

EXAMPLE 1.10

The magnetic circuit of Fig. 1.17 is modified so that the air-gap area is reduced to $A_g = 2.0\,\text{cm}^2$, as shown in Fig. 1.18. Find the minimum magnet volume required to achieve an air-gap flux density of 0.8 T.

■ Solution

The smallest magnet volume will be achieved with the magnet operating at its point of maximum energy product, as shown in Fig. 1.16a. At this operating point, $B_m = 1.0$ T and $H_m = -40$ kA/m.

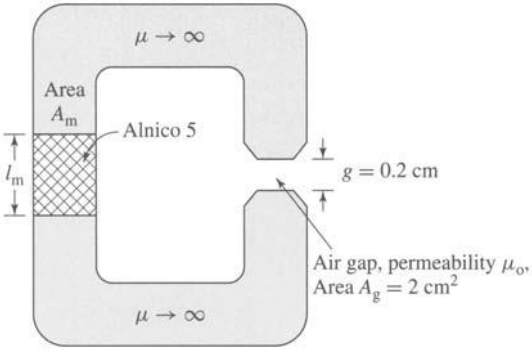

Figure 1.18 Magnetic circuit for Example 1.10.

Thus from Eq. 1.57,

$$A_m = A_g\left(\frac{B_g}{B_m}\right)$$

$$= 2\text{ cm}^2\left(\frac{0.8}{1.0}\right) = 1.6\text{ cm}^2$$

and from Eq. 1.58

$$l_m = -g\left(\frac{H_g}{H_m}\right) = -g\left(\frac{B_g}{\mu_0 H_m}\right)$$

$$= -0.2\text{ cm}\left(\frac{0.8}{(4\pi \times 10^{-7})(-40 \times 10^3)}\right)$$

$$= 3.18\text{ cm}$$

Thus the minimum magnet volume is equal to $1.6\text{ cm}^2 \times 3.18\text{ cm} = 5.09\text{ cm}^3$.

Practice Problem 1.8

Repeat Example 1.10 assuming the air-gap area is further reduced to $A_g = 1.8\text{ cm}^2$ and that the desired air-gap flux density is 0.6 T.

Solution

Minimum magnet volume $= 2.58\text{ cm}^3$.

1.6 APPLICATION OF PERMANENT MAGNET MATERIALS

Examples 1.9 and 1.10 consider the operation of permanent magnetic materials under the assumption that the operating point can be determined simply from a knowledge of the geometry of the magnetic circuit and the properties of the various magnetic

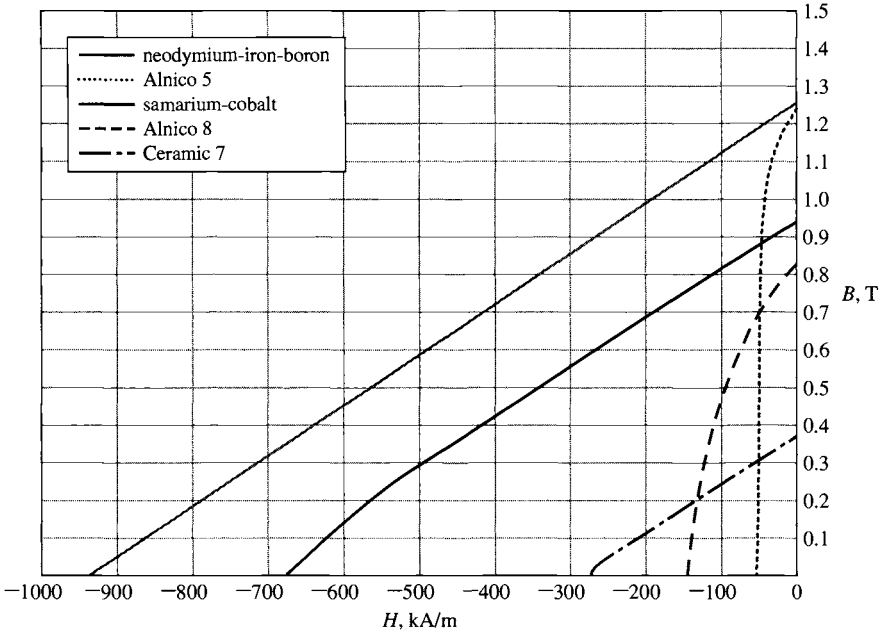

Figure 1.19 Magnetization curves for common permanent-magnet materials.

materials involved. In fact, the situation is more complex.[8] This section will expand upon these issues.

Figure 1.19 shows the magnetization characteristics for a few common permanent magnet materials. Alnico 5 is a widely used alloy of iron, nickel, aluminum, and cobalt, originally discovered in 1931. It has a relatively large residual flux density. Alnico 8 has a lower residual flux density and a higher coercivity than Alnico 5. Hence, it is less subject to demagnetization than Alnico 5. Disadvantages of the Alnico materials are their relatively low coercivity and their mechanical brittleness.

Ceramic permanent magnet materials (also known as *ferrite magnets*) are made from iron-oxide and barium- or strontium-carbonate powders and have lower residual flux densities than Alnico materials but significantly higher coercivities. As a result, they are much less prone to demagnetization. One such material, Ceramic 7, is shown in Fig. 1.19, where its magnetization characteristic is almost a straight line. Ceramic magnets have good mechanical characteristics and are inexpensive to manufacture; as a result, they are the widely used in many permanent magnet applications.

[8] For a further discussion of permanent magnets and their application, see P. Campbell, *Permanent Magnet Materials and Their Application,* Cambridge University Press, 1994; R. J. Parker, *Advances in Permanent Magnetism,* John Wiley & Sons, 1990; A. Bosak, *Permanent-Magnet DC Linear Motors,* Clarendon Press·Oxford, 1996; G. R. Slemon and A. Straughen, *Electric Machines,* Addison-Wesley, 1980, Secs 1.20–1.25; and T. J. E. Miller, *Brushless Permanent-Magnet and Reluctance Motor Drives,* Clarendon Press·Oxford, 1989, Chapter 3.

Samarium-cobalt represents a significant advance in permanent magnet technology which began in the 1960s with the discovery of rare earth permanent magnet materials. From Fig. 1.19 it can be seen to have a high residual flux density such as is found with the Alnico materials, while at the same time having a much higher coercivity and maximum energy product. The newest of the rare earth magnetic materials is the neodymium-iron-boron material. It features even larger residual flux density, coercivity, and maximum energy product than does samarium-cobalt.

Consider the magnetic circuit of Fig. 1.20. This includes a section of hard magnetic material in a core of highly permeable soft magnetic material as well as an N-turn excitation winding. With reference to Fig. 1.21, we assume that the hard

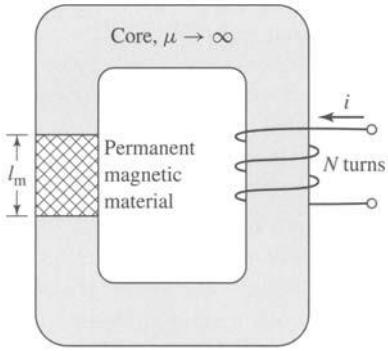

Figure 1.20 Magnetic circuit including both a permanent magnet and an excitation winding.

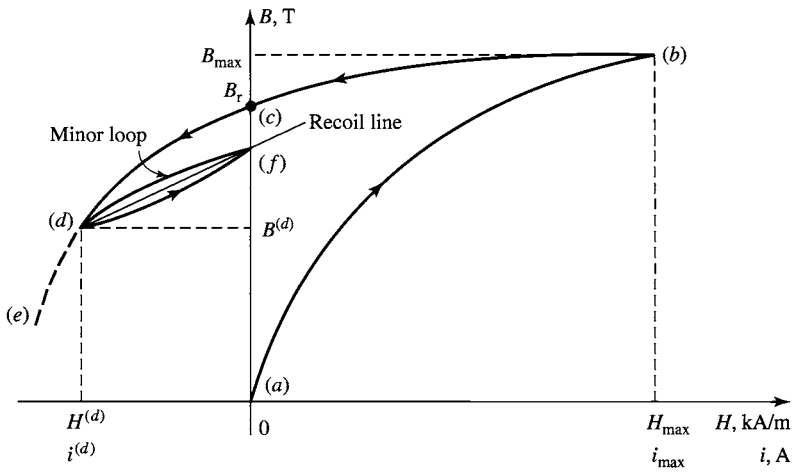

Figure 1.21 Portion of a B-H characteristic showing a minor loop and a recoil line.

magnetic material is initially unmagnetized (corresponding to point a of the figure) and consider what happens as current is applied to the excitation winding. Because the core is assumed to be of infinite permeability, the horizontal axis of Fig. 1.21 can be considered to be both a measure of the applied current $i = Hl_m/N$ as well as a measure of H in the magnetic material.

As the current i is increased to its maximum value, the B-H trajectory rises from point a in Fig. 1.21 toward its maximum value at point b. To fully magnetize the material, we assume that the current has been increased to a value i_{max} sufficiently large that the material has been driven well into saturation at point b. When the current is then decreased to zero, the B-H characteristic will begin to form a hysteresis loop, arriving at point c at zero current. At point c, notice that H in the material is zero but B is at its remanent value B_r.

As the current then goes negative, the B-H characteristic continues to trace out a hysteresis loop. In Fig. 1.21, this is seen as the trajectory between points c and d. If the current is then maintained at the value $-i^{(d)}$, the operating point of the magnet will be that of point d. Note that, as in Example 1.9, this same operating point would be reached if the material were to start at point c and, with the excitation held at zero, an air gap of length $g = l_m(A_g/A_m)(-\mu_0 H^{(d)}/B^{(d)})$ were then inserted in the core.

Should the current then be made more negative, the trajectory would continue tracing out the hysteresis loop toward point e. However, if instead the current is returned to zero, the trajectory does not in general retrace the hysteresis loop toward point c. Rather it begins to trace out a *minor hysteresis loop,* reaching point f when the current reaches zero. If the current is then varied between zero and $-i^{(d)}$, the B-H characteristic will trace out the minor loop as shown.

As can be seen from Fig. 1.21, the B-H trajectory between points d and f can be represented by a straight line, known as the *recoil line*. The slope of this line is called the *recoil permeability* μ_R. We see that once this material has been demagnetized to point d, the effective remanent magnetization of the magnetic material is that of point f which is less than the remanent magnetization B_r which would be expected based on the hysteresis loop. Note that should the demagnetization be increased past point d, for example, to point e of Fig. 1.21, a new minor loop will be created, with a new recoil line and recoil permeability.

The demagnetization effects of negative excitation which have just been discussed are equivalent to those of an air gap in the magnetic circuit. For example, clearly the magnetic circuit of Fig. 1.20 could be used as a system to magnetize hard magnetic materials. The process would simply require that a large excitation be applied to the winding and then reduced to zero, leaving the material at a remanent magnetization B_r (point c in Fig. 1.21).

Following this magnetization process, if the material were removed from the core, this would be equivalent to opening a large air gap in the magnetic circuit, demagnetizing the material in a fashion similar to that seen in Example 1.9. At this point, the magnet has been effectively weakened, since if it were again inserted in the magnetic core, it would follow a recoil line and return to a remanent magnetization somewhat less than B_r. As a result, hard magnetic materials, such as the Alnico materials of Fig. 1.19, often do not operate stably in situations with varying mmf and

geometry, and there is often the risk that improper operation can significantly demagnetize them. A significant advantage of materials such as Ceramic 7, samarium-cobalt and neodymium-iron-boron is that, because of their "straight-line" characteristic in the second quadrant (with slope close to μ_0), their recoil lines closely match their magnetization characteristic. As a result, demagnetization effects are significantly reduced in these materials and often can be ignored.

At the expense of a reduction in value of the remanent magnetization, hard magnetic materials can be stabilized to operate over a specified region. This procedure, based on the recoil trajectory shown in Fig. 1.21, can best be illustrated by an example.

EXAMPLE 1.11

Figure 1.22 shows a magnetic circuit containing hard magnetic material, a core and plunger of high (assumed infinite) permeability, and a single-turn winding which will be used to magnetize the hard magnetic material. The winding will be removed after the system is magnetized. The plunger moves in the x direction as indicated, with the result that the air-gap area can vary ($2\,\text{cm}^2 \le A_g \le 4\,\text{cm}^2$). Assuming that the hard magnetic material is Alnico 5 and that the system is initially magnetized with $A_g = 2$ cm, (*a*) find the magnet length l_m such that the system will operate on a recoil line which intersects the maximum B-H product point on the magnetization curve for Alnico 5, (*b*) devise a procedure for magnetizing the magnet, and (*c*) calculate the flux density B_g in the air gap as the plunger moves back and forth and the air gap varies between these two limits.

■ Solution

a. Figure 1.23a shows the magnetization curve for Alnico 5 and two load lines corresponding to the two extremes of the air gap, $A_g = 2\,\text{cm}^2$ and $A_g = 4\,\text{cm}^2$. We see that the system will operate on the desired recoil line if the load line for $A_g = 2\,\text{cm}^2$ intersects the B-H characteristic at the maximum energy product point (labeled point a in Fig. 1.23a), $B_m^{(a)} = 1.0$ T and $H_m^{(a)} = -40$ kA/m.

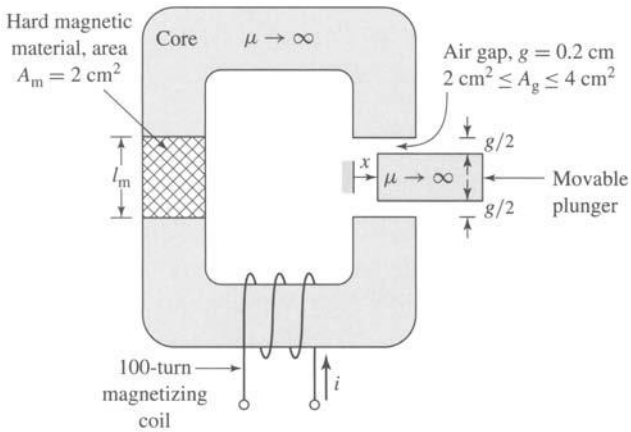

Figure 1.22 Magnetic circuit for Example 1.11.

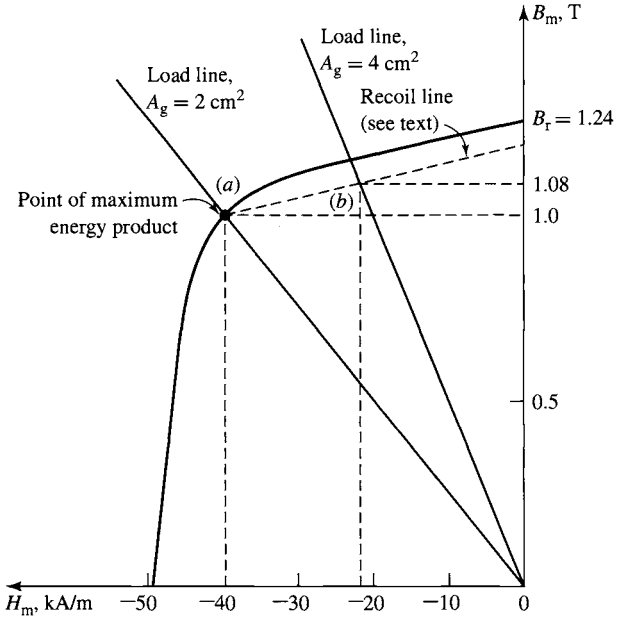

(a)

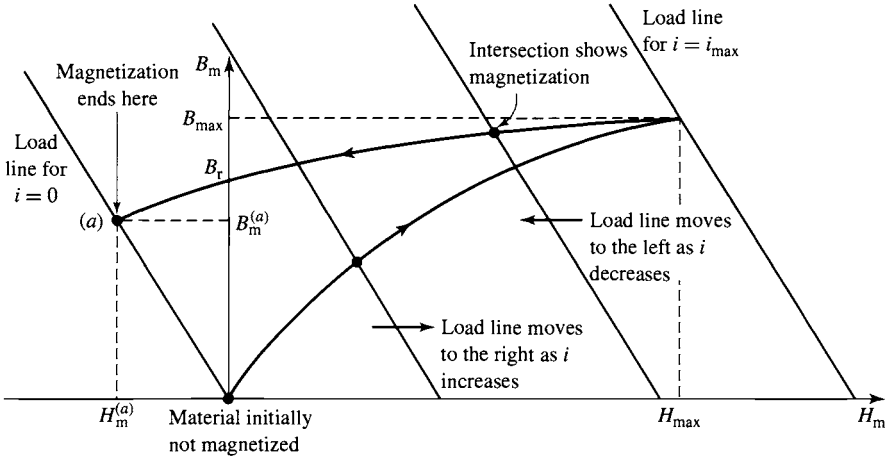

(b)

Figure 1.23 (a) Magnetization curve for Alnico 5 for Example 1.11; (b) series of load lines for $A_g = 2$ cm^2 and varying values of i showing the magnetization procedure for Example 1.11.

From Eqs. 1.57 and 1.58, we see that the slope of the required load line is given by

$$\frac{B_m^{(a)}}{-H_m^{(a)}} = \frac{B_g}{H_g}\frac{A_g}{A_m}\frac{l_m}{g}$$

and thus

$$\begin{aligned} l_m &= g\left(\frac{A_m}{A_g}\right)\left(\frac{B_m^{(a)}}{-\mu_0 H_m^{(a)}}\right) \\ &= 0.2\text{ cm}\left(\frac{2}{2}\right)\left(\frac{1.0}{4\pi\times 10^{-7}\times 4\times 10^4}\right) = 3.98\text{ cm} \end{aligned}$$

b. Figure 1.23b shows a series of load lines for the system with $A_g = 2\text{ cm}^2$ and with current i applied to the excitation winding. The general equation for these load lines can be readily derived since from Eq. 1.5

$$Ni = H_m l_m + H_g g$$

and from Eqs. 1.3 and 1.7

$$B_m A_m = B_g A_g = \mu_0 H_g A_g$$

Thus

$$\begin{aligned} B_m &= -\mu_0\left(\frac{A_g}{A_m}\right)\left(\frac{l_m}{g}\right)H_m + \frac{\mu_0 N}{g}\left(\frac{A_g}{A_m}\right)i \\ &= \mu_0\left[-\left(\frac{2}{2}\right)\left(\frac{3.98}{0.2}\right)H_m + \frac{100}{2\times 10^{-3}}\left(\frac{2}{2}\right)i\right] \\ &= -2.50\times 10^{-5}H_m + 6.28\times 10^{-2}i \end{aligned}$$

From this equation and Fig. 1.23b, we see that to drive the magnetic material into saturation to the point $B_{max} - H_{max}$, the current in the magnetizing winding must be increased to the value i_{max} where

$$i_{max} = \frac{B_{max} + 2.50\times 10^{-5}H_{max}}{6.28\times 10^{-2}}\text{ A}$$

In this case, we do not have a complete hysteresis loop for Alnico 5, and hence we will have to estimate B_{max} and H_{max}. Linearly extrapolating the B-H curve at $H = 0$ back to 4 times the coercivity, that is, $H_{max} = 4\times 50 = 200$ kA/m, yields $B_{max} = 2.1$ T. This value is undoubtedly extreme and will overestimate the required current somewhat. However, using $B_{max} = 2.1$ T and $H_{max} = 200$ kA/m yields $i_{max} = 45.2$ A.

Thus with the air-gap area set to 2 cm^2, increasing the current to 45.2 A and then reducing it to zero will achieve the desired magnetization.

c. Because we do not have specific information about the slope of the recoil line, we shall assume that its slope is the same as that of the B-H characteristic at the point $H = 0$, $B = B_r$. From Fig. 1.23a, with the recoil line drawn with this slope, we see that as the air-gap area varies between 2 and 4 cm^2, the magnet flux density B_m varies between 1.00 and 1.08 T. Since the air-gap flux density equals A_m/A_g times this value, the airgap flux density will equal $(2/2)1.00 = 1.0$ T when $A_g = 2.0\text{ cm}^2$ and $(2/4)1.08 = 0.54$ T when

$A_g = 4.0\,\text{cm}^2$. Note from Fig. 1.23a that, when operated with these air-gap variations, the magnet appears to have an effective residual flux density of 1.17 T instead of the initial value of 1.24 T. Note that as long as the air-gap variation is limited to the range considered here, the system will continue to operate on the line labeled "Recoil line" in Fig. 1.23a and the magnet can be said to be *stabilized*.

As has been discussed, hard magnetic materials such as Alnico 5 can be subject to demagnetization, should their operating point be varied excessively. As shown in Example 1.11, these materials can be stabilized with some loss in effective remanent magnetization. However, this procedure does not guarantee absolute stability of operation. For example, if the material in Example 1.11 were subjected to an air-gap area smaller than 2 cm^2 or to excessive demagnetizing current, the effect of the stabilization would be erased and the material would be found to operate on a new recoil line with further reduced magnetization.

However, many materials, such as samarium-cobalt, Ceramic 7, and neodymium-iron-boron (see Fig. 1.19), which have large values of coercivity, tend to have very low values of recoil permeability, and the recoil line is essentially tangent to the B-H characteristic for a large portion of the useful operating region. For example, this can be seen in Fig. 1.19, which shows the dc magnetization curve for neodymium-iron-boron, from which we see that this material has a remanent magnetization of 1.25 T and a coercivity of −940 kA/m. The portion of the curve between these points is a straight line with a slope equal to $1.06\mu_0$, which is the same as the slope of its recoil line. As long as these materials are operated on this low-incremental-permeability portion of their B-H characteristic, they do not require stabilization, provided they are not excessively demagnetized.

For these materials, it is often convenient to assume that their dc magnetization curve is linear over their useful operating range with a slope equal to the recoil permeability μ_R. Under this assumption, the dc magnetization curve for these materials can be written in the form

$$B = \mu_R(H - H_c') = B_r + \mu_R H \tag{1.61}$$

Here, H_c' is the *apparent coercivity* associated with this linear representation. As can be seen from Fig. 1.19, the apparent coercivity is typically somewhat larger in magnitude (i.e. a larger negative value) than the material coercivity H_c because the dc magnetization characteristic tends to bend downward for low values of flux density.

1.7 SUMMARY

Electromechanical devices which employ magnetic fields often use ferromagnetic materials for guiding and concentrating these fields. Because the magnetic permeability of ferromagnetic materials can be large (up to tens of thousands times that of the surrounding space), most of the magnetic flux is confined to fairly well-defined paths determined by the geometry of the magnetic material. In addition, often the frequencies of interest are low enough to permit the magnetic fields to be considered

quasi-static, and hence they can be determined simply from a knowledge of the net mmf acting on the magnetic structure.

As a result, the solution for the magnetic fields in these structures can be obtained in a straightforward fashion by using the techniques of magnetic-circuit analysis. These techniques can be used to reduce a complex three-dimensional magnetic field solution to what is essentially a one-dimensional problem. As in all engineering solutions, a certain amount of experience and judgment is required, but the technique gives useful results in many situations of practical engineering interest.

Ferromagnetic materials are available with a wide variety of characteristics. In general, their behavior is nonlinear, and their B-H characteristics are often represented in the form of a family of hysteresis (B-H) loops. Losses, both hysteretic and eddy-current, are functions of the flux level and frequency of operation as well as the material composition and the manufacturing process used. A basic understanding of the nature of these phenomena is extremely useful in the application of these materials in practical devices. Typically, important properties are available in the form of curves supplied by the material manufacturers.

Certain magnetic materials, commonly known as hard or permanent-magnet materials, are characterized by large values of remanent magnetization and coercivity. These materials produce significant magnetic flux even in magnetic circuits with air gaps. With proper design they can be made to operate stably in situations which subject them to a wide range of destabilizing forces and mmf's. Permanent magnets find application in many small devices, including loudspeakers, ac and dc motors, microphones, and analog electric meters.

1.8 PROBLEMS

1.1 A magnetic circuit with a single air gap is shown in Fig. 1.24. The core dimensions are:

Cross-sectional area $A_c = 1.8 \times 10^{-3}$ m^2
Mean core length $l_c = 0.6$ m
Gap length $g = 2.3 \times 10^{-3}$ m
$N = 83$ turns

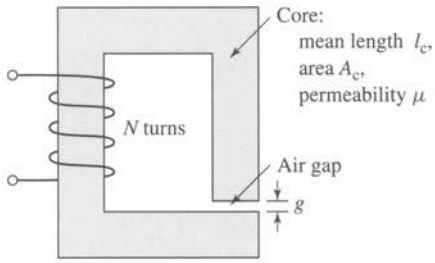

Figure 1.24 Magnetic circuit for Problem 1.1.

Assume that the core is of infinite permeability ($\mu \to \infty$) and neglect the effects of fringing fields at the air gap and leakage flux. (*a*) Calculate the reluctance of the core $\mathcal{R}_c$ and that of the gap $\mathcal{R}_g$. For a current of $i = 1.5$ A, calculate (*b*) the total flux ϕ, (*c*) the flux linkages λ of the coil, and (*d*) the coil inductance L.

1.2 Repeat Problem 1.1 for a finite core permeability of $\mu = 2500\mu_0$.

1.3 Consider the magnetic circuit of Fig. 1.24 with the dimensions of Problem 1.1. Assuming infinite core permeability, calculate (*a*) the number of turns required to achieve an inductance of 12 mH and (*b*) the inductor current which will result in a core flux density of 1.0 T.

1.4 Repeat Problem 1.3 for a core permeability of $\mu = 1300\mu_0$.

1.5 The magnetic circuit of Problem 1.1 has a nonlinear core material whose permeability as a function of B_m is given by

$$\mu = \mu_0 \left(1 + \frac{3499}{\sqrt{1 + 0.047(B_m)^{7.8}}} \right)$$

where B_m is the material flux density.

a. Using MATLAB, plot a dc magnetization curve for this material (B_m vs. H_m) over the range $0 \le B_m \le 2.2$ T.

b. Find the current required to achieve a flux density of 2.2 T in the core.

c. Again, using MATLAB, plot the coil flux linkages as a function of coil current as the current is varied from 0 to the value found in part (b).

1.6 The magnetic circuit of Fig. 1.25 consists of a core and a moveable plunger of width l_p, each of permeability μ. The core has cross-sectional area A_c and mean length l_c. The overlap area of the two air gaps A_g is a function of the plunger position x and can be assumed to vary as

$$A_g = A_c \left(1 - \frac{x}{X_0} \right)$$

You may neglect any fringing fields at the air gap and use approximations consistent with magnetic-circuit analysis.

a. Assuming that $\mu \to \infty$, derive an expression for the magnetic flux density in the air gap B_g as a function of the winding current I and as the

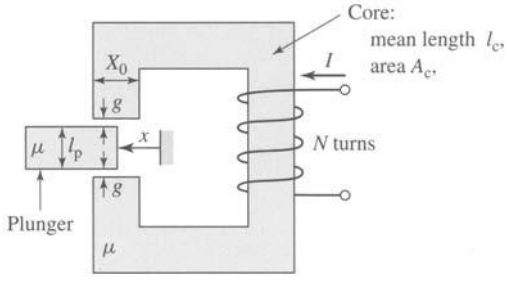

Figure 1.25 Magnetic circuit for Problem 1.6.

plunger position is varied ($0 \le x \le 0.8X_0$). What is the corresponding flux density in the core?

b. Repeat part (a) for a finite permeability μ.

1.7 The magnetic circuit of Fig. 1.25 and Problem 1.6 has the following dimensions:

$$A_c = 8.2\ \text{cm}^2 \quad l_c = 23\ \text{cm}$$
$$l_p = 2.8\ \text{cm} \quad g = 0.8\ \text{mm}$$
$$X_0 = 2.5\ \text{cm} \quad N = 430\ \text{turns}$$

a. Assuming a constant permeability of $\mu = 2800\mu_0$, calculate the current required to achieve a flux density of 1.3 T in the air gap when the plunger is fully retracted ($x = 0$).

b. Repeat the calculation of part (a) for the case in which the core and plunger are composed of a nonlinear material whose permeability is given by

$$\mu = \mu_0 \left(1 + \frac{1199}{\sqrt{1 + 0.05B_m^8}}\right)$$

where B_m is the magnetic flux density in the material.

c. For the nonlinear material of part (b), use MATLAB to plot the air-gap flux density as a function of winding current for $x = 0$ and $x = 0.5X_0$.

1.8 An inductor of the form of Fig. 1.24 has dimensions:

Cross-sectional area $A_c = 3.6\ \text{cm}^2$
Mean core length $l_c = 15$ cm
$N = 75$ turns

Assuming a core permeability of $\mu = 2100\mu_0$ and neglecting the effects of leakage flux and fringing fields, calculate the air-gap length required to achieve an inductance of 6.0 mH.

1.9 The magnetic circuit of Fig. 1.26 consists of rings of magnetic material in a stack of height h. The rings have inner radius R_i and outer radius R_o. Assume that the iron is of infinite permeability ($\mu \to \infty$) and neglect the effects of magnetic leakage and fringing. For:

$R_i = 3.4$ cm
$R_o = 4.0$ cm
$h = 2$ cm
$g = 0.2$ cm

calculate:

a. the mean core length l_c and the core cross-sectional area A_c.

b. the reluctance of the core $\mathcal{R}_c$ and that of the gap $\mathcal{R}_g$.

For $N = 65$ turns, calculate:

c. the inductance L.

d. current i required to operate at an air-gap flux density of $B_g = 1.35$T.

e. the corresponding flux linkages λ of the coil.

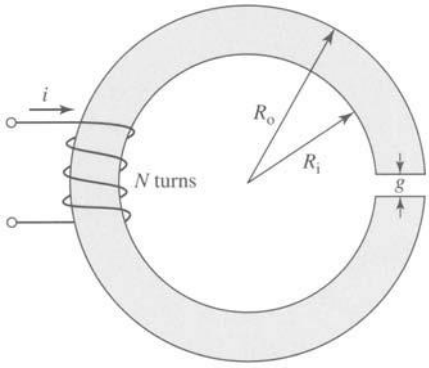

Figure 1.26 Magnetic circuit for Problem 1.9.

1.10 Repeat Problem 1.9 for a core permeability of $\mu = 750\mu_0$.

1.11 Using MATLAB, plot the inductance of the inductor of Problem 1.9 as a function of relative core permeability as the core permeability varies for $\mu_r = 100$ to $\mu_r = 10000$. (Hint: Plot the inductance versus the log of the relative permeability.) What is the minimum relative core permeability required to insure that the inductance is within 5 percent of the value calculated assuming that the core permeability is infinite?

1.12 The inductor of Fig. 1.27 has a core of uniform circular cross-section of area A_c, mean length l_c and relative permeability μ_r and an N-turn winding. Write an expression for the inductance L.

1.13 The inductor of Fig. 1.27 has the following dimensions:

$A_c = 1.0\ \text{cm}^2$
$l_c = 15\ \text{cm}$
$g = 0.8\ \text{mm}$
$N = 480$ turns

Neglecting leakage and fringing and assuming $\mu_r = 1000$, calculate the inductance.

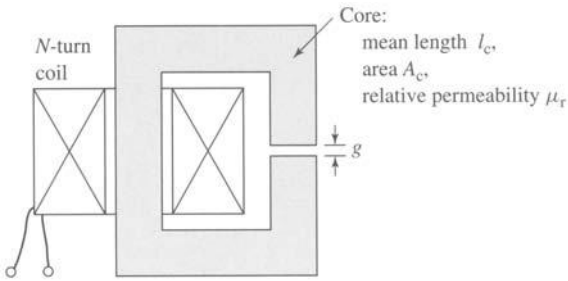

Figure 1.27 Inductor for Problem 1.12.

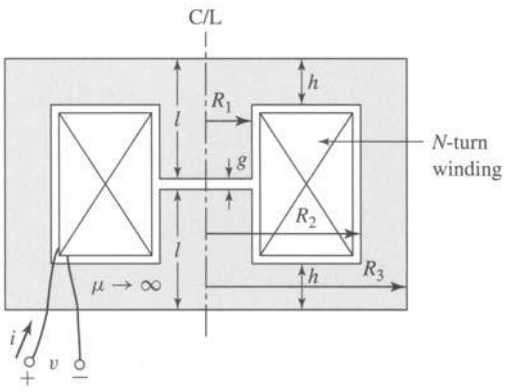

Figure 1.28 Pot-core inductor for Problem 1.15.

1.14 The inductor of Problem 1.13 is to be operated from a 60-Hz voltage source. (*a*) Assuming negligible coil resistance, calculate the rms inductor voltage corresponding to a peak core flux density of 1.5 T. (*b*) Under this operating condition, calculate the rms current and the peak stored energy.

1.15 Consider the magnetic circuit of Fig. 1.28. This structure, known as a *pot-core,* is typically made in two halves. The N-turn coil is wound on a cylindrical bobbin and can be easily inserted over the central post of the core as the two halves are assembled. Because the air gap is internal to the core, provided the core is not driven excessively into saturation, relatively little magnetic flux will "leak" from the core, making this a particularly attractive configuration for a wide variety of applications, both for inductors such as that of Fig. 1.27 and transformers.

Assume the core permeability to be $\mu = 2500\mu_0$ and $N = 200$ turns. The following dimensions are specified:

$$R_1 = 1.5\text{ cm} \quad R_2 = 4\text{ cm} \quad l = 2.5\text{ cm}$$
$$h = 0.75\text{ cm} \quad g = 0.5\text{ mm}$$

a. Find the value of R_3 such that the flux density in the outer wall of the core is equal to that within the central cylinder.

b. Although the flux density in the radial sections of the core (the sections of thickness h) actually decreases with radius, assume that the flux density remains uniform. (*i*) Write an expression for the coil inductance and (*ii*) evaluate it for the given dimensions.

c. The core is to be operated at a peak flux density of 0.8 T at a frequency of 60 Hz. Find (*i*) the corresponding rms value of the voltage induced in the winding, (*ii*) the rms coil current, and (*iii*) the peak stored energy.

d. Repeat part (c) for a frequency of 50 Hz.

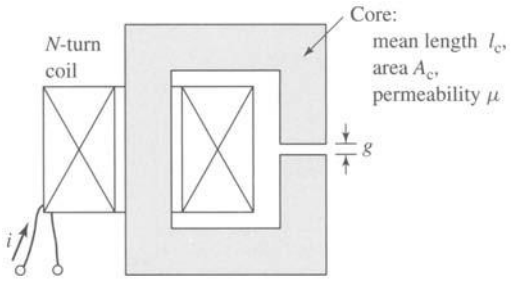

Figure 1.29 Inductor for Problem 1.17.

1.16 A square voltage wave having a fundamental frequency of 60 Hz and equal positive and negative half cycles of amplitude E is applied to a 1000-turn winding surrounding a closed iron core of $1.25 \times 10^{-3}\text{m}^2$ cross section. Neglect both the winding resistance and any effects of leakage flux.

a. Sketch the voltage, the winding flux linkage, and the core flux as a function of time.

b. Find the maximum permissible value of E if the maximum flux density is not to exceed 1.15 T.

1.17 An inductor is to be designed using a magnetic core of the form of that of Fig. 1.29. The core is of uniform cross-sectional area $A_c = 5.0\ \text{cm}^2$ and of mean length $l_c = 25$ cm.

a. Calculate the air-gap length g and the number of turns N such that the inductance is 1.4 mH and so that the inductor can operate at peak currents of 6 A without saturating. Assume that saturation occurs when the peak flux density in the core exceeds 1.7 T and that, below saturation, the core has permeability $\mu = 3200\mu_0$.

b. For an inductor current of 6 A, use Eq. 3.21 to calculate (*i*) the magnetic stored energy in the air gap and (*ii*) the magnetic stored energy in the core. Show that the total magnetic stored energy is given by Eq. 1.47.

1.18 Consider the inductor of Problem 1.17. Write a simple design program in the form of a MATLAB script to calculate the number of turns and air-gap length as a function of the desired inductance. The script should be written to request a value of inductance (in mH) from the user, with the output being the air-gap length in mm and the number of turns.

The inductor is to be operated with a sinusoidal current at 60 Hz, and it must be designed such that the peak core flux density will be equal to 1.7 T when the inductor current is equal to 4.5 A rms. Write your script to reject any designs for which the gap length is out of the range of 0.05 mm to 5.0 mm or for which the number of turns drops below 5.

Using your program find (*a*) the minimum and (*b*) the maximum inductances (to the nearest mH) which will satisfy the given constraints. For each of these values, find the required air-gap length and the number of turns as well as the rms voltage corresponding to the peak core flux.

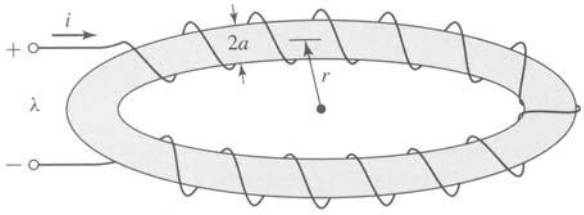

Figure 1.30 Toroidal winding for Problem 1.19.

1.19 A proposed energy storage mechanism consists of an N-turn coil wound around a large nonmagnetic ($\mu = \mu_0$) toroidal form as shown in Fig. 1.30. As can be seen from the figure, the toroidal form has a circular cross section of radius a and toroidal radius r, measured to the center of the cross section. The geometry of this device is such that the magnetic field can be considered to be zero everywhere outside the toroid. Under the assumption that $a \ll r$, the H field inside the toroid can be considered to be directed around the toroid and of uniform magnitude

$$H = \frac{Ni}{2\pi r}$$

For a coil with $N = 1000$ turns, $r = 10$ m, and $a = 0.45$ m:

a. Calculate the coil inductance L.

b. The coil is to be charged to a magnetic flux density of 1.75 T. Calculate the total stored magnetic energy in the torus when this flux density is achieved.

c. If the coil is to be charged at a uniform rate (i.e., $di/dt =$ constant), calculate the terminal voltage required to achieve the required flux density in 30 sec. Assume the coil resistance to be negligible.

1.20 Figure 1.31 shows an inductor wound on a laminated iron core of rectangular cross section. Assume that the permeability of the iron is infinite. Neglect magnetic leakage and fringing in the two air gaps (total gap length $= g$). The N-turn winding is insulated copper wire whose resistivity is ρ Ω·m. Assume

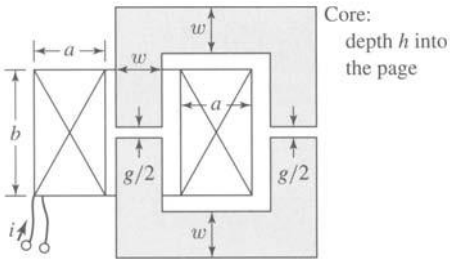

Figure 1.31 Iron-core inductor for Problem 1.20.

that the fraction f_w of the winding space is available for copper; the rest of the space is used for insulation.

a. Calculate the cross-sectional area and volume of the copper in the winding space.

b. Write an expression for the flux density B in the inductor in terms of the current density J_{cu} in the copper winding.

c. Write an expression for the copper current density J_{cu} in terms of the coil current I, the number of turns N, and the coil geometry.

d. Derive an expression for the electric power dissipation in the coil in terms of the current density J_{cu}.

e. Derive an expression for the magnetic stored energy in the inductor in terms of the applied current density J_{cu}.

f. From parts (d) and (e) derive an expression for the L/R time constant of the inductor. Note that this expression is independent of the number of turns in the coil and does not change as the inductance and coil resistance are changed by varying the number of turns.

1.21 The inductor of Fig. 1.31 has the following dimensions:

$$a = h = w = 1.5 \text{ cm} \quad b = 2 \text{ cm} \quad g = 0.2 \text{ cm}$$

The winding factor (i.e., the fraction of the total winding area occupied by conductor) is $f_w = 0.55$. The resistivity of copper is $1.73 \times 10^{-8}\ \Omega\cdot\text{m}$. When the coil is operated with a constant dc applied voltage of 35 V, the air-gap flux density is measured to be 1.4 T. Find the power dissipated in the coil, coil current, number of turns, coil resistance, inductance, time constant, and wire size to the nearest standard size. (Hint: Wire size can be found from the expression

$$\text{AWG} = 36 - 4.312 \ln\left(\frac{A_{\text{wire}}}{1.267 \times 10^{-8}}\right)$$

where AWG is the wire size, expressed in terms of the American Wire Gauge, and A_{wire} is the conductor cross-sectional area measured in m^2.)

1.22 The magnetic circuit of Fig. 1.32 has two windings and two air gaps. The core can be assumed to be of infinite permeability. The core dimensions are indicated in the figure.

a. Assuming coil 1 to be carrying a current I_1 and the current in coil 2 to be zero, calculate (*i*) the magnetic flux density in each of the air gaps, (*ii*) the flux linkage of winding 1, and (*iii*) the flux linkage of winding 2.

b. Repeat part (a), assuming zero current in winding 1 and a current I_2 in winding 2.

c. Repeat part (a), assuming the current in winding 1 to be I_1 and the current in winding 2 to be I_2.

d. Find the self-inductances of windings 1 and 2 and the mutual inductance between the windings.

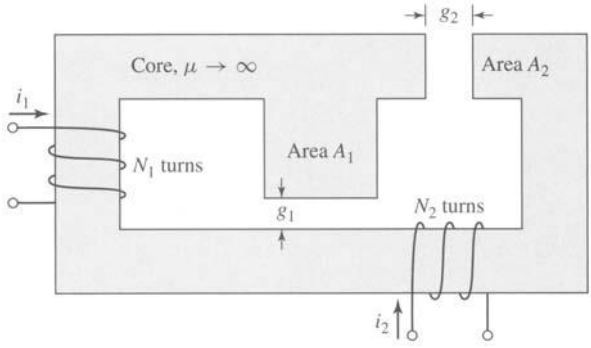

Figure 1.32 Magnetic circuit for Problem 1.22.

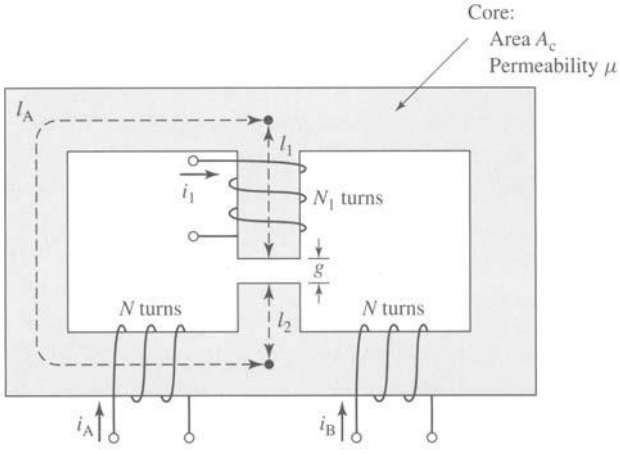

Figure 1.33 Symmetric magnetic circuit for Problem 1.23.

1.23 The symmetric magnetic circuit of Fig. 1.33 has three windings. Windings A and B each have N turns and are wound on the two bottom legs of the core. The core dimensions are indicated in the figure.

a. Find the self-inductances of each of the windings.

b. Find the mutual inductances between the three pairs of windings.

c. Find the voltage induced in winding 1 by time-varying currents $i_A(t)$ and $i_B(t)$ in windings A and B. Show that this voltage can be used to measure the imbalance between two sinusoidal currents of the same frequency.

1.24 The reciprocating generator of Fig. 1.34 has a movable plunger (position x) which is supported so that it can slide in and out of the magnetic yoke while maintaining a constant air gap of length g on each side adjacent to the yoke. Both the yoke and the plunger can be considered to be of infinite permeability. The motion of the plunger is constrained such that its position is limited to $0 \le x \le w$.

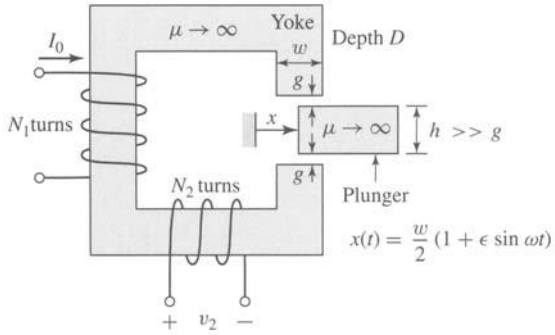

Figure 1.34 Reciprocating generator for Problem 1.24.

There are two windings on this magnetic circuit. The first has N_1 turns and carries a constant dc current I_0. The second, which has N_2 turns, is open-circuited and can be connected to a load.

a. Neglecting any fringing effects, find the mutual inductance between windings 1 and 2 as a function of the plunger position x.

b. The plunger is driven by an external source so that its motion is given by

$$x(t) = \frac{w(1 + \epsilon \sin \omega t)}{2}$$

where $\epsilon \leq 1$. Find an expression for the sinusoidal voltage which is generated as a result of this motion.

1.25 Figure 1.35 shows a configuration that can be used to measure the magnetic characteristics of electrical steel. The material to be tested is cut or punched into circular laminations which are then stacked (with interspersed insulation to avoid eddy-current formation). Two windings are wound over this stack of laminations: the first, with N_l turns, is used to excite a magnetic field in the lamination stack; the second, with N_2 turns, is used to sense the resultant magnetic flux.

The accuracy of the results requires that the magnetic flux density be uniform within the laminations. This can be accomplished if the lamination width $t = R_o - R_i$ is much smaller than the lamination radius and if the excitation winding is wound uniformly around the lamination stack. For the purposes of this analysis, assume there are n laminations, each of thickness Δ. Also assume that winding 1 is excited by a current $i_1 = I_0 \sin \omega t$.

a. Find the relationship between the magnetic field intensity H in the laminations and current i_1 in winding 1.

b. Find the relationship between the voltage v_2 and the time rate of change of the flux density B in the laminations.

c. Find the relationship between the voltage $v_0 = G \int v_2 \, dt$ and the flux density.

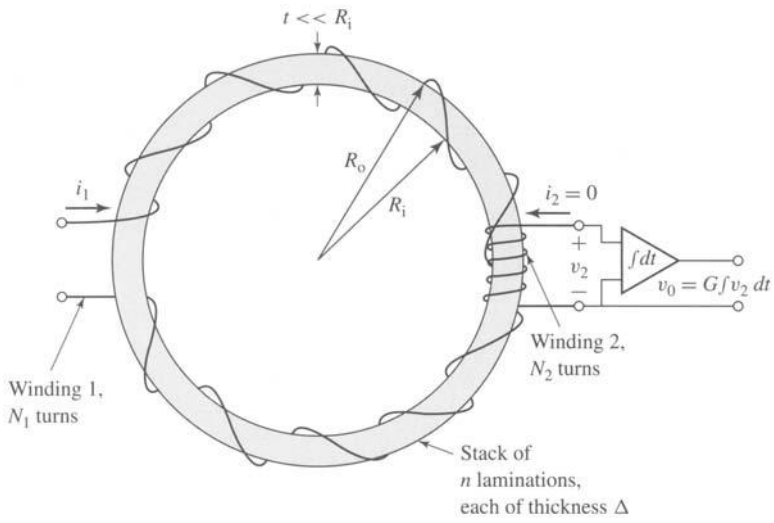

Figure 1.35 Configuration for measurement of magnetic properties of electrical steel.

In this problem, we have shown that the magnetic field intensity H and the magnetic flux density B in the laminations are proportional to the current i_1 and the voltage v_2 by known constants. Thus, B and H in the magnetic steel can be measured directly, and the B-H characteristics as discussed in Sections 1.3 and 1.4 can be determined.

1.26 From the dc magnetization curve of Fig. 1.10 it is possible to calculate the relative permeability $\mu_r = B_c/(\mu_0 H_c)$ for M-5 electrical steel as a function of the flux level B_c. Assuming the core of Fig. 1.2 to be made of M-5 electrical steel with the dimensions given in Example 1.1, calculate the maximum flux density such that the reluctance of the core never exceeds 5 percent of the reluctance of the total magnetic circuit.

1.27 In order to test the properties of a sample of electrical steel, a set of laminations of the form of Fig. 1.35 have been stamped out of a sheet of the electrical steel of thickness 3.0 mm. The radii of the laminations are $R_i = 75$ mm and $R_o = 82$ mm. They have been assembled in a stack of 10 laminations (separated by appropriate insulation to eliminate eddy currents) for the purposes of testing the magnetic properties at a frequency of 100 Hz.

a. The flux in the lamination stack will be excited from a variable-amplitude, 100-Hz voltage source whose peak amplitude is 30 V (peak-to-peak). Calculate the number of turns N_1 for the excitation winding required to insure that the lamination stack can be excited up to a peak flux density of 2.0 T.

b. With a secondary winding of $N_2 = 20$ turns and an integrator gain $G = 1000$, the output of the integrator is observed to be 7.0 V

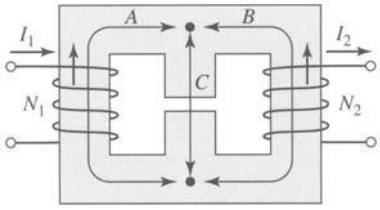

Figure 1.36 Magnetic circuit for Problem 1.28.

peak-to-peak. Calculate (*i*) the corresponding peak flux in the lamination stack and (*ii*) the corresponding amplitude of the voltage applied to the excitation winding.

1.28 The coils of the magnetic circuit shown in Fig. 1.36 are connected in series so that the mmf's of paths A and B both tend to set up flux in the center leg C in the same direction. The coils are wound with equal turns, $N_1 = N_2 = 100$. The dimensions are:

Cross-section area of A and B legs = 7 cm^2
Cross-section area of C legs = 14 cm^2
Length of A path = 17 cm
Length of B path = 17 cm
Length of C path = 5.5 cm
Air gap = 0.4 cm

The material is M-5 grade, 0.012-in steel, with a stacking factor of 0.94. Neglect fringing and leakage.

a. How many amperes are required to produce a flux density of 1.2 T in the air gap?
b. Under the condition of part (a), how many joules of energy are stored in the magnetic field in the air gap?
c. Calculate the inductance.

1.29 The following table includes data for the top half of a symmetric 60-Hz hysteresis loop for a specimen of magnetic steel:

B, T	0	0.2	0.4	0.6	0.7	0.8	0.9	1.0	0.95	0.9	0.8	0.7	0.6	0.4	0.2	0
$H, A \cdot$ turns/m	48	52	58	73	85	103	135	193	80	42	2	−18	−29	−40	−45	−48

Using MATLAB, (*a*) plot this data, (*b*) calculate the area of the hysteresis loop in joules, and (*c*) calculate the corresponding 60-Hz core loss in Watts/kg. The density of M-5 steel is 7.65 g/cm^3.

1.30 Assume the magnetic circuit of Problem 1.1 and Fig. 1.24 to be made up of M-5 electrical steel with the properties described in Figs. 1.10, 1.12, and 1.14. Assume the core to be operating with a 60-Hz sinusoidal flux density of the

rms flux density of 1.1 T. Neglect the winding resistance and leakage inductance. Find the winding voltage, rms winding current, and core loss for this operating condition. The density of M-5 steel is 7.65 g/cm^3.

1.31 Repeat Example 1.8 under the assumption that all the core dimensions are doubled.

1.32 Using the magnetization characteristics for samarium cobalt given in Fig. 1.19, find the point of maximum energy product and the corresponding flux density and magnetic field intensity. Using these values, repeat Example 1.10 with the Alnico 5 magnet replaced by a samarium-cobalt magnet. By what factor does this reduce the magnet volume required to achieve the desired air-gap flux density?

1.33 Using the magnetization characteristics for neodymium-iron-boron given in Fig. 1.19, find the point of maximum-energy product and the corresponding flux density and magnetic field intensity. Using these values, repeat Example 1.10 with the Alnico 5 magnet replaced by a neodymium-iron-boron magnet. By what factor does this reduce the magnet volume required to achieve the desired air-gap flux density?

1.34 Figure 1.37 shows the magnetic circuit for a permanent-magnet loudspeaker. The voice coil (not shown) is in the form of a circular cylindrical coil which fits in the air gap. A samarium-cobalt magnet is used to create the air-gap dc magnetic field which interacts with the voice coil currents to produce the motion of the voice coil. The designer has determined that the air gap must have radius $R = 1.8$ cm, length $g = 0.1$ cm, and height $h = 0.9$ cm.

Assuming that the yoke and pole piece are of infinite magnetic permeability ($\mu \to \infty$), find the magnet height h_m and the magnet radius R_m that will result in an air-gap magnetic flux density of 1.2 T and require the smallest magnet volume.

(Hint: Refer to Example 1.10 and to Fig. 1.19 to find the point of maximum energy product for samarium cobalt.)

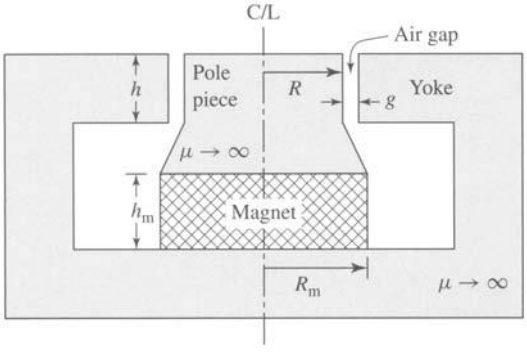

Figure 1.37 Magnetic circuit for the loudspeaker of Problem 1.34 (voice coil not shown).

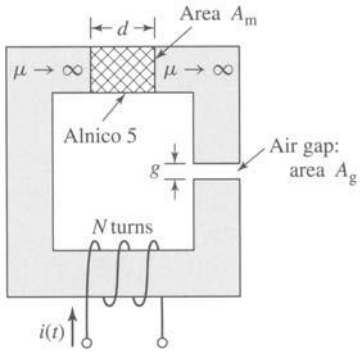

Figure 1.38 Magnetic circuit for Problem 1.35.

1.35 It is desired to achieve a time-varying magnetic flux density in the air gap of the magnetic circuit of Fig. 1.38 of the form

$$B_g = B_0 + B_1 \sin \omega t$$

where $B_0 = 0.5$ T and $B_l = 0.25$ T. The dc field B_0 is to be created by a neodimium-iron-boron magnet, whereas the time-varying field is to be created by a time-varying current.

For $A_g = 6\ \text{cm}^2$, $g = 0.4$ cm, and $N = 200$ turns, find:

a. the magnet length d and the magnet area A_m that will achieve the desired dc air-gap flux density and minimize the magnet volume.

b. the minimum and maximum values of the time-varying current required to achieve the desired time-varying air-gap flux density. Will this current vary sinusoidally in time?

CHAPTER 2

Transformers

Before we proceed with a study of electric machinery, it is desirable to discuss certain aspects of the theory of magnetically-coupled circuits, with emphasis on transformer action. Although the static transformer is not an energy conversion device, it is an indispensable component in many energy conversion systems. A significant component of ac power systems, it makes possible electric generation at the most economical generator voltage, power transfer at the most economical transmission voltage, and power utilization at the most suitable voltage for the particular utilization device. The transformer is also widely used in low-power, low-current electronic and control circuits for performing such functions as matching the impedances of a source and its load for maximum power transfer, isolating one circuit from another, or isolating direct current while maintaining ac continuity between two circuits.

The transformer is one of the simpler devices comprising two or more electric circuits coupled by a common magnetic circuit. Its analysis involves many of the principles essential to the study of electric machinery. Thus, our study of the transformer will serve as a bridge between the introduction to magnetic-circuit analysis of Chapter 1 and the more detailed study of electric machinery to follow.

2.1 INTRODUCTION TO TRANSFORMERS

Essentially, a transformer consists of two or more windings coupled by mutual magnetic flux. If one of these windings, the *primary,* is connected to an alternating-voltage source, an alternating flux will be produced whose amplitude will depend on the primary voltage, the frequency of the applied voltage, and the number of turns. The mutual flux will link the other winding, the *secondary,*[1] and will induce a voltage in it

[1] It is conventional to think of the "input" to the transformer as the primary and the "output" as the secondary. However, in many applications, power can flow either way and the concept of primary and secondary windings can become confusing. An alternate terminology, which refers to the windings as "high-voltage" and "low-voltage," is often used and eliminates this confusion.

whose value will depend on the number of secondary turns as well as the magnitude of the mutual flux and the frequency. By properly proportioning the number of primary and secondary turns, almost any desired *voltage ratio,* or *ratio of transformation,* can be obtained.

The essence of transformer action requires only the existence of time-varying mutual flux linking two windings. Such action can occur for two windings coupled through air, but coupling between the windings can be made much more effectively using a core of iron or other ferromagnetic material, because most of the flux is then confined to a definite, high-permeability path linking the windings. Such a transformer is commonly called an *iron-core transformer.* Most transformers are of this type. The following discussion is concerned almost wholly with iron-core transformers.

As discussed in Section 1.4, to reduce the losses caused by eddy currents in the core, the magnetic circuit usually consists of a stack of thin laminations. Two common types of construction are shown schematically in Fig. 2.1. In the *core type* (Fig. 2.1a) the windings are wound around two legs of a rectangular magnetic core; in the *shell type* (Fig. 2.1b) the windings are wound around the center leg of a three-legged core. Silicon-steel laminations 0.014 in thick are generally used for transformers operating at frequencies below a few hundred hertz. Silicon steel has the desirable properties of low cost, low core loss, and high permeability at high flux densities (1.0 to 1.5 T). The cores of small transformers used in communication circuits at high frequencies and low energy levels are sometimes made of compressed powdered ferromagnetic alloys known as *ferrites.*

In each of these configurations, most of the flux is confined to the core and therefore links both windings. The windings also produce additional flux, known as *leakage flux,* which links one winding without linking the other. Although leakage flux is a small fraction of the total flux, it plays an important role in determining the behavior of the transformer. In practical transformers, leakage is reduced by

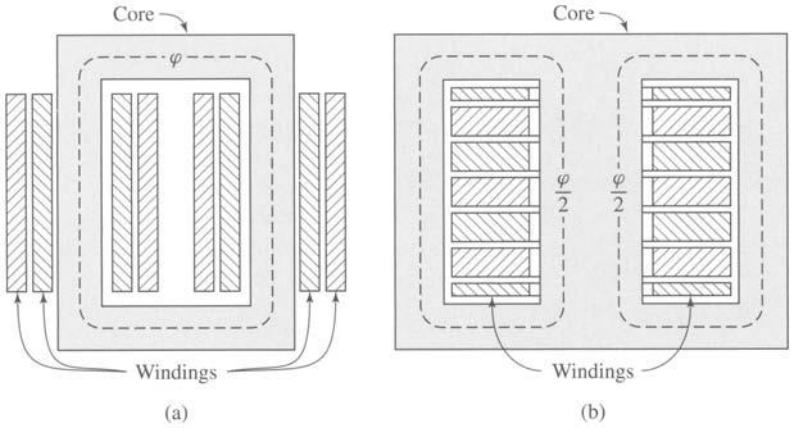

Figure 2.1 Schematic views of (a) core-type and (b) shell-type transformers.

subdividing the windings into sections placed as close together as possible. In the core-type construction, each winding consists of two sections, one section on each of the two legs of the core, the primary and secondary windings being concentric coils. In the shell-type construction, variations of the concentric-winding arrangement may be used, or the windings may consist of a number of thin "pancake" coils assembled in a stack with primary and secondary coils interleaved.

Figure 2.2 illustrates the internal construction of a *distribution transformer* such as is used in public utility systems to provide the appropriate voltage for use by residential consumers. A large power transformer is shown in Fig. 2.3.

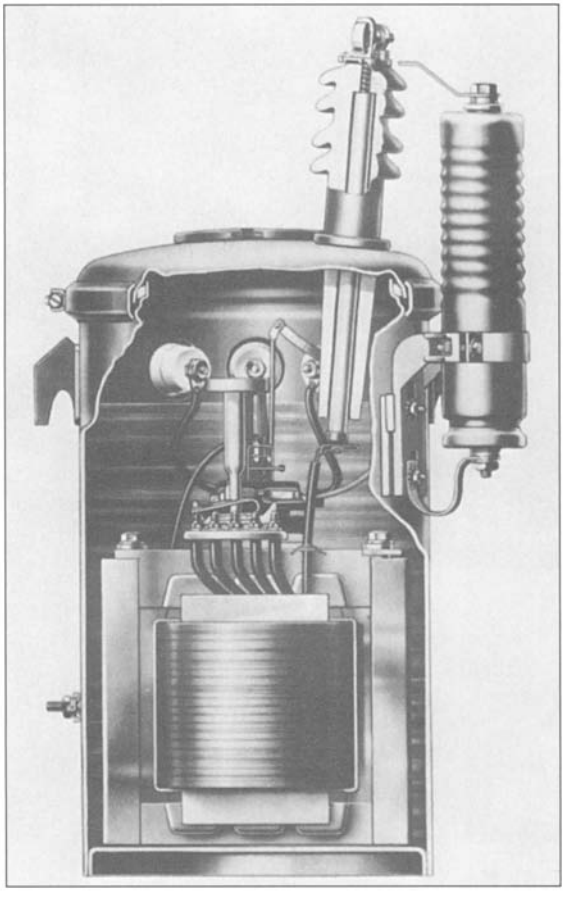

Figure 2.2 Cutaway view of self-protected distribution transformer typical of sizes 2 to 25 kVA, 7200:240/120 V. Only one high-voltage insulator and lightning arrester is needed because one side of the 7200-V line and one side of the primary are grounded. (*General Electric Company.*)

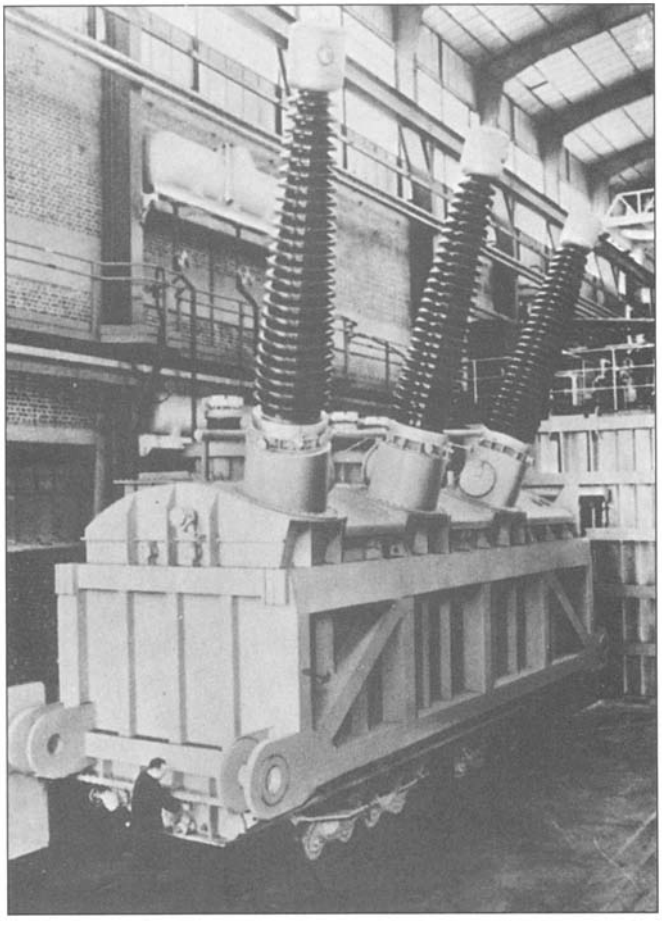

Figure 2.3 A 660-MVA three-phase 50-Hz transformer used to step up generator voltage of 20 kV to transmission voltage of 405 kV. (*CEM Le Havre, French Member of the Brown Boveri Corporation.*)

2.2 NO-LOAD CONDITIONS

Figure 2.4 shows in schematic form a transformer with its secondary circuit open and an alternating voltage v_1 applied to its primary terminals. To simplify the drawings, it is common on schematic diagrams of transformers to show the primary and secondary windings as if they were on separate legs of the core, as in Fig. 2.4, even though the windings are actually interleaved in practice. As discussed in Section 1.4, a small steady-state current i_φ, called the *exciting current,* flows in the primary and establishes

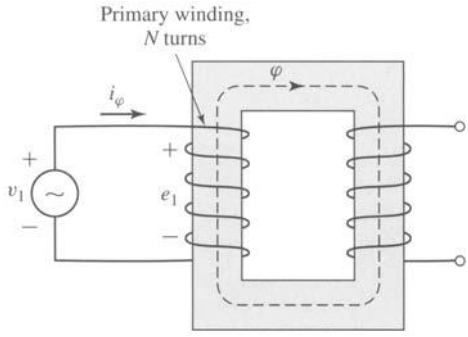

Figure 2.4 Transformer with open secondary.

an alternating flux in the magnetic circuit.[2] This flux induces an emf in the primary equal to

$$e_1 = \frac{d\lambda_1}{dt} = N_1 \frac{d\varphi}{dt} \tag{2.1}$$

where

λ_1 = flux linkage of the primary winding
φ = flux in the core linking both windings
N_1 = number of turns in the primary winding

The voltage e_1 is in volts when φ is in webers. This emf, together with the voltage drop in the *primary resistance* R_1, must balance the applied voltage v_1; thus

$$v_1 = R_1 i_\varphi + e_1 \tag{2.2}$$

Note that for the purposes of the current discussion, we are neglecting the effects of primary leakage flux, which will add an additional induced-emf term in Eq. 2.2. In typical transformers, this flux is a small percentage of the core flux, and it is quite justifiable to neglect it for our current purposes. It does however play an important role in the behavior of transformers and is discussed in some detail in Section 2.4.

In most large transformers, the no-load resistance drop is very small indeed, and the induced emf e_1 very nearly equals the applied voltage v_1. Furthermore, the waveforms of voltage and flux are very nearly sinusoidal. The analysis can then be greatly simplified, as we have shown in Section 1.4. Thus, if the instantaneous flux is

$$\varphi = \phi_{\max} \sin \omega t \tag{2.3}$$

[2] In general, the exciting current corresponds to the net ampere-turns (mmf) acting on the magnetic circuit, and it is not possible to distinguish whether it flows in the primary or secondary winding or partially in each winding.

the induced voltage is

$$e_1 = N_1 \frac{d\varphi}{dt} = \omega N_1 \phi_{\max} \cos \omega t \tag{2.4}$$

where $\phi_{\max}$ is the maximum value of the flux and $\omega = 2\pi f$, the frequency being f Hz. For the current and voltage reference directions shown in Fig. 2.4, the induced emf leads the flux by 90°. The rms value of the induced emf e_1 is

$$E_1 = \frac{2\pi}{\sqrt{2}} f N_1 \phi_{\max} = \sqrt{2}\pi f N_1 \phi_{\max} \tag{2.5}$$

If the resistive voltage drop is negligible, the counter emf equals the applied voltage. Under these conditions, if a sinusoidal voltage is applied to a winding, a sinusoidally varying core flux must be established whose maximum value $\phi_{\max}$ satisfies the requirement that E_1 in Eq. 2.5 equal the rms value V_1 of the applied voltage; thus

$$\phi_{\max} = \frac{V_1}{\sqrt{2}\pi f N_1} \tag{2.6}$$

Under these conditions, the core flux is determined solely by the applied voltage, its frequency, and the number of turns in the winding. This important relation applies not only to transformers but also to any device operated with a sinusoidally-alternating impressed voltage, as long as the resistance and leakage-inductance voltage drops are negligible. The core flux is fixed by the applied voltage, and the required exciting current is determined by the magnetic properties of the core; the exciting current must adjust itself so as to produce the mmf required to create the flux demanded by Eq. 2.6.

Because of the nonlinear magnetic properties of iron, the waveform of the exciting current differs from the waveform of the flux. A curve of the exciting current as a function of time can be found graphically from the ac hysteresis loop, as is discussed in Section 1.4 and shown in Fig. 1.11.

If the exciting current is analyzed by Fourier-series methods, it is found to consist of a fundamental component and a series of odd harmonics. The fundamental component can, in turn, be resolved into two components, one in phase with the counter emf and the other lagging the counter emf by 90°. The in-phase component supplies the power absorbed by hysteresis and eddy-current losses in the core. It is referred to as *core-loss component* of the exciting current. When the core-loss component is subtracted from the total exciting current, the remainder is called the *magnetizing current*. It comprises a fundamental component lagging the counter emf by 90°, together with all the harmonics. The principal harmonic is the third. For typical power transformers, the third harmonic usually is about 40 percent of the exciting current.

Except in problems concerned directly with the effects of harmonic currents, the peculiarities of the exciting-current waveform usually need not be taken into account, because the exciting current itself is small, especially in large transformers. For example, the exciting current of a typical power transformer is about 1 to 2 percent of full-load current. Consequently the effects of the harmonics usually are swamped

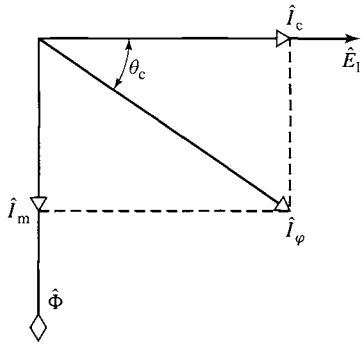

Figure 2.5 No-load phasor diagram.

out by the sinusoidal-currents supplied to other linear elements in the circuit. The exciting current can then be represented by an equivalent sinusoidal current which has the same rms value and frequency and produces the same average power as the actual exciting current. Such representation is essential to the construction of a *phasor diagram*, which represents the phase relationship between the various voltages and currents in a system in vector form. Each signal is represented by a phasor whose length is proportional to the amplitude of the signal and whose angle is equal to the phase angle of that signal as measured with respect to a chosen reference signal.

In Fig. 2.5, the phasors $\hat{E}_1$ and $\hat{\Phi}$ respectively, represent the rms values of the induced emf and the flux. The phasor $\hat{I}_\varphi$ represents the rms value of the equivalent sinusoidal exciting current. It lags the induced emf $\hat{E}_1$ by a phase angle θ_c.

The core loss P_c, equal to the product of the in-phase components of the $\hat{E}_1$ and $\hat{I}_\varphi$, is given by

$$P_c = E_1 I_\varphi \cos\theta_c \tag{2.7}$$

The component $\hat{I}_c$ in phase with $\hat{E}_1$ is the core-loss current. The component $\hat{I}_m$ in phase with the flux represents an equivalent sine wave current having the same rms value as the magnetizing current. Typical exciting volt-ampere and core-loss characteristics of high-quality silicon steel used for power and distribution transformer laminations are shown in Figs. 1.12 and 1.14.

EXAMPLE 2.1

In Example 1.8 the core loss and exciting voltamperes for the core of Fig. 1.15 at $B_{max} = 1.5$ T and 60 Hz were found to be

$$P_c = 16\text{ W} \qquad (VI)_{rms} = 20\text{ VA}$$

and the induced voltage was $274/\sqrt{2} = 194$ V rms when the winding had 200 turns.

Find the power factor, the core-loss current I_c, and the magnetizing current I_m.

■ Solution

$$\text{Power factor } \cos\theta_c = \tfrac{16}{20} = 0.80 \text{ (lag)} \quad \text{thus} \quad \theta_c = -36.9^\circ$$

Note that we know that the power factor is lagging because the system is inductive.

Exciting current $I_\varphi = \frac{20}{194} = 0.10$ A rms

Core-loss component $I_c = \frac{16}{194} = 0.082$ A rms

Magnetizing component $I_m = I_\varphi |\sin\theta_c| = 0.060$ A rms

---

2.3 EFFECT OF SECONDARY CURRENT; IDEAL TRANSFORMER

As a first approximation to a quantitative theory, consider a transformer with a primary winding of N_1 turns and a secondary winding of N_2 turns, as shown schematically in Fig. 2.6. Notice that the secondary current is defined as positive out of the winding; thus positive secondary current produces an mmf in the opposite direction from that created by positive primary current. Let the properties of this transformer be idealized under the assumption that winding resistances are negligible, that all the flux is confined to the core and links both windings (i.e., leakage flux is assumed negligible), that there are no losses in the core, and that the permeability of the core is so high that only a negligible exciting mmf is required to establish the flux. These properties are closely approached but never actually attained in practical transformers. A hypothetical transformer having these properties is often called an *ideal transformer*.

Under the above assumptions, when a time-varying voltage v_1 is impressed on the primary terminals, a core flux φ must be established such that the counter emf e_1 equals the impressed voltage. Thus

$$v_1 = e_1 = N_1 \frac{d\varphi}{dt} \tag{2.8}$$

The core flux also links the secondary and produces an induced emf e_2, and an equal secondary terminal voltage v_2, given by

$$v_2 = e_2 = N_2 \frac{d\varphi}{dt} \tag{2.9}$$

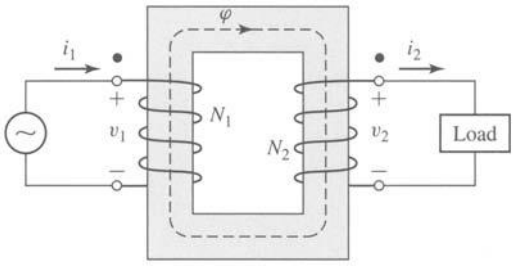

Figure 2.6 Ideal transformer and load.

From the ratio of Eqs. 2.8 and 2.9,

$$\frac{v_1}{v_2} = \frac{N_1}{N_2} \tag{2.10}$$

Thus an ideal transformer transforms voltages in the direct ratio of the turns in its windings.

Now let a load be connected to the secondary. A current i_2 and an mmf $N_2 i_2$ are then present in the secondary. Since the core permeability is assumed very large and since the impressed primary voltage sets the core flux as specfied by Eq. 2.8, the core flux is unchanged by the presence of a load on the secondary, and hence the net exciting mmf acting on the core (equal to $N_1 i_1 - N_2 i_2$) will not change and hence will remain negligible. Thus

$$N_1 i_1 - N_2 i_2 = 0 \tag{2.11}$$

From Eq. 2.11 we see that a compensating primary mmf must result to cancel that of the secondary. Hence

$$N_1 i_1 = N_2 i_2 \tag{2.12}$$

Thus we see that the requirement that the net mmf remain unchanged is the means by which the primary "knows" of the presence of load current in the secondary; any change in mmf flowing in the secondary as the result of a load must be accompanied by a corresponding change in the primary mmf. Note that for the reference directions shown in Fig. 2.6 the mmf's of i_1 and i_2 are in opposite directions and therefore compensate. The net mmf acting on the core therefore is zero, in accordance with the assumption that the exciting current of an ideal transformer is zero.

From Eq. 2.12

$$\frac{i_1}{i_2} = \frac{N_2}{N_1} \tag{2.13}$$

Thus an ideal transformer transforms currents in the inverse ratio of the turns in its windings.

Also notice from Eqs. 2.10 and 2.13 that

$$v_1 i_1 = v_2 i_2 \tag{2.14}$$

i.e., instantaneous power input to the primary equals the instantaneous power output from the secondary, a necessary condition because all dissipative and energy storage mechanisms in the transformer have been neglected.

An additional property of the ideal transformer can be seen by considering the case of a sinusoidal applied voltage and an impedance load. Phasor symbolism can be used. The circuit is shown in simplified form in Fig. 2.7a, in which the dot-marked terminals of the transformer correspond to the similarly marked terminals in Fig. 2.6. The dot markings indicate terminals of corresponding polarity; i.e., if one follows through the primary and secondary windings of Fig. 2.6, beginning at their dot-marked terminals, one will find that both windings encircle the core in the same direction with respect to the flux. Therefore, if one compares the voltages of the two windings, the voltages from a dot-marked to an unmarked terminal will be of the

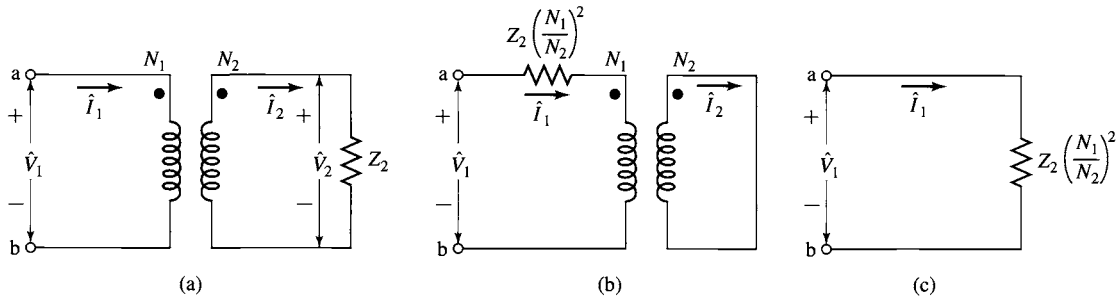

Figure 2.7 Three circuits which are identical at terminals ab when the transformer is ideal.

same instantaneous polarity for primary and secondary. In other words, the voltages $\hat{V}_1$ and $\hat{V}_2$ in Fig. 2.7a are in phase. Also currents $\hat{I}_1$ and $\hat{I}_2$ are in phase as seen from Eq. 2.12. Note again that the polarity of $\hat{I}_1$ is defined as into the dotted terminal and the polarity of $\hat{I}_2$ is defined as out of the dotted terminal.

We next investigate the impendance transformation properties of the ideal transformer. In phasor form, Eqs. 2.10 and 2.13 can be expressed as

$$\hat{V}_1 = \frac{N_1}{N_2}\hat{V}_2 \quad \text{and} \quad \hat{V}_2 = \frac{N_2}{N_1}\hat{V}_1 \tag{2.15}$$

$$\hat{I}_1 = \frac{N_2}{N_1}\hat{I}_2 \quad \text{and} \quad \hat{I}_2 = \frac{N_1}{N_2}\hat{I}_1 \tag{2.16}$$

From these equations

$$\frac{\hat{V}_1}{\hat{I}_1} = \left(\frac{N_1}{N_2}\right)^2 \frac{\hat{V}_2}{\hat{I}_2} \tag{2.17}$$

Noting that the load impedance Z_2 is related to the secondary voltages and currents

$$Z_2 = \frac{\hat{V}_2}{\hat{I}_2} \tag{2.18}$$

where Z_2 is the complex impedance of the load. Consequently, as far as its effect is concerned, an impedance Z_2 in the secondary circuit can be replaced by an equivalent impedance Z_1 in the primary circuit, provided that

$$Z_1 = \left(\frac{N_1}{N_2}\right)^2 Z_2 \tag{2.19}$$

Thus, the three circuits of Fig. 2.7 are indistinguishable as far as their performance viewed from terminals ab is concerned. Transferring an impedance from one side of a transformer to the other in this fashion is called *referring the impedance* to the

other side; impedances transform as the square of the turns ratio. In a similar manner, voltages and currents can be *referred* to one side or the other by using Eqs. 2.15 and 2.16 to evaluate the equivalent voltage and current on that side.

To summarize, *in an ideal transformer, voltages are transformed in the direct ratio of turns, currents in the inverse ratio, and impedances in the direct ratio squared; power and voltamperes are unchanged.*

EXAMPLE 2.2

The equivalent circuit of Fig. 2.8a shows an ideal transformer with an impedance $R_2 + jX_2 = 1 + j4\ \Omega$ connected in series with the secondary. The turns ratio $N_1/N_2 = 5{:}1$. (*a*) Draw an equivalent circuit with the series impedance referred to the primary side. (*b*) For a primary voltage of 120 V rms and a short connected across the terminals A-B, calculate the primary current and the current flowing in the short.

■ Solution

a. The new equivalent is shown in Fig. 2.8b. The secondary impedance is referred to the primary by the turns ratio squared. Thus

$$R_2' + jX_2' = \left(\frac{N_1}{N_2}\right)^2 (R_2 + jX_2)$$
$$= 25 + j100\ \Omega$$

b. From Eq. 2.19, a short at terminals A-B will appear as a short at the primary of the ideal transformer in Fig. 2.8b since the zero voltage of the short is reflected by the turns ratio N_1/N_2 to the primary. Hence the primary current will be given by

$$\hat{I}_1 = \frac{\hat{V}_1}{R_2' + jX_2'} = \frac{120}{25 + j100} = 0.28 - j1.13 \text{ A rms}$$

corresponding to a magnitude of 1.16 A rms. From Eq. 2.13, the secondary current will equal $N_1/N_2 = 5$ times that of the current in the primary. Thus the current in the short will have a magnitude of $5(1.16) = 5.8$ A rms.

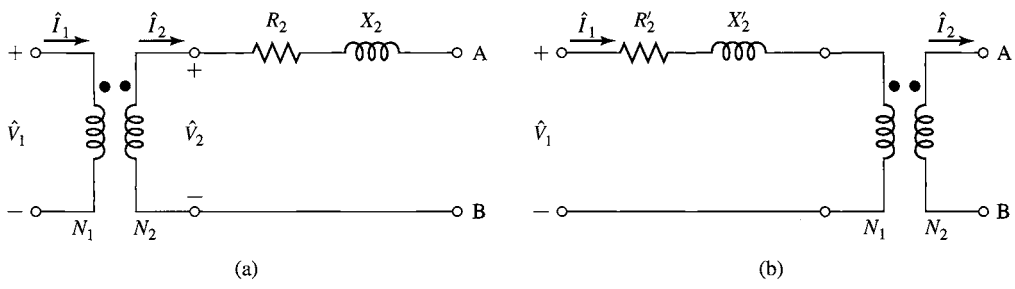

Figure 2.8 Equivalent circuits for Example 2.2. (a) Impedance in series with the secondary. (b) Impedance referred to the primary.

Practice Problem 2.1

Repeat part (*b*) of Example 2.2 for a series impedance $R_2 + jX_2 = 0.05 + j0.97\ \Omega$ and a turns ratio of 14:1.

Solution

The primary current is $0.03 - j0.63$ A rms, corresponding to a magnitude of 0.63 A rms. The current in the short will be 14 times larger and thus will be of magnitude 8.82 A rms.

2.4 TRANSFORMER REACTANCES AND EQUIVALENT CIRCUITS

The departures of an actual transformer from those of an ideal transformer must be included to a greater or lesser degree in most analyses of transformer performance. A more complete model must take into account the effects of winding resistances, leakage fluxes, and finite exciting current due to the finite (and indeed nonlinear) permeability of the core. In some cases, the capacitances of the windings also have important effects, notably in problems involving transformer behavior at frequencies above the audio range or during rapidly changing transient conditions such as those encountered in power system transformers as a result of voltage surges caused by lightning or switching transients. The analysis of these high-frequency problems is beyond the scope of the present treatment however, and accordingly the capacitances of the windings will be neglected.

Two methods of analysis by which departures from the ideal can be taken into account are (1) an equivalent-circuit technique based on physical reasoning and (2) a mathematical approach based on the classical theory of magnetically coupled circuits. Both methods are in everyday use, and both have very close parallels in the theories of rotating machines. Because it offers an excellent example of the thought process involved in translating physical concepts to a quantitative theory, the equivalent circuit technique is presented here.

To begin the development of a transformer equivalent circuit, we first consider the primary winding. The total flux linking the primary winding can be divided into two components: the resultant mutual flux, confined essentially to the iron core and produced by the combined effect of the primary and secondary currents, and the primary leakage flux, which links only the primary. These components are identified in the schematic transformer shown in Fig. 2.9, where for simplicity the primary and secondary windings are shown on opposite legs of the core. In an actual transformer with interleaved windings, the details of the flux distribution are more complicated, but the essential features remain the same.

The leakage flux induces voltage in the primary winding which adds to that produced by the mutual flux. Because the leakage path is largely in air, this flux and the voltage induced by it vary linearly with primary current $\hat{I}_1$. It can therefore be represented by a *primary leakage inductance* L_{l_1} (equal to the leakage-flux linkages

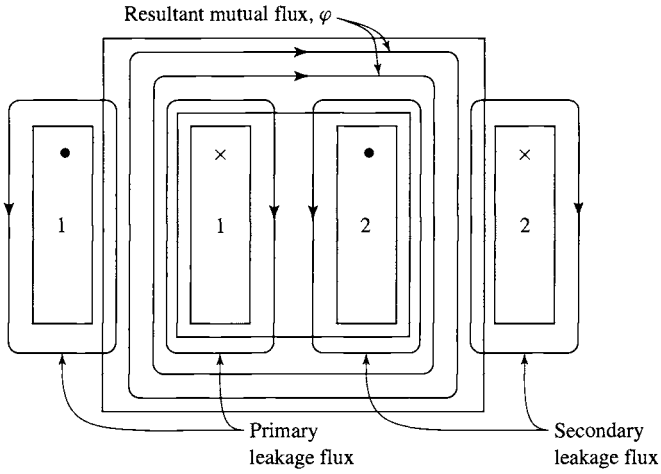

Figure 2.9 Schematic view of mutual and leakage fluxes in a transformer.

with the primary per unit of primary current). The corresponding *primary leakage reactance* X_{l_1} is found as

$$X_{l_1} = 2\pi f L_{l_1} \tag{2.20}$$

In addition, there will be a voltage drop in the primary resistance R_1.

We now see that the primary terminal voltage $\hat{V}_1$ consists of three components: the $\hat{I}_1 R_1$ drop in the primary resistance, the $\hat{I}_1 X_{l_1}$ drop arising from primary leakage flux, and the emf $\hat{E}_1$ induced in the primary by the resultant mutual flux. Fig. 2.10a shows an equivalent circuit for the primary winding which includes each of these voltages.

The resultant mutual flux links both the primary and secondary windings and is created by their combined mmf's. It is convenient to treat these mmf's by considering that the primary current must meet two requirements of the magnetic circuit: It must not only produce the mmf required to produce the resultant mutual flux, but it must also counteract the effect of the secondary mmf which acts to demagnetize the core. An alternative viewpoint is that the primary current must not only magnetize the core, it must also supply current to the load connected to the secondary. According to this picture, it is convenient to resolve the primary current into two components: an exciting component and a load component. The *exciting component* $\hat{I}_\varphi$ is defined as the additional primary current required to produce the resultant mutual flux. It is a nonsinusoidal current of the nature described in Section 2.2.[3] The *load component*

[3] In fact, the exciting current corresponds to the net mmf acting on the transformer core and cannot, in general, be considered to flow in the primary alone. However, for the purposes of this discussion, this distinction is not significant.

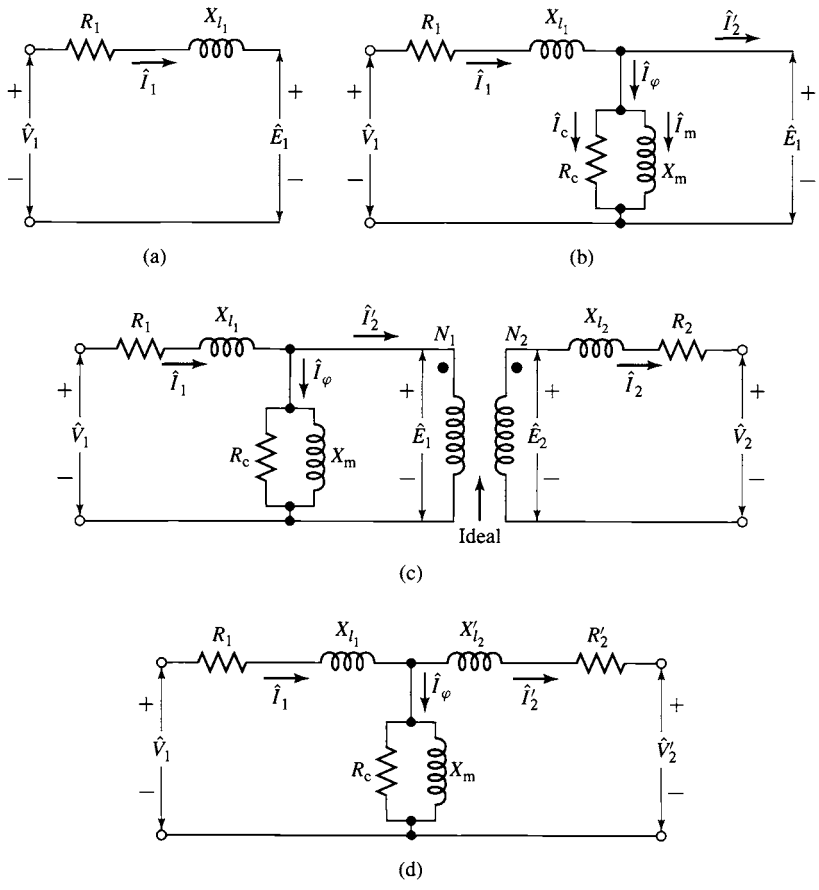

Figure 2.10 Steps in the development of the transformer equivalent circuit.

$\hat{I}_2'$ is defined as the component current in the primary which would exactly counteract the mmf of secondary current $\hat{I}_2$.

Since it is the exciting component which produces the core flux, the net mmf must equal $N_1\hat{I}_\varphi$ and thus we see that

$$\begin{aligned} N_1\hat{I}_\varphi &= N_1\hat{I}_1 - N_2\hat{I}_2 \\ &= N_1(\hat{I}_\varphi + \hat{I}_2') - N_2\hat{I}_2 \end{aligned} \tag{2.21}$$

and from Eq. 2.21 we see that

$$\hat{I}_2' = \frac{N_2}{N_1}\hat{I}_2 \tag{2.22}$$

From Eq. 2.22, we see that the load component of the primary current equals the secondary current referred to the primary as in an ideal transformer.

The exciting current can be treated as an equivalent sinusoidal current $\hat{I}_\varphi$, in the manner described in Section 2.2, and can be resolved into a core-loss component $\hat{I}_c$ in phase with the emf $\hat{E}_1$ and a magnetizing component $\hat{I}_m$ lagging $\hat{E}_1$ by 90°. In the equivalent circuit (Fig. 2.10b) the equivalent sinusoidal exciting current is accounted for by means of a shunt branch connected across $\hat{E}_1$, comprising a *core-loss resistance* R_c in parallel with a *magnetizing inductance* L_m whose reactance, known as the *magnetizing reactance,* is given by

$$X_m = 2\pi f L_m \tag{2.23}$$

In the equivalent circuit of (Fig. 2.10b) the power E_1^2/R_c accounts for the core loss due to the resultant mutual flux. R_c is referred to as the *magnetizing resistance* or *core-loss resistance* and together with X_m forms the *excitation branch* of the equivalent circuit, and we will refer to the parallel combination of R_c and X_m as the *exciting impedance* Z_φ. When R_c is assumed constant, the core loss is thereby assumed to vary as E_1^2 or (for sine waves) as $\phi_{max}^2 f^2$, where ϕ_{max} is the maximum value of the resultant mutual flux. Strictly speaking, the magnetizing reactance X_m varies with the saturation of the iron. When X_m is assumed constant, the magnetizing current is thereby assumed to be independent of frequency and directly proportional to the resultant mutual flux. Both R_c and X_m are usually determined at rated voltage and frequency; they are then assumed to remain constant for the small departures from rated values associated with normal operation.

We will next add to our equivalent circuit a representation of the secondary winding. We begin by recognizing that the resultant mutual flux $\hat{\Phi}$ induces an emf $\hat{E}_2$ in the secondary, and since this flux links both windings, the induced-emf ratio must equal the winding turns ratio, i.e.,

$$\frac{\hat{E}_1}{\hat{E}_2} = \frac{N_1}{N_2} \tag{2.24}$$

just as in an ideal transformer. This voltage transformation and the current transformation of Eq. 2.22 can be accounted for by introducing an ideal transformer in the equivalent circuit, as in Fig. 2.10c. Just as is the case for the primary winding, the emf $\hat{E}_2$ is not the secondary terminal voltage, however, because of the *secondary resistance* R_2 and because the secondary current $\hat{I}_2$ creates secondary leakage flux (see Fig. 2.9). The secondary terminal voltage $\hat{V}_2$ differs from the induced voltage $\hat{E}_2$ by the voltage drops due to secondary resistance R_2 and *secondary leakage reactance* X_{l_2} (corresponding to the *secondary leakage inductance* L_{l_2}), as in the portion of the complete transformer equivalent circuit (Fig. 2.10c) to the right of $\hat{E}_2$.

From the equivalent circuit of Fig. 2.10, the actual transformer therefore can be seen to be equivalent to an ideal transformer plus external impedances. By referring all quantities to the primary or secondary, the ideal transformer in Fig. 2.10c can be moved out to the right or left, respectively, of the equivalent circuit. This is almost invariably done, and the equivalent circuit is usually drawn as in Fig. 2.10d, with the ideal transformer not shown and all voltages, currents, and impedances referred to

either the primary or secondary winding. Specifically, for Fig. 2.10d,

$$X'_{l_2} = \left(\frac{N_1}{N_2}\right)^2 X_{l_2} \tag{2.25}$$

$$R'_2 = \left(\frac{N_1}{N_2}\right)^2 R_2 \tag{2.26}$$

and

$$V'_2 = \frac{N_1}{N_2} V_2 \tag{2.27}$$

The circuit of Fig. 2.10d is called the *equivalent-T circuit* for a transformer.

In Fig. 2.10d, in which the secondary quantities are referred to the primary, the referred secondary values are indicated with primes, for example, X'_{l_2} and R'_2, to distinguish them from the actual values of Fig. 2.10c. In the discussion that follows we almost always deal with referred values, and the primes will be omitted. One must simply keep in mind the side of the transformers to which all quantities have been referred.

EXAMPLE 2.3

A 50-kVA 2400:240-V 60-Hz distribution transformer has a leakage impedance of $0.72 + j0.92\ \Omega$ in the high-voltage winding and $0.0070 + j0.0090\ \Omega$ in the low-voltage winding. At rated voltage and frequency, the impedance Z_φ of the shunt branch (equal to the impedance of R_c and jX_m in parallel) accounting for the exciting current is $6.32 + j43.7\ \Omega$ when viewed from the low-voltage side. Draw the equivalent circuit referred to (*a*) the high-voltage side and (*b*) the low-voltage side, and label the impedances numerically.

■ Solution

The circuits are given in Fig. 2.11a and b, respectively, with the high-voltage side numbered 1 and the low-voltage side numbered 2. The voltages given on the nameplate of a power system transformer are based on the turns ratio and neglect the small leakage-impedance voltage drops under load. Since this is a 10-to-1 transformer, impedances are referred by multiplying or dividing by 100; for example, the value of an impedance referred to the high-voltage side is greater by a factor of 100 than its value referred to the low-voltage side.

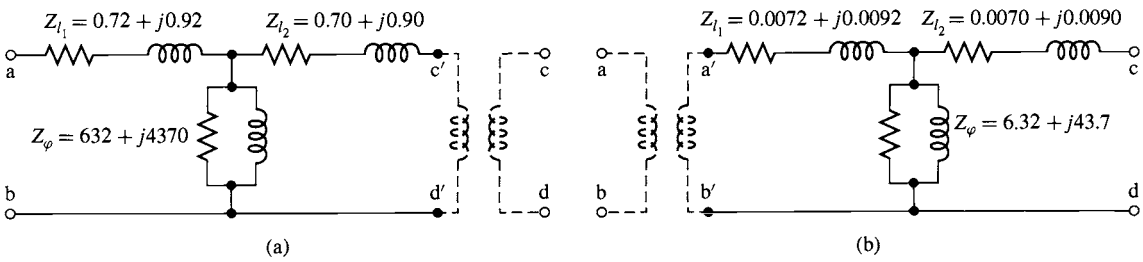

Figure 2.11 Equivalent circuits for transformer of Example 2.3 referred to (a) the high-voltage side and (b) the low-voltage side.

The ideal transformer may be explicitly drawn, as shown dotted in Fig. 2.11, or it may be omitted in the diagram and remembered mentally, making the unprimed letters the terminals. If this is done, one must of course remember to refer all connected impedances and sources to be consistent with the omission of the ideal transformer.

Practice Problem 2.2

If 2400 V rms is applied to the high-voltage side of the transformer of Example 2.3, calculate the magnitude of the current into the magnetizing impedance Z_φ in Figs. 2.11a and b respectively.

Solution

The current through Z_φ is 0.543 A rms when it is referred to the high-voltage side as in Fig. 2.11a and 5.43 A rms when it is referred to the low-voltage side.

2.5 ENGINEERING ASPECTS OF TRANSFORMER ANALYSIS

In engineering analyses involving the transformer as a circuit element, it is customary to adopt one of several approximate forms of the equivalent circuit of Fig. 2.10 rather than the full circuit. The approximations chosen in a particular case depend largely on physical reasoning based on orders of magnitude of the neglected quantities. The more common approximations are presented in this section. In addition, test methods are given for determining the transformer constants.

The approximate equivalent circuits commonly used for constant-frequency power transformer analyses are summarized for comparison in Fig. 2.12. All quantities in these circuits are referred to either the primary or the secondary, and the ideal transformer is not shown.

Computations can often be greatly simplified by moving the shunt branch representing the exciting current out from the middle of the T circuit to either the primary or the secondary terminals, as in Fig. 2.12a and b. These forms of the equivalent circuit are referred to as *cantilever circuits*. The series branch is the combined resistance and leakage reactance of the primary and secondary, referred to the same side. This impedance is sometimes called the *equivalent series impedance* and its components the *equivalent series resistance* R_{eq} and *equivalent series reactance* X_{eq}, as shown in Fig. 2.12a and b.

As compared to the equivalent-T circuit of Fig. 2.10d, the cantilever circuit is in error in that it neglects the voltage drop in the primary or secondary leakage impedance caused by the exciting current. Because the impedance of the exciting branch is typically quite large in large power transformers, the corresponding exciting current is quite small. This error is insignificant in most situations involving large transformers.

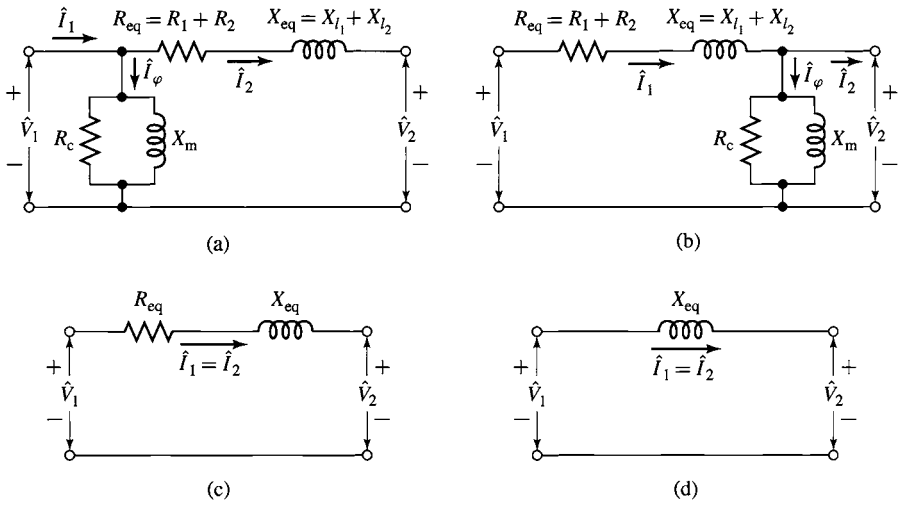

Figure 2.12 Approximate transformer equivalent circuits.

EXAMPLE 2.4

Consider the equivalent-T circuit of Fig. 2.11a of the 50-kVA 2400:240 V distribution transformer of Example 2.3 in which the impedances are referred to the high-voltage side. (*a*) Draw the cantilever equivalent circuit with the shunt branch at the high-voltage terminal. Calculate and label R_{eq} and X_{eq}. (*b*) With the low-voltage terminal open-circuit and 2400 V applied to the high-voltage terminal, calculate the voltage at the low-voltage terminal as predicted by each equivalent circuit.

■ Solution

a. The cantilever equivalent circuit is shown in Fig. 2.13. R_{eq} and X_{eq} are found simply as the sum of the high- and low-voltage winding series impedances of Fig. 2.11a

$$R_{eq} = 0.72 + 0.70 = 1.42\ \Omega$$

$$X_{eq} = 0.92 + 0.90 = 1.82\ \Omega$$

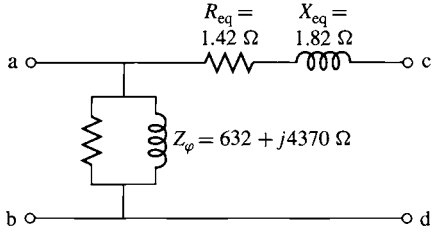

Figure 2.13 Cantilever equivalent circuit for Example 2.4.

b. For the equivalent-T circuit of Fig. 2.11a, the voltage at the terminal labeled c′-d′ will be given by

$$\hat{V}_{c'\text{-}d'} = 2400\left(\frac{Z_\varphi}{Z_\varphi + Z_{l_1}}\right) = 2399.4 + j0.315 \text{ V}$$

This corresponds to an rms magnitude of 2399.4 V. Reflected to the low-voltage terminals by the low- to high-voltage turns ratio, this in turn corresponds to a voltage of 239.94 V.

Because the exciting impedance is connected directly across the high-voltage terminals in the cantilever equivalent circuit of Fig. 2.13, there will be no voltage drop across any series leakage impedance and the predicted secondary voltage will be 240 V. These two solutions differ by 0.025 percent, well within reasonable engineering accuracy and clearly justifying the use of the cantilever equivalent circuit for analysis of this transformer.

Further analytical simplification results from neglecting the exciting current entirely, as in Fig. 2.12c, in which the transformer is represented as an equivalent series impedance. If the transformer is large (several hundred kilovoltamperes or more), the equivalent resistance R_{eq} is small compared with the equivalent reactance X_{eq} and can frequently be neglected, giving the equivalent circuit of Fig. 2.12d. The circuits of Fig. 2.12c and d are sufficiently accurate for most ordinary power system problems and are used in all but the most detailed analyses. Finally, in situations where the currents and voltages are determined almost wholly by the circuits external to the transformer or when a high degree of accuracy is not required, the entire transformer impedance can be neglected and the transformer considered to be ideal, as in Section 2.3.

The circuits of Fig. 2.12 have the additional advantage that the total equivalent resistance R_{eq} and equivalent reactance X_{eq} can be found from a very simple test in which one terminal is short-circuited. On the other hand, the process of determination of the individual leakage reactances X_{l_1} and X_{l_2} and a complete set of parameters for the equivalent-T circuit of Fig. 2.10c is more difficult. Example 2.4 illustrates that due to the voltage drop across leakage impedances, the ratio of the measured voltages of a transformer will not be indentically equal to the idealized voltage ratio which would be measured if the transformer were ideal. In fact, without some apriori knowledge of the turns ratio (based for example upon knowledge of the internal construction of the transformer), it is not possible to make a set of measurements which uniquely determine the turns ratio, the magnetizing inductance, and the individual leakage impedances.

It can be shown that, simply from terminal measurements, neither the turns ratio, the magnetizing reactance, or the leakage reactances are unique characteristics of a transformer equivalent circuit. For example, the turns ratio can be chosen arbitrarily and for each choice of turns ratio, there will be a corresponding set of values for the leakage and magnetizing reactances which matches the measured characteristic. Each of the resultant equivalent circuits will have the same electrical terminal characteristics, a fact which has the fortunate consequence that any self-consistent set of empirically determined parameters will adequately represent the transformer.

EXAMPLE 2.5

The 50-kVA 2400:240-V transformer whose parameters are given in Example 2.3 is used to step down the voltage at the load end of a feeder whose impedance is $0.30 + j1.60\ \Omega$. The voltage V_s at the sending end of the feeder is 2400 V.

Find the voltage at the secondary terminals of the transformer when the load connected to its secondary draws rated current from the transformer and the power factor of the load is 0.80 lagging. Neglect the voltage drops in the transformer and feeder caused by the exciting current.

■ Solution

The circuit with all quantities referred to the high-voltage (primary) side of the transformer is shown in Fig. 2.14a, where the transformer is represented by its equivalent impedance, as in Fig. 2.12c. From Fig. 2.11a, the value of the equivalent impedance is $Z_{eq} = 1.42 + j1.82\ \Omega$ and the combined impedance of the feeder and transformer in series is $Z = 1.72 + j3.42\ \Omega$. From the transformer rating, the load current referred to the high-voltage side is $I = 50{,}000/2400 = 20.8$ A.

This solution is most easily obtained with the aid of the phasor diagram referred to the high-voltage side as shown in Fig. 2.14b. Note that the power factor is defined at the load side of the transformer and hence defines the phase angle θ between the load current $\hat{I}$ and the voltage $\hat{V}_2$

$$\theta = -\cos^{-1}(0.80) = -36.87^\circ$$

From the phasor diagram

$$Ob = \sqrt{V_s^2 - (bc)^2} \quad \text{and} \quad V_2 = Ob - ab$$

Note that

$$bc = IX\cos\theta - IR\sin\theta \qquad ab = IR\cos\theta + IX\sin\theta$$

where R and X are the combined resistance and reactance, respectively. Thus

$$bc = 20.8(3.42)(0.80) - 20.8(1.72)(0.60) = 35.5 \text{ V}$$

$$ab = 20.8(1.72)(0.80) + 20.8(3.42)(0.60) = 71.4 \text{ V}$$

Substitution of numerical values shows that $V_2 = 2329$ V, referred to the high-voltage side. The actual voltage at the secondary terminals is 2329/10, or

$$V_2 = 233 \text{ V}$$

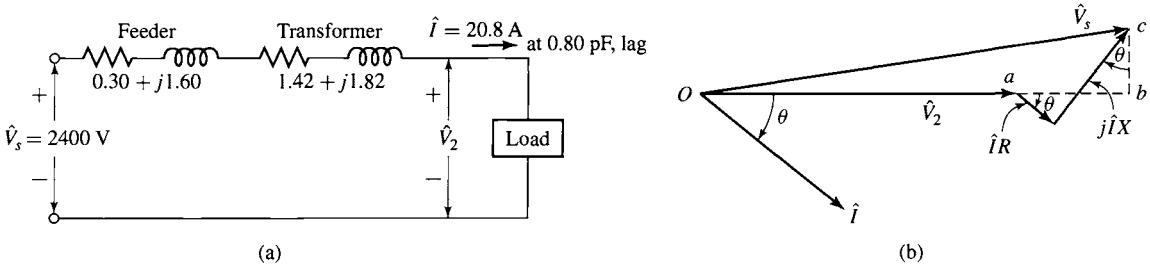

Figure 2.14 (a) Equivalent circuit and (b) phasor diagram for Example 2.5.

Practice Problem 2.3

Repeat Example 2.5 for a load which draws rated current from the transformer with a power factor of 0.8 leading.

Solution

$$V_2 = 239\,\text{V}$$

Two very simple tests serve to determine the parameters of the equivalent circuits of Fig. 2.10 and 2.12. These consist of measuring the input voltage, current, and power to the primary, first with the secondary short-circuited and then with the secondary open-circuited.

Short-Circuit Test The *short-circuit test* can be used to find the equivalent series impedance $R_{eq} + jX_{eq}$. Although the choice of winding to short-circuit is arbitrary, for the sake of this discussion we will consider the short circuit to be applied to the transformer secondary and voltage applied to primary. For convenience, the high-voltage side is usually taken as the primary in this test. Because the equivalent series impedance in a typical transformer is relatively small, typically an applied primary voltage on the order of 10 to 15 percent or less of the rated value will result in rated current.

Figure 2.15a shows the equivalent circuit with transformer secondary impedance referred to the primary side and a short circuit applied to the secondary. The short-circuit impedance Z_{sc} looking into the primary under these conditions is

$$Z_{sc} = R_1 + jX_{l_1} + \frac{Z_\varphi(R_2 + jX_{l_2})}{Z_\varphi + R_2 + jX_{l_2}} \tag{2.28}$$

Because the impedance Z_φ of the exciting branch is much larger than that of the secondary leakage impedance (which will be true unless the core is heavily saturated by excessive voltage applied to the primary; certainly not the case here), the short-circuit impedance can be approximated as

$$Z_{sc} \approx R_1 + jX_{l_1} + R_2 + jX_{l_2} = R_{eq} + jX_{eq} \tag{2.29}$$

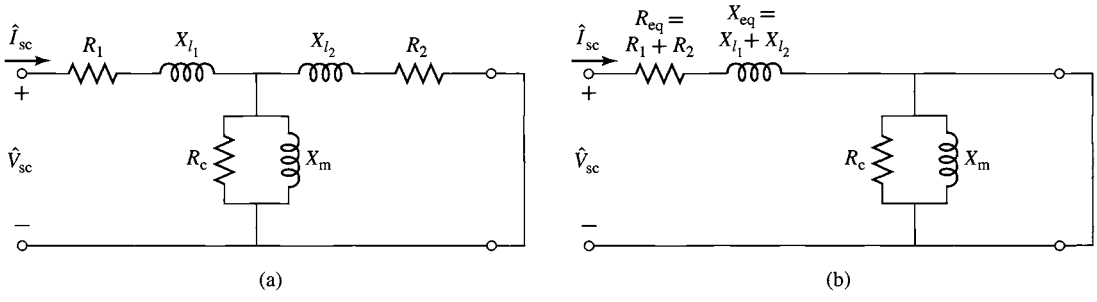

Figure 2.15 Equivalent circuit with short-circuited secondary. (a) Complete equivalent circuit. (b) Cantilever equivalent circuit with the exciting branch at the transformer secondary.

Note that the approximation made here is equivalent to the approximation made in reducing the equivalent-T circuit to the cantilever equivalent. This can be seen from Fig. 2.15b; the impedance seen at the input of this equivalent circuit is clearly $Z_{sc} = Z_{eq} = R_{eq} + jX_{eq}$ since the exciting branch is directly shorted out by the short on the secondary.

Typically the instrumentation used for this test will measure the rms magnitude of the applied voltage V_{sc}, the short-circuit current I_{sc}, and the power P_{sc}. Based upon these three measurements, the equivalent resistance and reactance (referred to the primary) can be found from

$$|Z_{eq}| = |Z_{sc}| = \frac{V_{sc}}{I_{sc}} \tag{2.30}$$

$$R_{eq} = R_{sc} = \frac{P_{sc}}{I_{sc}^2} \tag{2.31}$$

$$X_{eq} = X_{sc} = \sqrt{|Z_{sc}|^2 - R_{sc}^2} \tag{2.32}$$

where the symbol || indicates the magnitude of the enclosed complex quantity.

The equivalent impedance can, of course, be referred from one side to the other in the usual manner. On the rare occasions when the equivalent-T circuit in Fig. 2.10d must be resorted to, approximate values of the individual primary and secondary resistances and leakage reactances can be obtained by assuming that $R_1 = R_2 = 0.5R_{eq}$ and $X_{l_1} = X_{l_2} = 0.5X_{eq}$ when all impedances are referred to the same side. Strictly speaking, of course, it is possible to measure R_1 and R_2 directly by a dc resistance measurement on each winding (and then referring one or the other to the other side of the idea transformer). However, as has been discussed, no such simple test exists for the leakage reactances X_{l_1} and X_{l_2}.

Open-Circuit Test The *open-circuit test* is performed with the secondary open-circuited and rated voltage impressed on the primary. Under this condition an exciting current of a few percent of full-load current (less on large transformers and more on smaller ones) is obtained. Rated voltage is chosen to insure that the magnetizing reactance will be operating at a flux level close to that which will exist under normal operating conditions. If the transformer is to be used at other than its rated voltage, the test should be done at that voltage. For convenience, the low-voltage side is usually taken as the primary in this test. If the primary in this test is chosen to be the opposite winding from that of the short-circuit test, one must of course be careful to refer the various measured impedances to the same side of the transformer in order to obtain a self-consistent set of parameter values.

Figure 2.16a shows the equivalent circuit with the transformer secondary impedance referred to the primary side and the secondary open-circuited. The open-circuit impedance Z_{oc} looking into the primary under these conditions is

$$Z_{oc} = R_1 + jX_{l_1} + Z_\varphi = R_1 + jX_{l_1} + \frac{R_c\,(jX_m)}{R_c + jX_m} \tag{2.33}$$

Because the impedance of the exciting branch is quite large, the voltage drop in the primary leakage impedance caused by the exciting current is typically negligible, and

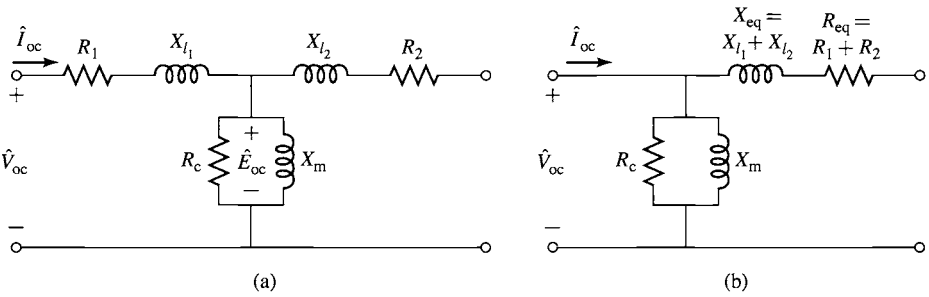

Figure 2.16 Equivalent circuit with open-circuited secondary. (a) Complete equivalent circuit. (b) Cantilever equivalent circuit with the exciting branch at the transformer primary.

the primary impressed voltage $\hat{V}_{oc}$ very nearly equals the emf $\hat{E}_{oc}$ induced by the resultant core flux. Similarly, the primary $I_{oc}^2 R_1$ loss caused by the exciting current is negligible, so that the power input P_{oc} very nearly equals the core loss E_{oc}^2/R_c. As a result, it is common to ignore the primary leakage impedance and to approximate the open-circuit impedance as being equal to the magnetizing impedance

$$Z_{oc} \approx Z_\varphi = \frac{R_c(jX_m)}{R_c + jX_m} \tag{2.34}$$

Note that the approximation made here is equivalent to the approximation made in reducing the equivalent-T circuit to the cantilever equivalent circuit of Fig. 2.16b; the impedance seen at the input of this equivalent circuit is clearly Z_φ since no current will flow in the open-circuited secondary.

As with the short-circuit test, typically the instrumentation used for this test will measure the rms magnititude of the applied voltage, V_{oc}, the open-circuit current I_{oc} and the power P_{oc}. Neglecting the primarly leakage impedance and based upon these three measurements, the magnetizing resistance and reactance (referred to the primary) can be found from

$$R_c = \frac{V_{oc}^2}{P_{oc}} \tag{2.35}$$

$$|Z_\varphi| = \frac{V_{oc}}{Z_{oc}} \tag{2.36}$$

$$X_m = \frac{1}{\sqrt{(1/|Z_\varphi|)^2 - (1/R_c)^2}} \tag{2.37}$$

The values obtained are, of course, referred to the side used as the primary in this test.

The open-circuit test can be used to obtain the core loss for efficiency computations and to check the magnitude of the exciting current. Sometimes the voltage at the terminals of the open-circuited secondary is measured as a check on the turns ratio.

Note that, if desired, a slightly more accurate calculation of X_m and R_c by retaining the measurements of R_1 and X_{l_1} obtained from the short-circuit test (referred to

the proper side of the transformer) and basing the derivation on Eq. 2.33. However, such additional effort is rarely necessary for the purposes of engineering accuracy.

EXAMPLE 2.6

With the instruments located on the high-voltage side and the low-voltage side short-circuited, the short-circuit test readings for the 50-kVA 2400:240-V transformer of Example 2.3 are 48 V, 20.8 A, and 617 W. An open-circuit test with the low-voltage side energized gives instrument readings on that side of 240 V, 5.41 A, and 186 W. Determine the efficiency and the voltage regulation at full load, 0.80 power factor lagging.

■ Solution

From the short-circuit test, the magnitude of the equivalent impedance, the equivalent resistance, and the equivalent reactance of the transformer (referred to the high-voltage side as denoted by the subscript H) are

$$|Z_{\text{eq,H}}| = \frac{48}{20.8} = 2.31\ \Omega \quad R_{\text{eq,H}} = \frac{617}{20.8^2} = 1.42\ \Omega$$

$$X_{\text{eq,H}} = \sqrt{2.31^2 - 1.42^2} = 1.82\ \Omega$$

Operation at full-load, 0.80 power factor lagging corresponds to a current of

$$I_{\text{H}} = \frac{50{,}000}{2400} = 20.8\ \text{A}$$

and an output power

$$P_{\text{output}} = P_{\text{load}} = (0.8)50{,}000 = 40{,}000\ \text{W}$$

The total loss under this operating condition is equal to the sum of the winding loss

$$P_{\text{winding}} = I_{\text{H}}^2 R_{\text{eq,H}} = 20.8^2(1.42) = 617\ \text{W}$$

and the core loss determined from the open-circuit test

$$P_{\text{core}} = 186\ \text{W}$$

Thus

$$P_{\text{loss}} = P_{\text{winding}} + P_{\text{core}} = 803\ \text{W}$$

and the power input to the transformer is

$$P_{\text{input}} = P_{\text{output}} + P_{\text{loss}} = 40{,}803\ \text{W}$$

The *efficiency* of a power conversion device is defined as

$$\text{efficiency} = \frac{P_{\text{output}}}{P_{\text{input}}} = \frac{P_{\text{input}} - P_{\text{loss}}}{P_{\text{input}}} = 1 - \frac{P_{\text{loss}}}{P_{\text{input}}}$$

which can be expressed in percent by multiplying by 100 percent. Hence, for this operating condition

$$\text{efficiency} = 100\% \left(\frac{P_{\text{output}}}{P_{\text{input}}}\right) = 100\% \left(\frac{40{,}000}{40{,}000 + 803}\right) = 98.0\%$$

The *voltage regulation* of a transformer is defined as the change in secondary terminal voltage from no load to full load and is usually expressed as a percentage of the full-load value. In power systems applications, regulation is one figure of merit for a transformer; a low value indicates that load variations on the secondary of that transformer will not significantly affect the magnitude of the voltage being supplied to the load. It is calculated under the assumption that the primary voltage remains constant as the load is removed from the transformer secondary.

The equivalent circuit of Fig. 2.12c will be used with all quantities referred to the high-voltage side. The primary voltage is assumed to be adjusted so that the secondary terminal voltage has its rated value at full load, or $V_{2H} = 2400$ V. For a load of rated value and 0.8 power factor lagging (corresponding to a power factor angle $\theta = -\cos^{-1}(0.8) = -36.9°$), the load current will be

$$\hat{I}_H = \left(\frac{50 \times 10^3}{2400}\right) e^{-j36.9°} = 20.8(0.8 - j0.6)\ \text{A}$$

The required value of the primary voltage V_{1H} can be calculated as

$$\begin{aligned}\hat{V}_{1H} &= \hat{V}_{2H} + \hat{I}_H(R_{eq,H} + jX_{eq,H}) \\ &= 2400 + 20.8(0.80 - j0.60)(1.42 + j1.82) \\ &= 2446 + j13\end{aligned}$$

The magnitude of $\hat{V}_{1H}$ is 2446 V. If this voltage were held constant and the load removed, the secondary voltage on open circuit would rise to 2446 V referred to the high-voltage side. Then

$$\text{Regulation} = \frac{2446 - 2400}{2400}(100\%) = 1.92\%$$

Practice Problem 2.4

Repeat the voltage-regulation calculation of Example 2.6 for a load of 50 kW (rated load, unity power factor).

Solution

$$\text{Regulation} = 1.24\%$$

2.6 AUTOTRANSFORMERS; MULTIWINDING TRANSFORMERS

The principles discussed in previous sections have been developed with specific reference to two-winding transformers. They are also applicable to transformers with other winding configurations. Aspects relating to autotransformers and multiwinding transformers are considered in this section.

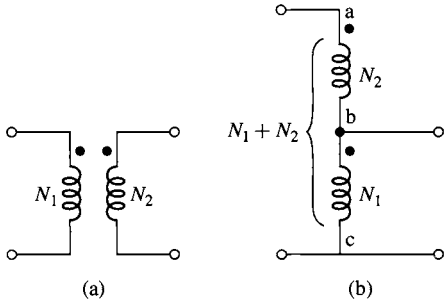

Figure 2.17 (a) Two-winding transformer. (b) Connection as an autotransformer.

2.6.1 Autotransformers

In Fig. 2.17a, a two-winding transformer is shown with N_1 and N_2 turns on the primary and secondary windings respectively. Substantially the same transformation effect on voltages, currents, and impedances can be obtained when these windings are connected as shown in Fig. 2.17b. Note that, however, in Fig. 2.17b, winding *bc* is common to both the primary and secondary circuits. This type of transformer is called an *autotransformer*. It is little more than a normal transformer connected in a special way.

One important difference between the two-winding transformer and the autotransformer is that the windings of the two-winding transformer are electrically isolated whereas those of the autotransformer are connected directly together. Also, in the autotransformer connection, winding *ab* must be provided with extra insulation since it must be insulated against the full maximum voltage of the autotransformer. Autotransformers have lower leakage reactances, lower losses, and smaller exciting current and cost less than two-winding transformers when the voltage ratio does not differ too greatly from 1:1.

The following example illustrates the benefits of an autotransformer for those situations where electrical isolation between the primary and secondary windings is not an important consideration.

EXAMPLE 2.7

The 2400:240-V 50-kVA transformer of Example 2.6 is connected as an autotransformer, as shown in Fig. 2.18a, in which ab is the 240-V winding and bc is the 2400-V winding. (It is assumed that the 240-V winding has enough insulation to withstand a voltage of 2640 V to ground.)

a. Compute the voltage ratings V_H and V_X of the high- and low-voltage sides, respectively, for this autotransformer connection.
b. Compute the kVA rating as an autotransformer.
c. Data with respect to the losses are given in Example 2.6. Compute the full-load efficiency as an autotransformer operating with a rated load of 0.80 power factor lagging.

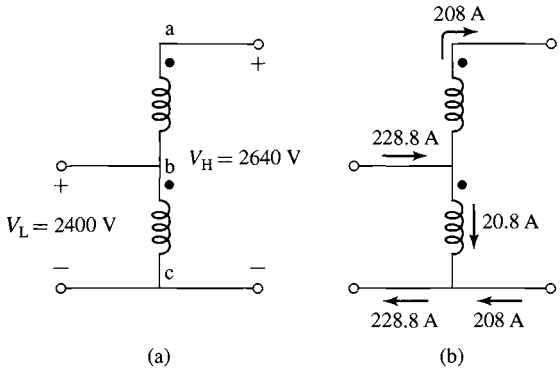

Figure 2.18 (a) Autotransformer connection for Example 2.7. (b) Currents under rated load.

■ Solution

a. Since the 2400-V winding bc is connected to the low-voltage circuit, $V_L = 2400$ V. When $V_{bc} = 2400$ V, a voltage $V_{ab} = 240$ V in phase with V_{bc} will be induced in winding ab (leakage-impedance voltage drops being neglected). The voltage of the high-voltage side therefore is

$$V_H = V_{ab} + V_{bc} = 2640 \text{ V}$$

b. From the rating of 50 kVA as a normal two-winding transformer, the rated current of the 240-V winding is $50{,}000/240 = 208$ A. Since the high-voltage lead of the autotransformer is connected to the 240-V winding, the rated current I_H at the high-voltage side of the autotransformer is equal to the rated current of the 240-V winding or 208 A. The kVA rating as an autotransformer therefore is

$$\frac{V_H I_H}{1000} = \frac{2640(208)}{1000} = 550 \text{ kVA}$$

Note that, in this connection, the autotransformer has an equivalent turns ratio of 2640/2400. Thus the rated current at the low-voltage winding (the 2400-V winding in this connection) must be

$$I_L = \left(\frac{2640}{2400}\right) 208 \text{ A} = 229 \text{ A}$$

At first, this seems rather unsettling since the 2400-V winding of the transformer has a rated current of 50 kVA/2400 V = 20.8 A. Further puzzling is that fact that this transformer, whose rating as a normal two-winding transformer is 50 kVA, is capable of handling 550 kVA as an autotransformer.

The higher rating as an autotransformer is a consequence of the fact that not all the 550 kVA has to be transformed by electromagnetic induction. In fact, all that the transformer has to do is to boost a current of 208 A through a potential rise of 240 V, corresponding to a power transformation capacity of 50 kVA. This fact is perhaps best illustrated by Fig. 2.18b which shows the currents in the autotransformer under rated

conditions. Note that the windings carry only their rated currents in spite of higher rating of the transformer.

c. When it is connected as an autotransformer with the currents and voltages shown in Fig. 2.18, the losses are the same as in Example 2.6, namely, 803 W. But the output as an autotransformer at full load, 0.80 power factor is 0.80(550,000) = 440,000 W. The efficiency therefore is

$$\left(1 - \frac{803}{440{,}803}\right) 100\% = 99.82\%$$

The efficiency is so high because the losses are those corresponding to transforming only 50 kVA.

Practice Problem 2.5

A 450-kVA, 460-V:7.97-kV transformer has an efficiency of 97.8 percent when supplying a rated load of unity power factor. If it is connected as a 7.97:8.43-kV autotransformer, calculate its rated terminal currents, rated kVA, and efficiency when supplying a unity-power-factor load.

Solution

The rated current at the 8.43-kV terminal is 978 A, at the 7.97-kV terminal is 1034 A and the transformer rating is 8.25 MVA. Its efficiency supplying a rated, unity-power-factor load is 99.88 percent.

From Example 2.7, we see that when a transformer is connected as an autotransformer as shown in Fig. 2.17, the rated voltages of the autotransformer can be expressed in terms of those of the two-winding transformer as

Low-voltage:

$$V_{L_{rated}} = V_{1_{rated}} \tag{2.38}$$

High-voltage:

$$V_{H_{rated}} = V_{1_{rated}} + V_{2_{rated}} = \left(\frac{N_1 + N_2}{N_1}\right) V_{L_{rated}} \tag{2.39}$$

The effective turns ratio of the autotransformer is thus $(N_1 + N_2)/N_1$. In addition, the power rating of the autotransformer is equal to $(N_1 + N_2)/N_2$ times that of the two-winding transformer, although the actual power processed by the transformer will not increase over that of the standard two-winding connection.

2.6.2 Multiwinding Transformers

Transformers having three or more windings, known as *multiwinding* or *multicircuit transformers,* are often used to interconnect three or more circuits which may have different voltages. For these purposes a multiwinding transformer costs less and is

more efficient than an equivalent number of two-winding transformers. Transformers having a primary and multiple secondaries are frequently found in multiple-output dc power supplies for electronic applications. Distribution transformers used to supply power for domestic purposes usually have two 120-V secondaries connected in series. Circuits for lighting and low-power applications are connected across each of the 120-V windings, while electric ranges, domestic hot-water heaters, clothes-dryers, and other high-power loads are supplied with 240-V power from the series-connected secondaries.

Similarly, a large distribution system may be supplied through a three-phase bank of multiwinding transformers from two or more transmission systems having different voltages. In addition, the three-phase transformer banks used to interconnect two transmission systems of different voltages often have a third, or tertiary, set of windings to provide voltage for auxiliary power purposes in substations or to supply a local distribution system. Static capacitors or synchronous condensers may be connected to the tertiary windings for power factor correction or voltage regulation. Sometimes Δ-connected tertiary windings are put on three-phase banks to provide a low-impedance path for third harmonic components of the exciting current to reduce third-harmonic components of the neutral voltage.

Some of the issues arising in the use of multiwinding transformers are associated with the effects of leakage impedances on voltage regulation, short-circuit currents, and division of load among circuits. These problems can be solved by an equivalent-circuit technique similar to that used in dealing with two-circuit transformers.

The equivalent circuits of multiwinding transformers are more complicated than in the two-winding case because they must take into account the leakage impedances associated with each pair of windings. Typically, in these equivalent circuits, all quantities are referred to a common base, either by use of the appropriate turns ratios as referring factors or by expressing all quantities in per unit. The exciting current usually is neglected.

2.7 TRANSFORMERS IN THREE-PHASE CIRCUITS

Three single-phase transformers can be connected to form a *three-phase transformer bank* in any of the four ways shown in Fig. 2.19. In all four parts of this figure, the windings at the left are the primaries, those at the right are the secondaries, and any primary winding in one transformer corresponds to the secondary winding drawn parallel to it. Also shown are the voltages and currents resulting from balanced impressed primary line-to-line voltages V and line currents I when the ratio of primary-to-secondary turns $N_1/N_2 = a$ and ideal transformers are assumed.[4] Note that the rated voltages and currents at the primary and secondary of the three-phase transformer bank depends upon the connection used but that the rated kVA of the three-phase bank is three times that of the individual single-phase transformers, regardless of the connection.

[4] The relationship between three-phase and single-phase quantities is discussed in Appendix A.

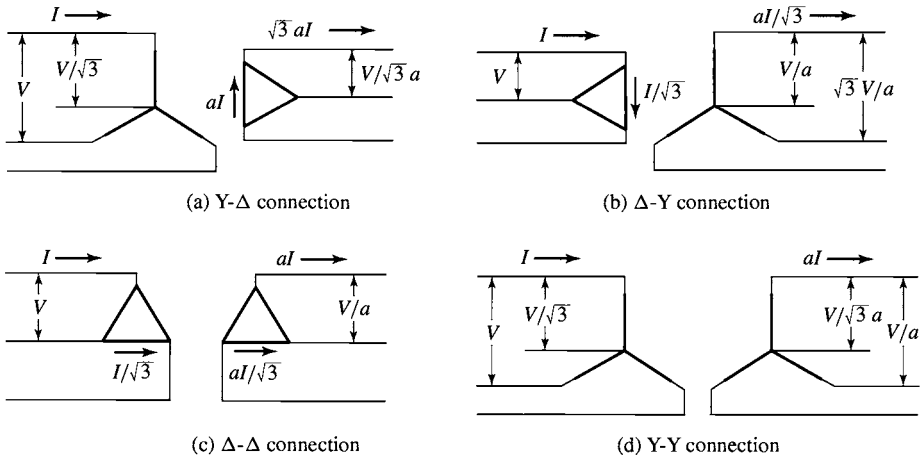

Figure 2.19 Common three-phase transformer connections; the transformer windings are indicated by the heavy lines.

The Y-Δ connection is commonly used in stepping down from a high voltage to a medium or low voltage. One reason is that a neutral is thereby provided for grounding on the high-voltage side, a procedure which can be shown to be desirable in many cases. Conversely, the Δ-Y connection is commonly used for stepping up to a high voltage. The Δ-Δ connection has the advantage that one transformer can be removed for repair or maintenance while the remaining two continue to function as a three-phase bank with the rating reduced to 58 percent of that of the original bank; this is known as the *open-delta,* or *V*, connection. The Y-Y connection is seldom used because of difficulties with exciting-current phenomena.[5]

Instead of three single-phase transformers, a three-phase bank may consist of one *three-phase transformer* having all six windings on a common multi-legged core and contained in a single tank. Advantages of three-phase transformers over connections of three single-phase transformers are that they cost less, weigh less, require less floor space, and have somewhat higher efficiency. A photograph of the internal parts of a large three-phase transformer is shown in Fig. 2.20.

Circuit computations involving three-phase transformer banks under balanced conditions can be made by dealing with only one of the transformers or phases and recognizing that conditions are the same in the other two phases except for the phase displacements associated with a three-phase system. It is usually convenient to carry out the computations on a single-phase (per-phase-Y, line-to-neutral) basis, since transformer impedances can then be added directly in series with transmission line impedances. The impedances of transmission lines can be referred from one side of the transformer bank to the other by use of the square of the ideal line-to-line voltage

[5] Because there is no neutral connection to carry harmonics of the exciting current, harmonic voltages are produced which significantly distort the transformer voltages.

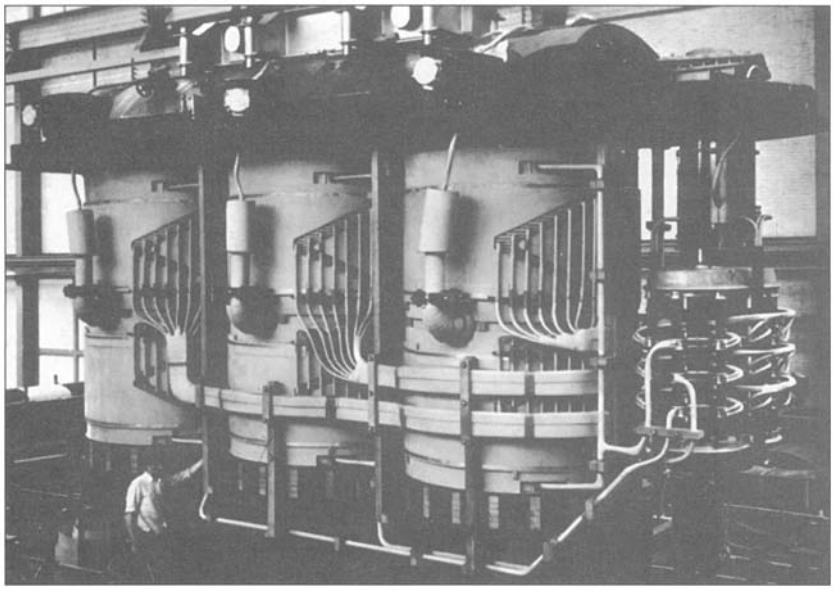

Figure 2.20 A 200-MVA, three-phase, 50-Hz, three-winding, 210/80/10.2-kV transformer removed from its tank. The 210-kV winding has an on-load tap changer for adjustment of the voltage. (*Brown Boveri Corporation.*)

ratio of the bank. In dealing with Y-Δ or Δ-Y banks, all quantities can be referred to the Y-connected side. In dealing with Δ-Δ banks in series with transmission lines, it is convenient to replace the Δ-connected impedances of the transformers by equivalent Y-connected impedances. It can be shown that a balanced Δ-connected circuit of Z_Δ Ω/phase is equivalent to a balanced Y-connected circuit of Z_Y Ω/phase if

$$Z_Y = \frac{1}{3} Z_\Delta \tag{2.40}$$

EXAMPLE 2.8

Three single-phase, 50-kVA 2400:240-V transformers, each identical with that of Example 2.6, are connected Y-Δ in a three-phase 150-kVA bank to step down the voltage at the load end of a feeder whose impedance is $0.15 + j1.00\,\Omega$/phase. The voltage at the sending end of the feeder is 4160 V line-to-line. On their secondary sides, the transformers supply a balanced three-phase load through a feeder whose impedance is $0.0005 + j0.0020\,\Omega$/phase. Find the line-to-line voltage at the load when the load draws rated current from the transformers at a power factor of 0.80 lagging.

■ Solution

The computations can be made on a single-phase basis by referring everything to the high-voltage, Y-connected side of the transformer bank. The voltage at the sending end of the feeder

is equivalent to a source voltage V_s of

$$V_s = \frac{4160}{\sqrt{3}} = 2400 \text{ V line-to-neutral}$$

From the transformer rating, the rated current on the high-voltage side is 20.8 A/phase Y. The low-voltage feeder impedance referred to the high voltage side by means of the square of the rated line-to-line voltage ratio of the transformer bank is

$$Z_{\text{lv,H}} = \left(\frac{4160}{240}\right)^2 (0.0005 + j0.0020) = 0.15 + j0.60\ \Omega$$

and the combined series impedance of the high- and low-voltage feeders referred to the high-voltage side is thus

$$Z_{\text{feeder,H}} = 0.30 + j1.60\ \Omega/\text{phase Y}$$

Because the transformer bank is Y-connected on its high-voltage side, its equivalent single-phase series impedance is equal to the single-phase series impedance of each single-phase transformer as referred to its high-voltage side. This impedance was originally calculated in Example 2.4 as

$$Z_{\text{eq,H}} = 1.42 + j1.82\ \Omega/\text{phase Y}$$

Due to the choice of values selected for this example, the single-phase equivalent circuit for the complete system is identical to that of Example 2.5, as can been seen with specific reference to Fig. 2.14a. In fact, the solution on a per-phase basis is exactly the same as the solution to Example 2.5, whence the load voltage referred to the high-voltage side is 2329 V to neutral. The actual line-neutral load voltage can then be calculated by referring this value to the low-voltage side of the transformer bank as

$$V_{\text{load}} = 2329\left(\frac{240}{4160}\right) = 134 \text{ V line-to-neutral}$$

which can be expressed as a line-to-line voltage by multiplying by $\sqrt{3}$

$$V_{\text{load}} = 134\sqrt{3} = 233 \text{ V line-to-line}$$

Note that this line-line voltage is equal to the line-neutral load voltage calculated in Example 2.5 because in this case the transformers are delta connected on their low-voltage side and hence the line-line voltage on the low-voltage side is equal to the low-voltage terminal voltage of the transformers.

Practice Problem 2.6

Repeat Example 2.8 with the transformers connected Y-Y and all other aspects of the problem statement remaining unchanged.

Solution

405 V line-line

EXAMPLE 2.9

The three transformers of Example 2.8 are reconnected Δ-Δ and supplied with power through a 2400-V (line-to-line) three-phase feeder whose reactance is 0.80 Ω/phase. At its sending end, the feeder is connected to the secondary terminals of a three-phase Y-Δ-connected transformer whose rating is 500 kVA, 24 kV:2400 V (line-to-line). The equivalent series impedance of the sending-end transformer is $0.17 + j0.92$ Ω/phase referred to the 2400-V side. The voltage applied to the primary terminals of the sending-end transformer is 24.0 kV line-to-line.

A three-phase short circuit occurs at the 240-V terminals of the receiving-end transformers. Compute the steady-state short-circuit current in the 2400-V feeder phase wires, in the primary and secondary windings of the receiving-end transformers, and at the 240-V terminals.

■ Solution

The computations will be made on an equivalent line-to-neutral basis with all quantities referred to the 2400-V feeder. The source voltage then is

$$\frac{2400}{\sqrt{3}} = 1385 \text{ V line-to-neutral}$$

From Eq. 2.40, the single-phase-equivalent series impedance of the Δ-Δ transformer seen at its 2400-V side is

$$Z_{eq} = R_{eq} + jX_{eq} = \frac{1.42 + j1.82}{3} = 0.47 + j0.61 \ \Omega/\text{phase}$$

The total series impedance to the short circuit is then the sum of this impedance, that of sending-end transformer and the reactance of the feeder

$$Z_{tot} = (0.47 + j0.61) + (0.17 + j0.92) + j0.80 = 0.64 + j2.33 \ \Omega/\text{phase}$$

which has a magnitude of

$$|Z_{tot}| = 2.42 \ \Omega/\text{phase}$$

The magnitude of the phase current in the 2400-V feeder can now simply be calculated as the line-neutral voltage divided by the series impedance

$$\text{Current in 2400-V feeder} = \frac{1385}{2.42} = 572 \text{ A}$$

and, as is shown in Fig. 2.19c, the winding current in the 2400-V winding of the receiving-end transformer is equal to the phase current divided by $\sqrt{3}$ or

$$\text{Current in 2400-V windings} = \frac{572}{\sqrt{3}} = 330 \text{ A}$$

while the current in the 240-V windings is 10 times this value

$$\text{Current in 240-V windings} = 10 \times 330 = 3300 \text{ A}$$

Finally, again with reference to Fig. 2.19c, the phase current at the 240-V terminals into the short circuit is given by

$$\text{Current at the 240-V terminals} = 3300\sqrt{3} = 5720 \text{ A}$$

Note of course that this same result could have been computed simply by recognizing that the turns ratio of the Δ-Δ transformer bank is equal to 10:1 and hence, under balanced-three-phase conditions, the phase current on the low voltage side will be 10 times that on the high-voltage side.

Practice Problem 2.7

Repeat Example 2.9 under the condition that the three transformers are connected Δ-Y instead of Δ-Δ such that the short low-voltage side of the three-phase transformer is rated 416 V line-to-line.

Solution

$$\text{Current in 2400-V feeder} = 572\ \text{A}$$

$$\text{Current in 2400-V windings} = 330\ \text{A}$$

$$\text{Current in 416-V windings} = 3300\ \text{A}$$

$$\text{Current at the 416-V terminals} = 3300\text{A}$$

2.8 VOLTAGE AND CURRENT TRANSFORMERS

Transformers are often used in instrumentation applications to match the magnitude of a voltage or current to the range of a meter or other instrumention. For example, most 60-Hz power-systems' instrumentation is based upon voltages in the range of 0–120 V rms and currents in the range of 0–5 A rms. Since power system voltages range up to 765-kV line-to-line and currents can be 10's of kA, some method of supplying an accurate, low-level representation of these signals to the instrumentation is required.

One common technique is through the use of specialized transformers known as *potential transformers* or *PT's* and *current transformers* or *CT's*. If constructed with a turns ratio of $N_1{:}N_2$, an ideal potential transformer would have a secondary voltage equal in magnitude to N_2/N_1 times that of the primary and identical in phase. Similarly, an ideal current transformer would have a secondary output current equal to N_1/N_2 times the current input to the primary, again identical in phase. In other words, potential and current transformers (also referred to as *instrumentation transformers*) are designed to approximate ideal transformers as closely as is practically possible.

The equivalent circuit of Fig. 2.21 shows a transformer loaded with an impedance $Z_b = R_b + jX_b$ at its secondary. For the sake of this discussion, the core-loss resistance R_c has been neglected; if desired, the analysis presented here can be easily expanded to include its effect. Following conventional terminology, the load on an instrumentation transformer is frequently referred to as the *burden* on that transformer, hence the subscript b. To simplify our discussion, we have chosen to refer all the secondary quantities to the primary side of the ideal transformer.

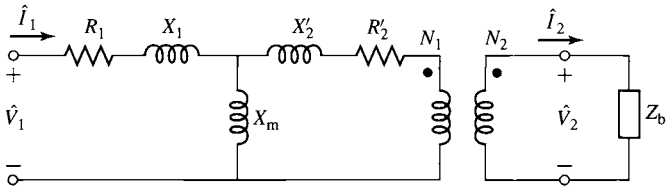

Figure 2.21 Equivalent circuit for an instrumentation transformer.

Consider first a potential transformer. Ideally it should accurately measure voltage while appearing as an open circuit to the system under measurement, i.e., drawing negligible current and power. Thus, its load impedance should be "large" in a sense we will now quantify.

First, let us assume that the transformer secondary is open-circuited (i.e., $|Z_b| = \infty$). In this case we can write that

$$\frac{\hat{V}_2}{\hat{V}_1} = \left(\frac{N_2}{N_1}\right) \frac{jX_m}{R_1 + j(X_1 + X_m)} \tag{2.41}$$

From this equation, we see that a potential transformer with an open-circuited secondary has an inherent error (in both magnitude and phase) due to the voltage drop of the magnetizing current through the primary resistance and leakage reactance. To the extent that the primary resistance and leakage reactance can be made small compared to the magnetizing reactance, this inherent error can be made quite small.

The situation is worsened by the presence of a finite burden. Including the effect of the burden impedance, Eq. 2.41 becomes

$$\frac{\hat{V}_2}{\hat{V}_1} = \left(\frac{N_2}{N_1}\right) \frac{Z_{eq} Z'_b}{(R_1 + jX_1)(Z_{eq} + Z'_b + R'_2 + jX'_2)} \tag{2.42}$$

where

$$Z_{eq} = \frac{jX_m(R_1 + jX_1)}{R_1 + j(X_m + X_1)} \tag{2.43}$$

and

$$Z'_b = \left(\frac{N_1}{N_2}\right)^2 Z_b \tag{2.44}$$

is the burden impedance referred to the transformer primary.

From these equations, it can be seen that the characterstics of an accurate potential transformer include a large magnetizing reactance (more accurately, a large exciting impedance since the effects of core loss, although neglected in the analysis presented here, must also be minimized) and relatively small winding resistances and leakage reactances. Finally, as will be seen in Example 2.10, the burden impedance must be kept above a minimum value to avoid introducing excessive errors in the magnitude and phase angle of the measured voltage.

EXAMPLE 2.10

A 2400:120-V, 60-Hz potential transformer has the following parameter values (referred to the 2400-V winding):

$$X_1 = 143\ \Omega \quad X_2' = 164\ \Omega \quad X_m = 163\ \text{k}\Omega$$

$$R_1 = 128\ \Omega \quad R_2' = 141\ \Omega$$

(*a*) Assuming a 2400-V input, which ideally should produce a voltage of 120 V at the low-voltage winding, calculate the magnitude and relative phase-angle errors of the secondary voltage if the secondary winding is open-circuited. (*b*) Assuming the burden impedance to be purely resistive ($Z_b = R_b$), calculate the minimum resistance (maximum burden) that can be applied to the secondary such that the magnitude error is less than 0.5 percent. (*c*) Repeat part (*b*) but find the minimum resistance such that the phase-angle error is less than 1.0 degree.

■ Solution

a. This problem is most easily solved using MATLAB.† From Eq. 2.41 with $\hat{V}_1 = 2400$ V, the following MATLAB script gives

$$\hat{V}_2 = 119.90\ \angle 0.045^\circ\ \text{V}$$

Here is the MATLAB script:

```
clc
clear

%PT parameters
R1 = 128;
X1 = 143;
Xm = 163e3;

N1 = 2400;
N2 = 120;
N = N1/N2;

%Primary voltage
V1 = 2400;

%Secondary voltage
V2 = V1*(N2/N1)*(j*Xm/(R1+ j*(X1+Xm)));
magV2 = abs(V2);
phaseV2 = 180*angle(V2)/pi;

fprintf('\nMagnitude of V2 = %g [V]',magV2)
fprintf('\n    and angle = %g [degrees]\n\n',phaseV2)
```

b. Here, again, it is relatively straight forward to write a MATLAB script to implement Eq. 2.42 and to calculate the percentage error in the magnitude of voltage $\hat{V}_2$ as compared to the 120 Volts that would be measured if the PT were ideal. The resistive burden R_b

† MATLAB is a registered trademark of The MathWorks, Inc.

can be initialized to a large value and then reduced until the magnitude error reaches 0.5 percent. The result of such an analysis would show that the minimum resistance is 162.5 Ω, corresponding to a magnitude error of 0.50 percent and a phase angle of 0.22°. (Note that this appears as a resistance of 65 kΩ when referred to the primary.)

c. The MATLAB script of part (*b*) can be modified to search for the minimum resistive burden that will keep the phase angle error less than 1.0 degrees. The result would show that the minimum resistance is 41.4 Ω, corresponding to a phase angle of 1.00° and a magnitude error of 1.70 percent.

Practice Problem 2.8

Using MATLAB, repeat parts (*b*) and (*c*) of Example 2.10 assuming the burden impedance is purely reactive ($Z_b = jX_b$) and finding the corresponding minimum impedance X_b in each case.

Solution

The minimum burden reactance which results in a secondary voltage magnitude within 0.5 percent of the expected 120 V is $X_b = 185.4\ \Omega$, for which the phase angle is 0.25°. The minimum burden reactance which results in a secondary voltage phase-angle of within 1.0° of that of the primary voltage is $X_b = 39.5\ \Omega$, for which the voltage-magnitude error is 2.0 percent.

Consider next a current transformer. An ideal current transformer would accurately measure voltage while appearing as a short circuit to the system under measurement, i.e., developing negligible voltage drop and drawing negligible power. Thus, its load impedance should be "small" in a sense we will now quantify.

Let us begin with the assumption that the transformer secondary is short-circuited (i.e., $|Z_b| = 0$). In this case we can write that

$$\frac{\hat{I}_2}{\hat{I}_1} = \left(\frac{N_1}{N_2}\right) \frac{jX_m}{R_2' + j(X_2' + X_m)} \tag{2.45}$$

In a fashion quite analogous to that of a potential transformer, Eq. 2.45 shows that a current transformer with a shorted secondary has an inherent error (in both magnitude and phase) due to the fact that some of the primary current is shunted through the magnetizing reactance and does not reach the secondary. To the extent that the magnetizing reactance can be made large in comparison to the secondary resistance and leakage reactance, this error can be made quite small.

A finite burden appears in series with the secondary impedance and increases the error. Including the effect of the burden impedance, Eq. 2.45 becomes

$$\frac{\hat{I}_2}{\hat{I}_1} = \left(\frac{N_1}{N_2}\right) \frac{jX_m}{Z_b' + R_2' + j(X_2' + X_m)} \tag{2.46}$$

From these equations, it can be seen that an accurate current transformer has a large magnetizing impedance and relatively small winding resistances and leakage

reactances. In addition, as is seen in Example 2.11, the burden impedance on a current transformer must be kept below a maximum value to avoid introducing excessive additional magnitude and phase errors in the measured current.

EXAMPLE 2.11

A 800:5-A, 60-Hz current transformer has the following parameter values (referred to the 800-A winding):

$$X_1 = 44.8\ \mu\Omega \quad X_2' = 54.3\ \mu\Omega \quad X_m = 17.7\ \text{m}\Omega$$

$$R_1 = 10.3\ \mu\Omega \quad R_2' = 9.6\ \mu\Omega$$

Assuming that the high-current winding is carrying a current of 800 amperes, calculate the magnitude and relative phase of the current in the low-current winding if the load impedance is purely resistive with $R_b = 2.5\ \Omega$.

■ Solution

The secondary current can be found from Eq. 2.46 by setting $\hat{I}_1 = 800\,\text{A}$ and $R_b' = (N_1/N_2)^2 R_b = 0.097\ \text{m}\Omega$. The following MATLAB script gives

$$\hat{I}_2 = 4.98\ \angle 0.346^\circ\ \text{A}$$

Here is the MATLAB script:

```
clc
clear

%CT parameters
R_2p = 9.6e-6;
X_2p = 54.3e-6;
X_m = 17.7e-3;

N_1 = 5;
N_2 = 800;
N = N_1/N_2;

%Load impedance
R_b = 2.5;
X_b = 0;
Z_bp = N^2*(R_b + j * X_b);

% Primary current
I1 = 800;

%Secondary current
I2 = I1*N*j*X_m/(Z_bp + R_2p + j*(X_2p + X_m));

magI2 = abs(I2);
phaseI2 = 180*angle(I2)/pi;

fprintf('\nSecondary current magnitude = %g [A]',magI2)
fprintf('\n    and phase angle = %g [degrees]\n\n',phaseI2)
```

Practice Problem 2.9

For the current transformer of Example 2.11, find the maximum purely reactive burden $Z_b = jX_b$ such that, for 800 A flowing in the transformer primary, the secondary current will be greater than 4.95 A (i.e., there will be at most a 1.0 percent error in current magnitude).

Solution

X_b must be less than 3.19 Ω

2.9 THE PER-UNIT SYSTEM

Computations relating to machines, transformers, and systems of machines are often carried out in *per-unit* form, i.e., with all pertinent quantities expressed as decimal fractions of appropriately chosen *base values*. All the usual computations are then carried out in these per unit values instead of the familiar volts, amperes, ohms, and so on.

There are a number of advantages to the system. One is that the parameter values of machines and transformers typically fall in a reasonably narrow numerical range when expressed in a per-unit system based upon their rating. The correctness of their values is thus subject to a rapid approximate check. A second advantage is that when transformer equivalent-circuit parameters are converted to their per-unit values, the ideal transformer turns ratio becomes 1:1 and hence the ideal transformer can be eliminated. This greatly simplifies analyses since it eliminates the need to refer impedances to one side or the other of transformers. For complicated systems involving many transformers of different turns ratios, this advantage is a significant one in that a possible cause of serious mistakes is removed.

Quantities such as voltage V, current I, power P, reactive power Q, voltamperes VA, resistance R, reactance X, impedance Z, conductance G, susceptance B, and admittance Y can be translated to and from per-unit form as follows:

$$\text{Quantity in per unit} = \frac{\text{Actual quantity}}{\text{Base value of quantity}} \tag{2.47}$$

where "Actual quantity" refers to the value in volts, amperes, ohms, and so on. To a certain extent, base values can be chosen arbitrarily, but certain relations between them must be observed for the normal electrical laws to hold in the per-unit system. Thus, for a single-phase system,

$$P_{\text{base}},\ Q_{\text{base}},\ VA_{\text{base}} = V_{\text{base}}\, I_{\text{base}} \tag{2.48}$$

$$R_{\text{base}},\ X_{\text{base}},\ Z_{\text{base}} = \frac{V_{\text{base}}}{I_{\text{base}}} \tag{2.49}$$

The net result is that *only two independent base quantities can be chosen arbitrarily;* the remaining quantities are determined by the relationships of Eqs. 2.48 and 2.49. In typical usage, values of VA_{base} and V_{base} are chosen first; values of I_{base} and all other quantities in Eqs. 2.48 and 2.49 are then uniquely established.

The value of VA_{base} must be the same over the entire system under analysis. When a transformer is encountered, the values of V_{base} differ on each side and should

be chosen in the same ratio as the turns ratio of the transformer. Usually the rated or nominal voltages of the respective sides are chosen. The process of referring quantities to one side of the transformer is then taken care of automatically by using Eqs. 2.48 and 2.49 in finding and interpreting per-unit values.

This can be seen with reference to the equivalent circuit of Fig. 2.10c. If the base voltages of the primary and secondary are chosen to be in the ratio of the turns of the ideal transformer, the per-unit ideal transformer will have a unity turns ratio and hence can be eliminated.

If these rules are followed, the procedure for performing system analyses in per-unit can be summarized as follows:

1. Select a *VA* base and a base voltage at some point in the system.
2. Convert all quantities to per unit on the chosen *VA* base and with a voltage base that transforms as the turns ratio of any transformer which is encountered as one moves through the system.
3. Perform a standard electrical analysis with all quantities in per unit.
4. When the analysis is completed, all quantities can be converted back to real units (e.g., volts, amperes, watts, etc.) by multiplying their per-unit values by their corresponding base values.

When only one electric device, such as a transformer, is involved, the device's own rating is generally used for the volt-ampere base. When expressed in per-unit form on their rating as a base, the characteristics of power and distribution transformers do not vary much over a wide range of ratings. For example, the exciting current is usually between 0.02 and 0.06 per unit, the equivalent resistance is usually between 0.005 and 0.02 per unit (the smaller values applying to large transformers), and the equivalent reactance is usually between 0.015 and 0.10 per unit (the larger values applying to large high-voltage transformers). Similarly, the per-unit values of synchronous- and induction-machine parameters fall within a relatively narrow range. The reason for this is that the physics behind each type of device is the same and, in a crude sense, they can each be considered to be simply scaled versions of the same basic device. As a result, when normalized to their own rating, the effect of the scaling is eliminated and the result is a set of per-unit parameter values which is quite similar over the whole size range of that device.

Often, manufacturers supply device parameters in per unit on the device base. When several devices are involved, however, an arbitrary choice of volt-ampere base must usually be made, and that value must then be used for the overall system. As a result, when performing a system analysis, it may be necessary to convert the supplied per-unit parameter values to per-unit values on the base chosen for the analysis. The following relations can be used to convert per-unit (pu) values from one base to another:

$$(P, Q, VA)_{\text{pu on base 2}} = (P, Q, VA)_{\text{pu on base 1}} \left[\frac{VA_{\text{base 1}}}{VA_{\text{base 2}}}\right] \tag{2.50}$$

$$(R, X, Z)_{\text{pu on base 2}} = (R, X, Z)_{\text{pu on base 1}} \left[\frac{(V_{\text{base 1}})^2 VA_{\text{base 2}}}{(V_{\text{base 2}})^2 VA_{\text{base 1}}}\right] \tag{2.51}$$

$$V_{\text{pu on base 2}} = V_{\text{pu on base 1}} \left[\frac{V_{\text{base 1}}}{V_{\text{base 2}}} \right] \tag{2.52}$$

$$I_{\text{pu on base 2}} = I_{\text{pu on base 1}} \left[\frac{V_{\text{base 2}} VA_{\text{base 1}}}{V_{\text{base 1}} VA_{\text{base 2}}} \right] \tag{2.53}$$

EXAMPLE 2.12

The equivalent circuit for a 100-MVA, 7.97-kV:79.7-kV transformer is shown in Fig. 2.22a. The equivalent-circuit parameters are:

$$X_L = 0.040\ \Omega \quad X_H = 3.75\ \Omega \quad X_m = 114\ \Omega$$

$$R_L = 0.76\ \text{m}\Omega \quad R_H = 0.085\ \Omega$$

Note that the magnetizing inductance has been referred to the low-voltage side of the equivalent circuit. Convert the equivalent circuit parameters to per unit using the transformer rating as base.

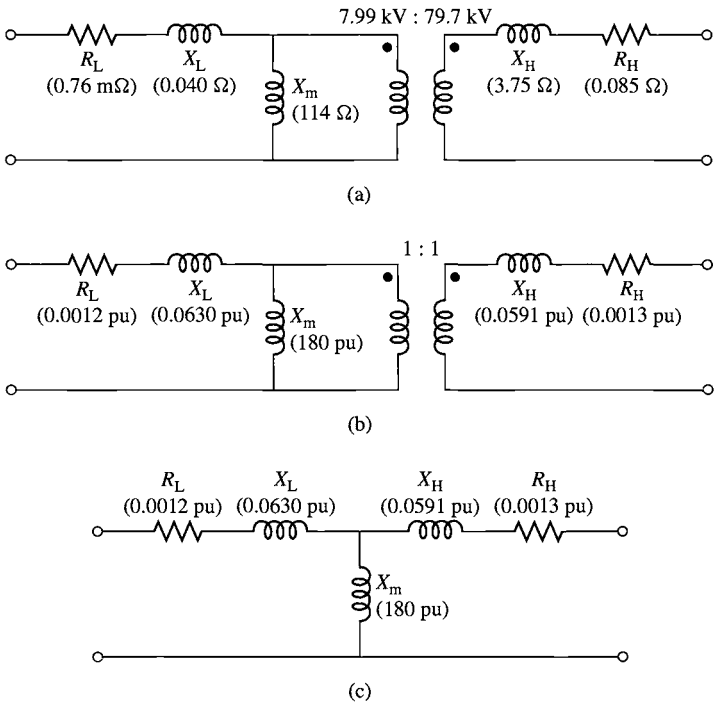

Figure 2.22 Transformer equivalent circuits for Example 2.12. (a) Equivalent circuit in actual units. (b) Per-unit equivalent circuit with 1:1 ideal transformer. (c) Per-unit equivalent circuit following elimination of the ideal transformer.

■ Solution

The base quantities for the transformer are:

Low-voltage side:

$$VA_{\text{base}} = 100\ \text{MVA} \quad V_{\text{base}} = 7.97\ \text{kV}$$

and from Eqs. 2.48 and 2.49

$$R_{\text{base}} = X_{\text{base}} = \frac{V_{\text{base}}^2}{VA_{\text{base}}} = 0.635\ \Omega$$

High-voltage side:

$$VA_{\text{base}} = 100\ \text{MVA} \quad V_{\text{base}} = 79.7\ \text{kV}$$

and from Eqs. 2.48 and 2.49

$$R_{\text{base}} = X_{\text{base}} = \frac{V_{\text{base}}^2}{VA_{\text{base}}} = 63.5\ \Omega$$

The per-unit values of the transformer parameters can now be calculated by division by their corresponding base quantities.

$$X_{\text{L}} = \frac{0.040}{0.635} = 0.0630 \text{ per unit}$$

$$X_{\text{H}} = \frac{3.75}{63.5} = 0.0591 \text{ per unit}$$

$$X_{\text{m}} = \frac{114}{0.635} = 180 \text{ per unit}$$

$$R_{\text{L}} = \frac{7.6 \times 10^{-4}}{0.635} = 0.0012 \text{ per unit}$$

$$R_{\text{H}} = \frac{0.085}{63.5} = 0.0013 \text{ per unit}$$

Finally, the voltages representing the turns ratio of the ideal transformer must each be divided by the base voltage on that side of the transformer. Thus the turns ratio of 7.97-kV:79.7-kV becomes in per unit

$$\text{Per-unit turns ratio} = \left(\frac{7.97\ \text{kV}}{7.97\ \text{kV}}\right) : \left(\frac{79.7\ \text{kV}}{79.7\ \text{kV}}\right) = 1 : 1$$

The resultant per-unit equivalent circuit is shown in Fig. 2.22b. Because it has unity turns ratio, there is no need to keep the ideal transformer and hence this equivalent circuit can be reduced to the form of Fig. 2.22c.

EXAMPLE 2.13

The exciting current measured on the low-voltage side of a 50-kVA, 2400:240-V transformer is 5.41 A. Its equivalent impedance referred to the high-voltage side is $1.42 + j1.82\ \Omega$. Using the transformer rating as the base, express in per unit on the low- and high-voltage sides (*a*) the exciting current and (*b*) the equivalent impedance.

■ Solution

The base values of voltages and currents are

$$V_{\text{base,H}} = 2400 \text{ V} \quad V_{\text{base,L}} = 240 \text{ V} \quad I_{\text{base,H}} = 20.8 \text{ A} \quad I_{\text{base,L}} = 208 \text{ A}$$

where subscripts H and L indicate the high- and low-voltage sides, respectively.

From Eq. 2.49

$$Z_{\text{base,H}} = \frac{2400}{20.8} = 115.2\ \Omega \quad Z_{\text{base,L}} = \frac{240}{208} = 1.152\ \Omega$$

a. From Eq. 2.47, the exciting current in per unit referred to the low-voltage side can be calculated as:

$$I_{\varphi,\text{L}} = \frac{5.41}{208} = 0.0260 \text{ per unit}$$

The exciting current referred to the high-voltage side is 0.541 A. Its per-unit value is

$$I_{\varphi,\text{H}} = \frac{0.541}{20.8} = 0.0260 \text{ per unit}$$

Note that, as expected, the per-unit values are the same referred to either side, corresponding to a unity turns ratio for the ideal transformer in the per-unit transformer. This is a direct consequence of the choice of base voltages in the ratio of the transformer turns ratio and the choice of a constant volt-ampere base.

b. From Eq. 2.47 and the value for Z_{base}

$$Z_{\text{eq,H}} = \frac{1.42 + j1.82}{115.2} = 0.0123 + j0.0158 \text{ per unit}$$

The equivalent impedance referred to the low-voltage side is $0.0142 + j0.0182\Omega$. Its per-unit value is

$$Z_{\text{eq,L}} = \frac{0.142 + 0.0182}{1.152} = 0.0123 + j0.0158 \text{ per unit}$$

The per-unit values referred to the high- and low-voltage sides are the same, the transformer turns ratio being accounted for in per unit by the base values. Note again that this is consistent with a unity turns ratio of the ideal transformer in the per-unit transformer equivalent circuit.

Practice Problem 2.10

A 15-kVA 120:460-V transformer has an equivalent series impedance of $0.018 + j0.042$ per unit. Calculate the equivalent series impedance in ohms (*a*) referred to the low-voltage side and (*b*) referred to the high-voltage side.

Solution

$$Z_{\text{eq,L}} = 0.017 + j0.040\ \Omega \quad \text{and} \quad Z_{\text{eq,H}} = 0.25 + j0.60\ \Omega$$

When they are applied to the analysis of three-phase systems, the base values for the per-unit system are chosen so that the relations for a balanced three-phase system

hold between them:

$$(P_{\text{base}}, Q_{\text{base}}, VA_{\text{base}})_{\text{3-phase}} = 3VA_{\text{base, per phase}} \tag{2.54}$$

In dealing with three-phase systems, $VA_{\text{base, 3-phase}}$, the three-phase volt-ampere base, and $V_{\text{base, 3-phase}} = V_{\text{base, l-l}}$, the line-to-line voltage base are usually chosen first. The base values for the phase (line-to-neutral) voltage then follows as

$$V_{\text{base, l-n}} = \frac{1}{\sqrt{3}} V_{\text{base, l-l}} \tag{2.55}$$

Note that the base current for three-phase systems is equal to the phase current, which is the same as the base current for a single-phase (per-phase) analysis. Hence

$$I_{\text{base, 3-phase}} = I_{\text{base, per phase}} = \frac{VA_{\text{base, 3-phase}}}{\sqrt{3}\, V_{\text{base, 3-phase}}} \tag{2.56}$$

Finally, the three-phase base impedance is chosen to the be the single-phase base impedance. Thus

$$\begin{aligned} Z_{\text{base, 3-phase}} &= Z_{\text{base, per phase}} \\ &= \frac{V_{\text{base, l-n}}}{I_{\text{base, per phase}}} \\ &= \frac{V_{\text{base, 3-phase}}}{\sqrt{3} I_{\text{base, 3-phase}}} \\ &= \frac{(V_{\text{base, 3-phase}})^2}{VA_{\text{base, 3-phase}}} \end{aligned} \tag{2.57}$$

The equations for conversion from base to base, Eqs. 2.50 through 2.53, apply equally to three-phase base conversion. Note that the factors of $\sqrt{3}$ and 3 relating Δ to Y quantities of volts, amperes, and ohms in a balanced three-phase system are automatically taken care of in per unit by the base values. Three-phase problems can thus be solved in per unit as if they were single-phase problems and the details of transformer (Y vs Δ on the primary and secondary of the transformer) and impedance (Y vs Δ) connections disappear, except in translating volt, ampere, and ohm values into and out of the per-unit system.

EXAMPLE 2.14

Rework Example 2.9 in per unit, specifically calculating the short-circuit phase currents which will flow in the feeder and at the 240-V terminals of the receiving-end transformer bank. Perform the calculations in per unit on the three-phase, 150-kVA, rated-voltage base of the receiving-end transformer.

■ Solution

We start by converting all the impedances to per unit. The impedance of the 500-kVA, 24 kV:2400 V sending end transformer is $0.17 + j0.92\ \Omega$/phase as referred to the 2400-V

side. From Eq. 2.57, the base impedance corresponding to a 2400-V, 150-kVA base is

$$Z_{\text{base}} = \frac{2400^2}{150 \times 10^3} = 38.4\ \Omega$$

From Example 2.9, the total series impedance is equal to $Z_{\text{tot}} = 0.64 + j2.33\ \Omega$/phase and thus in per unit it is equal to

$$Z_{\text{tot}} = \frac{0.64 + j2.33}{38.4} = 0.0167 + j0.0607 \text{ per unit}$$

which is of magnitude

$$|Z_{\text{tot}}| = 0.0629 \text{ per unit}$$

The voltage applied to the high-voltage side of the sending-end transformer is $V_s = 24.0$ kV $= 1.0$ per unit on a rated-voltage base and hence the short-circuit current will equal

$$I_{\text{sc}} = \frac{V_s}{|Z_{\text{tot}}|} = \frac{1.0}{0.0629} = 15.9 \text{ per unit}$$

To calculate the phase currents in amperes, it is simply necessary to multiply the per-unit short-circuit current by the appropriate base current. Thus, at the 2400-V feeder the base current is

$$I_{\text{base, 2400-V}} = \frac{150 \times 10^3}{\sqrt{3}\,2400} = 36.1 \text{ A}$$

and hence the feeder current will be

$$I_{\text{feeder}} = 15.9 \times 36.1 = 574 \text{ A}$$

The base current at the 240-V secondary of the receiving-end transformers is

$$I_{\text{base, 240-V}} = \frac{150 \times 10^3}{\sqrt{3}\,240} = 361 \text{ A}$$

and hence the short-circuit current is

$$I_{\text{240-V secondary}} = 15.9 \times 361 = 5.74 \text{ kA}$$

As expected, these values are equivalent within numerical accuracy to those calculated in Example 2.9.

Practice Problem 2.11

Calculate the magnitude of the short-circuit current in the feeder of Example 2.9 if the 2400-V feeder is replaced by a feeder with an impedance of $0.07 + j0.68\ \Omega$/phase. Perform this calculation on the 500-kVA, rated-voltage base of the sending-end transformer and express your solution both in per unit and in amperes per phase.

Solution

$$\text{Short-circuit current} = 5.20 \text{ per unit} = 636 \text{ A}$$

EXAMPLE 2.15

A three-phase load is supplied from a 2.4-kV:460-V, 250-kVA transformer whose equivalent series impedance is $0.026 + j0.12$ per unit on its own base. The load voltage is observed to be 438-V line-line, and it is drawing 95 kW at unity power factor. Calculate the voltage at the high-voltage side of the transformer. Perform the calculations on a 460-V, 100-kVA base.

■ Solution

The 460-V side base impedance for the transformer is

$$Z_{\text{base, transformer}} = \frac{460^2}{250 \times 10^3} = 0.846\ \Omega$$

while that based upon a 100-kVA base is

$$Z_{\text{base, 100-kVA}} = \frac{460^2}{100 \times 10^3} = 2.12\ \Omega$$

Thus, from Eq. 2.51 the per-unit transformer impedance on a 100-kVA base is

$$Z_{\text{transformer}} = (0.026 + j0.12)\left(\frac{0.864}{2.12}\right) = 0.0106 + j.0489 \text{ per unit}$$

The per unit load voltage is

$$\hat{V}_{\text{load}} = \frac{438}{460} = 0.952\ \angle 0^\circ \text{ per unit}$$

where the load voltage has been chosen as the reference for phase-angle calculations.

The per-unit load power is

$$P_{\text{load}} = \frac{95}{100} = 0.95 \text{ per unit}$$

and hence the per-unit load current, which is in phase with the load voltage because the load is operating at unity power factor, is

$$\hat{I}_{\text{load}} = \frac{P_{\text{load}}}{V_{\text{load}}} = \frac{0.95}{0.952} = 0.998\ \angle 0^\circ \text{ per unit}$$

Thus we can now calculate the high-side voltage of the transformer

$$\begin{aligned}\hat{V}_{\text{H}} &= \hat{V}_{\text{load}} + \hat{I}_{\text{load}} Z_{\text{transformer}} \\ &= 0.952 + 0.998(0.0106 + j0.0489) \\ &= 0.963 + j0.0488 = 0.964\ \angle 29.0^\circ \text{ per unit}\end{aligned}$$

Thus the high-side voltage is equal to 0.964×2400 V $= 2313$ V (line-line).

Practice Problem 2.12

Repeat Example 2.15 if the 250-kV three-phase transformer is replaced by a 150-kV transformer also rated at 2.4-kV:460-V and whose equivalent series impedance is $0.038 + j0.135$ per unit on its own base. Perform the calculations on a 460-V, 100-kVA base.

Solution

$$\text{High-side voltage} = 0.982 \text{ per unit} = 2357 \text{ V (line-line)}$$

2.10 SUMMARY

Although not an electromechanical device, the transformer is a common and indispensable component of ac systems where it is used to transform voltages, currents, and impedances to appropriate levels for optimal use. For the purposes of our study of electromechanical systems, transformers serve as valuable examples of the analysis techniques which must be employed. They offer us opportunities to investigate the properties of magnetic circuits, including the concepts of mmf, magnetizing current, and magnetizing, mutual, and leakage fluxes and their associated inductances.

In both transformers and rotating machines, a magnetic field is created by the combined action of the currents in the windings. In an iron-core transformer, most of this flux is confined to the core and links all the windings. This resultant mutual flux induces voltages in the windings proportional to their number of turns and is responsible for the voltage-changing property of a transformer. In rotating machines, the situation is similar, although there is an air gap which separates the rotating and stationary components of the machine. Directly analogous to the manner in which transformer core flux links the various windings on a transformer core, the mutual flux in rotating machines crosses the air gap, linking the windings on the rotor and stator. As in a transformer, the mutual flux induces voltages in these windings proportional to the number of turns and the time rate of change of the flux.

A significant difference between transformers and rotating machines is that in rotating machines there is relative motion between the windings on the rotor and stator. This relative motion produces an additional component of the time rate of change of the various winding flux linkages. As will be discussed in Chapter 3, the resultant voltage component, known as the *speed voltage,* is characteristic of the process of electromechanical energy conversion. In a static transformer, however, the time variation of flux linkages is caused simply by the time variation of winding currents; no mechanical motion is involved, and no electromechanical energy conversion takes place.

The resultant core flux in a transformer induces a counter emf in the primary which, together with the primary resistance and leakage-reactance voltage drops, must balance the applied voltage. Since the resistance and leakage-reactance voltage drops usually are small, the counter emf must approximately equal the applied voltage and the core flux must adjust itself accordingly. Exactly similar phenomena must take place in the armature windings of an ac motor; the resultant air-gap flux wave must adjust itself to generate a counter emf approximately equal to the applied voltage.

In both transformers and rotating machines, the net mmf of all the currents must accordingly adjust itself to create the resultant flux required by this voltage balance. In any ac electromagnetic device in which the resistance and leakage-reactance voltage drops are small, the resultant flux is very nearly determined by the applied voltage and frequency, and the currents must adjust themselves accordingly to produce the mmf required to create this flux.

In a transformer, the secondary current is determined by the voltage induced in the secondary, the secondary leakage impedance, and the electric load. In an induction motor, the secondary (rotor) current is determined by the voltage induced in the secondary, the secondary leakage impedance, and the mechanical load on its shaft. Essentially the same phenomena take place in the primary winding of the transformer and in the armature (stator) windings of induction and synchronous motors. In all three, the primary, or armature, current must adjust itself so that the combined mmf of all currents creates the flux required by the applied voltage.

In addition to the useful mutual fluxes, in both transformers and rotating machines there are leakage fluxes which link individual windings without linking others. Although the detailed picture of the leakage fluxes in rotating machines is more complicated than that in transformers, their effects are essentially the same. In both, the leakage fluxes induce voltages in ac windings which are accounted for as leakage-reactance voltage drops. In both, the reluctances of the leakage-flux paths are dominanted by that of a path through air, and hence the leakage fluxes are nearly linearly proportional to the currents producing them. The leakage reactances therefore are often assumed to be constant, independent of the degree of saturation of the main magnetic circuit.

Further examples of the basic similarities between transformers and rotating machines can be cited. Except for friction and windage, the losses in transformers and rotating machines are essentially the same. Tests for determining the losses and equivalent circuit parameters are similar: an open-circuit, or no-load, test gives information regarding the excitation requirements and core losses (along with friction and windage losses in rotating machines), while a short-circuit test together with dc resistance measurements gives information regarding leakage reactances and winding resistances. Modeling of the effects of magnetic saturation is another example: In both transformers and ac rotating machines, the leakage reactances are usually assumed to be unaffected by saturation, and the saturation of the main magnetic circuit is assumed to be determined by the resultant mutual or air-gap flux.

2.11 PROBLEMS

2.1 A transformer is made up of a 1200-turn primary coil and an open-circuited 75-turn secondary coil wound around a closed core of cross-sectional area 42 cm^2. The core material can be considered to saturate when the rms applied flux density reaches 1.45 T. What maximum 60-Hz rms primary voltage is possible without reaching this saturation level? What is the corresponding secondary voltage? How are these values modified if the applied frequency is lowered to 50 Hz?

2.2 A magnetic circuit with a cross-sectional area of 15 cm^2 is to be operated at 60 Hz from a 120-V rms supply. Calculate the number of turns required to achieve a peak magnetic flux density of 1.8 T in the core.

2.3 A transformer is to be used to transform the impedance of a 8-Ω resistor to an impedance of 75 Ω. Calculate the required turns ratio, assuming the transformer to be ideal.

2.4 A 100-Ω resistor is connected to the secondary of an idea transformer with a turns ratio of 1:4 (primary to secondary). A 10-V rms, 1-kHz voltage source is connected to the primary. Calculate the primary current and the voltage across the 100-Ω resistor.

2.5 A source which can be represented by a voltage source of 8 V rms in series with an internal resistance of 2 kΩ is connected to a 50-Ω load resistance through an ideal transformer. Calculate the value of turns ratio for which maximum power is supplied to the load and the corresponding load power? Using MATLAB, plot the the power in milliwatts supplied to the load as a function of the transformer ratio, covering ratios from 1.0 to 10.0.

2.6 Repeat Problem 2.5 with the source resistance replaced by a 2-kΩ reactance.

2.7 A single-phase 60-Hz transformer has a nameplate voltage rating of 7.97 kV:266 V, which is based on its winding turns ratio. The manufacturer calculates that the primary (7.97-kV) leakage inductance is 165 mH and the primary magnetizing inductance is 135 H. For an applied primary voltage of 7970 V at 60 Hz, calculate the resultant open-circuit secondary voltage.

2.8 The manufacturer calculates that the transformer of Problem 2.7 has a secondary leakage inductance of 0.225 mH.

a. Calculate the magnetizing inductance as referred to the secondary side.

b. A voltage of 266 V, 60 Hz is applied to the secondary. Calculate (*i*) the resultant open-circuit primary voltage and (*ii*) the secondary current which would result if the primary were short-circuited.

2.9 A 120-V:2400-V, 60-Hz, 50-kVA transformer has a magnetizing reactance (as measured from the 120-V terminals) of 34.6 Ω. The 120-V winding has a leakage reactance of 27.4 mΩ and the 2400-V winding has a leakage reactance of 11.2 Ω.

a. With the secondary open-circuited and 120 V applied to the primary (120-V) winding, calculate the primary current and the secondary voltage.

b. With the secondary short-circuited, calculate the primary voltage which will result in rated current in the primary winding. Calculate the corresponding current in the secondary winding.

2.10 A 460-V:2400-V transformer has a series leakage reactance of 37.2 Ω as referred to the high-voltage side. A load connected to the low-voltage side is observed to be absorbing 25 kW, unity power factor, and the voltage is measured to be 450 V. Calculate the corresponding voltage and power factor as measured at the high-voltage terminals.

2.11 The resistances and leakage reactances of a 30-kVA, 60-Hz, 2400-V:240-V distribution transformer are

$$R_1 = 0.68\ \Omega \quad R_2 = 0.0068\ \Omega$$
$$X_{l_1} = 7.8\ \Omega \quad X_{l_2} = 0.0780\ \Omega$$

where subscript 1 denotes the 2400-V winding and subscript 2 denotes the 240-V winding. Each quantity is referred to its own side of the transformer.

a. Draw the equivalent circuit referred to (*i*) the high- and (*ii*) the low-voltage sides. Label the impedances numerically.

b. Consider the transformer to deliver its rated kVA to a load on the low-voltage side with 230 V across the load. (*i*) Find the high-side terminal voltage for a load power factor of 0.85 power factor lagging. (*ii*) Find the high-side terminal voltage for a load power factor of 0.85 power factor leading.

c. Consider a rated-kVA load connected at the low-voltage terminals operating at 240V. Use MATLAB to plot the high-side terminal voltage as a function of the power-factor angle as the load power factor varies from 0.6 leading through unity power factor to 0.6 pf lagging.

2.12 Repeat Problem 2.11 for a 75-kVA, 60-Hz, 4600-V:240-V distribution transformer whose resistances and leakage reactances are

$$R_1 = 0.846\ \Omega \quad R_2 = 0.00261\ \Omega$$
$$X_{l_1} = 26.8\ \Omega \quad X_{l_2} = 0.0745\ \Omega$$

where subscript 1 denotes the 4600-V winding and subscript 2 denotes the 240-V winding. Each quantity is referred to its own side of the transformer.

2.13 A single-phase load is supplied through a 35-kV feeder whose impedance is $95 + j360\ \Omega$ and a 35-kV:2400-V transformer whose equivalent impedance is $0.23 + j1.27\ \Omega$ referred to its low-voltage side. The load is 160 kW at 0.89 leading power factor and 2340 V.

a. Compute the voltage at the high-voltage terminals of the transformer.

b. Compute the voltage at the sending end of the feeder.

c. Compute the power and reactive power input at the sending end of the feeder.

2.14 Repeat Example 2.6 with the transformer operating at full load and unity power factor.

2.15 The nameplate on a 50-MVA, 60-Hz single-phase transformer indicates that it has a voltage rating of 8.0-kV:78-kV. An open-circuit test is conducted from the low-voltage side, and the corresponding instrument readings are 8.0 kV, 62.1 A, and 206 kW. Similarly, a short-circuit test from the low-voltage side gives readings of 674 V, 6.25 kA, and 187 kW.

a. Calculate the equivalent series impedance, resistance, and reactance of the transformer as referred to the low-voltage terminals.

b. Calculate the equivalent series impedance of the transformer as referred to the high-voltage terminals.

c. Making appropriate approximations, draw a T equivalent circuit for the transformer.

d. Determine the efficiency and voltage regulation if the transformer is operating at the rated voltage and load (unity power factor).

e. Repeat part (d), assuming the load to be at 0.9 power factor leading.

2.16 A 550-kVA, 60-Hz transformer with a 13.8-kV primary winding draws 4.93 A and 3420 W at no load, rated voltage and frequency. Another transformer has a core with all its linear dimensions $\sqrt{2}$ times as large as the corresponding dimensions of the first transformer. The core material and lamination thickness are the same in both transformers. If the primary windings of both transformers have the same number of turns, what no-load current and power will the second transformer draw with 27.6 kV at 60 Hz impressed on its primary?

2.17 The following data were obtained for a 20-kVA, 60-Hz, 2400:240-V distribution transformer tested at 60 Hz:

	Voltage, V	Current, A	Power, W
With high-voltage winding open-circuited	240	1.038	122
With low-voltage terminals short-circuited	61.3	8.33	257

a. Compute the efficiency at full-load current and the rated terminal voltage at 0.8 power factor.

b. Assume that the load power factor is varied while the load current and secondary terminal voltage are held constant. Use a phasor diagram to determine the load power factor for which the regulation is greatest. What is this regulation?

2.18 A 75-kVa, 240-V:7970-V, 60-Hz single-phase distribution transformer has the following parameters referred to the high-voltage side:

$$R_1 = 5.93\ \Omega \quad X_1 = 43.2\ \Omega$$
$$R_2 = 3.39\ \Omega \quad X_2 = 40.6\ \Omega$$
$$R_c = 244\ \text{k}\Omega \quad X_m = 114\ \text{k}\Omega$$

Assume that the transformer is supplying its rated kVA at its low-voltage terminals. Write a MATLAB script to determine the efficiency and regulation of the transformer for any specified load power factor (leading or lagging). You may use reasonable engineering approximations to simplify your analysis. Use your MATLAB script to determine the efficiency and regulation for a load power factor of 0.87 leading.

2.19 The transformer of Problem 2.11 is to be connected as an autotransformer. Determine (*a*) the voltage ratings of the high- and low-voltage windings for this connection and (*b*) the kVA rating of the autotransformer connection.

2.20 A 120:480-V, 10-kVA transformer is to be used as an autotransformer to supply a 480-V circuit from a 600-V source. When it is tested as a two-winding transformer at rated load, unity power factor, its efficiency is 0.979.

a. Make a diagram of connections as an autotransformer.

b. Determine its kVA rating as an autotransformer.

c. Find its efficiency as an autotransformer at full load, with 0.85 power factor lagging.

2.21 Consider the 8-kV:78-kV, 50-MVA transformer of Problem 2.15 connected as an autotransformer.

a. Determine the voltage ratings of the high- and low-voltage windings for this connection and the kVA rating of the autotransformer connection.

b. Calculate the efficiency of the transformer in this connection when it is supplying its rated load at unity power factor.

2.22 Write a MATLAB script whose inputs are the rating (voltage and kVA) and rated-load, unity-power-factor efficiency of a single-transformer and whose output is the transformer rating and rated-load, unity-power-factor efficiency when connected as an autotransformer.

2.23 The high-voltage terminals of a three-phase bank of three single-phase transformers are supplied from a three-wire, three-phase 13.8-kV (line-to-line) system. The low-voltage terminals are to be connected to a three-wire, three-phase substation load drawing up to 4500 kVA at 2300 V line-to-line. Specify the required voltage, current, and kVA ratings of each transformer (both high- and low-voltage windings) for the following connections:

	High-voltage Windings	Low-voltage Windings
a.	Y	Δ
b.	Δ	Y
c.	Y	Y
d.	Δ	Δ

2.24 Three 100-MVA single-phase transformers, rated at 13.8 kV:66.4 kV, are to be connected in a three-phase bank. Each transformer has a series impedance of $0.0045 + j0.19\ \Omega$ referred to its 13.8-kV winding.

a. If the transformers are connected Y-Y, calculate (*i*) the voltage and power rating of the three-phase connection, (*ii*) the equivalent impedance as referred to its low-voltage terminals, and (*iii*) the equivalent impedance as referred to its high-voltage terminals.

b. Repeat part (a) if the transformer is connected Y on its low-voltage side and Δ on its high-voltage side.

2.25 Repeat Example 2.8 for a load drawing rated current from the transformers at unity power factor.

2.26 A three-phase Y-Δ transformer is rated 225-kV:24-kV, 400 MVA and has a series reactance of 11.7 Ω as referred to its high-voltage terminals. The transformer is supplying a load of 325 MVA, with 0.93 power factor lagging at a voltage of 24 kV (line-to-line) on its low-voltage side. It is supplied from a feeder whose impedance is $0.11 + j2.2\ \Omega$ connected to its high-voltage terminals. For these conditions, calculate (*a*) the line-to-line voltage at the high-voltage terminals of the transformer and (*b*) the line-to-line voltage at the sending end of the feeder.

2.27 Assume the total load in the system of Problem 2.26 to remain constant at 325 MVA. Write a MATLAB script to plot the line-to-line voltage which must be applied to the sending end of the feeder to maintain the load voltage at 24 kV line-to-line for load power factors in range from 0.75 lagging to unity to 0.75 leading. Plot the sending-end voltage as a function of power factor angle.

2.28 A Δ-Y-connected bank of three identical 100-kVA, 2400-V:120-V, 60-Hz transformers is supplied with power through a feeder whose impedance is $0.065 + j0.87\ \Omega$ per phase. The voltage at the sending end of the feeder is held constant at 2400 V line-to-line. The results of a single-phase short-circuit test on one of the transformers with its low-voltage terminals short-circuited are

$$V_H = 53.4\ \text{V} \quad f = 60\ \text{Hz} \quad I_H = 41.7\ \text{A} \quad P = 832\ \text{W}$$

a. Determine the line-to-line voltage on the low-voltage side of the transformer when the bank delivers rated current to a balanced three-phase unity power factor load.

b. Compute the currents in the transformer's high- and low-voltage windings and in the feeder wires if a solid three-phase short circuit occurs at the secondary line terminals.

2.29 A 7970-V:120-V, 60-Hz potential transformer has the following parameters as seen from the high-voltage (primary) winding:

$$X_1 = 1721\ \Omega \quad X_2' = 1897\ \Omega \quad X_m = 782\ \text{k}\Omega$$
$$R_1 = 1378\ \Omega \quad R_2' = 1602\ \Omega$$

a. Assuming that the secondary is open-circuited and that the primary is connected to a 7.97-kV source, calculate the magnitude and phase angle (with respect to the high-voltage source) of the voltage at the secondary terminals.

b. Calculate the magnitude and phase angle of the secondary voltage if a 1-kΩ resistive load is connected to the secondary terminals.

c. Repeat part (b) if the burden is changed to a 1-kΩ reactance.

2.30 For the potential transformer of Problem 2.29, find the maximum reactive burden (mimimum reactance) which can be applied at the secondary terminals such that the voltage magnitude error does not exceed 0.5 percent.

2.31 Consider the potential transformer of Problem 2.29.

a. Use MATLAB to plot the percentage error in voltage magnitude as a function of the magnitude of the burden impedance (*i*) for a resistive burden of $100\ \Omega \le R_b \le 3000\ \Omega$ and (*ii*) for a reactive burden of $100\ \Omega \le X_b \le 3000\ \Omega$. Plot these curves on the same axis.

b. Next plot the phase error in degrees as a function of the magnitude of the burden impedance (*i*) for a resistive burden of $100\ \Omega \le R_b \le 3000\ \Omega$ and (*ii*) for a reactive burden of $100\ \Omega \le X_b \le 3000\ \Omega$. Again, plot these curves on the same axis.

2.32 A 200-A:5-A, 60-Hz current transformer has the following parameters as seen from the 200-A (primary) winding:

$$X_1 = 745\ \mu\Omega \quad X_2' = 813\ \mu\Omega \quad X_m = 307\ \text{m}\Omega$$
$$R_1 = 136\ \mu\Omega \quad R_2' = 128\ \mu\Omega$$

a. Assuming a current of 200 A in the primary and that the secondary is short-circuited, find the magnitude and phase angle of the secondary current.

b. Repeat the calculation of part (a) if the CT is shorted through a $250\ \mu\Omega$ burden.

2.33 Consider the current transformer of Problem 2.32.

a. Use MATLAB to plot the percentage error in current magnitude as a function of the magnitude of the burden impedance (*i*) for a resistive burden of $100\ \Omega \le R_b \le 1000\ \Omega$ and (*ii*) for a reactive burden of $100\ \Omega \le X_b \le 1000\ \Omega$. Plot these curves on the same axis.

b. Next plot the phase error in degrees as a function of the magnitude of the burden impedance (*i*) for a resistive burden of $100\ \Omega \le R_b \le 1000\ \Omega$ and (*ii*) for a reactive burden of $100\ \Omega \le X_b \le 1000\ \Omega$. Again, plot these curves on the same axis.

2.34 A 15-kV:175-kV, 125-MVA, 60-Hz single-phase transformer has primary and secondary impedances of $0.0095 + j0.063$ per unit each. The magnetizing impedance is $j148$ per unit. All quantities are in per unit on the transformer base. Calculate the primary and secondary resistances and reactances and the magnetizing inductance (referred to the low-voltage side) in ohms and henrys.

2.35 The nameplate on a 7.97-kV:460-V, 75-kVA, single-phase transformer indicates that it has a series reactance of 12 percent (0.12 per unit).

a. Calculate the series reactance in ohms as referred to (*i*) the low-voltage terminal and (*ii*) the high-voltage terminal.

b. If three of these transformers are connected in a three-phase Y-Y connection, calculate (*i*) the three-phase voltage and power rating, (*ii*) the per unit impedance of the transformer bank, (*iii*) the series reactance in

ohms as referred to the high-voltage terminal, and (*iv*) the series reactance in ohms as referred to the low-voltage terminal.

c. Repeat part (b) if the three transformers are connected in Y on their HV side and Δ on their low-voltage side.

2.36 a. Consider the Y-Y transformer connection of Problem 2.35, part (b). If the rated voltage is applied to the high-voltage terminals and the three low-voltage terminals are short-circuited, calculate the magnitude of the phase current in per unit and in amperes on (*i*) the high-voltage side and (*ii*) the low-voltage side.

b. Repeat this calculation for the Y-Δ connection of Problem 2.35, part (c).

2.37 A three-phase generator step-up transformer is rated 26-kV:345-kV, 850 MVA and has a series impedance of $0.0035 + j0.087$ per unit on this base. It is connected to a 26-kV, 800-MVA generator, which can be represented as a voltage source in series with a reactance of $j1.57$ per unit on the generator base.

a. Convert the per unit generator reactance to the step-up transformer base.

b. The unit is supplying 700 MW at 345 kV and 0.95 power factor lagging to the system at the transformer high-voltage terminals. (*i*) Calculate the transformer low-side voltage and the generator internal voltage behind its reactance in kV. (*ii*) Find the generator output power in MW and the power factor.

3 CHAPTER

Electromechanical-Energy-Conversion Principles

We are concerned here with the electromechanical-energy-conversion process, which takes place through the medium of the electric or magnetic field of the conversion device. Although the various conversion devices operate on similar principles, their structures depend on their function. Devices for measurement and control are frequently referred to as *transducers;* they generally operate under linear input-output conditions and with relatively small signals. The many examples include microphones, pickups, sensors, and loudspeakers. A second category of devices encompasses *force-producing devices* and includes solenoids, relays, and electromagnets. A third category includes *continuous energy-conversion equipment* such as motors and generators.

This chapter is devoted to the principles of electromechanical energy conversion and the analysis of the devices which accomplish this function. Emphasis is placed on the analysis of systems which use magnetic fields as the conversion medium since the remaining chapters of the book deal with such devices. However, the analytical techniques for electric field systems are quite similar.

The purpose of such analysis is threefold: (1) to aid in understanding how energy conversion takes place, (2) to provide techniques for designing and optimizing the devices for specific requirements, and (3) to develop models of electromechanical-energy-conversion devices that can be used in analyzing their performance as components in engineering systems. Transducers and force-producing devices are treated in this chapter; continuous energy-conversion devices are treated in the rest of the book.

The concepts and techniques presented in this chapter are quite powerful and can be applied to a wide range of engineering situations involving electromechanical energy conversion. Sections 3.1 and 3.2 present a quantitative discussion of the forces in electromechanical systems and an overview of the energy method which forms the basis for the derivations presented here. Based upon the energy method, the remainder

of the chapter develops expressions for forces and torques in magnetic-field-based electromechanical systems.

3.1 FORCES AND TORQUES IN MAGNETIC FIELD SYSTEMS

The *Lorentz Force Law*

$$\mathbf{F} = q(\mathbf{E} + \mathbf{v} \times \mathbf{B}) \tag{3.1}$$

gives the force $\mathbf{F}$ on a particle of charge q in the presence of electric and magnetic fields. In SI units, $\mathbf{F}$ is in *newtons*, q in *coulombs*, E in *volts per meter*, $\mathbf{B}$ in *teslas*, and v, which is the velocity of the particle relative to the magnetic field, in *meters per second*.

Thus, in a pure electric-field system, the force is determined simply by the charge on the particle and the electric field

$$\mathbf{F} = q\mathbf{E} \tag{3.2}$$

The force acts in the direction of the electric field and is independent of any particle motion.

In pure magnetic-field systems, the situation is somewhat more complex. Here the force

$$\mathbf{F} = q(\mathbf{v} \times \mathbf{B}) \tag{3.3}$$

is determined by the magnitude of the charge on the particle and the magnitude of the $\mathbf{B}$ field as well as the velocity of the particle. In fact, the direction of the force is always perpendicular to the direction of both the particle motion and that of the magnetic field. Mathematically, this is indicated by the vector cross product $\mathbf{v} \times \mathbf{B}$ in Eq. 3.3. The magnitude of this cross product is equal to the product of the magnitudes of $\mathbf{v}$ and $\mathbf{B}$ and the sine of the angle between them; its direction can be found from the right-hand rule, which states that when the thumb of the right hand points in the direction of $\mathbf{v}$ and the index finger points in the direction of $\mathbf{B}$, the force, which is perpendicular to the directions of both $\mathbf{B}$ and $\mathbf{v}$, points in the direction normal to the palm of the hand, as shown in Fig. 3.1.

For situations where large numbers of charged particles are in motion, it is convenient to rewrite Eq. 3.1 in terms of the *charge density* ρ (measured in units of *coulombs per cubic meter*) as

$$\mathbf{F}_{\mathrm{v}} = \rho(\mathbf{E} + \mathbf{v} \times \mathbf{B}) \tag{3.4}$$

where the subscript v indicates that $\mathbf{F}_{\mathrm{v}}$ is a *force density* (force per unit volume) which in SI units is measured in *newtons per cubic meter*.

The product $\rho\mathbf{v}$ is known as the *current density*

$$\mathbf{J} = \rho\mathbf{v} \tag{3.5}$$

which has the units of *amperes per square meter*. The magnetic-system force density

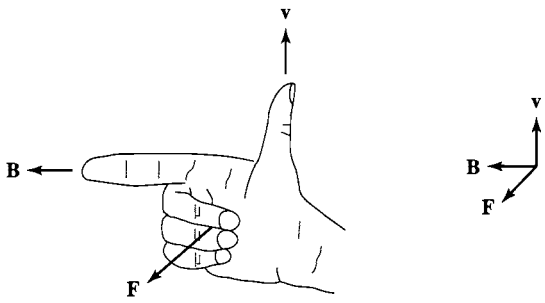

Figure 3.1 Right-hand rule for determining the direction magnetic-field component of the Lorentz force $\mathbf{F} = q(\mathbf{v} \times \mathbf{B})$.

corresponding to Eq. 3.3 can then be written as

$$\mathbf{F}_v = \mathbf{J} \times \mathbf{B} \tag{3.6}$$

For currents flowing in conducting media, Eq. 3.6 can be used to find the force density acting on the material itself. Note that a considerable amount of physics is hidden in this seemingly simple statement, since the mechanism by which the force is transferred from the moving charges to the conducting medium is a complex one.

EXAMPLE 3.1

A nonmagnetic rotor containing a single-turn coil is placed in a uniform magnetic field of magnitude B_0, as shown in Fig. 3.2. The coil sides are at radius R and the wire carries current I

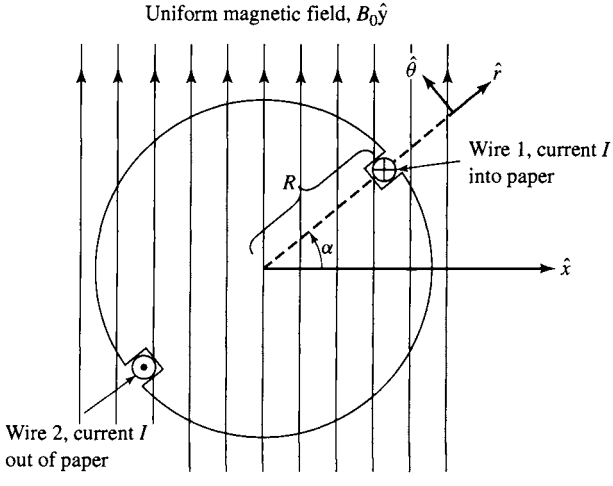

Figure 3.2 Single-coil rotor for Example 3.1.

as indicated. Find the θ-directed torque as a function of rotor position α when $I = 10$ A, $B_0 = 0.02$ T and $R = 0.05$ m. Assume that the rotor is of length $l = 0.3$ m.

■ Solution

The force per unit length on a wire carrying current I can be found by multiplying Eq. 3.6 by the cross-sectional area of the wire. When we recognize that the product of the cross-sectional area and the current density is simply the current **I**, the force per unit length acting on the wire is given by

$$\mathbf{F} = \mathbf{I} \times \mathbf{B}$$

Thus, for wire 1 carrying current I into the paper, the θ-directed force is given by

$$F_{1_\theta} = -I B_0 l \sin\alpha$$

and for wire 2 (which carries current in the opposite direction and is located 180° away from wire 1)

$$F_{2_\theta} = -I B_0 l \sin\alpha$$

where l is the length of the rotor. The torque T acting on the rotor is given by the sum of the force-moment-arm products for each wire

$$T = -2I B_0 R l \sin\alpha = -2(10)(0.02)(0.05)(0.3)\sin\alpha = -0.006\sin\alpha \quad \text{N}\cdot\text{m}$$

Practice Problem 3.1

Repeat Example 3.1 for the situation in which the uniform magnetic field points to the right instead of vertically upward as in Fig. 3.2.

Solution

$$T = -0.006\cos\alpha \quad \text{N}\cdot\text{m}$$

For situations in which the forces act only on current-carrying elements and which are of simple geometry (such as that of Example 3.1), Eq. 3.6 is generally the simplest and easiest way to calculate the forces acting on the system. Unfortunately, very few practical situations fall into this class. In fact, as discussed in Chapter 1, most electromechanical-energy-conversion devices contain magnetic material; in these systems, forces act directly on the magnetic material and clearly cannot be calculated from Eq. 3.6.

Techniques for calculating the detailed, localized forces acting on magnetic materials are extremely complex and require detailed knowledge of the field distribution throughout the structure. Fortunately, most electromechanical-energy-conversion devices are constructed of rigid, nondeforming structures. The performance of these devices is typically determined by the net force, or torque, acting on the moving component, and it is rarely necessary to calculate the details of the internal force distribution. For example, in a properly designed motor, the motor characteristics are determined by the net accelerating torque acting on the rotor; accompanying forces,

which act to squash or deform the rotor, play no significant role in the performance of the motor and generally are not calculated.

To understand the behavior of rotating machinery, a simple physical picture is quite useful. Associated with the rotor structure is a magnetic field (produced in many machines by currents in windings on the rotor), and similarly with the stator; one can picture them as a set of north and south magnetic poles associated with each structure. Just as a compass needle tries to align with the earth's magnetic field, these two sets of fields attempt to align, and torque is associated with their displacement from alignment. Thus, in a motor, the stator magnetic field rotates ahead of that of the rotor, pulling on it and performing work. The opposite is true for a generator, in which the rotor does the work on the stator.

Various techniques have evolved to calculate the net forces of concern in the electromechanical-energy-conversion process. The technique developed in this chapter and used throughout the book is known as the *energy method* and is based on the principle of *conservation of energy*. The basis for this method can be understood with reference to Fig. 3.3a, where a magnetic-field-based electromechanical-energy-conversion device is indicated schematically as a lossless magnetic-energy-storage system with two terminals. The electric terminal has two terminal variables, a voltage e and a current i, and the mechanical terminal also has two terminal variables, a force f_{fld} and a position x.

This sort of representation is valid in situations where the loss mechanism can be separated (at least conceptually) from the energy-storage mechanism. In these cases the electrical losses, such as ohmic losses in windings, can be represented as external elements (i.e., resistors) connected to the electric terminals, and the mechanical losses, such as friction and windage, can be included external to the mechanical terminals. Figure 3.3b shows an example of such a system; a simple force-producing device with a single coil forming the electric terminal, and a movable plunger serving as the mechanical terminal.

The interaction between the electric and mechanical terminals, i.e., the electromechanical energy conversion, occurs through the medium of the magnetic stored

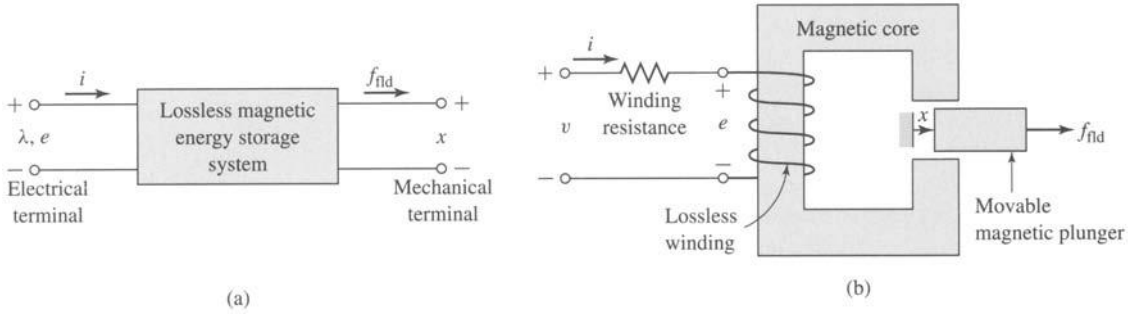

Figure 3.3 (a) Schematic magnetic-field electromechanical-energy-conversion device; (b) simple force-producing device.

energy. Since the energy-storage system is lossless, it is a simple matter to write that the time rate of change of W_{fld}, the stored energy in the magnetic field, is equal to the electric power input (given by the product of the terminal voltage and current) less the mechanical power output of the energy storage system (given by the product of the mechanical force and the mechanical velocity):

$$\frac{dW_{\text{fld}}}{dt} = ei - f_{\text{fld}}\frac{dx}{dt} \tag{3.7}$$

Recognizing that, from Eq. 1.27, the voltage at the terminals of our lossless winding is given by the time-derivative of the winding flux linkages

$$e = \frac{d\lambda}{dt} \tag{3.8}$$

and multiplying Eq. 3.7 by dt, we get

$$dW_{\text{fld}} = i\,d\lambda - f_{\text{fld}}\,dx \tag{3.9}$$

As shown in Section 3.4, Eq. 3.9 permits us to solve for the force simply as a function of the flux λ and the mechanical terminal position x. Note that this result comes about as a consequence of our assumption that it is possible to separate the losses out of the physical problem, resulting in a lossless energy-storage system, as in Fig. 3.3a.

Equations 3.7 and 3.9 form the basis for the energy method. This technique is quite powerful in its ability to calculate forces and torques in complex electromechanical-energy-conversion systems. The reader should recognize that this power comes at the expense of a detailed picture of the force-producing mechanism. The forces themselves are produced by such well-known physical phenomena as the Lorentz force on current carrying elements, described by Eq. 3.6, and the interaction of the magnetic fields with the dipoles in the magnetic material.

3.2 ENERGY BALANCE

The principle of conservation of energy states that energy is neither created nor destroyed; it is merely changed in form. For example, a golf ball leaves the tee with a certain amount of kinetic energy; this energy is eventually dissipated as heat due to air friction or rolling friction by the time the ball comes to rest on the fairway. Similarly, the kinetic energy of a hammer is eventually dissipated as heat as a nail is driven into a piece of wood. For isolated systems with clearly identifiable boundaries, this fact permits us to keep track of energy in a simple fashion: the net flow of energy into the system across its boundary is equal to the sum of the time rate of change of energy stored in the system.

This result, which is a statement of the first law of thermodynamics, is quite general. We apply it in this chapter to electromechanical systems whose predominant energy-storage mechanism is in magnetic fields. In such systems, one can account for

Combining Eqs. 3.11 and 3.12 results in

$$dW_{\text{elec}} = ei\,dt = dW_{\text{mech}} + dW_{\text{fld}} \tag{3.13}$$

Equation 3.13, together with Faraday's law for induced voltage (Eq. 1.27), form the basis for the energy method; the following sections illustrate its use in the analysis of electromechanical-energy-conversion devices.

3.3 ENERGY IN SINGLY-EXCITED MAGNETIC FIELD SYSTEMS

In Chapters 1 and 2 we were concerned primarily with fixed-geometry magnetic circuits such as those used for transformers and inductors. Energy in those devices is stored in the leakage fields and to some extent in the core itself. However, the stored energy does not enter directly into the transformation process. In this chapter we are dealing with energy-conversion systems; the magnetic circuits have air gaps between the stationary and moving members in which considerable energy is stored in the magnetic field. This field acts as the energy-conversion medium, and its energy is the reservoir between the electric and mechanical systems.

Consider the electromagnetic relay shown schematically in Fig. 3.4. The resistance of the excitation coil is shown as an external resistance R, and the mechanical terminal variables are shown as a force f_{fld} produced by the magnetic field directed from the relay to the external mechanical system and a displacement x; mechanical losses can be included as external elements connected to the mechanical terminal. Similarly, the moving armature is shown as being massless; its mass represents mechanical energy storage and can be included as an external mass connected to the mechanical terminal. As a result, the magnetic core and armature constitute a lossless magnetic-energy-storage system, as is represented schematically in Fig. 3.3a.

This relay structure is essentially the same as the magnetic structures analyzed in Chapter 1. In Chapter 1 we saw that the magnetic circuit of Fig. 3.4 can be described by an inductance L which is a function of the geometry of the magnetic structure and the

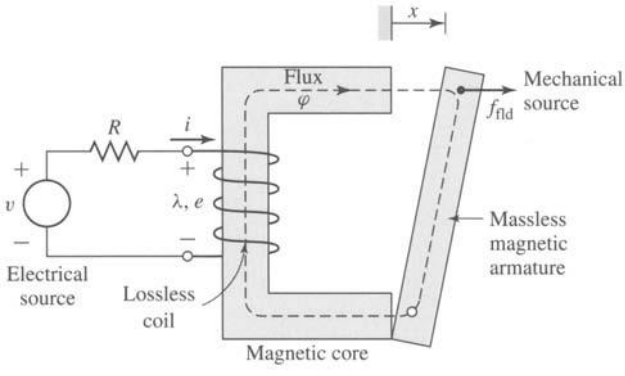

Figure 3.4 Schematic of an electromagnetic relay.

permeability of the magnetic material. Electromechanical-energy-conversion devices contain air gaps in their magnetic circuits to separate the moving parts. As discussed in Section 1.1, in most such cases the reluctance of the air gap is much larger than that of the magnetic material. Thus the predominant energy storage occurs in the air gap, and the properties of the magnetic circuit are determined by the dimensions of the air gap.

Because of the simplicity of the resulting relations, magnetic nonlinearity and core losses are often neglected in the analysis of practical devices. The final results of such approximate analyses can, if necessary, be corrected for the effects of these neglected factors by semi-empirical methods. Consequently, analyses are carried out under the assumption that the flux and mmf are directly proportional for the entire magnetic circuit. Thus the flux linkages λ and current i are considered to be linearly related by an inductance which depends solely on the geometry and hence on the armature position x.

$$\lambda = L(x)i \tag{3.14}$$

where the explicit dependence of L on x has been indicated.

Since the magnetic force f_{fld} has been defined as acting from the relay upon the external mechanical system and dW_{mech} is defined as the mechanical energy output of the relay, we can write

$$dW_{\text{mech}} = f_{\text{fld}}\, dx \tag{3.15}$$

Thus, using Eq. 3.15 and the substitution $dW_{\text{elec}} = i\, d\lambda$, we can write Eq. 3.11 as

$$dW_{\text{fld}} = i\, d\lambda - f_{\text{fld}}\, dx \tag{3.16}$$

Since the magnetic energy storage system is lossless, it is a *conservative system* and the value of W_{fld} is uniquely specified by the values of λ and x; λ and x are thus referred to as *state variables* since their values uniquely determine the state of the system.

From this discussion we see that W_{fld}, being uniquely determined by the values of λ and x, *is the same regardless of how λ and x are brought to their final values.* Consider Fig. 3.5, in which two separate paths are shown over which Eq. 3.16 can be integrated to find W_{fld} at the point (λ_0, x_0). Path 1 is the general case and is difficult to

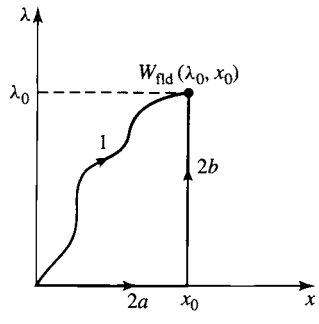

Figure 3.5 Integration paths for W_{fld}.

integrate unless both i and f_{fld} are known explicitly as a function of λ and x. However, because the integration of Eq. 3.16 is path independent, path 2 gives the same result and is much easier to integrate. From Eq. 3.16

$$W_{\text{fld}}(\lambda_0, x_0) = \int_{\text{path 2a}} dW_{\text{fld}} + \int_{\text{path 2b}} dW_{\text{fld}} \tag{3.17}$$

Notice that on path 2a, $d\lambda = 0$ and $f_{\text{fld}} = 0$ (since $\lambda = 0$ and there can be no magnetic force in the absence of magnetic fields). Thus from Eq. 3.16, $dW_{\text{fld}} = 0$ on path 2a. On path 2b, $dx = 0$, and, thus, from Eq. 3.16, Eq. 3.17 reduces to the integral of $i\,d\lambda$ over path 2b (for which $x = x_0$).

$$W_{\text{fld}}(\lambda_0, x_0) = \int_0^{\lambda_0} i(\lambda, x_0)\, d\lambda \tag{3.18}$$

For a linear system in which λ is proportional to i, as in Eq. 3.14, Eq. 3.18 gives

$$W_{\text{fld}}(\lambda, x) = \int_0^{\lambda} i(\lambda', x)\, d\lambda' = \int_0^{\lambda} \frac{\lambda'}{L(x)}\, d\lambda' = \frac{1}{2}\frac{\lambda^2}{L(x)} \tag{3.19}$$

It can be shown that the magnetic stored energy can also be expressed in terms of the energy density of the magnetic field integrated over the volume V of the magnetic field. In this case

$$W_{\text{fld}} = \int_V \left(\int_0^B \mathbf{H} \cdot \mathbf{dB}' \right) dV \tag{3.20}$$

For soft magnetic material of constant permeability ($\mathbf{B} = \mu\mathbf{H}$), this reduces to

$$W_{\text{fld}} = \int_V \left(\frac{B^2}{2\mu} \right) dV \tag{3.21}$$

EXAMPLE 3.2

The relay shown in Fig. 3.6a is made from infinitely-permeable magnetic material with a movable plunger, also of infinitely-permeable material. The height of the plunger is much greater than the air-gap length ($h \gg g$). Calculate the magnetic stored energy W_{fld} as a function of plunger position ($0 < x < d$) for $N = 1000$ turns, $g = 2.0$ mm, $d = 0.15$ m, $l = 0.1$ m, and $i = 10$ A.

■ Solution

Equation 3.19 can be used to solve for W_{fld} when λ is known. For this situation, i is held constant, and thus it would be useful to have an expression for W_{fld} as a function of i and x. This can be obtained quite simply by substituting Eq. 3.14 into Eq. 3.19, with the result

$$W_{\text{fld}} = \frac{1}{2} L(x) i^2$$

The inductance is given by

$$L(x) = \frac{\mu_0 N^2 A_{\text{gap}}}{2g}$$

where A_{gap} is the gap cross-sectional area. From Fig. 3.6b, A_{gap} can be seen to be

$$A_{gap} = l(d - x) = ld\left(1 - \frac{x}{d}\right)$$

Thus

$$L(x) = \frac{\mu_0 N^2 ld(1 - x/d)}{2g}$$

and

$$\begin{aligned} W_{fld} &= \frac{1}{2}\frac{N^2\mu_0 ld(1 - x/d)}{2g} i^2 \\ &= \frac{1}{2}\frac{(1000^2)(4\pi \times 10^{-7})(0.1)(0.15)}{2(0.002)} \times 10^2\left(1 - \frac{x}{d}\right) \\ &= 236\left(1 - \frac{x}{d}\right) \text{ J} \end{aligned}$$

Practice Problem 3.2

The relay of Fig. 3.6 is modified in such a fashion that the air gaps surrounding the plunger are no longer uniform. The top air gap length is increased to $g_{top} = 3.5$ mm and that of the bottom gap is increased to $g_{bot} = 2.5$ mm. The number of turns is increased to $N = 1500$. Calculate the stored energy as a function of plunger position ($0 < x < d$) for a current of $i = 5$ A.

Solution

$$W_{fld} = 88.5\left(1 - \frac{x}{d}\right) \text{ J}$$

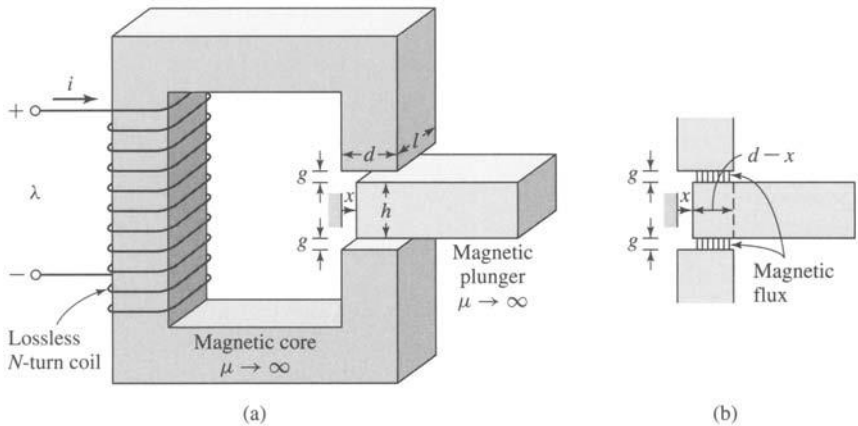

Figure 3.6 (a) Relay with movable plunger for Example 3.2. (b) Detail showing air-gap configuration with the plunger partially removed.

In this section we have seen the relationship between the magnetic stored energy and the electric and mechanical terminal variables for a system which can be represented in terms of a lossless-magnetic-energy-storage element. If we had chosen for our example a device with a rotating mechanical terminal instead of a linearly displacing one, the results would have been identical except that force would be replaced by torque and linear displacement by angular displacement. In Section 3.4 we see how knowledge of the magnetic stored energy permits us to solve for the mechanical force and torque.

3.4 DETERMINATION OF MAGNETIC FORCE AND TORQUE FROM ENERGY

As discussed in Section 3.3, for a lossless magnetic-energy-storage system, the magnetic stored energy W_{fld} is a *state function*, determined uniquely by the values of the independent state variables λ and x. This can be shown explicitly by rewriting Eq. 3.16 in the form

$$dW_{\text{fld}}(\lambda, x) = i\,d\lambda - f_{\text{fld}}\,dx \tag{3.22}$$

For any state function of two independent variables, e.g., $F(x_1, x_2)$, the total differential of F with respect to the two state variables x_1 and x_2 can be written

$$dF(x_1, x_2) = \left.\frac{\partial F}{\partial x_1}\right|_{x_2} dx_1 + \left.\frac{\partial F}{\partial x_2}\right|_{x_1} dx_2 \tag{3.23}$$

It is extremely important to recognize that the partial derivatives in Eq. 3.23 are each taken by holding the opposite state variable constant.

Equation 3.23 is valid for any state function F and hence it is certainly valid for W_{fld}; thus

$$dW_{\text{fld}}(\lambda, x) = \left.\frac{\partial W_{\text{fld}}}{\partial \lambda}\right|_{x} d\lambda + \left.\frac{\partial W_{\text{fld}}}{dx}\right|_{\lambda} dx \tag{3.24}$$

Since λ and x are independent variables, Eqs. 3.22 and 3.24 must be equal for all values of $d\lambda$ and dx, and so

$$i = \left.\frac{\partial W_{\text{fld}}(\lambda, x)}{\partial \lambda}\right|_{x} \tag{3.25}$$

where the partial derivative is taken while holding x constant and

$$f_{\text{fld}} = -\left.\frac{\partial W_{\text{fld}}(\lambda, x)}{\partial x}\right|_{\lambda} \tag{3.26}$$

in this case holding λ constant while taking the partial derivative.

This is the result we have been seeking. Once we know W_{fld} as a function of λ and x, Eq. 3.25 can be used to solve for $i(\lambda, x)$. More importantly, Eq. 3.26 can be used to solve for the mechanical force $f_{\text{fld}}(\lambda, x)$. It cannot be overemphasized that *the partial derivative of Eq. 3.26 is taken while holding the flux linkages λ constant.* This

is easily done provided W_{fld} is a known function of λ and x. Note that this is purely a mathematical requirement and has nothing to do with whether λ is held constant when operating the actual device.

The force f_{fld} is determined from Eq. 3.26 directly in terms of the electrical state variable λ. If we then want to express the force as a function of i, we can do so by substituting the appropriate expression for λ as a function of i into the expression for f_{fld} that is obtained by using Eq. 3.26.

For linear magnetic systems for which $\lambda = L(x)i$, the energy is expressed by Eq. 3.19 and the force can be found by direct substitution in Eq. 3.26

$$f_{\text{fld}} = -\frac{\partial}{\partial x}\left(\frac{1}{2}\frac{\lambda^2}{L(x)}\right)\bigg|_{\lambda} = \frac{\lambda^2}{2L(x)^2}\frac{dL(x)}{dx} \tag{3.27}$$

If desired, the force can now be expressed in directly in terms of the current i simply by substitution of $\lambda = L(x)i$

$$f_{\text{fld}} = \frac{i^2}{2}\frac{dL(x)}{dx} \tag{3.28}$$

EXAMPLE 3.3

Table 3.1 contains data from an experiment in which the inductance of a solenoid was measured as a function of position x, where $x = 0$ corresponds to the solenoid being fully retracted.

Table 3.1 Data for Example 3.3.

x [cm]	0	0.2	0.4	0.6	0.8	1.0	1.2	1.4	1.6	1.8	2.0
L [mH]	2.8	2.26	1.78	1.52	1.34	1.26	1.20	1.16	1.13	1.11	1.10

Plot the solenoid force as a function of position for a current of 0.75 A over the range $0.2 \leq x \leq 1.8$ cm.

■ Solution

The solution is most easily obtained using MATLAB.† First, a fourth-order polynomial fit of the inductance as a function of x is obtained using the MATLAB function *polyfit*. The result is of the form

$$L(x) = a(1)x^4 + a(2)x^3 + a(3)x^2 + a(4)x + a(5)$$

Figure 3.7a shows a plot of the data points along with the results of the polynomial fit.

Once this fit has been obtained, it is a straight forward matter to calculate the force from Eq. 3.28.

$$f_{\text{fld}} = \frac{i^2}{2}\frac{dL(x)}{dx} = \frac{i^2}{2}(4a(1)x^3 + 3a(2)x^2 + 2a(3)x + a(4))$$

This force is plotted in Figure 3.7b. Note that the force is negative, which means that it is acting in such a direction as to pull the solenoid inwards towards $x = 0$.

† MATLAB is a registered trademark of The MathWorks, Inc.

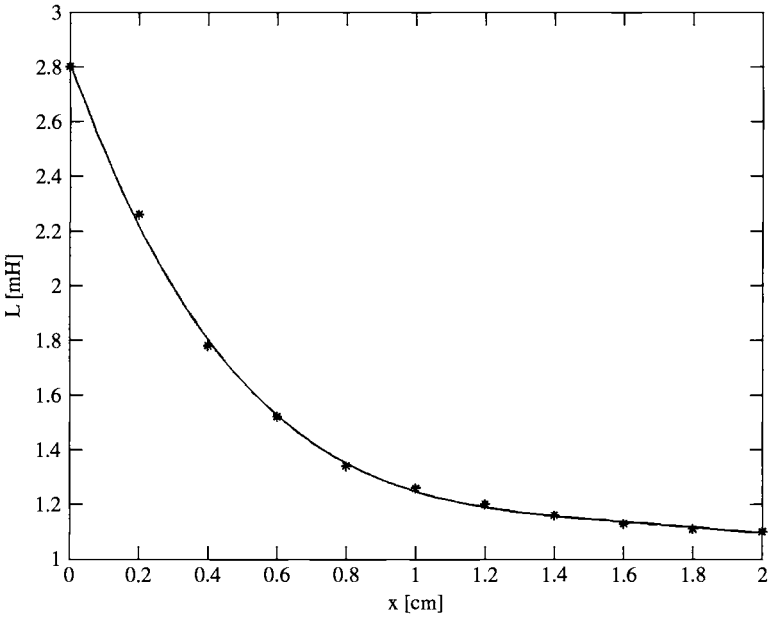

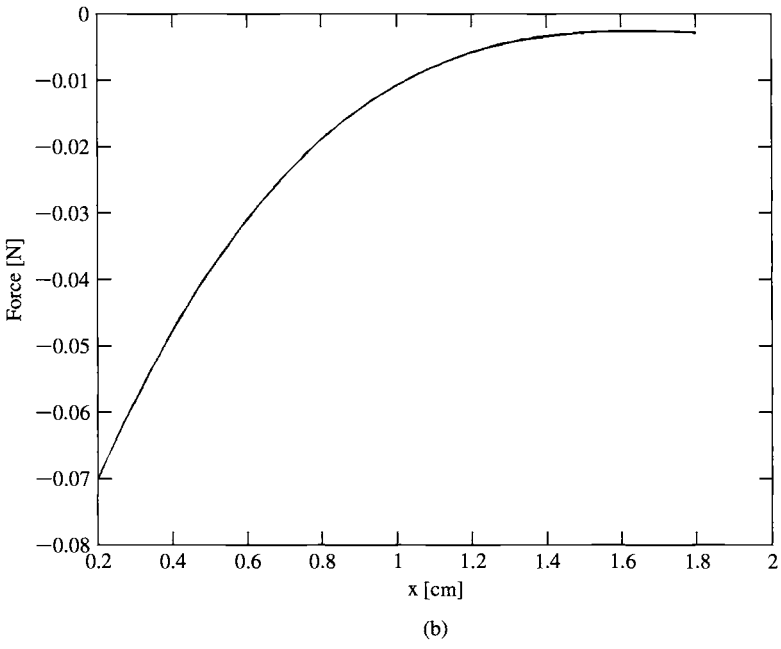

Figure 3.7 Example 3.3. (a) Polynomial curve fit of inductance. (b) Force as a function of position x for $i = 0.75$ A.

Here is the MATLAB script:

```
clc
clear

% Here is the data: x in cm, L in mH
xdata = [0 0.2 0.4 0.6 0.8 1.0 1.2 1.4 1.6 1.8 2.0];
Ldata = [2.8 2.26 1.78 1.52 1.34 1.26 1.20 1.16 1.13 1.11 1.10];

%Convert to SI units
x = xdata*1.e-2;
L = Ldata*1.e-3;

len = length(x);
xmax = x(len);

% Use polyfit to perform a 4'th order fit of L to x. Store
% the polynomial coefficients in vector a. The fit will be
% of the form:
%
%       Lfit = a(1)*x^4 + a(2)*x^3 + a(3)*x^2 + a(4)*x + a(5);
%

a = polyfit(x,L,4);

% Let's check the fit

for n = 1:101
  xfit(n) = xmax*(n-1)/100;
  Lfit(n) = a(1)*xfit(n)^4 + a(2)*xfit(n)^3 + a(3)*xfit(n)^2 ...
  + a(4)*xfit(n) + a(5);
end

% Plot the data and then the fit to compare (convert xfit to cm and
% Lfit to mH)

plot(xdata,Ldata,'*')
hold
plot(xfit*100,Lfit*1000)
hold
xlabel('x [cm]')
ylabel('L [mH]')

fprintf('\n Paused. Hit any key to plot the force.\n')
pause;

% Now plot the force. The force will be given by
%
%   i^2    dL    i^2
%   --- * ---- = --- ( 4*a(1)*x^3 + 3*a(2)*x^2 + 2*a(3)*x + a(4))
%    2     dx     2
```

```
%Set current to 0.75 A
I = 0.75;

for n = 1:101
  xfit(n) = 0.002 + 0.016*(n-1)/100;
  F(n)=4*a(1)*xfit(n)^3+3*a(2)*xfit(n)^2+2*a(3)*xfit(n)+a(4);
  F(n)=(I^2/2)*F(n);
end

plot(xfit*100,F)
xlabel('x [cm]')
ylabel('Force [N]')
```

Practice Problem 3.3

An external controller is connected to the solenoid of Example 3.3 which maintains the coil flux linkages constant at $\lambda = 1.5$ mWb. Plot the resultant solenoid force over the range $0.2 \leq x \leq 1.8$ cm.

Solution

The resultant force is plotted in Fig. 3.8.

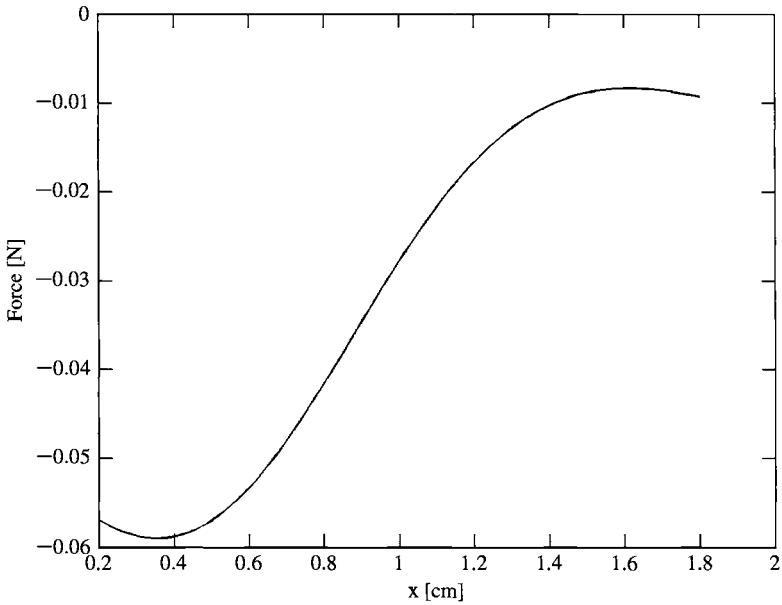

Figure 3.8 Practice problem 3.3. Plot of force vs. x for $\lambda = 1.5$ mWb.

For a system with a rotating mechanical terminal, the mechanical terminal variables become the angular displacement θ and the torque T_{fld}. In this case, Eq. 3.22 becomes

$$dW_{\text{fld}}(\lambda, \theta) = i\, d\lambda - T_{\text{fld}}\, d\theta \tag{3.29}$$

where the explicit dependence of W_{fld} on state variables λ and θ has been indicated.

By analogy to the development that led to Eq. 3.26, the torque can be found from the negative of the partial derivative of the energy with respect to θ taken holding λ constant

$$T_{\text{fld}} = -\left.\frac{\partial W_{\text{fld}}(\lambda, \theta)}{\partial \theta}\right|_{\lambda} \tag{3.30}$$

For linear magnetic systems for which $\lambda = L(\theta)i$, by analogy to Eq. 3.19 the energy is given by

$$W_{\text{fld}}(\lambda, \theta) = \frac{1}{2}\frac{\lambda^2}{L(\theta)} \tag{3.31}$$

The torque is therefore given by

$$T_{\text{fld}} = -\frac{\partial}{\partial \theta}\left.\left(\frac{1}{2}\frac{\lambda^2}{L(\theta)}\right)\right|_{\lambda} = \frac{1}{2}\frac{\lambda^2}{L(\theta)^2}\frac{dL(\theta)}{d\theta} \tag{3.32}$$

which can be expressed indirectly in terms of the current i as

$$T_{\text{fld}} = \frac{i^2}{2}\frac{dL(\theta)}{d\theta} \tag{3.33}$$

EXAMPLE 3.4

The magnetic circuit of Fig. 3.9 consists of a single-coil stator and an oval rotor. Because the air-gap is nonuniform, the coil inductance varies with rotor angular position, measured between the magnetic axis of the stator coil and the major axis of the rotor, as

$$L(\theta) = L_0 + L_2 \cos(2\theta)$$

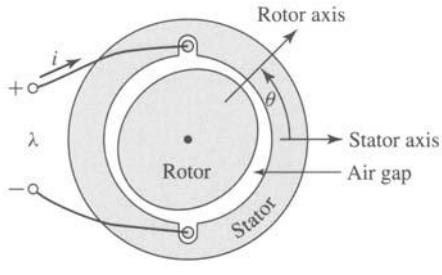

Figure 3.9 Magnetic circuit for Example 3.4.

where $L_0 = 10.6$ mH and $L_2 = 2.7$ mH. Note the second-harmonic variation of inductance with rotor angle θ. This is consistent with the fact that the inductance is unchanged if the rotor is rotated through an angle of 180°.

Find the torque as a function of θ for a coil current of 2 A.

■ Solution

From Eq. 3.33

$$T_{\text{fld}}(\theta) = \frac{i^2}{2}\frac{dL(\theta)}{d\theta} = \frac{i^2}{2}\left(-2L_2 \sin(2\theta)\right)$$

Numerical substitution gives

$$T_{\text{fld}}(\theta) = -1.08 \times 10^{-2} \sin(2\theta) \quad \text{N} \cdot \text{m}$$

Note that in this case the torque acts in such a direction as to pull the rotor axis in alignment with the coil axis and hence to maximize the coil inductance.

Practice Problem 3.4

The inductance of a coil on a magnetic circuit similar to that of Fig. 3.9 is found to vary with rotor position as

$$L(\theta) = L_0 + L_2 \cos(2\theta) + L_4 \sin(4\theta)$$

where $L_0 = 25.4$ mH, $L_2 = 8.3$ mH and $L_4 = 1.8$ mH. (*a*) Find the torque as a function of θ for a winding current of 3.5 A. (*b*) Find a rotor position $\theta_{\max}$ that produces the largest negative torque.

Solution

a. $T_{\text{fld}}(\theta) = -0.1017 \sin(2\theta) + 0.044 \cos(4\theta) \quad \text{N} \cdot \text{m}$
b. The largest negative torque occurs when $\theta = 45°$ and $\theta = 225°$. This can be determined analytically, but it is helpful to plot the torque using MATLAB.

3.5 DETERMINATION OF MAGNETIC FORCE AND TORQUE FROM COENERGY

A mathematical manipulation of Eq. 3.22 can be used to define a new state function, known as the *coenergy,* from which the force can be obtained directly as a function of the current. The selection of energy or coenergy as the state function is purely a matter of convenience; they both give the same result, but one or the other may be simpler analytically, depending on the desired result and the characteristics of the system being analyzed.

The coenergy W'_{fld} is defined as a function of i and x such that

$$W'_{\text{fld}}(i, x) = i\lambda - W_{\text{fld}}(\lambda, x) \tag{3.34}$$

The desired derivation is carried out by using the differential of $i\lambda$

$$d(i\lambda) = i\,d\lambda + \lambda\,di \tag{3.35}$$

and the differential of $dW_{\text{fld}}(\lambda, x)$ from Eq. 3.22. From Eq. 3.34

$$dW'_{\text{fld}}(i, x) = d(i\lambda) - dW_{\text{fld}}(\lambda, x) \tag{3.36}$$

Substitution of Eqs. 3.22 and 3.35 into Eq. 3.36 results in

$$dW'_{\text{fld}}(i, x) = \lambda\,di + f_{\text{fld}}\,dx \tag{3.37}$$

From Eq. 3.37, the coenergy $W'_{\text{fld}}(i, x)$ can be seen to be a state function of the two independent variables i and x. Thus, its differential can be expressed as

$$dW'_{\text{fld}}(i, x) = \left.\frac{\partial W'_{\text{fld}}}{\partial i}\right|_x di + \left.\frac{\partial W'_{\text{fld}}}{\partial x}\right|_i dx \tag{3.38}$$

Equations 3.37 and 3.38 must be equal for all values of di and dx; thus

$$\lambda = \left.\frac{\partial W'_{\text{fld}}(i, x)}{\partial i}\right|_x \tag{3.39}$$

$$f_{\text{fld}} = \left.\frac{\partial W'_{\text{fld}}(i, x)}{\partial x}\right|_i \tag{3.40}$$

Equation 3.40 gives the mechanical force directly in terms of i and x. Note that *the partial derivative in* Eq. 3.40 *is taken while holding i constant;* thus W'_{fld} must be a known function of i and x. For any given system, Eqs. 3.26 and 3.40 will give the same result; the choice as to which to use to calculate the force is dictated by user preference and convenience.

By analogy to the derivation of Eq. 3.18, the coenergy can be found from the integral of $\lambda\,di$

$$W'_{\text{fld}}(i, x) = \int_0^i \lambda(i', x)\,di' \tag{3.41}$$

For linear magnetic systems for which $\lambda = L(x)i$, the coenergy is therefore given by

$$W'_{\text{fld}}(i, x) = \frac{1}{2}L(x)i^2 \tag{3.42}$$

and the force can be found from Eq. 3.40

$$f_{\text{fld}} = \frac{i^2}{2}\frac{dL(x)}{dx} \tag{3.43}$$

which, as expected, is identical to the expression given by Eq. 3.28.

Similarly, for a system with a rotating mechanical displacement, the coenergy can be expressed in terms of the current and the angular displacement θ

$$W'_{\text{fld}}(i, \theta) = \int_0^i \lambda(i', \theta)\,di' \tag{3.44}$$

and the torque is given by

$$T_{\text{fld}} = \left.\frac{\partial W'_{\text{fld}}(i,\theta)}{\partial\theta}\right|_i \tag{3.45}$$

If the system is magnetically linear,

$$W'_{\text{fld}}(i,\theta) = \frac{1}{2}L(\theta)i^2 \tag{3.46}$$

and

$$T_{\text{fld}} = \frac{i^2}{2}\frac{dL(\theta)}{d\theta} \tag{3.47}$$

which is identical to Eq. 3.33.

In field-theory terms, for soft magnetic materials (for which $\mathbf{B} = 0$ when $\mathbf{H} = 0$), it can be shown that

$$W'_{\text{fld}} = \int_V \left(\int_0^{H_0} \mathbf{B}\cdot d\mathbf{H}\right) dV \tag{3.48}$$

For soft magnetic material with constant permeability ($\mathbf{B} = \mu\mathbf{H}$), this reduces to

$$W'_{\text{fld}} = \int_V \frac{\mu H^2}{2}\, dV \tag{3.49}$$

For permanent-magnet (hard) materials such as those which are discussed in Chapter 1 and for which $B = 0$ when $H = H_c$, the energy and coenergy are equal to zero when $B = 0$ and hence when $H = H_c$. Thus, although Eq. 3.20 still applies for calculating the energy, Eq. 3.48 must be modified to the form

$$W'_{\text{fld}} = \int_V \left(\int_{H_c}^{H_0} \mathbf{B}\cdot d\mathbf{H}\right) dV \tag{3.50}$$

Note that Eq. 3.50 can be considered to apply in general since soft magnetic materials can be considered to be simply hard magnetic materials with $H_c = 0$, in which case Eq. 3.50 reduces to Eq. 3.48.

In some cases, magnetic circuit representations may be difficult to realize or may not yield solutions of the desired accuracy. Often such situations are characterized by complex geometries and/or magnetic materials driven deeply into saturation. In such situations, numerical techniques can be used to evaluate the system energy using Eq. 3.20 or the coenergy using either Eqs. 3.48 or 3.50.

One such technique, known as the *finite-element method,*[1] has become widely used. For example, such programs, which are available commercially from a number of vendors, can be used to calculate the system coenergy for various values of the displacement x of a linear-displacement actuator (making sure to hold the current constant as x is varied). The force can then be obtained from Eq. 3.40, with the derivative of coenergy with respect to x being calculated numerically from the results of the finite-element analysis.

[1] See, for example, P. P. Sylvester and R. L. Ferrari, *Finite Elements for Electrical Engineers,* Cambridge University Press, New York, 1983.

EXAMPLE 3.5

For the relay of Example 3.2, find the force on the plunger as a function of x when the coil is driven by a controller which produces a current as a function of x of the form

$$i(x) = I_0 \left(\frac{x}{d}\right) \text{ A}$$

■ Solution

From Example 3.2

$$L(x) = \frac{\mu_0 N^2 l d(1 - x/d)}{2g}$$

This is a magnetically-linear system for which the force can be calculated as

$$f_{\text{fld}} = \frac{i^2}{2}\frac{dL(x)}{dx} = -\frac{i^2}{2}\left(\frac{\mu_0 N^2 l}{2g}\right)$$

Substituting for $i(x)$, the expression for the force as a function of x can be determined as

$$f_{\text{fld}} = -\frac{I_0^2 \mu_0 N^2 l}{4g}\left(\frac{x}{d}\right)^2$$

Note that from Eq. 3.46, the coenergy for this system is equal to

$$W'_{\text{fld}}(i, x) = \frac{i^2}{2}L(x) = \frac{i^2}{2}\frac{N^2 \mu_0 l d(1 - x/d)}{2g}$$

Substituting for $i(x)$, this can be written as

$$W'_{\text{fld}}(i, x) = \frac{I_0^2 N^2 \mu_0 l d(1 - x/d)}{4g}\left(\frac{x}{d}\right)^2$$

Note that, although this is a perfectly correct expression for the coenergy as a function of x under the specified operating conditions, if one were to attempt to calculate the force from taking the partial derivative of this expression for W'_{fld} with respect to x, the resultant expression would not give the correct expression for the force. The reason for this is quite simple: As seen from Eq. 3.40, the partial derivative must be taken holding the current constant. Having substituted the expression for $i(x)$ to obtain the expression, the current is no longer a constant, and this requirement cannot be met. This illustrates the problems that can arise if the various force and torque expressions developed here are misapplied.

Practice Problem 3.5

Consider a plunger whose inductance varies as

$$L(x) = L_0(1 - (x/d)^2)$$

Find the force on the plunger as a function of x when the coil is driven by a controller which produces a current as a function of x of the form

$$i(x) = I_0 \left(\frac{x}{d}\right)^2 \text{ A}$$

Solution

$$f_{\text{fld}} = -\left(\frac{2L_0 I_0^2}{d}\right)\left(\frac{x}{d}\right)^3$$

For a magnetically-linear system, the energy and coenergy are numerically equal: $\frac{1}{2}\lambda^2/L = \frac{1}{2}Li^2$. The same is true for the energy and coenergy densities: $\frac{1}{2}B^2/\mu = \frac{1}{2}\mu H^2$. For a nonlinear system in which λ and i or B and H are not linearly proportional, the two functions are not even numerically equal. A graphical interpretation of the energy and coenergy for a nonlinear system is shown in Fig. 3.10. The area between the $\lambda - i$ curve and the vertical axis, equal to the integral of $i\,d\lambda$, is the energy. The area to the horizontal axis given by the integral of $\lambda\,di$ is the coenergy. For this singly-excited system, the sum of the energy and coenergy is, by definition (see Eq. 3.34),

$$W_{\text{fld}} + W'_{\text{fld}} = \lambda i \tag{3.51}$$

The force produced by the magnetic field in a device such as that of Fig. 3.4 for some particular value of x and i or λ cannot, of course, depend upon whether it is calculated from the energy or coenergy. A graphical illustration will demonstrate that both methods must give the same result.

Assume that the relay armature of Fig. 3.4 is at position x so that the device is operating at point a in Fig. 3.11a. The partial derivative of Eq. 3.26 can be interpreted as the limit of $-\Delta W_{\text{fld}}/\Delta x$ with λ constant as $\Delta x \to 0$. If we allow a change Δx, the change $-\Delta W_{\text{fld}}$ is shown by the shaded area in Fig. 3.11a. Hence, the force $f_{\text{fld}} =$ (shaded area)$/\Delta x$ as $\Delta x \to 0$. On the other hand, the partial derivative of Eq. 3.40 can be interpreted as the limit of $\Delta W'_{\text{fld}}/\Delta x$ with i constant as $\Delta x \to 0$. This perturbation of the device is shown in Fig. 3.11b; the force $f_{\text{fld}} =$ (shaded area)$/\Delta x$ as $\Delta x \to 0$. The shaded areas differ only by the small triangle abc of sides Δi and $\Delta\lambda$, so that in the limit the shaded areas resulting from Δx at constant λ or at constant i are

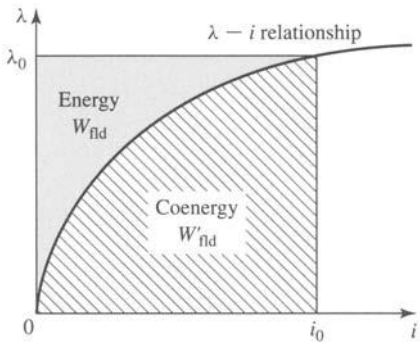

Figure 3.10 Graphical interpretation of energy and coenergy in a singly-excited system.

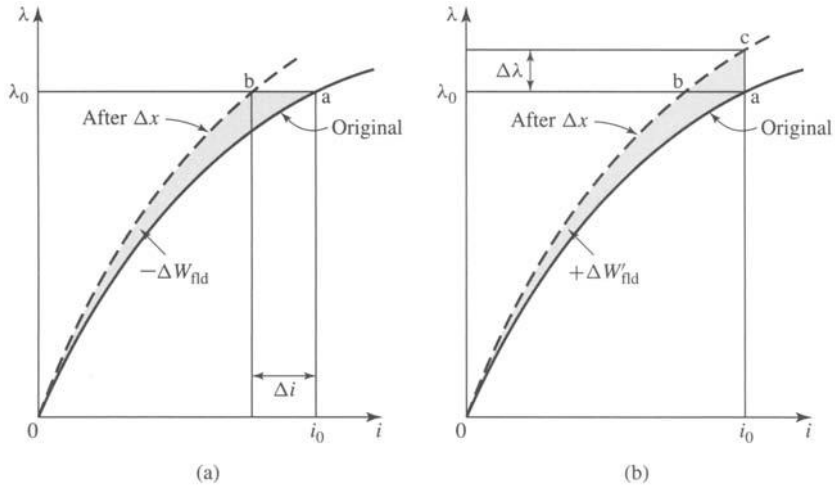

Figure 3.11 Effect of Δx on the energy and coenergy of a singly-excited device: (a) change of energy with λ held constant; (b) change of coenergy with i held constant.

equal. Thus the force produced by the magnetic field is independent of whether the determination is made with energy or coenergy.

Equations 3.26 and 3.40 express the mechanical force of electrical origin in terms of partial derivatives of the energy and coenergy functions $W_{\text{fld}}(\lambda, x)$ and $W'_{\text{fld}}(i, x)$. It is important to note two things about them: the variables in terms of which they must be expressed and their algebraic signs. Physically, of course, the force depends on the dimension x and the magnetic field. The field (and hence the energy or coenergy) can be specified in terms of flux linkage λ, or current i, or related variables. We again emphasize that the selection of the energy or coenergy function as a basis for analysis is a matter of convenience.

The algebraic signs in Eqs. 3.26 and 3.40 show that the force acts in a direction to decrease the magnetic field stored energy at constant flux or to increase the coenergy at constant current. In a singly-excited device, the force acts to increase the inductance by pulling on members so as to reduce the reluctance of the magnetic path linking the winding.

EXAMPLE 3.6

The magnetic circuit shown in Fig. 3.12 is made of high-permeability electrical steel. The rotor is free to turn about a vertical axis. The dimensions are shown in the figure.

a. Derive an expression for the torque acting on the rotor in terms of the dimensions and the magnetic field in the two air gaps. Assume the reluctance of the steel to be negligible (i.e., $\mu \to \infty$) and neglect the effects of fringing.
b. The maximum flux density in the overlapping portions of the air gaps is to be limited to approximately 1.65 T to avoid excessive saturation of the steel. Compute the maximum torque for $r_1 = 2.5$ cm, $h = 1.8$ cm, and $g = 3$ mm.

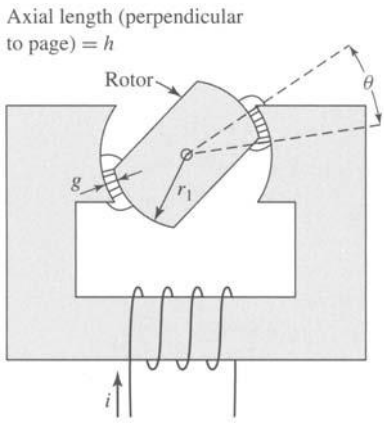

Figure 3.12 Magnetic system of Example 3.6.

■ Solution

a. There are two air gaps in series, each of length g, and hence the air-gap field intensity H_{ag} is equal to

$$H_{ag} = \frac{Ni}{2g}$$

Because the permeability of the steel is assumed infinite and B_{steel} must remain finite, $H_{steel} = B_{steel}/\mu$ is zero and the coenergy density (Eq. 3.49) in the steel is zero ($\mu H_{steel}^2/2 = B_{steel}^2/2\mu = 0$). Hence the system coenergy is equal to that of the air gaps, in which the coenergy density in the air gap is $\mu_0 H_{ag}^2/2$. The volume of the two overlapping air gaps is $2gh(r_1 + 0.5g)\theta$. Consequently, the coenergy is equal to the product of the air-gap coenergy density and the air-gap volume

$$W'_{ag} = \left(\frac{\mu_0 H_{ag}^2}{2}\right)(2gh(r_1 + 0.5g)\theta) = \frac{\mu_0 (Ni)^2 h(r_1 + 0.5g)\theta}{4g}$$

and thus, from Eq. 3.40

$$T_{fld} = \left.\frac{\partial W'_{ag}(i,\theta)}{\partial \theta}\right|_i = \frac{\mu_0 (Ni)^2 h(r_1 + 0.5g)}{4g}$$

The sign of the torque is positive, hence acting in the direction to increase the overlap angle θ and thus to align the rotor with the stator pole faces.

b. For $B_{ag} = 1.65$ T,

$$H_{ag} = \frac{B_{ag}}{\mu_0} = \frac{1.65}{4\pi \times 10^{-7}} = 1.31 \times 10^6 \text{ A/m}$$

and thus

$$Ni = 2gH_{ag} = 2(3 \times 10^{-3})1.31 \times 10^6 = 7860 \text{ A-turns}$$

T_{fld} can now be calculated as

$$T_{\text{fld}} = \frac{4\pi \times 10^{-7}(7860)^2(1.8 \times 10^{-2})(2.5 \times 10^{-2} + 0.5(3 \times 10^{-3}))}{4(3 \times 10^{-3})}$$
$$= 3.09\ \text{N} \cdot \text{m}$$

Practice Problem 3.6

(*a*) Write an expression for the inductance of the magnetic circuit of Fig. 3.12 as a function of θ. (*b*) Using this expression, derive an expression for the torque acting on the rotor as a function of the winding current i and the rotor angle θ.

Solution

a.

$$L(\theta) = \frac{\mu_0 N^2 h(r_1 + 0.5g)\theta}{2g}$$

b.

$$T_{\text{fld}} = \frac{i^2}{2}\frac{dL(\theta)}{d\theta} = \frac{i^2}{2}\left(\frac{\mu_0 N^2 h(r_1 + 0.5g)}{2g}\right)$$

3.6 MULTIPLY-EXCITED MAGNETIC FIELD SYSTEMS

Many electromechanical devices have multiple electrical terminals. In measurement systems it is often desirable to obtain torques proportional to two electric signals; a meter which determines power as the product of voltage and current is one example. Similarly, most electromechanical-energy-conversion devices consist of multiply-excited magnetic field systems.

Analysis of these systems follows directly from the techniques discussed in previous sections. This section illustrates these techniques based on a system with two electric terminals. A schematic representation of a simple system with two electrical terminals and one mechanical terminal is shown in Fig. 3.13. In this case it represents a system with rotary motion, and the mechanical terminal variables are torque T_{fld} and angular displacement θ. Since there are three terminals, the system must be described in terms of three independent variables; these can be the mechanical angle θ along with the flux linkages λ_1 and λ_2, currents i_1 and i_2, or a hybrid set including one current and one flux.[2]

When the fluxes are used, the differential energy function $dW_{\text{fld}}(\lambda_1, \lambda_2, \theta)$ corresponding to Eq. 3.29 is

$$dW_{\text{fld}}(\lambda_1, \lambda_2, \theta) = i_1\, d\lambda_1 + i_2\, d\lambda_2 - T_{\text{fld}}\, d\theta \tag{3.52}$$

[2] See, for example, H. H. Woodson and J. R. Melcher, *Electromechanical Dynamics*, Wiley, New York, 1968, Pt. I, Chap. 3.

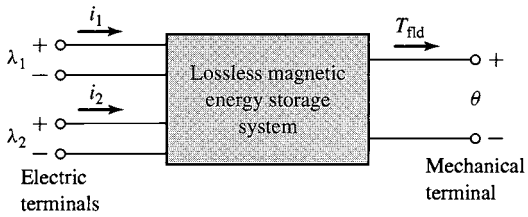

Figure 3.13 Multiply-excited magnetic energy storage system.

and in direct analogy to the previous development for a singly-excited system

$$i_1 = \left.\frac{\partial W_{fld}(\lambda_1, \lambda_2, \theta)}{\partial \lambda_1}\right|_{\lambda_2, \theta} \tag{3.53}$$

$$i_2 = \left.\frac{\partial W_{fld}(\lambda_1, \lambda_2, \theta)}{\partial \lambda_2}\right|_{\lambda_1, \theta} \tag{3.54}$$

and

$$T_{fld} = -\left.\frac{\partial W_{fld}(\lambda_1, \lambda_2, \theta)}{\partial \theta}\right|_{\lambda_1, \lambda_2} \tag{3.55}$$

Note that in each of these equations, *the partial derivative with respect to each independent variable must be taken holding the other two independent variables constant.*

The energy W_{fld} can be found by integrating Eq. 3.52. As in the singly-excited case, this is most conveniently done by holding λ_1 and λ_2 fixed at zero and integrating first over θ; under these conditions, T_{fld} is zero, and thus this integral is zero. One can then integrate over λ_2 (while holding λ_1 zero) and finally over λ_1. Thus

$$W_{fld}(\lambda_{1_0}, \lambda_{2_0}, \theta_0) = \int_0^{\lambda_{2_0}} i_2(\lambda_1 = 0, \lambda_2, \theta = \theta_0)\, d\lambda_2 + \int_0^{\lambda_{1_0}} i_1(\lambda_1, \lambda_2 = \lambda_{2_0}, \theta = \theta_0)\, d\lambda_1 \tag{3.56}$$

This path of integration is illustrated in Fig. 3.14 and is directly analogous to that of Fig. 3.5. One could, of course, interchange the order of integration for λ_2 and λ_1. It is extremely important to recognize, however, that the state variables are integrated over a specific path over which only one state variable is varied at a time; for example, λ_1 is maintained at zero while integrating over λ_2 in Eq. 3.56. This is explicitly indicated in Eq. 3.56 and can also be seen from Fig. 3.14. Failure to observe this requirement is one of the most common errors made in analyzing these systems.

In a magnetically-linear system, the relationships between λ and i can be specified in terms of inductances as is discussed in Section 1.2

$$\lambda_1 = L_{11} i_1 + L_{12} i_2 \tag{3.57}$$

$$\lambda_2 = L_{21} i_1 + L_{22} i_2 \tag{3.58}$$

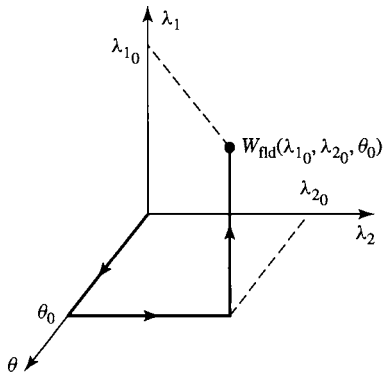

Figure 3.14 Integration path to obtain $W_{fld}(\lambda_{1_0}, \lambda_{2_0}, \theta_0)$.

where

$$L_{12} = L_{21} \tag{3.59}$$

Here the inductances are, in general, functions of angular position θ.

These equations can be inverted to obtain expressions for the i's as a function of the θ's

$$i_1 = \frac{L_{22}\lambda_1 - L_{12}\lambda_2}{D} \tag{3.60}$$

$$i_2 = \frac{-L_{21}\lambda_1 + L_{11}\lambda_2}{D} \tag{3.61}$$

where

$$D = L_{11}L_{22} - L_{12}L_{21} \tag{3.62}$$

The energy for this linear system can be found from Eq. 3.56

$$\begin{aligned} W_{fld}(\lambda_{1_0}, \lambda_{2_0}, \theta_0) &= \int_0^{\lambda_{2_0}} \frac{L_{11}(\theta_0)\lambda_2}{D(\theta_0)}\, d\lambda_2 \\ &\quad + \int_0^{\lambda_{1_0}} \frac{(L_{22}(\theta_0)\lambda_1 - L_{12}(\theta_0)\lambda_{2_0})}{D(\theta_0)}\, d\lambda_1 \\ &= \frac{1}{2D(\theta_0)} L_{11}(\theta_0)\lambda_{2_0}^2 + \frac{1}{2D(\theta_0)} L_{22}(\theta_0)\lambda_{1_0}^2 \\ &\quad - \frac{L_{12}(\theta_0)}{D(\theta_0)} \lambda_{1_0}\lambda_{2_0} \end{aligned} \tag{3.63}$$

where the dependence of the inductances and the determinant $D(\theta)$ on the angular displacement θ has been explicitly indicated.

In Section 3.5, the coenergy function was defined to permit determination of force and torque directly in terms of the current for a single-winding system. A

similar coenergy function can be defined in the case of systems with two windings as

$$W'_{\text{fld}}(i_1, i_2, \theta) = \lambda_1 i_1 + \lambda_2 i_2 - W_{\text{fld}} \tag{3.64}$$

It is a state function of the two terminal currents and the mechanical displacement. Its differential, following substitution of Eq. 3.52, is given by

$$dW'_{\text{fld}}(i_1, i_2, \theta) = \lambda_1\, di_1 + \lambda_2\, di_2 + T_{\text{fld}}\, d\theta \tag{3.65}$$

From Eq. 3.65 we see that

$$\lambda_1 = \left.\frac{\partial W'_{\text{fld}}(i_1, i_2, \theta)}{\partial i_1}\right|_{i_2,\theta} \tag{3.66}$$

$$\lambda_2 = \left.\frac{\partial W'_{\text{fld}}(i_1, i_2, \theta)}{\partial i_2}\right|_{i_1,\theta} \tag{3.67}$$

Most significantly, the torque can now be determined directly in terms of the currents as

$$T_{\text{fld}} = \left.\frac{\partial W'_{\text{fld}}(i_1, i_2, \theta)}{\partial \theta}\right|_{i_1,i_2} \tag{3.68}$$

Analogous to Eq. 3.56, the coenergy can be found as

$$\begin{aligned} W'_{\text{fld}}(i_{1_0}, i_{2_0}, \theta_0) = &\int_0^{i_{2_0}} \lambda_2(i_1 = 0, i_2, \theta = \theta_0)\, di_2 \\ &+ \int_0^{i_{1_0}} \lambda_1(i_1, i_2 = i_{2_0}, \theta = \theta_0)\, di_1 \end{aligned} \tag{3.69}$$

For the linear system of Eqs. 3.57 to 3.59

$$W'_{\text{fld}}(i_1, i_2, \theta) = \frac{1}{2}L_{11}(\theta)i_1^2 + \frac{1}{2}L_{22}(\theta)i_2^2 + L_{12}(\theta)i_1 i_2 \tag{3.70}$$

For such a linear system, the torque can be found either from the energy of Eq. 3.63 using Eq. 3.55 or from the coenergy of Eq. 3.70 using Eq. 3.68. It is at this point that the utility of the coenergy function becomes apparent. The energy expression of Eq. 3.63 is a complex function of displacement, and its derivative is even more so. Alternatively, the coenergy function is a relatively simple function of displacement, and from its derivative a straightforward expression for torque can be determined as a function of the winding currents i_1 and i_2 as

$$\begin{aligned} T_{\text{fld}} &= \left.\frac{\partial W'_{\text{fld}}(i_1, i_2, \theta)}{\partial \theta}\right|_{i_1,i_2} \\ &= \frac{i_1^2}{2}\frac{dL_{11}(\theta)}{d\theta} + \frac{i_2^2}{2}\frac{dL_{22}(\theta)}{d\theta} + i_1 i_2 \frac{dL_{12}(\theta)}{d\theta} \end{aligned} \tag{3.71}$$

Systems with more than two electrical terminals are handled in analogous fashion. As with the two-terminal-pair system above, the use of a coenergy function of the terminal currents greatly simplifies the determination of torque or force.

EXAMPLE 3.7

In the system shown in Fig. 3.15, the inductances in henrys are given as $L_{11} = (3 + \cos 2\theta) \times 10^{-3}$; $L_{12} = 0.3 \cos\theta$; $L_{22} = 30 + 10 \cos 2\theta$. Find and plot the torque $T_{\text{fld}}(\theta)$ for current $i_1 = 0.8$ A and $i_2 = 0.01$ A.

■ Solution

The torque can be determined from Eq. 3.71.

$$T_{\text{fld}} = \frac{i_1^2}{2}\frac{dL_{11}(\theta)}{d\theta} + \frac{i_2^2}{2}\frac{dL_{22}(\theta)}{d\theta} + i_1 i_2 \frac{dL_{12}(\theta)}{d\theta}$$

$$= \frac{i_1^2}{2}(-2 \times 10^{-3}) \sin 2\theta + \frac{i_2^2}{2}(-20 \sin 2\theta) - i_1 i_2 (0.3) \sin\theta$$

For $i_1 = 0.8$ A and $i_2 = 0.01$ A, the torque is

$$T_{\text{fld}} = -1.64 \times 10^{-3} \sin 2\theta - 2.4 \times 10^{-3} \sin\theta$$

Notice that the torque expression consists of terms of two types. One term, proportional to $i_1 i_2 \sin\theta$, is due to the mutual interaction between the rotor and stator currents; it acts in a direction to align the rotor and stator so as to maximize their mutual inductance. Alternately, it can be thought of as being due to the tendency of two magnetic fields (in this case those of the rotor and stator) to align.

The torque expression also has two terms each proportional to $\sin 2\theta$ and to the square of one of the coil currents. These terms are due to the action of the individual winding currents alone and correspond to the torques one sees in singly-excited systems. Here the torque is due to the fact that the self inductances are a function of rotor position and the corresponding torque acts in a direction to maximize each inductance so as to maximize the coenergy. The 2θ variation is due to the corresponding variation in the self inductances (exactly as was seen previously in Example 3.4), which in turn is due to the variation of the air-gap reluctance;

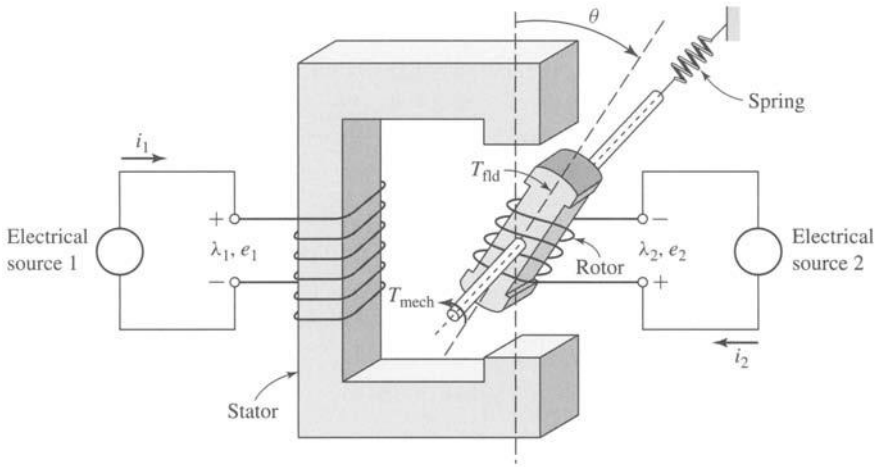

Figure 3.15 Multiply-excited magnetic system for Example 3.7.

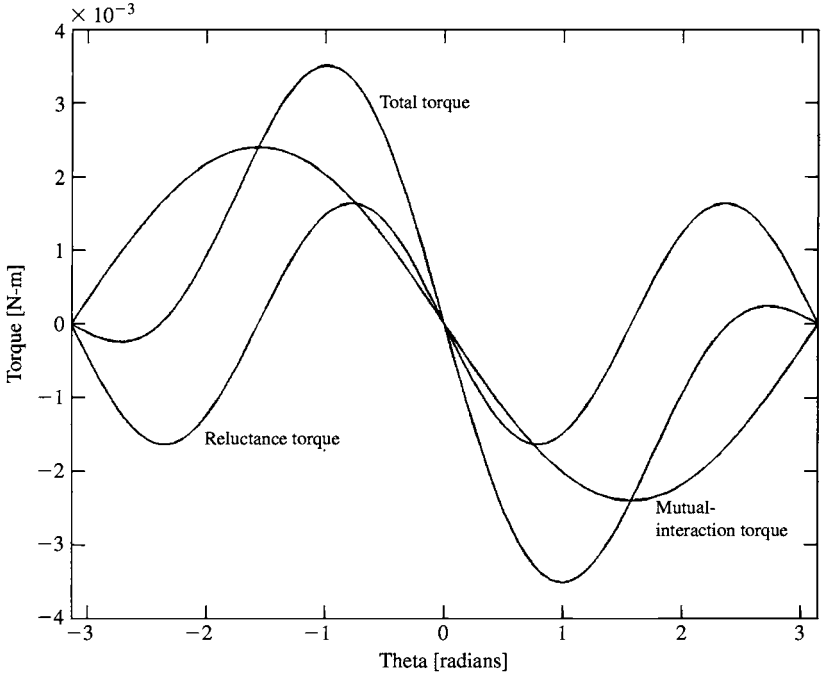

Figure 3.16 Plot of torque components for the multiply-excited system of Example 3.7.

notice that rotating the rotor by 180° from any given position gives the same air-gap reluctance (hence the twice-angle variation). This torque component is known as the *reluctance torque*. The two torque components (mutual and reluctance), along with the total torque, are plotted with MATLAB in Fig. 3.16.

Practice Problem 3.7

Find an expression for the torque of a symmetrical two-winding system whose inductances vary as

$$L_{11} = L_{22} = 0.8 + 0.27\cos 4\theta$$

$$L_{12} = 0.65\cos 2\theta$$

for the condition that $i_1 = -i_2 = 0.37$ A.

Solution

$$T_{\text{fld}} = -0.296\sin(4\theta) + 0.178\sin(2\theta)$$

The derivation presented above for angular displacement can be repeated in an analogous fashion for the systems with linear displacement. If this is done, the

expressions for energy and coenergy will be found to be

$$W_{\text{fld}}(\lambda_{1_0}, \lambda_{2_0}, x_0) = \int_0^{\lambda_{2_0}} i_2(\lambda_1 = 0, \lambda_2, x = x_0)\, d\lambda_2 + \int_0^{\lambda_{1_0}} i_1(\lambda_1, \lambda_2 = \lambda_{2_0}, x = x_0)\, d\lambda_1 \tag{3.72}$$

$$W'_{\text{fld}}(i_{1_0}, i_{2_0}, x_0) = \int_0^{i_{2_0}} \lambda_2(i_1 = 0, i_2, x = x_0)\, di_2 + \int_0^{i_{1_0}} \lambda_1(i_1, i_2 = i_{2_0}, x = x_0)\, di_1 \tag{3.73}$$

Similarly the force can be found from

$$f_{\text{fld}} = -\left.\frac{\partial W_{\text{fld}}(\lambda_1, \lambda_2, x)}{\partial x}\right|_{\lambda_1, \lambda_2} \tag{3.74}$$

or

$$f_{\text{fld}} = \left.\frac{\partial W'_{\text{fld}}(i_1, i_2, x)}{\partial x}\right|_{i_1, i_2} \tag{3.75}$$

For a magnetically-linear system, the coenergy expression of Eq. 3.70 becomes

$$W'_{\text{fld}}(i_1, i_2, x) = \frac{1}{2}L_{11}(x)i_1^2 + \frac{1}{2}L_{22}(x)i_2^2 + L_{12}(x)i_1 i_2 \tag{3.76}$$

and the force is thus given by

$$f_{\text{fld}} = \frac{i_1^2}{2}\frac{dL_{11}(x)}{dx} + \frac{i_2^2}{2}\frac{dL_{22}(x)}{dx} + i_1 i_2 \frac{dL_{12}(x)}{dx} \tag{3.77}$$

3.7 FORCES AND TORQUES IN SYSTEMS WITH PERMANENT MAGNETS

The derivations of the force and torque expressions of Sections 3.4 through 3.6 focus on systems in which the magnetic fields are produced by the electrical excitation of specific windings in the system. However, in Section 3.5, it is seen that special care must be taken when considering systems which contain permanent magnets (also referred to as *hard* magnetic materials). Specifically, the discussion associated with the derivation of the coenergy expression of Eq. 3.50 points out that in such systems the magnetic flux density is zero when $H = H_c$, not when $H = 0$.

For this reason, the derivation of the expressions for force and torque in Sections 3.4 through 3.6 must be modified for systems which contain permanent magnets. Consider for example that the derivation of Eq. 3.18 depends on the fact that in Eq. 3.17 the force can be assumed zero when integrating over path $2a$ because there is no electrical excitation in the system. A similar argument applies in the derivation of the coenergy expressions of Eqs. 3.41 and 3.69.

In systems with permanent magnets, these derivations must be carefully revisited. In some cases, such systems have no windings at all, their magnetic fields are due solely to the presence of permanent-magnet material, and it is not possible to base a derivation purely upon winding fluxes and currents. In other cases, magnetic fields may be produced by a combination of permanent magnets and windings.

A modification of the techniques presented in the previous sections can be used in systems which contain permanent magnets. Although the derivation presented here applies specifically to systems in which the magnet appears as an element of a magnetic circuit with a uniform internal field, it can be generalized to more complex situations; in the most general case, the field theory expressions for energy (Eq. 3.20) and coenergy (Eq. 3.50) can be used.

The essence of this technique is to consider the system as having an additional *fictitious winding* acting upon the same portion of the magnetic circuit as does the permanent magnet. Under normal operating conditions, the fictitious winding carries zero current. Its function is simply that of a mathematical "crutch" which can be used to accomplish the required analysis. The current in this winding can be adjusted to zero-out the magnetic fields produced by the permanent magnet in order to achieve the "zero-force" starting point for the analyses such as that leading from Eq. 3.17 to Eq. 3.18.

For the purpose of calculating the energy and coenergy of the system, this winding is treated as any other winding, with its own set of current and flux linkages. As a result, energy and coenergy expressions can be obtained as a function of all the winding flux linkages or currents, including those of the fictitious winding. Since under normal operating conditions the current in this winding will be set equal to zero, it is useful to derive the expression for the force from the system coenergy since the winding currents are explicitly expressed in this representation.

Figure 3.17a shows a magnetic circuit with a permanent magnet and a movable plunger. To find the force on the plunger as a function of the plunger position, we assume that there is a fictitious winding of N_f turns carrying a current i_f wound so as to produce flux through the permanent magnet, as shown in Fig. 3.17b.

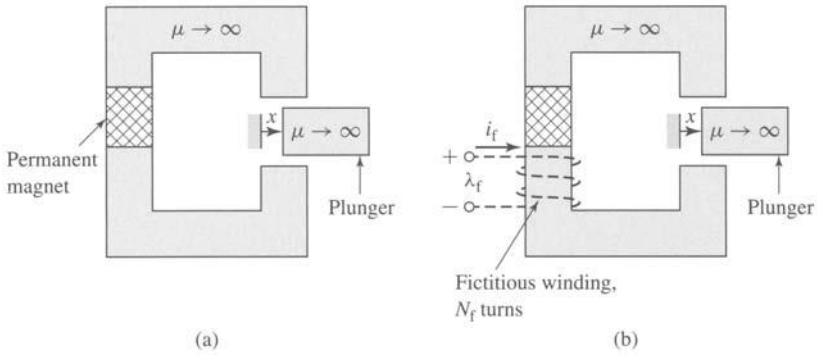

Figure 3.17 (a) Magnetic circuit with permanent magnet and movable plunger; (b) fictitious winding added.

For this single-winding system we can write the expression for the differential in coenergy from Eq. 3.37 as

$$dW'_{\text{fld}}(i_{\text{f}}, x) = \lambda_{\text{f}}\, di_{\text{f}} + f_{\text{fld}}\, dx \tag{3.78}$$

where the subscript 'f' indicates the fictitious winding. Corresponding to Eq. 3.40, the force in this system can be written as

$$f_{\text{fld}} = \left.\frac{\partial W'_{\text{fld}}(i_{\text{f}} = 0, x)}{\partial x}\right|_{i_{\text{f}}} \tag{3.79}$$

where the partial derivative is taken while holding i_{f} constant, and the resultant expression is then evaluated at $i_{\text{f}} = 0$, which is equivalent to setting $i_{\text{f}} = 0$ in the expression for W'_{fld} before taking the derivative. As we have seen, holding i_{f} constant for the derivative in Eq. 3.79 is a requirement of the energy method; it must be set to zero to properly calculate the force due to the magnet alone so as not to include a force component from current in the fictitious winding.

To calculate the coenergy $W'_{\text{fld}}(i_{\text{f}}, x)$ in this system, it is necessary to integrate Eq. 3.78. Since W'_{fld} is a state function of i_{f} and x, we are free to choose any integration path we wish. Figure 3.18 illustrates a path over which this integration is particularly simple. For this path we can write the expression for coenergy in this system as

$$\begin{aligned} W'_{\text{fld}}(i_{\text{f}} = 0, x) &= \int_{\text{path 1a}} dW'_{\text{fld}} + \int_{\text{path 1b}} dW'_{\text{fld}} \\ &= \int_0^x f_{\text{fld}}(i_{\text{f}} = I_{\text{f0}}, x')\, dx' + \int_{I_{\text{f0}}}^0 \lambda_{\text{f}}(i_{\text{f}}, x)\, di_{\text{f}} \end{aligned} \tag{3.80}$$

which corresponds directly to the analogous expression for energy found in Eq. 3.17.

Note that the integration is initially over x with the current i_{f} held fixed at $i_{\text{f}} = I_{\text{f0}}$. This is a very specific current, equal to that fictitious-winding current which reduces the magnetic flux in the system to zero. In other words, the current I_{f0} is that current in the fictitious winding which totally counteracts the magnetic field produced by the permanent magnet. Thus, the force f_{fld} is zero at point A in Fig. 3.18 and remains so for the integral over x of path 1a. Hence the integral over path 1a in Eq. 3.80 is zero,

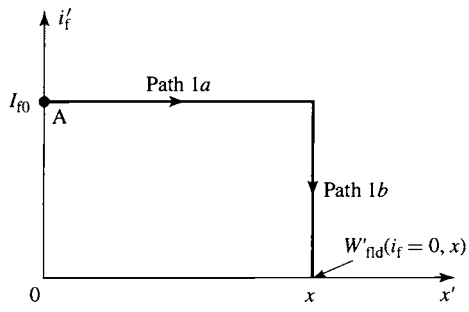

Figure 3.18 Integration path for calculating $W_{\text{fld}}(i_{\text{f}} = 0, x)$ in the permanent magnet system of Fig. 3.17.

and Eq. 3.80 reduces to

$$W'_{\text{fld}}(i_f = 0, x) = \int_{I_{f0}}^{0} \lambda_f(i'_f, x)\, di'_f \tag{3.81}$$

Note that Eq. 3.81 is perfectly general and does not require either the permanent magnet or the magnetic material in the magnetic circuit to be linear. Once Eq. 3.81 has been evaluated, the force at a given plunger position x can be readily found from Eq. 3.79. Note also that due to the presence of the permanent magnet, neither the coenergy nor the force is zero when i_f is zero, as we would expect.

EXAMPLE 3.8

The magnetic circuit of Fig. 3.19 is excited by a samarium-cobalt permanent magnet and includes a movable plunger. Also shown is the fictitious winding of N_f turns carrying a current i_f which is included here for the sake of the analysis. The dimensions are:

$$W_m = 2.0 \text{ cm} \quad W_g = 3.0 \text{ cm} \quad W_0 = 2.0 \text{ cm}$$
$$d = 2.0 \text{ cm} \quad g_0 = 0.2 \text{ cm} \quad D = 3.0 \text{ cm}$$

Find (*a*) an expression for the coenergy of the system as a function of plunger position x and (*b*) an expression for the force on the plunger as a function of x. Finally, (*c*) calculate the force at $x = 0$ and $x = 0.5$ cm. Neglect any effects of fringing fluxes in this calculation.

■ Solution

a. Because it is quite linear over most of its useful operating range, the dc magnetization curve for samarium-cobalt can be represented as a straight line of the form of Eq. 1.61

$$B_m = \mu_R(H_m - H'_c) = \mu_R H_m + B_r$$

where the subscript 'm' is used here to refer specifically to the fields within the samarium-cobalt magnet and

$$\mu_R = 1.05\mu_0$$
$$H'_c = -712 \text{ kA/m}$$
$$B_r = 0.94 \text{ T}$$

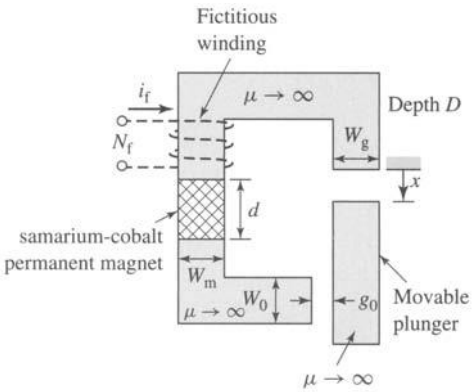

Figure 3.19 Magnetic circuit for Example 3.8.

Note from Fig. 1.19 that the DC magnetization curve for samarium-cobalt is not completely linear; it bends slightly downward for low flux densities. Hence, in the linearized B-H characteristic given above, the apparent coercivity H_c' is somewhat larger than the actual coercivity of samarium-cobalt.

From Eq. 1.5 we can write

$$N_f i_f = H_m d + H_g x + H_0 g_0$$

where the subscript 'g' refers to the variable gap and the subscript '0' refers to the fixed gap. Similarly from the continuity of flux condition, Eq. 1.3, we can write

$$B_m W_m D = B_g W_g D = B_0 W_0 D$$

Recognizing that in the air gaps $B_g = \mu_0 H_g$ and $B_0 = \mu_0 H_0$, we can solve the above equations for B_m:

$$B_m = \frac{\mu_R (N_f i_f - H_c' d)}{d + W_m \left(\frac{\mu_R}{\mu_0}\right)\left(\frac{x}{W_g} + \frac{g_0}{W_0}\right)}$$

Finally we can solve for the flux linkages λ_f of the fictitious winding as

$$\lambda_f = N_f W_m D B_m = \frac{N_f W_m D \mu_R (N_f i_f - H_c' d)}{d + W_m \left(\frac{\mu_R}{\mu_0}\right)\left(\frac{x}{W_g} + \frac{g_0}{W_0}\right)}$$

Thus we see that the flux linkages λ_f will be zero when $i_f = I_{f0} = H_c' d / N_f = -B_r d / (\mu_R N_f)$ and from Eq. 3.81 we can find the coenergy as

$$W_{fld}'(x) = \int_{H_c' d/N_f}^{0} \left[\frac{N_f W_m D \mu_R (N_f i_f - H_c' d)}{d + W_m \left(\frac{\mu_R}{\mu_0}\right)\left(\frac{x}{W_g} + \frac{g_0}{W_0}\right)} \right] di_f$$

$$= \frac{W_m D (B_r d)^2}{2\mu_R \left[d + W_m \left(\frac{\mu_R}{\mu_0}\right)\left(\frac{x}{W_g} + \frac{g_0}{W_0}\right) \right]}$$

Note that the answer does not depend upon N_f or i_f which is as we would expect since the fictitious winding does not actually exist in this system.

b. Once the coenergy has been found, the force can be found from Eq. 3.79 as

$$f_{fld} = -\frac{W_m^2 D (B_r d)^2}{2\mu_0 W_g \left[d + W_m \left(\frac{\mu_R}{\mu_0}\right)\left(\frac{x}{W_g} + \frac{g_0}{W_0}\right) \right]^2}$$

Notice that the force is negative, indicating that the force is acting in the direction to decrease x, that is to pull the plunger in the direction which decreases the gap.

c. Finally, substitution into the force expression yields

$$f_{fld} = \begin{cases} -115 \text{ N} & \text{at } x = 0 \text{ cm} \\ -85.8 \text{ N} & \text{at } x = 0.5 \text{ cm} \end{cases}$$

Practice Problem 3.8

(*a*) Derive an expression for the coenergy in the magnetic circuit of Fig. 3.20 as a function of the plunger position x. (*b*) Derive an expression for the x-directed force on the plunger and evaluate it at $x = W_g/2$. Neglect any effects of fringing fluxes. The dimensions are:

$$W_m = 2.0 \text{ cm} \quad W_g = 2.5 \text{ cm} \quad D = 3.0 \text{ cm}$$
$$d = 1.0 \text{ cm} \quad g_0 = 0.2 \text{ cm}$$

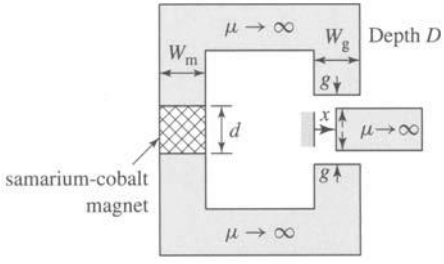

Figure 3.20 Magnetic circuit for Practice Problem 3.8.

Solution

a.

$$W'_{fld} = \frac{W_m D (B_r d)^2}{2\mu_R \left[d + \left(\frac{\mu_R}{\mu_0}\right)\left(\frac{2gW_m}{(W_g - x)}\right)\right]}$$

b.

$$f_{fld} = -\frac{g W_m^2 D B_r^2}{\mu_0 (W_g - x)^2 \left[1 + \left(\frac{\mu_R}{\mu_0}\right)\left(\frac{wgW_m}{(W_g - x)}\right)\right]^2}$$

At $x = W_g/2$, $f_{fld} = -107$ N.

Consider the schematic magnetic circuit of Fig. 3.21a. It consists of a section of linear, hard magnetic material ($B_m = \mu_R(H_m - H'_c)$) of area A and length d. It is connected in series with an external magnetic circuit of mmf $\mathcal{F}_e$.

From Eq. 1.21, since there are no ampere-turns acting on this magnetic circuit,

$$H_m d + \mathcal{F}_e = 0 \tag{3.82}$$

The flux produced in the external magnetic circuit by the permanent magnet is given by

$$\Phi = AB_m = \mu_R A(H_m - H'_c) \tag{3.83}$$

Substitution for H_m from Eq. 3.82 in Eq. 3.83 gives

$$\Phi = \mu_R A \left(-H'_c - \frac{\mathcal{F}_e}{d}\right) \tag{3.84}$$

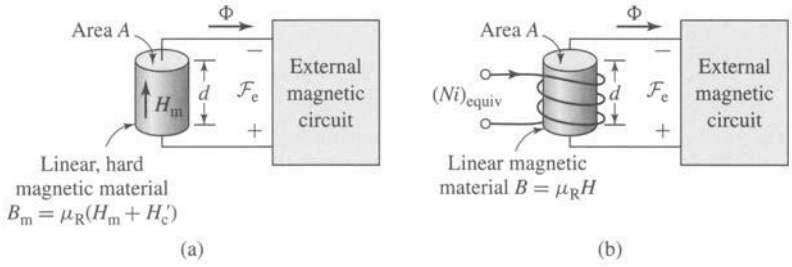

Figure 3.21 (a) Generic magnetic circuit containing a section of linear, permanent-magnet material. (b) Generic magnetic circuit in which the permanent-magnet material has been replaced by a section of linear magnetic material and a fictitious winding.

Now consider the schematic magnetic circuit of Fig. 3.21b in which the linear, hard magnetic material of Fig. 3.21a has been replaced by soft, linear magnetic material of the same permeability ($B = \mu_R H$) and of the same dimensions, length d and area A. In addition, a winding carrying $(Ni)_{equiv}$ ampere-turns has been included.

For this magnetic circuit, the flux can be shown to be given by

$$\Phi = \mu_R A \left(\frac{(Ni)_{equiv}}{d} - \frac{\mathcal{F}_e}{d} \right) \tag{3.85}$$

Comparing Eqs. 3.84 and 3.85, we see that the same flux is produced in the external magnetic circuit if the ampere-turns, $(Ni)_{equiv}$, in the winding of Fig. 3.21b is equal to $-H_c'd$.

This is a useful result for analyzing magnetic-circuit structures which contain linear, permanent-magnet materials whose B-H characteristic can be represented in the form of Eq. 1.61. In such cases, replacing the permanent-magnet section with a section of linear-magnetic material of the same permeability μ_R and geometry and an equivalent winding of ampere-turns

$$(Ni)_{equiv} = -H_c'd \tag{3.86}$$

results in the same flux in the external magnetic circuit. As a result, both the linear permanent magnet and the combination of the linear magnetic material and the winding are indistinguishable with regard to the production of magnetic fields in the external magnetic circuit, and hence they produce identical forces. Thus, the analysis of such systems may be simplified by this subsitution, as is shown in Example 3.9. This technique is especially useful in the analysis of magnetic circuits containing both a permanet magnetic and one or more windings.

EXAMPLE 3.9

Figure 3.22a shows an actuator consisting of an infinitely-permeable yoke and plunger, excited by a section of neodymium-iron-boron magnet and an excitation winding of $N_1 = 1500$ turns.

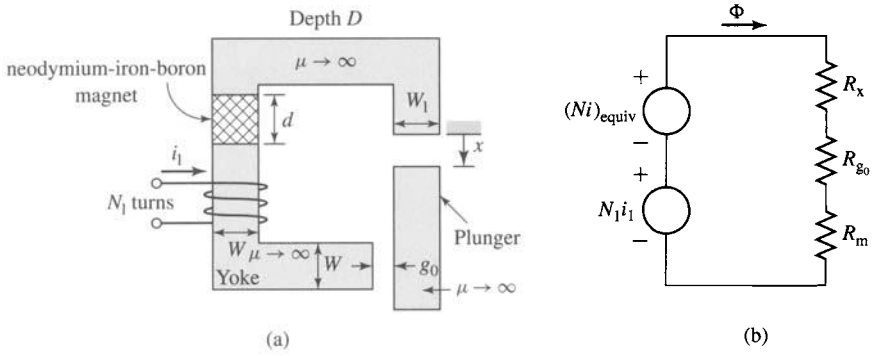

Figure 3.22 (a) Actuator for Example 3.9. (b) Equivalent circuit for the actuator with the permanent magnet replaced by linear material and an equivalent winding carrying $(Ni)_{\text{equiv}}$ ampere-turns.

The dimensions are:

$$W = 4.0 \text{ cm} \quad W_1 = 4.5 \text{ cm} \quad D = 3.5 \text{ cm}$$
$$d = 8 \text{ mm} \quad g_0 = 1 \text{ mm}$$

Find (*a*) the x-directed force on the plunger when the current in the excitation winding is zero and $x = 3$ mm. (*b*) Calculate the current in the excitation winding required to reduce the plunger force to zero.

■ Solution

a. As discussed in Section 1.6, the dc-magnetization characteristic of neodymium-iron-boron can be represented by a linear relationship of the form

$$B = \mu_R(H - H_c') = B_r + \mu_R H$$

where $\mu_R = 1.06\mu_0$, $H_c' = -940$ kA/m and $B_r = 1.25$ T. As discussed in this section, we can replace the magnet by a section of linear material of permeability μ_R and an equivalent winding of ampere-turns

$$(Ni)_{\text{equiv}} = -H_c'd = -(-9.4 \times 10^5)(8 \times 10^{-3}) = 7520 \text{ ampere-turns}$$

Based upon this substitution, the equivalent circuit for the system becomes that of Fig. 3.22b. There are two sources of mmf in series with three reluctances: the variable gap $\mathcal{R}_x$, the fixed gap $\mathcal{R}_0$, and the magnet $\mathcal{R}_m$.

$$\mathcal{R}_x = \frac{x}{\mu_0 W_1 D}$$

$$\mathcal{R}_0 = \frac{g_0}{\mu_0 W D}$$

$$\mathcal{R}_m = \frac{d}{\mu_R W D}$$

With $i_1 = 0$, the actuator is equivalent to a single-winding system whose coenergy is given by

$$W'_{\text{fld}} = \frac{1}{2}Li_1^2 = \frac{1}{2}\left(\frac{(Ni)^2_{\text{equiv}}}{\mathcal{R}_x + \mathcal{R}_0 + \mathcal{R}_m}\right)$$

The force on the plunger can then be found from

$$f_{\text{fld}} = \left.\frac{\partial W'_{\text{fld}}}{\partial x}\right|_{i_{\text{equiv}}} = -\frac{(Ni)^2_{\text{equiv}}}{(\mathcal{R}_x + \mathcal{R}_0 + \mathcal{R}_m)^2}\left(\frac{d\mathcal{R}_x}{dx}\right)$$

$$= -\frac{(Ni)^2_{\text{equiv}}}{\mu_0 W_1 D(\mathcal{R}_x + \mathcal{R}_0 + \mathcal{R}_m)^2}$$

Substituting the given values gives $f_{\text{fld}} = -703$ N, where the minus sign indicates that the force acts in the direction to reduce x (i.e., to close the gap).

b. The flux in the actuator is proportional to the total effective ampere-turns $(Ni)_{\text{equiv}} + N_1 i_1$ acting on the magnetic circuit. Thus, the force will be zero when the net ampere-turns is equal to zero or when

$$i_1 = \frac{(Ni)_{\text{equiv}}}{N_1} = \frac{7520}{1500} = 5.01 \text{ A}$$

Note however that the sign of the current (i.e., in which direction it should be applied to the excitation winding) cannot be determined from the information given here since we do not know the direction of magnetization of the magnet. Since the force depends upon the square of the magnetic flux density, the magnet can be oriented to produce flux either upward or downward in the left-hand leg of the magnetic circuit, and the force calculated in part (*a*) will be the same. To reduce the force to zero, the excitation winding current of 5.01 amperes must be applied in such a direction as to reduce the flux to zero; if the opposite current is applied, the flux density will increase, as will the force.

Practice Problem 3.9

Practice Problem 3.8 is to be reworked replacing the samarium-cobalt magnet by a section of linear material and an equivalent winding. Write (*a*) expressions for $\mathcal{R}_m$, the reluctance of the section of linear material; $\mathcal{R}_g$, the reluctance of the air gap; and $(Ni)_{\text{equiv}}$, the ampere-turns of the equivalent winding; and (*b*) an expression for the inductance of the equivalent winding and the coenergy.

$$W_m = 2.0 \text{ cm} \quad W_g = 2.5 \text{ cm} \quad D = 3.0 \text{ cm}$$
$$d = 1.0 \text{ cm} \quad g_0 = 0.2 \text{ cm}$$

Solution

a.

$$\mathcal{R}_m = \frac{d}{\mu_R W_m D}$$

$$\mathcal{R}_g = \frac{2g}{\mu_0(W_g - x)D}$$

$$(Ni)_{\text{equiv}} = -H'_c d = \frac{(B_r d)}{\mu_R}$$

b.

$$L = \frac{N_{\text{equiv}}^2}{(\mathcal{R}_{\text{m}} + \mathcal{R}_{\text{g}})}$$

$$W'_{\text{fld}} = \frac{L i_{\text{equiv}}^2}{2} = \frac{(B_{\text{r}} d)^2}{2\mu_{\text{R}}^2(\mathcal{R}_{\text{m}} + \mathcal{R}_{\text{g}})} = \frac{W_{\text{m}} D (B_{\text{r}} d)^2}{2\mu_{\text{R}}\left[d + \left(\frac{\mu_{\text{R}}}{\mu_0}\right)\left(\frac{2gW_{\text{m}}}{(W_{\text{g}} - x)}\right)\right]}$$

Clearly the methods described in this chapter can be extended to handle situations in which there are permanent magnets and multiple current-carrying windings. In many devices of practical interest, the geometry is sufficiently complex, independent of the number of windings and/or permanent magnets, that magnetic-circuit analysis is not necessarily applicable, and analytical solutions can be expected to be inaccurate, if they can be found at all. In these cases, numerical techniques, such as the finite-element method discussed previously, can be employed. Using this method, the coenergy of Eq. 3.48, or Eq. 3.50 if permanet magnets are involved, can be evaluated numerically at constant winding currents and for varying values of displacement.

3.8 DYNAMIC EQUATIONS

We have derived expressions for the forces and torques produced in electromechanical-energy-conversion devices as functions of electrical terminal variables and mechanical displacement. These expressions were derived for conservative energy-conversion systems for which it can be assumed that losses can be assigned to external electrical and mechanical elements connected to the terminals of the energy-conversion system. Such energy-conversion devices are intended to operate as a coupling means between electric and mechanical systems. Hence, we are ultimately interested in the operation of the complete electromechanical system and not just of the electromechanical-energy-conversion system around which it is built.

The model of a simple electromechancal system shown in Fig. 3.23 shows the basic system components, the details of which may vary from system to system. The system shown consists of three parts: an external electric system, the electromechanical-energy-conversion system, and an external mechanical system. The electric system

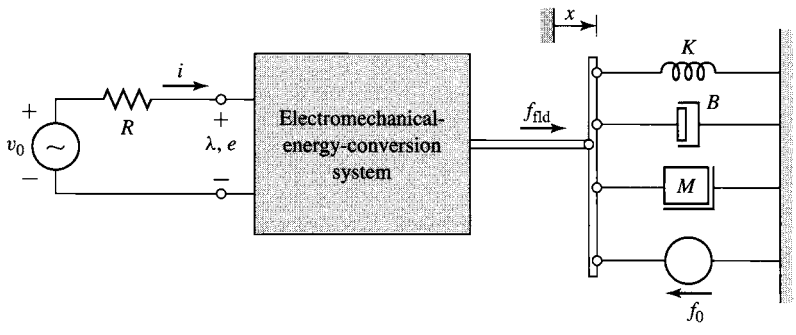

Figure 3.23 Model of a singly-excited electromechanical system.

is represented by a voltage source v_0 and resistance R; the source could alternatively be represented by a current source and a parallel conductance G.

Note that all the electrical losses in the system, including those which are inherent to the electromechanical-energy-conversion system are assigned to the resistance R in this model. For example, if the voltage source has an equivalent resistance R_s and the winding resistance of the electromechanical-energy-conversion system is R_w, the resistance R would equal the sum of these two resistances; $R = R_s + R_w$.

The electric equation for this model is

$$v_0 = iR + \frac{d\lambda}{dt} \tag{3.87}$$

If the flux linkage λ can be expressed as $\lambda = L(x)i$, the external equation becomes

$$v_0 = iR + L(x)\frac{di}{dt} + i\frac{dL(x)}{dx}\frac{dx}{dt} \tag{3.88}$$

The second term on the right, $L(di/dt)$, is the self-inductance voltage term. The third term $i(dL/dx)(dx/dt)$ includes the multiplier dx/dt. This is the speed of the mechanical terminal, and the third term is often called simply the *speed voltage*. The speed-voltage term is common to all electromechanical-energy-conversion systems and is responsible for energy transfer to and from the mechanical system by the electrical system.

For a multiply-excited system, electric equations corresponding to Eq. 3.87 are written for each input pair. If the expressions for the λ's are to be expanded in terms of inductances, as in Eq. 3.88, both self- and mutual-inductance terms will be required.

The mechanical system of Fig. 3.23 includes the representation for a spring (spring constant K), a damper (damping constant B), a mass M, and an external mechanical excitation force f_0. Here, as for the electrical system, the damper represents the losses both of the external mechanical system as well as any mechanical losses of the electromechanical-energy-conversion system.

The x-directed forces and displacement x are related as follows:

Spring:

$$f_K = -K(x - x_0) \tag{3.89}$$

Damper:

$$f_D = -B\frac{dx}{dt} \tag{3.90}$$

Mass:

$$f_M = -M\frac{d^2x}{dt^2} \tag{3.91}$$

where x_0 is the value of x with the spring normally unstretched. Force equilibrium thus requires that

$$f_{fld} + f_K + f_D + f_M - f_0 = f_{fld} - K(x - x_0) - B\frac{dx}{dt} - M\frac{d^2x}{dt^2} - f_0 = 0 \tag{3.92}$$

Combining Eqs. 3.88 and 3.92, the differential equations for the overall system of Fig. 3.23 for arbitrary inputs $v_0(t)$ and $f_0(t)$ are thus

$$v_0(t) = iR + L(x)\frac{di}{dt} + i\frac{dL(x)}{dx} \tag{3.93}$$

$$f_0(t) = -M\frac{d^2x}{dt^2} - B\frac{dx}{dt} - K(x - x_0) + f_{\text{fld}}(x, i) \tag{3.94}$$

The functions $L(x)$ and $f_{\text{fld}}(x, i)$ depend on the properties of the electromechanical-energy-conversion system and are calculated as previously discussed.

EXAMPLE 3.10

Figure 3.24 shows in cross section a cylindrical solenoid magnet in which the cylindrical plunger of mass M moves vertically in brass guide rings of thickness g and mean diameter d.

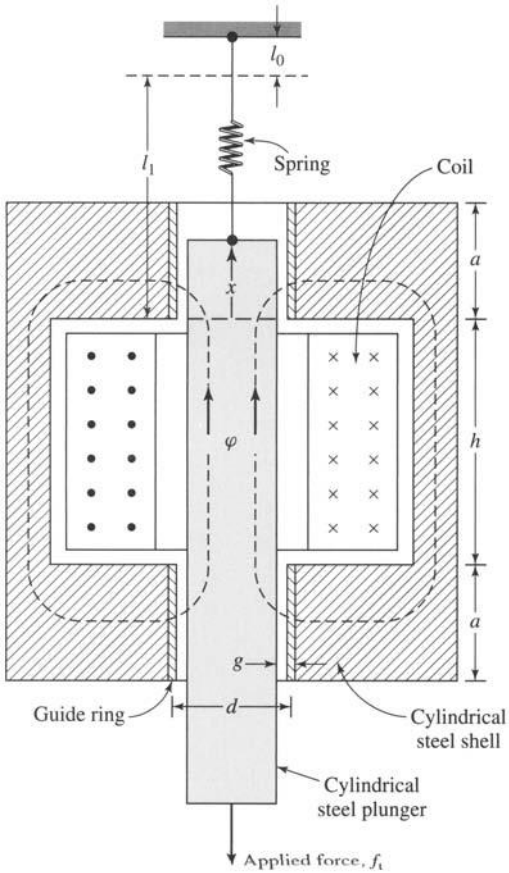

Figure 3.24 Solenoid magnet for Example 3.10.

The permeability of brass is the same as that of free space and is $\mu_0 = 4\pi \times 10^{-7}$ H/m in SI units. The plunger is supported by a spring whose spring constant is K. Its unstretched length is l_0. A mechanical load force f_t is applied to the plunger from the mechanical system connected to it, as shown in Fig. 3.24. Assume that frictional force is linearly proportional to the velocity and that the coefficient of friction is B. The coil has N turns and resistance R. Its terminal voltage is v_t and its current is i. The effects of magnetic leakage and reluctance of the steel are negligible.

Derive the dynamic equations of motion of the electromechanical system, i.e., the differential equations expressing the dependent variables i and x in terms of v_t, f_t, and the given constants and dimensions.

■ Solution

We begin by expressing the inductance as functions of x. The coupling terms, i.e., the magnetic force f_{fld} and induced emf e, can then be expressed in terms of x and i and these relations substituted in the equations for the mechanical and electric systems.

The reluctance of the magnetic circuit is that of the two guide rings in series, with the flux directed radially through them, as shown by the dashed flux lines φ in Fig. 3.24. Because $g \ll d$, the flux density in the guide rings is very nearly constant with respect to the radial distance. In a region where the flux density is constant, the reluctance is

$$\frac{\text{Length of flux path in direction of field}}{\mu\ (\text{area of flux path perpendicular to field})}$$

The reluctance of the upper gap is

$$\mathcal{R}_1 = \frac{g}{\mu_0 \pi x d}$$

in which it is assumed that the field is concentrated in the area between the upper end of the plunger and the lower end of the upper guide ring. Similarly, the reluctance of the lower gap is

$$\mathcal{R}_2 = \frac{g}{\mu_0 \pi a d}$$

The total reluctance is

$$\mathcal{R} = \mathcal{R}_1 + \mathcal{R}_2 = \frac{g}{\mu_0 \pi d}\left(\frac{1}{x} + \frac{1}{a}\right) = \frac{g}{\mu_0 \pi a d}\left(\frac{a+x}{x}\right)$$

Hence, the inductance is

$$L(x) = \frac{N^2}{\mathcal{R}} = \frac{\mu_0 \pi a d N^2}{g}\left(\frac{x}{a+x}\right) = L'\left(\frac{x}{a+x}\right)$$

where

$$L' = \frac{\mu_0 \pi a d N^2}{g}$$

The magnetic force acting upward on the plunger in the positive x direction is

$$f_{fld} = \left.\frac{\partial W'_{fld}(i,x)}{\partial x}\right|_i = \frac{i^2}{2}\frac{dL}{dx} = \frac{i^2}{2}\frac{aL'}{(a+x)^2}$$

The induced emf in the coil is

$$e = \frac{d}{dt}(Li) = L\frac{di}{dt} + i\frac{dL}{dx}\frac{dx}{dt}$$

or

$$e = L'\left(\frac{x}{a+x}\right)\frac{di}{dt} + L'\left(\frac{ai}{(a+x)^2}\right)\frac{dx}{dt}$$

Substitution of the magnetic force in the differential equation of motion of the mechanical system (Eq. 3.94) gives

$$f_t = -M\frac{d^2x}{dt^2} - B\frac{dx}{dt} - K(x - l_0) + \frac{1}{2}L'\frac{ai^2}{(a+x)^2}$$

The voltage equation for the electric system is (from Eq. 3.93)

$$v_t = iR + L'\left(\frac{x}{a+x}\right)\frac{di}{dt} + iL'\left(\frac{a}{(a+x)^2}\right)\frac{dx}{dt}$$

These last two equations are the desired results. They are valid only as long as the upper end of the plunger is well within the upper guide ring, say, between the limits $0.1a < x < 0.9a$. This is the normal working range of the solenoid.

3.9 ANALYTICAL TECHNIQUES

We have described relatively simple devices in this chapter. The devices have one or two electrical terminals and one mechanical terminal, which is usually constrained to incremental motion. More complicated devices capable of continuous energy conversion are treated in the following chapters. The analytical techniques discussed here apply to the simple devices, but the principles are applicable to the more complicated devices as well.

Some of the devices described in this chapter are used to produce gross motion, such as in relays and solenoids, where the devices operate under essentially "on" and "off" conditions. Analysis of these devices is carried out to determine force as a function of displacement and reaction on the electric source. Such calculations have already been made in this chapter. If the details of the motion are required, such as the displacement as a function of time after the device is energized, nonlinear differential equations of the form of Eqs. 3.93 and 3.94 must be solved.

In contrast to gross-motion devices, other devices such as loudspeakers, pickups, and transducers of various kinds are intended to operate with relatively small displacements and to produce a linear relationship between electrical signals and mechanical motion, and vice versa. The relationship between the electrical and mechanical variables is made linear either by the design of the device or by restricting the excursion of the signals to a linear range. In either case the differential equations are linear and can be solved using standard techniques for transient response, frequency response, and so forth, as required.

3.9.1 Gross Motion

The differential equations for a singly-excited device as derived in Example 3.10 are of the form

$$\frac{1}{2}L'\left(\frac{ai^2}{(a+x)^2}\right) = M\frac{d^2x}{dt^2} + B\frac{dx}{dt} + K(x - l_0) + f_t \tag{3.95}$$

$$v_t = iR + L'\left(\frac{x}{a+x}\right)\frac{di}{dt} + L'\left(\frac{ai}{(a+x)^2}\right)\frac{dx}{dt} \tag{3.96}$$

A typical problem using these differential equations is to find the excursion $x(t)$ when a prescribed voltage $v_t = V_0$ is applied at $t = 0$. An even simpler problem is to find the time required for the armature to move from its position $x(0)$ at $t = 0$ to a given displacement $x = X$ when a voltage $v_t = V$ is applied at $t = 0$. There is no general analytical solution for these differential equations; they are nonlinear, involving products and powers of the variables x and i and their derivatives. They can be solved using computer-based numerical integration techniques.

In many cases the gross-motion problem can be simplified and a solution found by relatively simple methods. For example, when the winding of the device is connected to the voltage source with a relatively large resistance, the iR term dominates on the right-hand side of Eq. 3.96 compared with the di/dt self-inductance voltage term and the dx/dt speed-voltage term. The current i can then be assumed equal to V/R and inserted directly into Eq. 3.95. The same assumption can be made when the winding is driven from power electronic circuitry which directly controls the current to the winding. With the assumption that $i = V/R$, two cases can be solved easily.

Case 1 The first case includes those devices in which the dynamic motion is dominated by damping rather than inertia, e.g., devices purposely having low inertia or relays having dashpots or dampers to slow down the motion. For example, under such conditions, with $f_t = 0$, the differential equation of Eq. 3.95 reduces to

$$B\frac{dx}{dt} = f(x) = \frac{1}{2}L'\left(\frac{a}{(a+x)^2}\right)\left(\frac{V}{R}\right)^2 - K(x - l_0) \tag{3.97}$$

where $f(x)$ is the difference between the force of electrical origin and the spring force in the device of Fig. 3.24. The velocity at any value of x is merely $dx/dt = f(x)/B$; the time t to reach $x = X$ is given by

$$t = \int_0^X \frac{B}{f(x)}\,dx \tag{3.98}$$

The integration of Eq. 3.98 can be carried out analytically or numerically.

Case 2 In this case, the dynamic motion is governed by the inertia rather than the damping. Again with $f_t = 0$, the differential equation of Eq. 3.95 reduces to

$$M\frac{d^2x}{dt^2} = f(x) = \frac{1}{2}L'\left(\frac{a}{(a+x)^2}\right)\left(\frac{V}{R}\right)^2 - K(x - l_0) \tag{3.99}$$

Equation 3.99 can be written in the form

$$\frac{M}{2}\frac{d}{dx}\left(\frac{dx}{dt}\right)^2 = f(x) \tag{3.100}$$

and the velocity $v(x)$ at any value x is then given by

$$v(x) = \frac{dx}{dt} = \sqrt{\frac{2}{M}\int_0^x f(x')\,dx'} \tag{3.101}$$

The integration of Eq. 3.101 can be carried out analytically or numerically to find $v(x)$ and to find the time t to reach any value of x.

3.9.2 Linearization

Devices characterized by nonlinear differential equations such as Eqs. 3.95 and 3.96 will yield nonlinear responses to input signals when used as transducers. To obtain linear behavior, such devices must be restricted to small excursions of displacement and electrical signals about their equilibrium values. The equilibrium displacement is determined either by a bias mmf produced by a dc winding current, or a permanent magnet acting against a spring, or by a pair of windings producing mmf's whose forces cancel at the equilibrium point. The equilibrium point must be stable; the transducer following a small disturbance should return to the equilibrium position.

With the current and applied force set equal to their equilibrium values, I_0 and f_{t_0} respectively, the equilibrium displacement X_0 and voltage V_0 can be determined for the system described by Eqs. 3.95 and 3.96 by setting the time derivatives equal to zero. Thus

$$\frac{1}{2}L'\left(\frac{aI_0^2}{(a+l_0)^2}\right) = K(X_0 - l_0) + f_{t_0} \tag{3.102}$$

$$V_0 = I_0 R \tag{3.103}$$

The incremental operation can be described by expressing each variable as the sum of its equilibrium and incremental values; thus $i = I_0 + i'$, $f_t = f_{t_0} + f'$, $v_t = V_0 + v'$, and $x = X_0 + x'$. The equations are then linearized by canceling any products of increments as being of second order. Equations 3.95 and 3.96 thus become

$$\frac{1}{2}\frac{L'a(I_0+i')^2}{(a+X_0+x')^2} = M\frac{d^2x'}{dt^2} + B\frac{dx'}{dt} + K(X_0 + x' - l_0) + f_{t_0} + f' \tag{3.104}$$

and

$$V_0 + v' = (I_0 + i')R + \frac{L'(X_0+x')}{a+X_0+x'}\frac{di'}{dt} + \frac{L'a(I_0+i')}{(a+X_0+x')^2}\frac{dx'}{dt} \tag{3.105}$$

The equilibrium terms cancel, and retaining only first-order incremental terms yields a set of linear differential equations in terms of just the incremental variables

of first order as

$$\frac{L'aI_0}{(a+X_0)^2}\,i' = M\frac{d^2x'}{dt^2} + B\frac{dx'}{dt} + \left[K + \frac{L'aI_0^2}{(a+X_0)^3}\right]x' + f' \tag{3.106}$$

$$v' = i'R + \frac{L'X_0}{a+X_0}\frac{di'}{dt} + \frac{L'aI_0}{(a+X_0)^2}\frac{dx'}{dt} \tag{3.107}$$

Standard techniques can be used to solve for the time response of this set of linear differential equations. Alternatively, sinusoidal-steady-state operation can be assumed, and Eqs. 3.106 and 3.107 can be converted to a set of linear, complex algebraic equations and solved in the frequency domain.

3.10 SUMMARY

In electromechanical systems, energy is stored in magnetic and electric fields. When the energy in the field is influenced by the configuration of the mechanical parts constituting the boundaries of the field, mechanical forces are created which tend to move the mechanical elements so that energy is transmitted from the field to the mechanical system.

Singly excited magnetic systems are considered first in Section 3.3. By removing electric and mechanical loss elements from the electromechanical-energy-conversion system (and incorporating them as loss elements in the external electrical and mechanical systems), the energy conversion device can be modeled as a conservative system. Its energy then becomes a state function, determined by its state variables λ and x. Section 3.4 derives expressions for determining the force and torque as the negative of partial derivative of the energy with respect to the displacement, taken while holding the flux-linkage λ constant.

In Section 3.5 the state function coenergy, with state variables i and x or θ, is introduced. The force and torque are then shown to be given by the partial derivative of the coenergy with respect to displacement, taken while holding the current i constant.

These concepts are extended in Section 3.6 to include systems with multiple windings. Section 3.7 further extends the development to include systems in which permanent magnets are included among the sources of the magnetic energy storage.

Energy conversion devices operate between electric and mechanical systems. Their behavior is described by differential equations which include the coupling terms between the systems, as discussed in Section 3.8. These equations are usually nonlinear and can be solved by numerical methods if necessary. As discussed in Section 3.9, in some cases approximations can be made to simplify the equations. For example, in many cases, linearized analyses can provide useful insight, both with respect to device design and performance.

This chapter has been concerned with basic principles applying broadly to the electromechanical-energy-conversion process, with emphasis on magnetic-field systems. Basically, rotating machines and linear-motion transducers work in the same way. The remainder of this text is devoted almost entirely to rotating machines. Rotating machines typically include multiple windings and may include permanent

magnets. Their performance can be analyzed by using the techniques and principles developed in this chapter.

3.11 PROBLEMS

3.1 The rotor of Fig. 3.25 is similar to that of Fig. 3.2 (Example 3.1) except that it has two coils instead of one. The rotor is nonmagnetic and is placed in a uniform magnetic field of magnitude B_0. The coil sides are of radius R and are uniformly spaced around the rotor surface. The first coil is carrying a current I_1 and the second coil is carrying a current I_2.

Assuming that the rotor is 0.30 m long, $R = 0.13$ m, and $B_0 = 0.85$ T, find the θ-directed torque as a function of rotor position α for (*a*) $I_1 = 0$ A and $I_2 = 5$ A, (*b*) $I_1 = 5$ A and $I_2 = 0$ A, and (*c*) $I_1 = 8$ A and $I_2 = 8$ A.

3.2 The winding currents of the rotor of Problem 3.1 are controlled as a function of rotor angle α such that

$$I_1 = 8\sin\alpha \quad \text{A} \qquad \text{and} \qquad I_2 = 8\cos\alpha \quad \text{A}$$

Write an expression for the rotor torque as a function of the rotor position α.

3.3 Calculate the magnetic stored energy in the magnetic circuit of Example 1.2.

3.4 An inductor has an inductance which is found experimentally to be of the form

$$L = \frac{2L_0}{1 + x/x_0}$$

where $L_0 = 30$ mH, $x_0 = 0.87$ mm, and x is the displacement of a movable element. Its winding resistance is measured and found to equal 110 mΩ.

a. The displacement x is held constant at 0.90 mm, and the current is increased from 0 to 6.0 A. Find the resultant magnetic stored energy in the inductor.

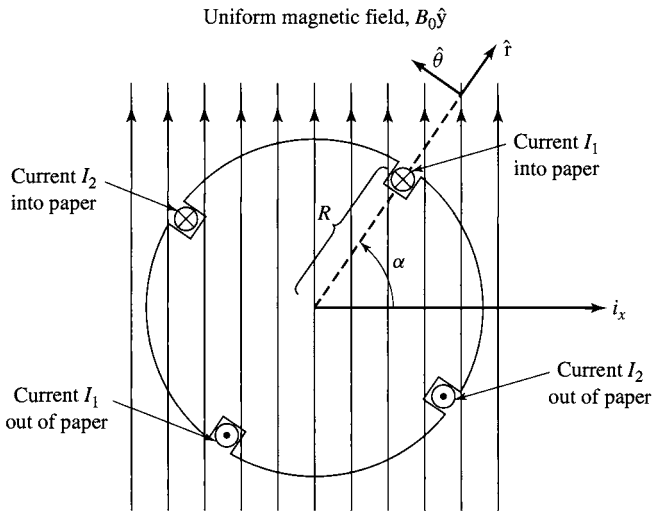

Figure 3.25 Two-coil rotor for Problem 3.1.

b. The current is then held constant at 6.0 A, and the displacement is increased to 1.80 mm. Find the corresponding change in magnetic stored energy.

3.5 Repeat Problem 3.4, assuming that the inductor is connected to a voltage source which increases from 0 to 0.4 V (part [a]) and then is held constant at 0.4 V (part [b]). For both calculations, assume that all electric transients can be ignored.

3.6 The inductor of Problem 3.4 is driven by a sinusoidal current source of the form

$$i(t) = I_0 \sin \omega t$$

where $I_0 = 5.5$ A and $\omega = 100\pi$ (50 Hz). With the displacement held fixed at $x = x_0$, calculate (*a*) the time-averaged magnetic stored energy (W_{fld}) in the inductor and (*b*) the time-averaged power dissipated in the winding resistance.

3.7 An actuator with a rotating vane is shown in Fig. 3.26. You may assume that the permeability of both the core and the vane are infinite ($\mu \to \infty$). The total air-gap length is $2g$ and shape of the vane is such that the effective area of the air gap can be assumed to be of the form

$$A_g = A_0 \left(1 - \left(\frac{4\theta}{\pi}\right)^2\right)$$

(valid only in the range $|\theta| \leq \pi/6$). The actuator dimensions are $g = 0.8$ mm, $A_0 = 6.0$ mm^2, and $N = 650$ turns.

a. Assuming the coil to be carrying current i, write an expression for the magnetic stored energy in the actuator as a function of angle θ for $|\theta| \leq \pi/6$.

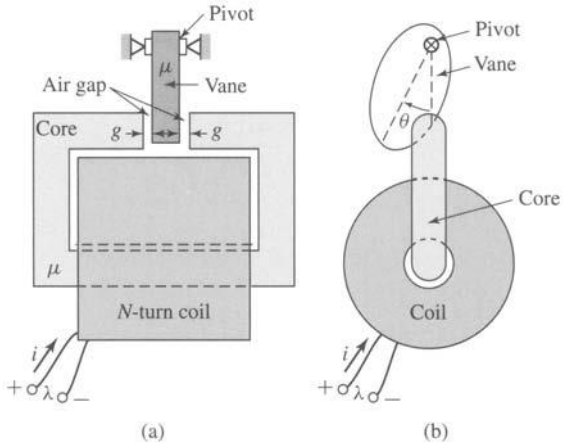

Figure 3.26 Actuator with rotating vane for Problem 3.7. (a) Side view. (b) End view.

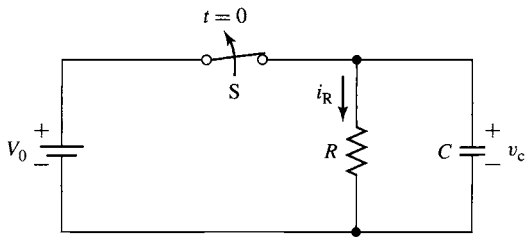

Figure 3.27 An RC circuit for Problem 3.8.

b. Find the corresponding inductance $L(\theta)$. Use MATLAB to plot this inductance as a function of θ.

3.8 An RC circuit is connected to a battery, as shown in Fig. 3.27. Switch S is initially closed and is opened at time $t = 0$.

a. Find the capacitor voltage $v_C(t)$ for $t \geq 0$

b. What are the initial and final ($t = \infty$) values of the stored energy in the capacitor? (Hint: $W_{fld} = \frac{1}{2}q^2/C$, where $q = CV_0$.) What is the energy stored in the capacitor as a function of time?

c. What is the power dissipated in the resistor as a function of time? What is the total energy dissipated in the resistor?

3.9 An RL circuit is connected to a battery, as shown in Fig. 3.28. Switch S is initially closed and is opened at time $t = 0$.

a. Find the inductor current $i_L(t)$ for $t \geq 0$. (Hint: Note that while the switch is closed, the diode is reverse-biased and can be assumed to be an open circuit. Immediately after the switch is opened, the diode becomes forward-biased and can be assumed to be a short circuit.)

b. What are the initial and final ($t = \infty$) values of the stored energy in the inductor? What is the energy stored in the inductor as a function of time?

c. What is the power dissipated in the resistor as a function of time? What is the total energy dissipated in the resistor?

3.10 The L/R time constant of the field winding of an 500-MVA synchronous generator is 4.8 s. At normal operating conditions, the field winding is known to be dissipating 1.3 MW. Calculate the corresponding magnetic stored energy.

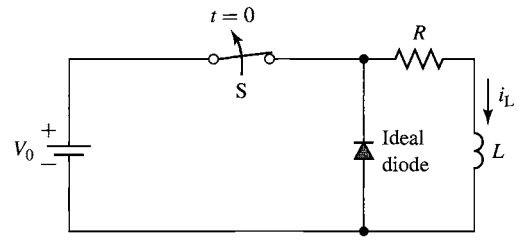

Figure 3.28 An RL circuit for Problem 3.9.

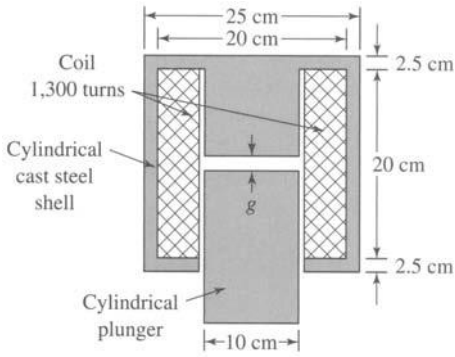

Figure 3.29 Plunger actuator for Problem 3.12.

3.11 The inductance of a phase winding of a three-phase salient-pole motor is measured to be of the form

$$L(\theta_m) = L_0 + L_2 \cos 2\theta_m$$

where θ_m is the angular position of the rotor.

a. How many poles are on the rotor of this motor?

b. Assuming that all other winding currents are zero and that this phase is excited by a constant current I_0, find the torque $T_{fld}(\theta)$ acting on the rotor.

3.12 Cylindrical iron-clad solenoid actuators of the form shown in Fig. 3.29 are used for tripping circuit breakers, for operating valves, and in other applications in which a relatively large force is applied to a member which moves a relatively short distance. When the coil current is zero, the plunger drops against a stop such that the gap g is 2.25 cm. When the coil is energized by a direct current of sufficient magnitude, the plunger is raised until it hits another stop set so that g is 0.2 cm. The plunger is supported so that it can move freely in the vertical direction. The radial air gap between the shell and the plunger can be assumed to be uniform and 0.05 cm in length.

For this problem neglect the magnetic leakage and fringing in the air gaps. The exciting coil has 1300 turns and carries a constant current of 2.3 A. Assume that the mmf in the iron can be neglected and use MATLAB to

a. plot the flux density in the variable gap between the yoke and the plunger for the range of travel of the plunger,

b. plot the corresponding values of the total energy stored in the magnetic field in μJ, and

c. plot the corresponding values of the coil inductance in μH.

3.13 Consider the plunger actuator of Fig. 3.29. Assume that the plunger is initially fully opened ($g = 2.25$ cm) and that a battery is used to supply a current of 2.5 A to the winding.

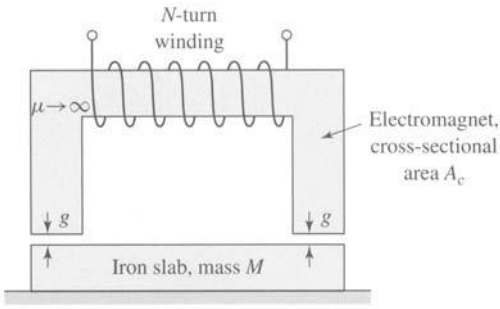

Figure 3.30 Electromagnet lifting an iron slab (Problem 3.14).

a. If the plunger is constrained to move very slowly (i.e., slowly compared to the electrical time constant of the actuator), reducing the gap g from 2.25 to 0.20 cm, how much mechanical work in joules will be supplied to the plunger?

b. For the conditions of part (a), how much energy will be supplied by the battery (in excess of the power dissipated in the coil)?

3.14 As shown in Fig. 3.30, an N-turn electromagnet is to be used to lift a slab of iron of mass M. The surface roughness of the iron is such that when the iron and the electromagnet are in contact, there is a minimum air gap of $g_{\min} = 0.18$ mm in each leg. The electromagnet cross-sectional area $A_c = 32$ cm and coil resistance is 2.8 Ω. Calculate the minimum coil voltage which must be used to lift a slab of mass 95 kg against the force of gravity. Neglect the reluctance of the iron.

3.15 Data for the magnetization curve of the iron portion of the magnetic circuit of the plunger actuator of Problem 3.12 are given below:

Flux (mWb)	5.12	8.42	9.95	10.6	10.9	11.1	11.3	11.4	11.5	11.6
mmf (A · turns)	68	135	203	271	338	406	474	542	609	677

a. Use the MATLAB polyfit function to obtain a 3'rd-order fit of reluctance and total flux versus mmf for the iron portions of the magnetic circuit. Your fits will be of the form:

$$\mathcal{R}_{\text{iron}} = a_1\mathcal{F}_{\text{iron}}^3 + a_2\mathcal{F}_{\text{iron}}^2 + a_3\mathcal{F}_{\text{iron}} + a_4$$

$$\phi_{\text{iron}} = b_1\mathcal{F}_{\text{iron}}^3 + b_2\mathcal{F}_{\text{iron}}^2 + b_3\mathcal{F}_{\text{iron}} + b_4$$

List the coefficients.

b. (*i*) Using MATLAB and the functional forms found in part (a), plot the magnetization curve for the complete magnetic circuit (flux linkages λ versus winding current i) for a variable-gap length of $g = 0.2$ cm. On the

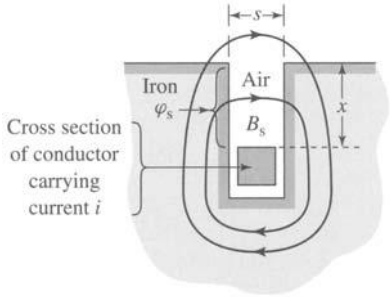

Figure 3.31 Conductor in a slot (Problem 3.17).

same axes, plot the magnetization curve corresponding to the assumption that the iron is of infinite permeability. The maximum current in your plot should correspond to a flux in the magnetic circuit of 600 mWb. (*ii*) Calculate the magnetic field energy and coenergy for each of these cases corresponding to a winding current of 2.0 A.

c. Repeat part (b) for a variable-gap length of $g = 2.25$ cm. In part (ii), calculate the magnetic field energy and coenergy corresponding to a winding current of 20 A.

3.16 An inductor is made up of a 525-turn coil on a core of 14-cm^2 cross-sectional area and gap length 0.16 mm. The coil is connected directly to a 120-V 60-Hz voltage source. Neglect the coil resistance and leakage inductance. Assuming the coil reluctance to be negligible, calculate the time-averaged force acting on the core tending to close the air gap. How would this force vary if the air-gap length were doubled?

3.17 Figure 3.31 shows the general nature of the slot-leakage flux produced by current i in a rectangular conductor embedded in a rectangular slot in iron. Assume that the iron reluctance is negligible and that the slot leakage flux goes straight across the slot in the region between the top of the conductor and the top of the slot.

a. Derive an expression for the flux density B_s in the region between the top of the conductor and the top of the slot.

b. Derive an expression for the slot-leakage φ_s sits crossing the slot above the conductor, in terms of the height x of the slot above the conductor, the slot width s, and the embedded length l perpendicular to the paper.

c. Derive an expression for the force f created by this magnetic field on a conductor of length l. In what direction does this force act on the conductor?

d. When the conductor current is 850 A, compute the force per meter on a conductor in a slot 2.5 cm wide.

3.18 A long, thin solenoid of radius r_0 and height h is shown in Fig. 3.32. The magnetic field inside such a solenoid is axially directed, essentially uniform and equal to $H = Ni/h$. The magnetic field outside the solenoid can be

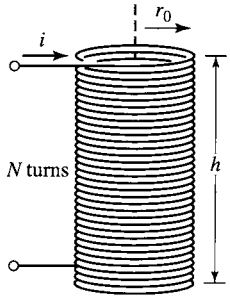

Figure 3.32 Solenoid coil (Problem 3.18).

shown to be negligible. Calculate the radial pressure in newtons per square meter acting on the sides of the solenoid for constant coil current $i = I_0$.

3.19 An electromechanical system in which electric energy storage is in electric fields can be analyzed by techniques directly analogous to those derived in this chapter for magnetic field systems. Consider such a system in which it is possible to separate the loss mechanism mathematically from those of energy storage in electric fields. Then the system can be represented as in Fig. 3.33. For a single electric terminal, Eq. 3.11 applies, where

$$dW_{\text{elec}} = vi\,dt = v\,dq$$

where v is the electric terminal voltage and q is the net charge associated with electric energy storage. Thus, by analogy to Eq. 3.16,

$$dW_{\text{fld}} = v\,dq - f_{\text{fld}}\,dx$$

a. Derive an expression for the electric stored energy $W_{\text{fld}}(q, x)$ analogous to that for the magnetic stored energy in Eq. 3.18.

b. Derive an expression for the force of electric origin f_{fld} analogous to that of Eq. 3.26. State clearly which variable must be held constant when the derivative is taken.

c. By analogy to the derivation of Eqs. 3.34 to 3.41, derive an expression for the coenergy $W'_{\text{fld}}(v, x)$ and the corresponding force of electric origin.

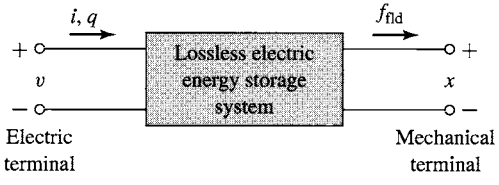

Figure 3.33 Lossless electric energy storage system.

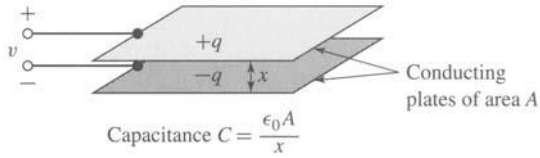

Figure 3.34 Capacitor plates (Problem 3.20).

3.20 A capacitor (Fig. 3.34) is made of two conducting plates of area A separated in air by a spacing x. The terminal voltage is v, and the charge on the plates is q. The capacitance C, defined as the ratio of charge to voltage, is

$$C = \frac{q}{v} = \frac{\epsilon_0 A}{x}$$

where ϵ_0 is the dielectric constant of free space (in SI units $\epsilon_0 = 8.85 \times 10^{-12}$ F/m).

a. Using the results of Problem 3.19, derive expressions for the energy $W_{\text{fld}}(q, x)$ and the coenergy $W'_{\text{fld}}(v, x)$.

b. The terminals of the capacitor are connected to a source of constant voltage V_0. Derive an expression for the force required to maintain the plates separated by a constant spacing $x = \delta$.

3.21 Figure 3.35 shows in schematic form an *electrostatic voltmeter,* a capacitive system consisting of a fixed electrode and a moveable electrode. The moveable electrode is connected to a vane which rotates on a pivot such that the air gap between the two electrodes remains fixed as the vane rotates. The capacitance of this system is given by

$$C(\theta) = \frac{\epsilon_0 R d(\alpha - |\theta|)}{g} \qquad (|\theta| \le \alpha)$$

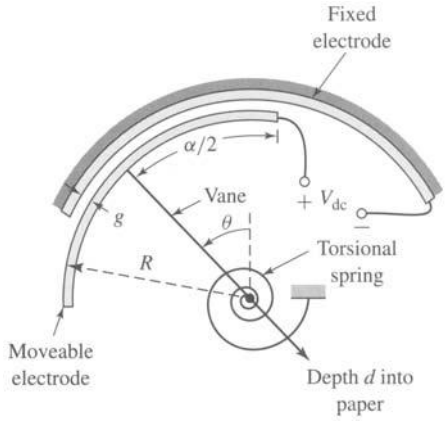

Figure 3.35 Schematic electrostatic voltmeter (Problem 3.21).

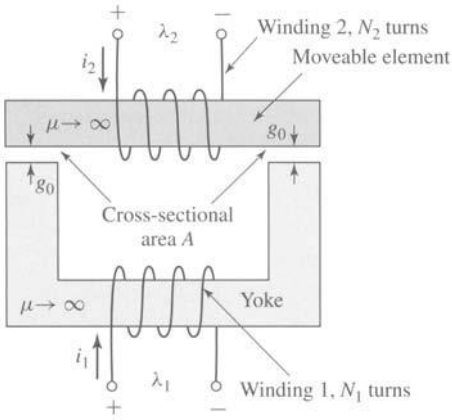

Figure 3.36 Two-winding magnetic circuit for Problem 3.22.

A torsional spring is connected to the moveable vane, producing a torque

$$T_{\text{spring}} = -K(\theta - \theta_0)$$

a. For $0 \le \theta \le \alpha$, using the results of Problem 3.19, derive an expression for the electromagnetic torque T_{fld} in terms of the applied voltage V_{dc}.

b. Find an expression for the angular position of the moveable vane as a function of the applied voltage V_{dc}.

c. For a system with

$$R = 12 \text{ cm}, \quad d = 4 \text{ cm}, \quad g = 0.2 \text{ mm}$$
$$\alpha = \pi/3 \text{ rad}, \quad \theta_0 = 0 \text{ rad}, \quad K = 3.65 \text{ N} \cdot \text{m/rad}$$

Plot the vane position in degrees as a function of applied voltage for $0 \le V_{\text{dc}} \le 1500$ V.

3.22 The two-winding magnetic circuit of Fig. 3.36 has a winding on a fixed yoke and a second winding on a moveable element. The moveable element is constrained to motion such that the lengths of both air gaps remain equal.

a. Find the self-inductances of windings 1 and 2 in terms of the core dimensions and the number of turns.

b. Find the mutual inductance between the two windings.

c. Calculate the coenergy $W'_{\text{fld}}(i_1, i_2)$.

d. Find an expression for the force acting on the moveable element as a function of the winding currents.

3.23 Two coils, one mounted on a stator and the other on a rotor, have self- and mutual inductances of

$$L_{11} = 3.5 \text{ mH} \quad L_{22} = 1.8 \text{ mH} \quad L_{12} = 2.1 \cos\theta \text{ mH}$$

where θ is the angle between the axes of the coils. The coils are connected in

series and carry a current

$$i = \sqrt{2} I \sin \omega t$$

a. Derive an expression for the instantaneous torque T on the rotor as a function of the angular position θ.
b. Find an expression for the time-averaged torque T_{avg} as a function of θ.
c. Compute the numerical value of T_{avg} for $I = 10$ A and $\theta = 90°$.
d. Sketch curves of T_{avg} versus θ for currents $I = 5, 7.07$, and 10 A.
e. A helical restraining spring which tends to hold the rotor at $\theta = 90°$ is now attached to the rotor. The restraining torque of the spring is proportional to the angular deflection from $\theta = 90°$ and is -0.1 N · m when the rotor is turned to $\theta = 0°$. Show on the curves of part (d) how you could find the angular position of the rotor-plus-spring combination for coil currents $I = 5, 7.07$, and 10 A. From your curves, estimate the rotor angle for each of these currents.
f. Write a MATLAB script to plot the angular position of the rotor as a function of rms current for $0 \leq I \leq 10$ A.

(Note that this problem illustrates the principles of the dynamometer-type ac ammeter.)

3.24 Two windings, one mounted on a stator and the other on a rotor, have self- and mutual inductances of

$$L_{11} = 4.5\,\text{H} \quad L_{22} = 2.5\,\text{H} \quad L_{12} = 2.8 \cos\theta\ \text{H}$$

where θ is the angle between the axes of the windings. The resistances of the windings may be neglected. Winding 2 is short-circuited, and the current in winding 1 as a function of time is $i_1 = 10 \sin \omega t$ A.

a. Derive an expression for the numerical value in newton-meters of the instantaneous torque on the rotor in terms of the angle θ.
b. Compute the time-averaged torque in newton-meters when $\theta = 45°$.
c. If the rotor is allowed to move, will it rotate continuously or will it tend to come to rest? If the latter, at what value of θ_0?

3.25 A loudspeaker is made of a magnetic core of infinite permeability and circular symmetry, as shown in Figs. 3.37a and b. The air-gap length g is much less than the radius r_0 of the central core. The voice coil is constrained to move only in the x direction and is attached to the speaker cone, which is not shown in the figure. A constant radial magnetic field is produced in the air gap by a direct current in coil 1, $i_1 = I_1$. An audio-frequency signal $i_2 = I_2 \cos \omega t$ is then applied to the voice coil. Assume the voice coil to be of negligible thickness and composed of N_2 turns uniformly distributed over its height h. Also assume that its displacement is such that it remains in the air gap ($0 \leq x \leq l - h$).

a. Calculate the force on the voice coil, using the Lorentz Force Law (Eq. 3.1).

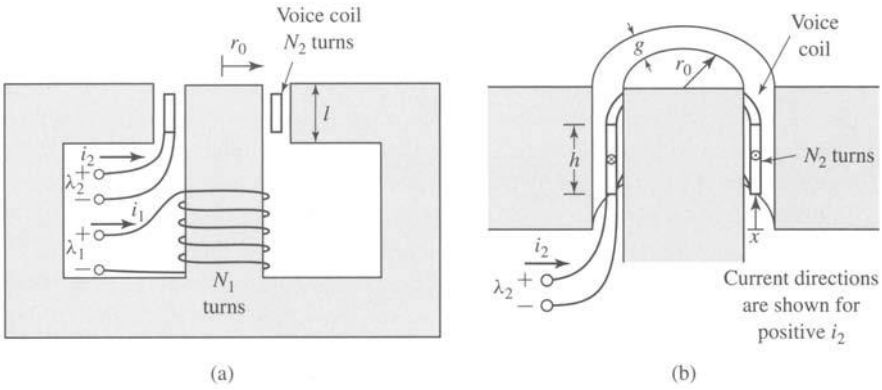

Figure 3.37 Loudspeaker for Problem 3.25.

b. Calculate the self-inductance of each coil.

c. Calculate the mutual inductance between the coils. (Hint: Assume that current is applied to the voice coil, and calculate the flux linkages of coil 1. Note that these flux linkages vary with the displacement x.)

d. Calculate the force on the voice coil from the coenergy W'_{fld}.

3.26 Repeat Example 3.8 with the samarium-cobalt magnet replaced by a neodymium-iron-boron magnet.

3.27 The magnetic structure of Fig. 3.38 is a schematic view of a system designed to support a block of magnetic material ($\mu \to \infty$) of mass M against the force of gravity. The system includes a permanent magnet and a winding. Under normal conditions, the force is supplied by the permanent magnet alone. The function of the winding is to counteract the field produced by the magnet so that the mass can be removed from the device. The system is designed such that the air gaps at each side of the mass remain constant at length $g_0/2$.

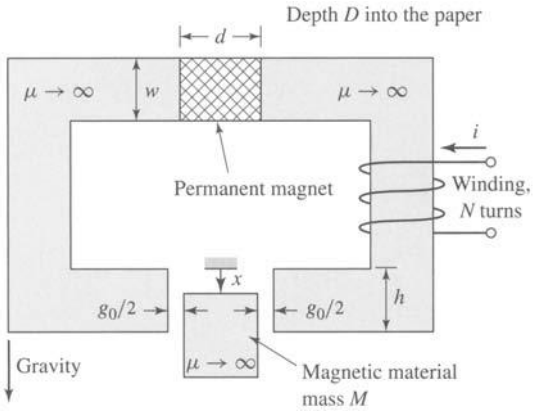

Figure 3.38 Magnetic support system for Problem 3.27.

Assume that the permanent magnet can be represented by a linear characteristic of the form

$$B_m = \mu_R(H_m - H_c)$$

and that the winding direction is such that positive winding current reduces the air-gap flux produced by the permanent magnet. Neglect the effects of magnetic fringing.

a. Assume the winding current to be zero. (*i*) Find the force f_{fld} acting on the mass in the x direction due to the permanent magnet alone as a function of x ($0 \le x \le h$). (*ii*) Find the maximum mass M_{max} that can be supported against gravity for $0 \le x \le h$.

b. For $M = M_{max}/2$, find the minimum current required to ensure that the mass will fall out of the system when the current is applied.

3.28 Winding 1 in the loudspeaker of Problem 3.25 (Fig. 3.37) is replaced by a permanent magnet as shown in Fig. 3.39. The magnet can be represented by the linear characteristic $B_m = \mu_R(H_m - H_c)$.

a. Assuming the voice coil current to be zero, ($i_2 = 0$), calculate the magnetic flux density in the air gap.

b. Calculate the flux linkage of the voice coil due to the permanent magnet as a function of the displacement x.

c. Calculate the coenergy $W'_{fld}(i_2, x)$ assuming that the voice coil current is sufficiently small so that the component of W'_{fld} due to the voice coil self inductance can be ignored.

d. Calculate the force on the voice coil.

3.29 Figure 3.40 shows a circularly symmetric system in which a moveable plunger (constrained to move only in the vertical direction) is supported by a spring of spring constant $K = 5.28$ N/m. The system is excited by a

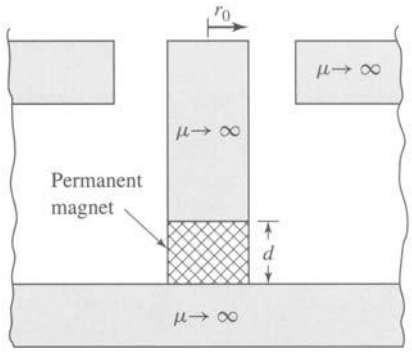

Figure 3.39 Central core of loudspeaker of Fig. 3.37 with winding 1 replaced by a permanent magnet (Problem 3.28).

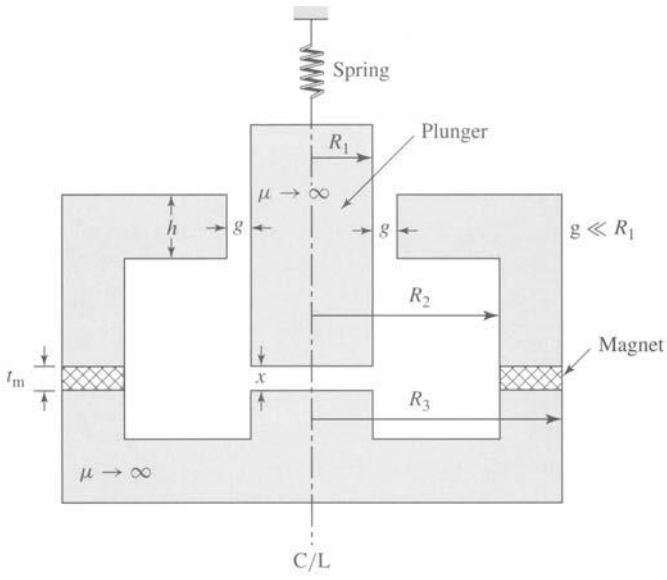

Figure 3.40 Permanent-magnet system for Problem 3.29.

samarium-cobalt permanent-magnet in the shape of a washer of outer radius R_3, inner radius R_2, and thickness t_m. The system dimensions are:

$$R_1 = 2.1 \text{ cm}, \quad R_2 = 4 \text{ cm}, \quad R_3 = 4.5 \text{ cm}$$
$$h = 1 \text{ cm}, \quad g = 1 \text{ mm}, \quad t_m = 3 \text{ mm}$$

The equilibrium position of the plunger is observed to be $x = 1.0$ mm.

a. Find the magnetic flux density B_g in the fixed gap and B_x in the variable gap.

b. Calculate the x-directed magnetic force pulling down on the plunger.

c. The spring force is of the form $f_{\text{spring}} = K(X_0 - x)$. Find X_0.

3.30 The plunger of a solenoid is connected to a spring. The spring force is given by $f = K_0(0.9a - x)$, where x is the air-gap length. The inductance of the solenoid is of the form $L = L_0(1 - x/a)$, and its winding resistance is R.

The plunger is initially stationary at position $x = 0.9a$ when a dc voltage of magnitude V_0 is applied to the solenoid.

a. Find an expression for the force as a function of time required to hold the plunger at position $a/2$.

b. If the plunger is then released and allowed to come to equilibrium, find the equilibrium position X_0. You may assume that this position falls in the range $0 \le X_0 \le a$.

3.31 Consider the solenoid system of Problem 3.30. Assume the following parameter values:

$$L_0 = 4.0 \text{ mH} \quad a = 2.2 \text{ cm} \quad R = 1.5\,\Omega \quad K_0 = 3.5 \text{ N/cm}$$

The plunger has mass $M = 0.2$ kg. Assume the coil to be connected to a dc source of magnitude 4 A. Neglect any effects of gravity.

a. Find the equilibrium displacement X_0.

b. Write the dynamic equations of motion for the system.

c. Linearize these dynamic equations for incremental motion of the system around its equilibrium position.

d. If the plunger is displaced by an incremental distance ϵ from its equilibrium position X_0 and released with zero velocity at time $t = 0$, find (*i*) The resultant motion of the plunger as a function of time, and (*ii*) The corresponding time-varying component of current induced across the coil terminals.

3.32 The solenoid of Problem 3.31 is now connected to a dc voltage source of magnitude 6 V.

a. Find the equilibrium displacement X_0.

b. Write the dynamic equations of motion for the system.

c. Linearize these dynamic equations for incremental motion of the system around its equilibrium position.

3.33 Consider the single-coil rotor of Example 3.1. Assume the rotor winding to be carrying a constant current of $I = 8$ A and the rotor to have a moment of inertia $J = 0.0125\ \text{kg} \cdot \text{m}^2$.

a. Find the equilibrium position of the rotor. Is it stable?

b. Write the dynamic equations for the system.

c. Find the natural frequency in hertz for incremental rotor motion around this equilibrium position.

3.34 Consider a solenoid magnet similar to that of Example 3.10 (Fig. 3.24) except that the length of the cylindrical plunger is reduced to $a + h$. Derive the dynamic equations of motion of the system.